Biological evaluation of biomaterials for bone tissue regeneration

Pedro de Sousa Gomes

FACULDADE DE
MEDICINA DENTÁRIA
UNIVERSIDADE DO PORTO

U.PORTO

Porto, 2011

Dissertação de candidatura ao grau de Doutor em Medicina Dentária, submetida à Faculdade de Medicina Dentária, Universidade do Porto.

Conselho Científico da Faculdade de Medicina Dentária, Universidade do Porto

Prof. Doutor Afonso Pinhão Ferreira - Presidente

Prof. Doutor António Cabral Campos Felino – Vice-presidente

Prof. Doutor Américo dos Santos Afonso

Prof. Doutor César Fernando Coelho Leal da Silva

Prof. Doutor Fernando Jorge Morais Branco

Prof. Doutor Germano Neves Pinto Rocha

Prof. Doutora Irene Graça Azevedo Pina Vaz

Prof. Doutor João Carlos Antunes Sampaio Fernandes

Prof. Doutor João Carlos Gonçalves Ferreira de Pinho

Prof. Doutor João Fernando Costa Carvalho

Prof. Doutor Jorge Manuel Carvalho Dias Lopes

Prof. Doutor José Albertino Cruz Lordelo

Prof. Doutor José António Macedo Carvalho Capelas

Prof. Doutor José Carlos Reis Campos

Prof. Doutor Manuel José Fontes de Carvalho

Prof. Doutora Maria Cristina P. C. M. F. Pollmann

Prof. Doutora Maria de Lurdes Ferreira Lobo Pereira

Prof. Doutora Maria Helena Guimarães Figueiral da Silva

Prof. Doutora Maria Helena Raposo Fernandes

Prof. Doutor Mário Augusto Pires Vaz

Prof. Doutor Mário Jorge Rebolho da Silva

Prof. Doutor Mário Ramalho Vasconcelos

Prof. Doutor Miguel Fernando Silva Gonçalves Pinto

Prof. Doutor Paulo Rui Galrão Ribeiro Melo

Prof. Doutor Ricardo Manuel C. L. Faria de Almeida

Docentes Jubilados e Aposentados

Professor Doutor Adão Fernando Pereira

Prof. Doutor Amílcar Almeida Oliveira

Prof. Doutor António Manuel Guerra Capelas

Prof. Doutor António Manuel Machado Capelas †

Dr. António Ulisses Matos dos Santos

Prof. Doutor Artur Manuel Osório de Araújo

Prof. Doutor Durval Manuel Belo Moreira

Prof. Doutor Fernando José Brandão Martins Peres

Prof. Doutor Francisco António Rebelo Morais Caldas

Prof. Doutor José Carlos Pina de Almeida Rebelo

Prof. Doutor José Serra Silva Campos Neves

Dr. José Maria Vaz Osório

Prof. Doutor Manuel Desport Marques †

Prof. Doutor Manuel Guedes de Figueiredo

Prof. Doutor Manuel Pedro Fonseca Paulo

Prof. Doutora Maria Adelaide Macedo Carvalho Capelas

Prof. Doutor Rogério Serapião Martins de Aguiar Branco

…. to Sara

"The scientific method," Thomas Henry Huxley once wrote, "is nothing but the normal working of the human mind." That is to say, when the mind is working; that is to say further, when it is engaged in corrrecting its mistakes.

Taking this point of view, we may conclude that science is not physics, biology, or chemistry - is not even a "subject" - but a moral imperative drawn from a larger narrative whose purpose is to give perspective, balance, and humility to learning.

Quoted in: Neil Postman, *The End of Education,* Alfred A. Knopf, New York, 1995, p 68

Contents

x

Agradecimentos

À Professora Doutora Maria Helena Raposo Fernandes, Professora Catedrática da Faculdade de Medicina Dentária, Universidade do Porto, agradeço os ensinamentos e a motivação que transmitiu durante toda a minha formação académica pré- e pós-graduada, nomeadamente a supervisão do trabalho de investigação que conduziu à elaboração desta dissertação. Agradeço profundamente a amizade e a disponibilidade, bem como o exemplo de rigor, voluntariedade, capacidade de trabalho, conhecimento científico e humanismo, que tiveram um impacto determinante na minha vida, no plano profissional e pessoal.

Ao Professor Doutor João Carlos Sampaio Fernandes, Professor Catedrático da Faculdade de Medicina Dentária, Universidade do Porto, agradeço o apoio constante e os ensinamentos desde o meu tempo de estudante, a motivação para o desenvolvimento de trabalho de investigação, e a amizade, que em muito contribuíram para a realização desta dissertação.

Ao Professor Doutor António Cabral de Campos Felino, Professor Catedrático da Faculdade de Medicina Dentária, Universidade do Porto, agradeço a força e motivação manifestadas durante o desenvolvimento deste trabalho. Agradeço também a cordialidade com que me acolheu no Serviço de Cirurgia Oral como colaborador, e o quanto essa oportunidade contribuiu para o meu desenvolvimento pessoal e profissional.

Ao Professor Doutor Afonso Pinhão Ferreira, Professor Catedrático e Director da Faculdade de Medicina Dentária, Universidade do Porto, agradeço todo o apoio pessoal e institucional, determinantes para a minha actividade profissional, e que em muito contribuíram para a efectivação do presente trabalho de investigação. Agradeço também o voto de confiança para os cargos de natureza científica e órgãos de gestão universitária.

Ao Professor Doutor José Domingos dos Santos, Professor Associado com Agregação da Faculdade de Engenharia, Universidade do Porto, agradeço o apoio e os ensinamentos na área dos Biomateriais, bem como a partilha de conhecimentos e a estreita colaboração no trabalho de investigação.

Aos meus amigos, principalmente do Laboratório de Farmacologia e Biocompatibilidade Celular, e do Serviço de Cirurgia Oral, da Faculdade de Medicina Dentária, Universidade do Porto, João, Sara, Carlos e Pedro, a minha gratidão por todo o apoio e amizade.

À Sara, agradeço por me acompanhar, por partilhar e me guiar neste caminho, com todo o seu apoio e amor incondicionais.

Abstract

Bone tissue engineering strategies rely on the complex interplay between cells, biomaterials and biomodulators to achieve a successful regeneration of the bone tissue, in an intimate synergy with the hosts' biological capabilities. In these applications, a wide range of biomaterials has been assayed, in order to elicite an adequate response from the biological milieu. Regrettably, there is no current available material that meets all the desirable biochemical, mechanical and biological requirements for each individual bone-related clinical application. Moreover, the material's form and size, the close interface with body fluids and/or tissues, and the estimate duration of use, will further determine selected and individual properties. In this way, one material property alone is unlikely to lead to a successful and durable device, whereas a lack or inadequacy regarding a single key property, can lead to a disastrous failure.

In this way, biomaterial testing, specifically in which relates to the assessment of material's biocompatibility - the ability of a candidate biomaterial to perform its desired therapeutical function, without eliciting any undesirable local or systemic response, but engendering the most appropriate beneficial response in that specific situation – is regarded as the central theme concerning the clinical success of biomaterials application.

Initial approaches of biocompatibility assessment usually rely on *in vitro* biomaterial biological testing, embracing the general cytocompatibility evaluation with broadly available cell lines, usually of fibroblastic phenotype. A generic characterization of the biological behaviour of candidate materials is possible and the detection of cytotoxic and/or mutagenic compounds, in direct or indirect culture systems, is accomplishable. Nonetheless, a second *in vitro* phase, in which the specific cytocompatibility is assessed, is usually conducted to evaluate the material response to primary or early passaged cells of a type relevant to the proposed application of the medical device. In the case of bone-related applications, osteoblasts, osteoclasts and endothelial cells are commonly used in the biological evaluation.

Overall, i*n vitro* testing is an attempt to simulate the *in vivo* situation as closely as possible, in a strictly controlled environment. By selecting cell populations most likely to modulate the behaviour of implanted materials, a spectra of *in vitro* changes, ranging from inhibition of growth or inadequate expression of cell markers, to stimulation of cell proliferation and/or other cell functional factors, may be addressed and offer a method to tailor biomaterials in an early phase of development. However, *in vitro* testing, as exhaustive as it is, it does not eliminate the need to test the candidate

biomaterial in an *in vivo* biological system, reaching hand of animal experimental models.

Animal models are essential for evaluating biocompatibility, tissue response and mechanical function of candidate materials, prior to clinical use in human trials. They allow the evaluation of materials in a wide range of time frames, ages, and in different biological constrains, but while they may closely represent the biomechanical and physiological conditions of the human clinical situation, it must be remembered that it is only an estimated approximation, with each model having unique advantages and disadvantages.

In this work, the general and specific cytocompatibility profile of several candidate biomaterials for bone tissue regeneration is addressed, reaching hand of multiple *in vitro* cell culture systems. Materials ranging from calcium phosphate and silicon-based ceramics, to glass-substituted materials, composites and film-deposited constructs were deeply scrutinized regarding events of cell adhesion, proliferation and differentiation. Human cell populations most relevant for biocompatibility assessment were used, ranging from human fibroblastic or osteoblastic cell lines to primary or early passaged cultures of human fibroblasts, osteoblasts and endothelial cells. Moreover, the issue of the *in vivo* biocompatibility assessment has also been addressed, regarding the use of the rodents' calvaria model, for the evaluation of the bone regeneration process.

The development of new materials aiming clinical application within bone-related interventions has become progressively more sophisticated, both in terms of design and fabrication methodologies. From the biological point of view, recent advances have contributed to shed a new light into the development of research tools, and in the understanding of the mechanisms involved in cell and tissue cross-talk with biomaterials, during bone regeneration. The greatest challenge of this paradigm, that has emerged from the synergic multidisciplinary approach in biomaterials and regenerative medicine applications, relies on the exponential increase of possibilities that have to be tested and validated by trustworthy and effective methodologies. *In vitro* and *in vivo* testing both converge to establish a ground base for a preliminary biosafety criteria that materials aiming clinical application should obey, prior to any human contact, either in trials or perspective clinical applications.

Resumo

As estratégias de engenharia do tecido ósseo têm como base a interacção de células, biomateriais e biomoduladores, de forma a promoverem a regeneração óssea, numa estreita sinergia com o processo regenerativo do hospedeiro. Nestas aplicações, apesar de se utilizar uma grande variedade de biomateriais, nenhum dos actualmente disponíveis apresenta todas as características desejáveis de um biomaterial de regeneração óssea, do ponto de vista bioquímico, mecânico e biológico. Acresce o facto de que alguns factores, como a forma e as dimensões do material, a interacção com os fluidos e tecidos biológicos, e o tempo estimado de implantação, contribuem para a variabilidade das propriedades individuais do biomaterial, no âmbito de cada aplicação.

Deste modo, a caracterização de biomateriais de regeneração óssea, nomeadamente no que se refere à avaliação da biocompatibilidade – a capacidade de um material desempenhar a sua função terapêutica, sem desenvolver respostas adversas a nível local ou sistémico, ao mesmo tempo que induz a resposta mais apropriada por parte do organismo – revela-se fulcral no seu sucesso clínico.

De uma forma geral, o estudo da biocompatibilidade inicia-se com a caracterização *in vitro*, na qual se avalia a citocompatibilidade geral com recurso a linhas celulares de fenótipo fibroblástico. Este processo permite uma avaliação genérica do comportamento biológico dos materiais, nomeadamente a detecção de compostos e/ou componentes citotóxicos ou mutagénicos. No entanto, esta metodologia não dispensa uma segunda fase de caracterização *in vitro*, na qual se avalia a citocompatibilidade específica, utilizando culturas primárias ou subculturas iniciais de populações celulares relevantes no contexto da aplicação clínica do material. No que se refere às aplicações relacionadas com o tecido ósseo, as populações mais utilizadas nesta caracterização são os osteoblastos, osteoclastos e células endoteliais.

A caracterização *in vitro* procura mimetizar as condições observadas *in vivo*, num ambiente estritamente controlado. Este processo providencia um vasto leque de informações relativas à possibilidade de inibição ou estimulação da proliferação e/ou da actividade funcional. No entanto, a caracterização *in vitro*, por mais exaustiva que seja, não substitui a avaliação do material em questão num sistema biológico, *in vivo*, nomeadamente em modelos experimentais com animais de laboratório.

A avaliação biológica *in vivo* permite a caracterização exaustiva do material, considerando um leque variado de tempos de implantação, idades, condições fisiológicas e patológicas, mimetizando, desta forma, o contexto clínico. A

caracterização *in vivo* permite ainda a avaliação da resposta biológica local e sistémica, assim como a apreciação das propriedades mecânicas dos materiais em função. Não obstante, deve ser considerado o facto de que estes modelos são apenas aproximações mais ou menos fidedignas das condições fisio-patológicas humanas, pelo que cada modelo tem vantagens e limitações inerentes.

Neste trabalho, procedeu-se à caracterização dos processos de citocompatibilidade geral e específica de diversos materiais de regeneração óssea, utilizando para isso vários modelos de culturas celulares. Os estudos realizados incluíram a avaliação da adesão, proliferação e diferenciação das populações celulares na superfície de materiais cerâmicos à base de fosfatos de cálcio e de silício, biovidros, compósitos, e cerâmicos com modificações da superfície. Foram utilizadas diferentes populações celulares, nomeadamente, linhas celulares de origem fibroblástica e osteoblástica, culturas primárias ou culturas de passagens iniciais de fibroblastos, osteoblastos e células endoteliais humanas. Adicionalmente, a problemática da avaliação *in vivo* do processo de biocompatibilidade foi também considerada, no âmbito da utilização do modelo da calote craniana de roedores, na avaliação do processo de regeneração óssea.

O desenvolvimento de novos materiais que visam a utilização clínica em intervenções relacionadas com o processo de regeneração óssea é cada vez mais sofisticado, em termos de *design* e metodologias de fabrico. Do ponto de vista biológico, os recentes avanços tecnológicos têm permitido o desenvolvimento de novas ferramentas de investigação, bem como um melhor conhecimento dos mecanismos envolvidos na interacção célula-biomaterial, durante o processo regenerativo. O maior desafio deste paradigma, que emergiu da perspectiva sinergética e multidisciplinar dos biomateriais e estratégias da medicina regenerativa, é o aumento exponencial de hipóteses que necessitam de ser testadas e validadas por metodologias adequadas e eficazes. As técnicas de caracterização biológica, *in vitro* e *in vivo*, permitem assim a definição de critérios básicos de biosegurança subjacentes à utilização dos biomateriais em ensaios clínicos.

Aim and structure

The present thesis aims to compile a significant part of the research work in which I have been involved as a researcher of the Laboratory of Pharmacology and Cellular Biocompatibility of the Faculty of Dental Medicine, University of Porto, since 2005.

In the past years I was given the opportunity to develop collaborative work with several multidisciplinary research teams that approach the bone tissue regeneration process in different ways. All these projects were developed within the range of action of the Laboratory of Pharmacology and Cellular Biocompatibility, directed and supervised by Professor Maria Helena Fernandes, which is broadly centred in bone metabolism and regeneration, reaching hand of *in vitro* and *in vivo* methodological approaches.

Overall, the developed work aimed to contribute to a deeper understanding of the metabolic regulation of the bone regeneration process and the differentiation pathways of cells with an active role on the bone metabolism. Furthermore, a significant effort was also put on the assessment of the cytocompatibility and biocompatibility of newly developed or modified materials for bone tissue application and prospective bone tissue engineering strategies. A collaborative research endeavour has been developed with other academic and industrial institutions that have been responsible for the conception and production of materials, ranging from calcium phosphate and silicon-based ceramics, to glass-substituted materials, composites and film-deposited constructs. Close collaborations were established with FEUP - Faculty of Engineering, University of Porto; CICECO – Centre for Research in Ceramics & Composite Materials, University of Aveiro; DEM – Department of Mechanical Engineering, University of Minho; IST - Instituto Superior Técnico, Technical University of Lisbon, within the range of national funded research projects by FCT – Fundação para a Ciência e Tecnologia and, more recently, in a European covenant supported by the European Micro and Nano Technology program. Within the established partnerships, Laboratory of Pharmacology and Cellular Biocompatibility has been held responsible for the assessment of the biological characterization of developed materials broadly relying on *in vitro* testing with established cell culture models, which further contributed to improve materials' properties, based on data ascertained during the biological tests.

More recently, efforts have been directed into the establishment of reliable animal models of the bone regeneration process. Accordingly, specific post-graduation formation has been enrolled in order to develop specific competencies in Laboratory

Animals research. In 2007, the enrolment in the post-graduation course "Laboratory Animals Science", organized by the University of Porto, granted the accreditation by the National Veterinary Council as a Coordinator Researcher for animal experimentation (according to the Federation of European Laboratory Animal Science Associations, FELASA, category C guidelines). Later on, in 2009, the enrolment in the Master Program in Laboratory Animal Science and Welfare of the Autonomous University of Barcelona – which grants the FELASA category D affiliation as a Laboratory Animal Science Specialist – was also conducted and is currently under way. Meantime, Laboratory Animal research has been developed in close collaboration with several research centres, namely UC - University of Coimbra, and UTAD - University of Trás-os-Montes and Alto Douro, which account for accredited researchers and infrastructures for the establishment of experimental research with laboratory animals, according to the National Veterinary Council.

In a methodological approach, this thesis presents several stages of the biological characterization process of biomaterials, namely regarding cytocompatibility and biocompatibility analysis, aiming the potential clinical application of the developed constructs. A wide range of *in vitro* methodologies, using several human cell populations, namely cell lines of fibroblastic and osteoblastic origin, as well as normal primary and early subcultured osteoblasts and endothelial cells are portrayed in detail, as included in the assessment of the biological performance of candidate materials. Thus, this thesis is composed of eleven chapters. In chapter 1, a generally overview of the literature is conducted and focused on bone biology, bone grafts and cytotoxicity/biocompatibility assessment of materials for bone tissue regeneration. In chapters 2 to 9, several published papers in international referred journals are presented, describing a wide range of methodologies used for the *in vitro* evaluation of materials for bone regeneration. Chapter 10 presents a paper recently accepted for publication which critically appraises the use of the calvaria defect model in rodents, for the assessment of bone regeneration strategies. The last chapter, chapter 11, presents the broad concluding remarks, summarizing the most relevant considerations regarding the biological characterization of candidate materials aiming clinical application in bone tissue regeneration strategies.

Foreword

In the past half century, an explosive growth concerning the clinical use of medical implants has been witnessed by clinicians, patients and industry. Orthopaedic, cardiac, plastic and oral maxillofacial/dental surgeons are a small example of the medical specialities in which implantable devices, such as pacemakers, artificial joints, oral implants, synthetic cardiac valves, etc. are used in millions of patients every year. The economic burden of treating diseases and problems, directly or indirectly related to the loss of tissue function has been estimated to exceed US$39 billion in the USA alone [1]. Additionally, the chief challenges of population aging and the increase in life expectancy, now substantiates that tissues and organs may be forced into function longer than they may be able to independently withstand.

In order to deal with these concepts, and in cases where pharmacological treatments alone have been reported to be scarce, the gold standard approach has been the shifting of tissues from healthy anatomical locations into diseased areas, or the transplantation of living tissues or organs from other individuals [2]. Despite the satisfactory biological results in short to medium term, the donor site morbidity and the shortage of compatible donors moved forward early research into replacing stylish tissue and organ transplantation with artificially-produced substitutes. To date, tens of millions of individuals worldwide have the quality of their life enhanced for as long as 25 years, by the implantation of developed products [3]. Nonetheless, far from being reliable long-standing replacements, early devices behave as temporary devices for critically-ill patients, waiting for a more definitive alternative, while more recently developed substitutes report improved biofunctionality. Even so, the established question of how to solve the tissue/organ transplantation problems and limitations remained unanswered.

The absence of an adequate biological response by the use of biomaterials alone has been attributed to the poor responsiveness, flexibility and reactivity within the direct contact with tissues and/or organs. Material scientists alone are not able to solve the complex and intricate biological puzzle as the developing biomaterials, by definition, aim to interact with and function within living entities. The current strategy to develop smart biomaterials relies in their capacity to instruct biological entities to directly or indirectly regenerate the damaged tissues. The visionary of this strategy was Larry Hench, in the late 1960s; horrified by the multiple limb amputations of thousands of Vietnam war survivors, he aimed to produce biomaterials "to repair people, instead of making materials to destroy them" [4]. In this respect, he hypothesized that an implant, which was composed of calcium and phosphate at a proportion similar to the one of the

bone tissue would not be rejected by the organism – indeed Hench verified a direct bonding with the host bone tissue following the implantation of the material developed by himself (Bioglass®) [5].

Until now, calcium phosphate-based materials are relatively "old" but their ability to trigger bone formation in biological systems continues to be unmatched by more recently developed approaches. However, "classic" calcium phosphates are not able to support or substitute bone biomechanical demands, showing the yet unmet goal of developing a synthetic substitute that could account for the complete substitution, and simultaneously regeneration of a damaged or lost tissue.

Current strategies still follow the premises of Hench and aim to create synthetic systems with adequate responsiveness towards the biological milieu. In order to do so, the scrutiny of the detailed mechanisms occurring at organs and tissues, and specially at biomaterials interfaces – at molecular, cellular and macroscopic level – continues, aiming to point out the essential phenomena that can dictate the understanding and modulation of the processes occurring at these systems. The knowledge of these mechanisms is essential to develop synthetic substitutes that are able to heal and report long-term function within the implanted organism. In a natural way, the biomaterials field is shifting towards the development of biologically active materials, as a way to progress in performance and clinical usage. Complementary approaches have combined synthetic biomaterials with cells and/or biological modulators, i.e. in a tissue engineering approach, to render tissues with enhanced capacity to play their expected biological role [6].

References

1. Tissue Engineering and Cell Transplantation: Technologies, Opportunities and Evolving Markets. Medtech Insight. 2007.

2. Lalan S, Pomerantseva I, Vacanti J. Tissue engineering and its potential impact on surgery. World J Surg 2001;25:1458-1466.

3. Hench L, Polak J. Third-generation biomedical materials. Science 2002;8:1014-1017.

4. Hench L. Ethical Issues. In: Hench L, Wilson J, editors. An Introduction to Bioceramics. Singapore: World Scientific, 1993.

5. Hench L, Paschall H. Direct chemical bond of bioactive glass-ceramic materials to bone and muscle. J Biomed Mater Res 1973;7:25-42.

6. Burg K, Porter S, Kellam J. Biomaterial developments for bone tissue engineering. Biomaterials 2000;21:2347-2359.

Chapter 1

Literature Overview

Bone tissue

In the early times, around some 540 million years ago, and within a timeframe of a few million years, the evolutionary pathway lead a massive amount of multicellular organisms to begin the production of mineralized structures that were rapidly widespread among beings of higher complexity, like molluscs, echinoderms, plants and vertebrates. The mineralized structures were developed in order to fulfill specific functions. For instance, among vertebrates, apart from the negligible amount of magnetite minerals found in human brain that seem responsible for orientation, navigation and homing skills, apatitic calcium phosphate minerals are the main body's mineral component [1]. They are generally present on hard tissues such as bone and teeth, whose major functions include structural protection, motion, support and mastication.

The bone tissue is a specialized form of connective tissue that functions both as a tissue and an organ system, being the component of the skeleton that is committed with the protection, support and motion of the entire organism. Its high flexibility and elasticity allows for the protection of vital organs, e.g. skeletal components of the rib cage and vertebrae protect the heart, lungs and other organs and/or tissues in the thoracic cavity. The stiffness of the bone tissue also contributes to the maintenance of the structural support and mechanical action of muscles and tendons, which are broadly responsible for movement. At the cellular level, the bone tissue is a productive and metabolic active biological entity, i.e. the bone marrow lies within the trabeculae of the cancellous bone and is committed with cell proliferation and differentiation, including the hematopoietic process. The importance of bone becomes clearer in the case of bone-related diseases such as *osteogenesis imperfecta*, osteoarthritis, osteomyelitis, and osteoporosis in which the adequate physiological performance of the bone tissue is not attained. These diseases, along with traumatic injury, orthopaedic surgeries, and primary tumour resection lead to or induce the establishment of bone defects or voids. Nowadays, the clinical and economic impact of treatment of bone defects is astounding [2].

Structural and organizational composition

Structure, physicochemical and biomechanical properties

Bone is a complex organ which plays a wide variety of functions within human physiology. In its composition several tissues may be found: mineralized osseous tissue, marrow, endosteum and periosteum, nerves and blood vessels and, in close association, cartilage. The properties of hard tissues, namely in which regards to shape

and macrostructure, can be highly determined by genetic, metabolic and mechanical factors. For instance, flat bones, such as the scapula, function as anchors of large muscular masses, while, hollow and thick-walled long bones, such as the femur or the humerus, basically support weigh [3]. Either way, all bones consist of a basic twofold structure, for which its importance is highly correlated with its function. An external layer (cortical) of smooth, dense (of around 1.80 g/cm^3), and continuous tissue covers the bone; while on the interior, the bone reports a cancellous structure, highly porous (around 75-95%), and with a mean density of 0.2 g/cm^3.

Cortical bone consists of closely packed osteons or haversian systems. These osteons consist of a central canal (harversian or osteonic canal) that is surrounded by concentric lamellae of matrix. Between the concentric rings of matrix, bone cells (osteocytes) are located deep in distributed lacunae, while small channels (canaliculi) radiate from these lacunae into the harversian canal, which in turn can anastomose with obliquely oriented vascular branches (Volkmann's canals) that establish communication between the periosteum and the endosteum [4]. Osteons are closely packed in cortical bone and the harversian channel contains blood vessels parallel to the long axis of the bone – these vessels interconnect with vessels located on the surface of the bone [4].

Cancellous bone is less dense and is composed of plates (trabeculae) and struts of bone adjacent to small, irregular cavities that home the bone marrow. These calcified trabeculae are composed of irregular osteon fragments and are not generally penetrated by large blood vessels; in fact, canaliculi connect to adjacent marrow cavities – instead of the central harversian canal – to receive blood supply. Trabecular organization may appear arranged in a random manner but a meticulous organization follows the lines of stress and can realign if the direction of stress changes – providing the maximum strength – and a quick response to changes in mechanical loading and unloading [4].

The representation of the structural organization of cortical and cancellous bone is depicted on Figure 1.
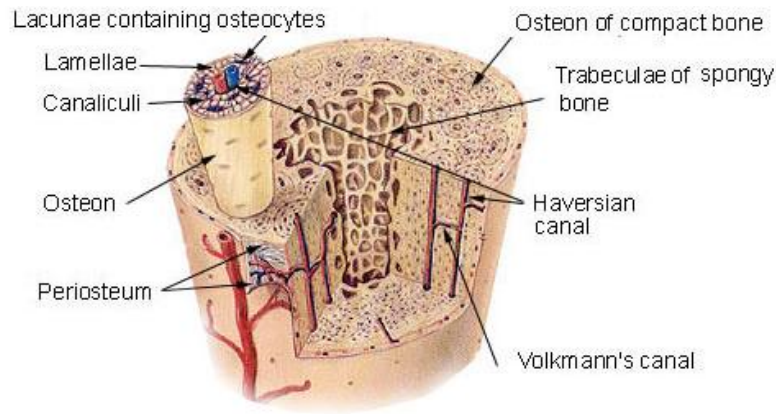
Figure 1 - Schematic representation of the structure of cortical and cancellous bone [5].

Cortical and cancellous bone can include, in their composition, either woven or lamellar bone. Woven bone (primary bone) is broadly found during the embryonic stage of bone development and is later resorbed and replaced by lamellar bone (secondary bone). Woven bone can also be found in epiphysial plates, ear ossicles, during fracture healing processes and the closure of cranial sutures. Comparing to the lamellar bone, woven bone has a higher metabolic rate, which substantiates an increased turnover during the remodelling phase. From a structural point of view, woven bone has a scattered and irregular display while lamellar bone is characterized by a highly and ordered arrangement whereas the cells are broadly uniform in size, shape and orientation [4].

The mechanical properties of bone patch up high stiffness and elasticity, in a way that has not been achieved in any other synthetic material. Cortical bone presents a tensile strength in the range of 75-150 MPa and a yield strength of 130-225 MPa in compression, in longitudinal direction; in the transverse axis, bone has a yield strength of 50-60 MPa in tension and 100-130 MPa in compression [6]. Estimates of the elastic module of the bone tissue are within the order of 15-20 GPa in longitudinal direction, and 5-15 GPa in the transversal direction [6]. These outstanding properties are the result of an intricate milieu of bone's microstructure, in which the organic matrix is complexly combined with mineral crystals of calcium phosphate-based apatite. These crystals are usually oriented in the longitudinal direction of the bone, contributing to the higher strength and stiffness in the longitudinal axis [7]. Cancellous bone is more isotropic and soft, and its mechanical properties vary widely and seem to be a function of the apparent density/porosity of the trabeculae. The strength and modulus of cancellous bone vary roughly as the square of the apparent density. Cancellous bone is highly viscoelastic and midrange values of the strength range between 5-10 MPa and the modulus ranges between 50-100 MPa [6].

Bone extracellular matrix

The overall extracellular structure of the bone tissue comprises around 90% of its volume, with only the remaining 10% being formed by the cellular component. By weight, the bone tissue is constituted of approximately 60% mineral content, 30% organic content (in which 90% represents collagenous proteins and the remaining 10% include proteoglycans and other non-collagenous proteins) and 10% water.
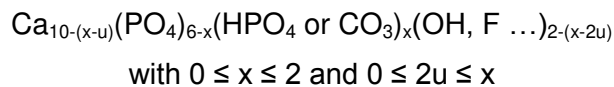
Collagen molecules are structurally assembled by tropocollagen, the small subunit of larger aggregates such as fibrils. It is approximately 300 nm long and 1.5 nm in diameter, made up of three polypeptide strands (α-chains), each possessing the conformation of a left-handed helix [8]. These helices are twisted together into a right-handed coiled coil, a triple helix, a cooperative quaternary structure stabilized by numerous hydrogen bonds. In fibrilar collagens, like collagen type I – by far the most abundant in the bone tissue, nevertheless types V, VI, VIII and XII are also present in small amounts - triple-helixes associate into a right-handed super-super-coil that is referred to as the collagen microfibril [8, 9]. Each microfibril is interdigitated with its neighbouring microfibrils to a degree that might suggest that they are individually unstable although within fibrilar organization they are so well ordered as to be crystalline. Larger fibrillar bundles are formed with the aid of several different classes of proteins, glycoproteins and proteoglycans to form the different types of mature tissues. Collagen fibrils/aggregates are arranged in different combinations and concentrations in various tissues, in order to provide a diverse range of tissue properties. In the bone tissue, entire collagen triple helices lie in a parallel, staggered array. Existing gaps of approximately 40 nm between the ends of the tropocollagen subunits probably serve as nucleation sites for the biomineralization process in which occurs the deposition of long, hard and fine crystals of hydroxyapatite [8, 9].

Several non-collagenous proteins can also be found among the extracellular organic component. Among the several, osteopontin (or bone sialoprotein-1, BSP-1), bone sialoprotein-2 (BSP-2), osteocalcin and osteonectin play an important role [10]. Their exact biological role is far from completely fulfilled but several functions have already been adequately established, e.g. osteopontin has RGD sequences that facilitate cell attachment and cell signalling pathways that seem particularly relevant during osteoclasts anchorage to the mineral matrix of bones [11]; bone sialoprotein-2 may act as a nucleation site for the initial apatite crystals and, following, as the apatite forms along the collagen fibres within the extracellular matrix, BSP-2 could then help direct, redirect or inhibit the crystal growth [12]; osteocalcin is a vitamin k-dependent protein and is exclusively produced by osteoblasts – it seems to play a role in hydroxyapatite crystals' nucleation and modulate osteoclasts migration [13];

osteonectin seems to contribute to the initiation of the mineralization and promotes mineral crystal formation by expressing several calcium and collagen binding locations [10].

Bone matrix also contains proteoglycans (e.g., decorin and biglycan) whose exact role is currently being investigated. These proteoglycans seem to play an important role in cell behaviour by blocking adhesion motifs from RGD-containing molecules and also by actively modulate collagen fibrillogenesis [14]. Bone proteoglycans also display selective patterns of reactivity with several bone constituents including cytokines and growth factors, namely transforming growth factor-beta or osteoprotegerin, thereby modulating their bio-availability and biological activity in the bone tissue [14]. Bone's extracellular matrix also contains glycoproteins, which play a distinctive role in cell signalling. Particular examples include fibronectin and vitronectin which contain the integrin-binding peptide motif RGD [15].

The inorganic component of the extracellular matrix plays an important role in the strengthening of the tissue and in ion storing. The chemical structure of human biological apatite can be represented as follows:

$$Ca_{10-(x-u)}(PO_4)_{6-x}(HPO_4 \text{ or } CO_3)_x(OH, F \ldots)_{2-(x-2u)}$$
$$\text{with } 0 \leq x \leq 2 \text{ and } 0 \leq 2u \leq x$$

in which (x-u) cationic vacancies and (x-2u) monovalent anionic vacancies coexist [16].

In the hard tissues, nucleation of the mineral component generally begins in the nanopores of the collagen fibrils – as the microenvironment is supersaturated in calcium and phosphate ionic species [17]. The process begins in a heterogeneous way and is catalyzed by the presence of phosphate esters and carboxylate groups at the surface of the collagen fibrils. The nucleation process is thoroughly developed until it embraces the entire collagenous network. The apatitic crystals are quite irregular in shape and formed of thin plates within the range of 20 – 1100 Å [18]. Due to the high surface area of crystallized minerals, an intimate contact with the extracellular fluids is established and allows a rapid ion exchange with these fluids – bone acts as a calcium and phosphor reservoir for the body metabolism [19]. A schematic representation of the interaction of apatitic crystals and collagen fibrils is presented on Figure 2.
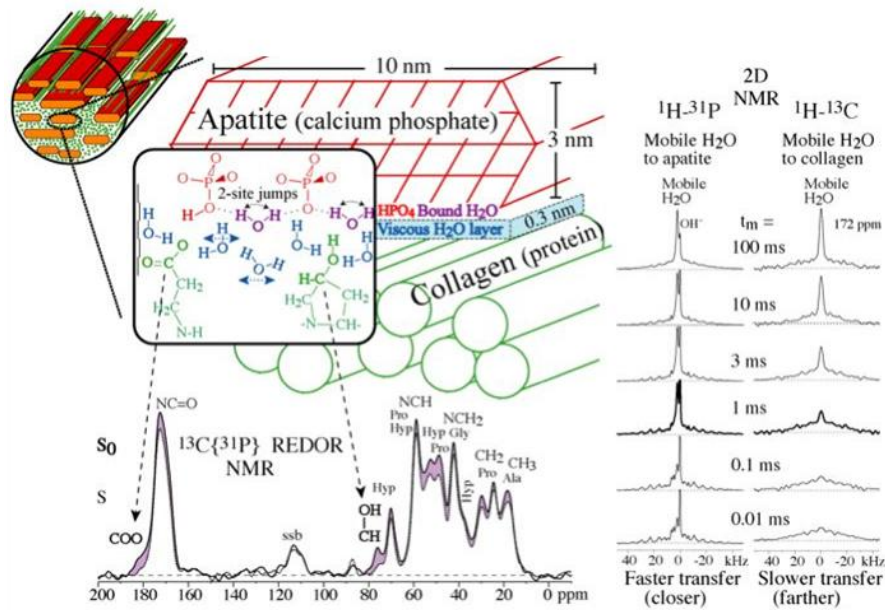
Figure 2 – Schematic representation of the apatite-collagen interface in the bone tissue [20].

Recent nuclear magnetic resonance (NMR) experiments have provided detailed information on the nanocrystal composition and thickness, the apatite surface composition, water layers at the apatite-collagen interface, and apatite-binding sites of collagen [21]. As reported, the carboxylic groups of most glutamates and around a quarter of the C-OH moieties of hydroxyprolines, in collagen fibrils, are near the interface, at a ~0.5 nm distance from phosphorus in apatite. A layer of viscous H_2O detected at the organic-inorganic interface may act as "glue" between apatite and collagen, providing continuous bonding. This view is supported by large-amplitude motions of the interfacial C-OH groups of hydroxyprolines, which make their specific binding to apatite surface sites unlikely [21, 22].

Cellular components

The skeletal tissue is, in essence, composed of five cellular elements: osteoprogenitor cells, osteoblasts, osteocytes, osteoclasts and bone lining cells. Cell populations can also be classified according to their biological origin and thus, osteoprogenitor cells, osteoblasts, osteocytes and bone lining cells are originated from mesenchymal cells, while osteoclasts are originated from hematopoietic progenitors.

Osteoprogenitor cells

Within the osteogenic commitment, mesenchymal stem cells sustain the differentiation cascade that generally trails the following sequence: mesenchymal stem cell → immature osteoprogenitor → mature osteoprogenitor → pre-osteoblast →

mature osteoblast → osteocyte or lining cell. The later on the differentiation phase, the reduced capacity for self renewal and proliferation [23].

Mesenchymal stem cells, in contrast with differentiated osteoblasts or osteocytes are migratory and highly proliferative in nature and have a greater differentiation potential. Immunofenotipically they are characterized by being uniformly positive for SH2, SH3, CD29, CD44, CD71, CD90, CD106, CD120a, CD124 [24]. These cells are able to migrate in a substrate or on blood flow by generating cycles of weak adhesion, traction, movement and detachment. At the end of the migration stage, progenitor cells adhere to the final targeted location by developing strong focal adhesion in order to proceed with the differentiation phase [24]. *In vitro* and *in vivo* reports have shown the capability of these cells to contribute to the regeneration of mesenchymal tissues such as bone, cartilage, muscle, ligament, tendon, fat, and stroma [24, 25]. Differentiation pathways of mesenchymal stem cells along several lineages are presented on Figure 3.

Inductive agents that cause the entrance into and progression along individual lineages such as bone, cartilage, fat and muscle, are known; nonetheless the molecular details that govern regulation of each lineage pathway continue to be active areas of research.
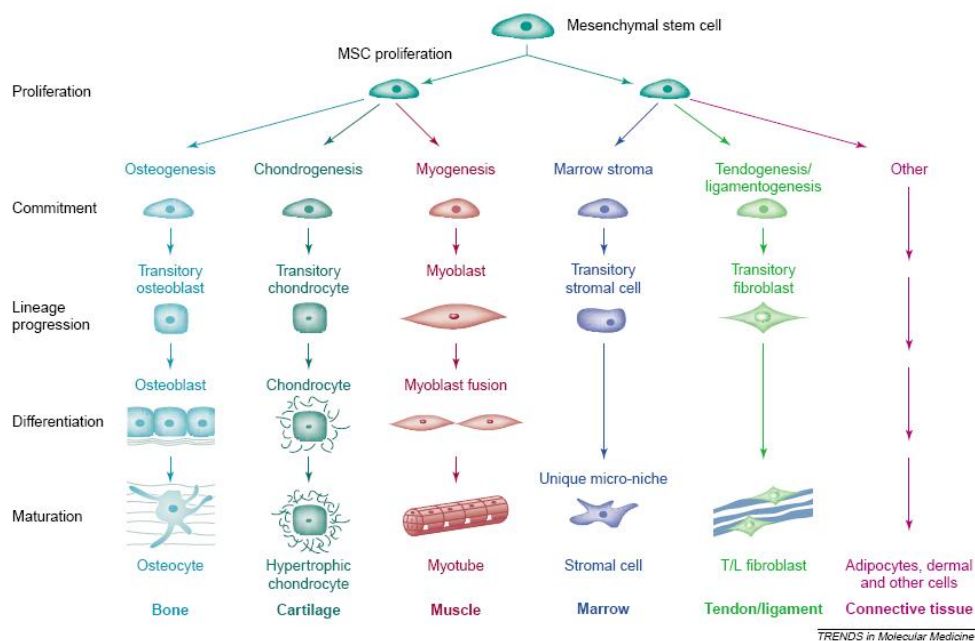

Figure 3 - Schematic representation of the stepwise cellular transitions from the putative mesenchymal stem cell (MSC) to highly differentiated phenotypes. Individual lineage pathways are arranged from the best comprehended (left) to the least comprehended (right). This simplified scheme does not represent all the transitions and complexities of each individual lineage, neither the potential interrelationships of cells moving between different pathways (plasticity) [26].

Osteoblasts, osteocytes and bone lining cells

Osteoblasts are highly differentiated, non-migratory cells that differ significantly depending on their stage of development – from which their function and phenotype varies and can be divided in several classes, as follows.

a) Osteocytes – these cells comprise more than 90% of the bone cells in adult skeleton [27]. Young osteocytes result from the embedment of mature osteoblasts within the non-mineralized bone matrix and share many characteristics with these cells [27]. As osteocytes mature, and more matrix is deposited and mineralized, these cells become smaller by cytoplasmic loss, and trapped in a small lacuna of 1-2 μm wide, around the cell. The lacunae have collagen fibrils in their composition, which support osteocytes cytoplasmic processes that establish a wide network of intracellular contact via canaliculi. This complex network, apart from being responsible for cell-mediated exchange of minerals, is believed to sense mechanical deformation that modulates bone formation or resorption, at a given site [27, 28]. During the resorptive phase, osteocytes are processed along with the extracellular matrix by osteoclasts. Osteocytes are non-mitotic cells and their turnover is only achieved during the remodelling process of the bone tissue.

b) Bone lining cells – these cells can be found along bone surfaces that undergo neither *de novo* bone formation nor resorption. They are elongated and compactly associated by tight junctions or cytoplasmic extensions which also connect them to osteocytes. They are metabolically less active than osteoblasts and though present fewer cytoplasmic organelles. The biological role of these cells has been a centre of interesting debate in the literature. Some authors support that, in the presence of parathyroid hormone, these cells secrete enzymes that are responsible for the removal of osteoid, preparing the matrix for osteoclastic activity [29]; others, substantiate that bone lining cells may be activated and enrol osteoblast-like functions [30].

c) Inactive osteoblasts – these are elongated cells, morphologically undistinguishable from bone lining cells. During bone forming activity, only active osteoblasts and their precursors seem to contribute to tissue production [31].

A schematic representation of osteoblasts functional activity within matrix production and mineralization is shown in Figure 4.
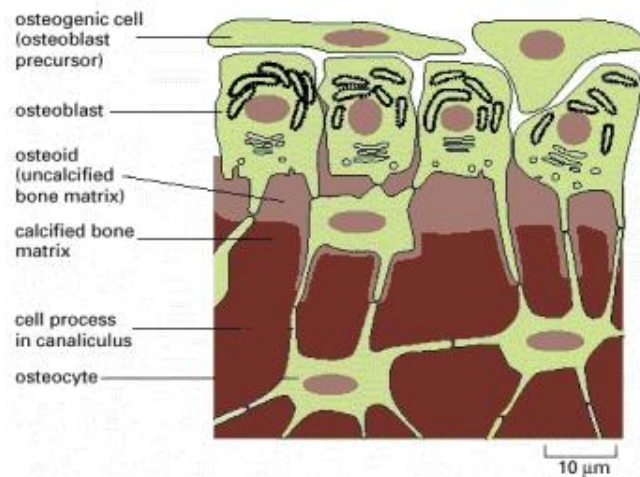
Figure 4 – Schematic representation of the deposition of bone matrix by osteoblasts apatite-collagen interface in the bone tissue [32].

Osteoclasts

Osteoclasts are giant multinucleated cells that derive from the fusion of several hematopoietic precursor cells that differentiate along the monocyte/macrophage lineage. They can be found along bone surfaces undergoing resorption and present a high mobility profile [33]. Osteoclasts regulate bone resorption process by acidification of their microenvironment – which leads to the dissolution of the mineral component – and is followed by an enzymatic degradation of the demineralised extracellular matrix [33, 34]. The mature cell is characterized for having 3 to 20 nuclei that tend to be oval and concentrated mid-cell. There are numerous mitochondria and lysossomal compartments but reduced endoplasmic reticulum, which contribute to the appearance of a foamy cytoplasm [33, 34]. The apical pole attaches to the bone matrix by the formation of a tight ring-zone of adhesion, known as the sealing zone, location where the resorptive actions take place. Integrins αvß3 of the osteoclasts cell membrane interact with RGD-containing proteins, initiating signals that lead to insertion, into the plasma membrane, of lysossomal vesicles that contain cathepsin K. Consequently, the cells generate a ruffled border above the resorption lacuna, into which is secreted hydrochloric acid and acidic proteases, such as cathepsin K. The acid is generated by the combined actions of a vacuolar H^+ ATPase, its coupled Cl^- channel, and a basolateral chloride–bicarbonate exchanger. Carbonic anhydrase converts CO_2 and H_2O into H^+ and HCO^{3-}. Solubilised mineral components are released when the cell migrates; organic degradation products are partially similarly released and partially transcytosed to the basolateral surface [33, 34]. A schematic representation of osteoclast structure and function is shown in Figure 5.
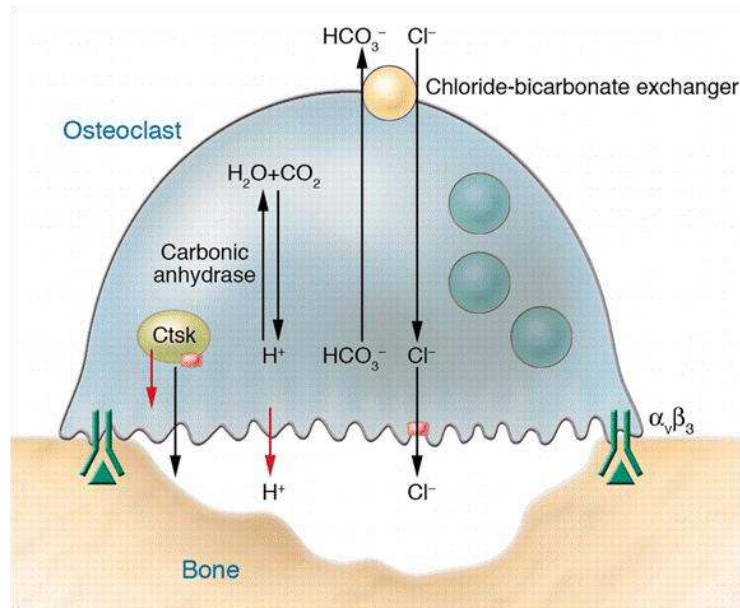
Figure 5 – Schematic representation of the mechanism of osteoclastic bone resorption [35]. Ctsk - cathepsin K.

Bone remodelling

Bone is a highly vascular, living and dynamic tissue, which is remarkable for its hardness and self regenerative capacity. In its extracellular mineralized matrix, bone embeds osteocytes that constitute the major cell type in the mature tissue. Vascular canals ramify and establish a dynamic network within bone, providing the living cells with the needed metabolic support.

Unlike other hard tissues, like enamel or dentin, bone is a very dynamic tissue and thus, following the initial ossification process of the embryonic skeleton, osteoclasts and osteoblasts begin modelling and remodelling processes that generally occur simultaneously. Modelling is generally concerned with changes in shape while remodelling deals with bone turnover without shape modification. During skeletal growth, removal and replacement of the bone tissue proceeds at a rapid pace – in the first year of life the rate of turnover of the skeleton approaches 100% per year, decreasing to about 10% in the late childhood, and usually continues at this rate or more slowly throughout life [36]. After completion of skeletal growth, bone turnover is mainly completed through remodelling. This physiological process occurs without affecting the shape or density of the bone, through an organized sequence of events that include osteoclast activation, resorption of the bone tissue, the reversal phase and formation of cement line, osteoblasts activation, and formation of new bone at the same anatomical location (Figure 6). The remodelling patterns vary with age, associated disease and environmental conditions [36].

The particularities of the remodelling and modelling processes are very intricate and still not fully understood, but one of the key mechanisms by which osteoblasts work in concern with osteoclasts is well established and following summarized. Differentiated osteoblasts express a transmembranar protein, receptor activator of NF-κB ligand (RANKL), which binds to its receptor RANK on osteoclasts membrane. Osteoblasts can downregulate osteoclasts activity through the expression of a transmembranar decoy receptor, osteoprotegerin (OPG), which inhibits osteoclast binding. Hormonal control can promote osteoclast activity through the elevation of RANKL expression. RANK-RANKL interaction not only activates a variety of downstream signalling pathways required for osteoclast development, but crosstalk with other signalling pathways that also fine-tune bone homeostasis both in physiological and pathological conditions [37].
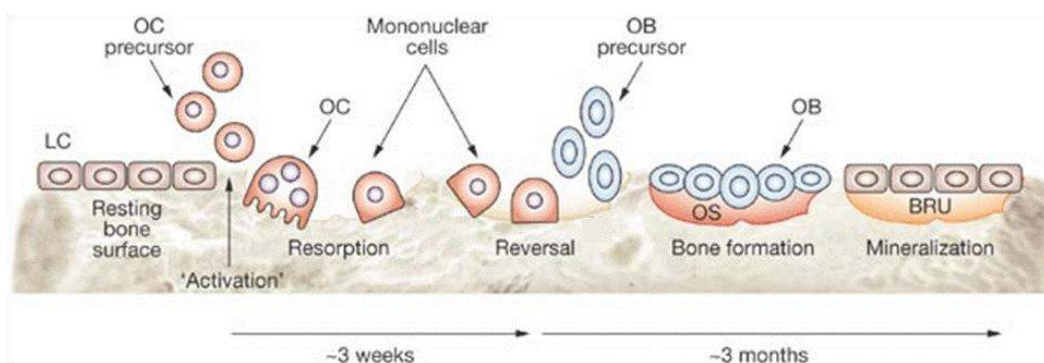

Figure 6 – Schematic representation of the sequence of bone remodeling in healthy individuals [38]. LC – bone lining cells; OC – osteoclasts; OB – osteoblasts; OS – osteoid; BRU – bone remodeling unit.

Regulators of bone metabolism

The source of the signalization process that determines bone modelling and remodelling relates to three broad functions of the skeletal tissue, i.e. homeostasis, haematopoiesis and mechanical, but not with the forth function, protection. Homeostasis in the skeleton is broadly concerned with the regulation of calcium and phosphate levels. Calcium plasma concentration averages about 9.4 mg/dL (generally between 9.0 and 10.0 mg/dL) whereas phosphate is present in two anionic forms – divalent and univalent anions – at concentration levels of 1.05 mmol/L and 0.26 mmol/L, respectively [39]. The titration of a regulated calcium concentration is achieved through feedback loops in which the liver, the kidney, 1,25-dihydroxy vitamin D_3 and parathyroid hormone (PTH) participate, as well as with the intestinal epithelium – where calcium is reabsorbed via the interaction with a calcium binding protein [39]. Phosphate

is a threshold ion, regulated by the kidney, where increased secretion occurs with the boost of PTH expression [39].

In response to homeostatic demands, cells of the basic remodelling unit (BRU) – the multitude of cell phenotypes responsible for remodelling a specific anatomical location – can be sensitized by 1,25-dihydroxy vitamin D_3, calcitonin, glucocorticoids, estrogen, androgen, PTH, growth hormone, and thyroid hormones [36]. PTH and 1,25-dihydroxy vitamin D_3 stimulate resorptive processes and are countered by calcitonin, which inhibits resorption – nonetheless, interactive mechanisms are still not completely understood. Overall, the key systemic signal for bone is estrogen, as a decline in this hormone causes resorption to outstrip formation, bone mass falls, converging to a clinical diagnostic of osteoporosis [40]. Estrogen is synthesized from testosterone and, with the advance of age, an increased level of PTH and a decrease in estrogen may evoke the increased expression of pro-inflammatory cytokines such as IL-1, IL-6, TNF-a and RANKL [40]. Estrogen depletion induces the apoptosis of osteocytes and can cause bone loss [41].

Local humoral regulators of the bone metabolism seem to include bone morphogenic proteins (BMPs), fibroblastic growth factor, insulin-like growth factor, transforming growth factor-β and platelet-derived growth factor, for formation, and granulocyte macrophage colony-stimulating factor and interleukins -1, -4, -6, -11, -13, -18 and macrophage colony-stimulating factor leading, for resorption [42]. Nonetheless, this dichotomy is not absolute and some controversies and contradictory data have been reported; for instance, transforming growth factor-β, in determined situations, can induce both formation and resorption. Among local factors, hematopoietic signals, namely cytokines and chemokines, secreted in response to local phenomenon – such as inflammation – can also influence bone homeostasis.

Osteoblasts also produce a fundamental enzyme, alkaline phosphatase (ALP), which is expressed in matrix vesicles also containing calcium and phosphorous. This enzyme is ubiquitous in bone, liver, kidney, intestine and placental tissues and seems to play a determinant role in the induction of hydroxyapatite deposition over extracellular matrix proteins. ALP facilitates the biomineralization process by hydrolyzing organic phosphate esters, thus producing an excess of free inorganic phosphate which initiates the biomineralization process [43]. Although ALP activity is an excellent local and systemic marker of osteodifferentiation and mineralization, the exact mechanism of action is still not fully understood.

Apart from the local and systemic determinants, cells must detect signals to elicit a biological response. Remodeling is thought to be initiated by the detection of the mechanical stress – the trigger is the deformation of bone due to load (fatigue-demand

bone deformation) [44]. The sensor for bone deformation is thought to include the osteocyte-bone lining cell complex but it is still unclear how messages are trafficked throughout the skeleton [45].

Bone grafts and bone Tissue Engineering

A bone graft is a tissue or material used to repair a defect or deficiency in contour and/or volume of the bone tissue. There is a wide range of opinions regarding what particulate materials should be employed in each clinical procedure, the rationale behind its aplication, the rationale for using combinations of materials, and the fractions of each material used [46]. The available options for clinical application in orthopaedic, trauma, maxillofacial and oral surgical interventions aim to restore the lost integrity and function of the skeletal system. The use of these materials in regenerative procedures is based on the assumption that they possess osteogenic potential (contain bone-forming cells), are osteoinductive (contain bone inducing substances), or simply are osteoconductive (provide a structure to guide bone formation). Overall, used grafts report fundamental biological and biomechanical functions that converge to establish an adequate framework for specific cell adhesion, proliferation and differentiation, that focus tissue healing.

General classification of clinically used bone grafts is established according to their origin. Thus, biological-derived grafts can be subdivided in autografts, if the grafted tissue is transplanted from one site to another within the same individual; isografts, if transferred from one monozygotic twin to another; allografts, if the grafted tissue is transferred between two genetically different individuals of the same species; and xenografts, if the grafted tissues is obtained from a donor of a different species. Moreover, synthetic grafts, also known as alloplastic materials, are non-biological in their origin and include a wide variety of prepared ceramic, metallic, polymeric and composite materials. Combination of more than one type of biological graft and/or alloplastic material is getting increasingly common.

Bone autografts

Currently, bone autografts remain as the gold standard treatment for bone-related clinical settings that require bone augmentation or regeneration procedures that are outshined by the boundary of physiological repair. Autograft bone reports the unique capacity to supply cells, biomodulators and a reliable matrix that supports cell adhesion and growth, as well as an adequate degradation profile. In fact, it provides optimal osteoconductive, osteoinductive and osteogenic properties, at the same time

that reports an established biosafety and prevention of immunologic rejection [47]. Clinical procedures includes the grafting of the bone tissue, either of cortical or cancellous structure, from the donor site of the patient, being the most frequently used donor site the iliac crest. Nonetheless, many other anatomical locations are being used, including intra-oral sites [48].

Harvesting of autologous bone, however, has several associated downsides as it lengthens the overall surgical procedure, outputs a limited amount of available material, and is commonly complicated by post-operative pain and aesthetical/functional disadvantages [49, 50]. Moreover, it may fail in clinical application as most of the osteogenic elements – the cellular component – may not survive the transplantation procedure [51]. Other potential complications associated with bone autografts are associated with the anatomical location, and may include haematoma formation, blood loss, vascular and nerve injury, hernia formation, infection, uretal injury, fracture, pelvic instability, aesthetical defects, tumour transplantation and chronic pain [52-54].

Bone allografts

The clinical use of allografts aimed to solve some of the limitations verified with the use of autograft materials, since they have become more and more available. In fact, more than one-third of the bone grafts used in North America are allografts [55]. Nonetheless, allograft bone reports more biological limitations in the essential bone graft characteristics described for autografts and yield more variable clinical results. Clinical studies have shown that allograft-based tissue reconstruction tends to incorporate and heal more slowly than with autografts, mainly due to the immunoresponse against histocompatibility antigens [56]. Apart from the risk of immunological intolerance that may converge to graft rejection, allografts carry the risk of disease transmission, namely of bacterial or viral origin [57].

The implementation of tissue processing aimed to allow off the shelf use and minimize the biological risk but, at the same time, induced significant changes that weakened the biological and biomechanical properties. Furthermore it is associated with an increase in cost production [58]. Accordingly, fresh allograft bone is practically out of use due to the inadequate time for disease screening. Allograft bone, either from cortical and cancellous origin, is generally prepared by demineralising, freeze or freeze-drying processes.

Demineralized bone matrix is produced by the acid extraction of allografts. The remaining biological material generally contains, following acid treatment, collagen type I, non-collagenous proteins and osteoinductive growth factors, mainly from the TGF-β

superfamily [59]. Several animal models have shown the plausibility of the osteoinductive effect of implanted demineralised bone matrix, as well as isolated case reports and uncontrolled retrospective reviews. Nevertheless, there is a generalized paucity of clinical studies with high evidence level [60, 61]. There are several bone matrix formulations, commercially available, based on developed refinements of the manufacturing process.

Frozen grafts are generally stored at temperatures below -60ºC, which aims to decrease the enzymatic degradation process and self immunological response. Freeze-drying technique is based on the removal of the water from the graft, following by packaging under vacuum – which allows storage at room temperature. Nevertheless, these grafts report a less vigorous host immunological response than that described for fresh or fresh-frozen grafts, mainly due to the destruction of cellular content – situation that also limites the osteoinductive capacity [62]. As for demineralised bone matrix, freeze and freeze-drying allografts can be produced in a diverse array of shapes and formats including powder, chips, wedges, pegs, dowels, struts, and can even be machined into specific components like rods or screws.

Sterility is a major issue in the clinical use of allografts, highlighting the conscious need for aseptic processing and careful donor screening. Tissue processing and sterilization aim to increase the biosafety of the graft, nevertheless the existing risk of transmission of viral infections – namely HIV and hepatitis B and C – bacterial infections, malignant diseases, systemic diseases (e.g. autoimmune diseases) and toxins [63]. Accordingly, a research report of the evaluation of candidate tissue for allograft banking reported a 8% prevalence of associated diseases – including malignant tumours – not previously diagnosed [64].

Bone xenografts

The clinical use of xenografts became increasingly popular in clinical application due to the wide availability and the possibility to be mixed with autografts or allografts, in order to augment graft quantity and modulate the eventual precocious resorption associated with the use of these materials [65].

Bone xenografts can be obtained from different origins but the most frequently available derive from mammalian bone (bovine, porcine and equine origin) and exoskeleton of corals. These grafts are considered to be biocompatible and osteoconductive. Nonetheless, safety issues, namely regarding the possibility of the development of immunological response against specific animal antigens and the development of bovine spongiform encephalopathy, following implantation of bovine-derived grafts, have been reported [66, 67].

Alloplastic biomaterials

Advances in the field of biomaterials and the limitations associated with the use of biological-derived grafts have directed attention toward the use of alloplastic graft materials in bone-related surgical interventions. An historical perspective shows that attempts to replace body parts, specifically hard tissues, dates back from centuries ago with the use of several synthetic materials. For instance, pre-Columbian civilizations used gold sheets to heal cranial cavities following trepanation, while Chinese reported the use of amalgam to repair decayed teeth in 659 AD. Many other attempts to create implantable materials have been carried out but generally lead to failure as a result of infection or lack of knowledge about toxicity of selected materials [68]. The safety in the use of materials to replace diseased body parts was only achieved with the practice of aseptic surgery at the end of the 19th century.

Early used materials included metals and non-degradable ceramics, due to their superior mechanical properties, namely regarding resistance to fatigue and high tensile strength [69]. In fact, until the 1960s, materials used to replace or substitute body parts were borrowed from industrial applications, and some of them are still used in clinical practice. Since the 1960s, a trend to develop specific materials for biomedical applications was established [68].

In spite of their composition or intended application, materials aiming to contact with living tissues must assemble both the aspects of biofunctionality and biocompatibility. The concept of biofunctionality concerns the capacity of the implanted material to perform the purpose for which it was designated. These requirements include: a) adequate mechanical properties, e.g. fatigue strength, elongation at fracture, fracture toughness, tensile strength, Young's module, etc.; b) adequate physical properties, such as the thermal expansion (in bone cements) and density (in bone implants); c) adequate surface chemistry, e.g. corrosion, oxidation, bone bonding ability, degradation resistance, etc. [68, 70]. Biocompatibility, on the other hand, is defined as the ability of a candidate biomaterial to perform its desired therapeutical function, without eliciting any undesirable local or systemic response, but engendering the most appropriate beneficial response in that specific situation [71].

Various types of synthetic materials have been developed in order to meet the terms of the proposed characteristics of biofuncionality and biocompatibility. General classification is established as follows: a) Metals – such as titanium, titanium alloys, stainless stell, cobalt-chromium alloys; b) Ceramics – such as aluminium oxide, carbon, calcium phosphates and glass-ceramics; c) Polymers – such as silicon, polymethyl methacrylate, polylactide, polyurethane, polyethylene; and d) Composites – such as

ceramic coatings on metal implants and ceramic-reinforced polymers. Commonly used materials and their application are depicted on Table 1.

The selection of one specific material over another will depend on the application and biological solicitations that need replacement. Regrettably, none of the described materials meets all the requirements for all desired applications. For instance, for load bearing applications, metals seem to be the only group of materials to meet the mechanical requirements. However, they have a limited capacity to establish a direct bond with bone tissue, comparing to other materials such as calcium phosphates, which have strong bone-bonding capacity but insufficient mechanical properties [72, 73].

Table 1 – Biomaterials clinically used for bone and related soft tissue repair. Adapted from [68, 74].

Composition	Type	Origin	Clinical applications	Main properties
Calcium phosphate, i.e. hydroxyapatite, tricalcium phosphate, etc.	Ceramic	Synthetic	Bone regeneration, non-loading sites, filler	Bone bonding, biodegradable, tunability of degradation
Alumina	Ceramic	Synthetic	Joint replacement	Good mechanical properties, non-bone bonding
Silica-based calcium phosphate	Glass ceramic	Synthetic	Bone regeneration, non-loading sites, filler	Bone bonding, biodegradable
Titanium and alloys	Metal	Synthetic	Bone replacement, load bearing sites	Bone connection in some cases, non-corrosive, resistance to fatigue
Stainless steel and Cobalt chrome alloys	Metal	Synthetic	Bone replacement, load bearing sites	Corrosive at long term
Polymethylmethacrylate	Polymer	Synthetic	Bone replacement, load bearing sites, filler	Non-degradable
Polyesthers, i.e. polylactide, polyglycolic acid, polycaprolactone	Polymer	Synthetic	Degradable bone fixation, filler, soft tissue suture	Tunability of degradation and mechanical properties
Ultra high molecular weight polyethylene	Polymer	Synthetic	Articular surfaces of orthopaedic prosthesis, load bearing sites	Lubricating properties
Polyethylene oxide, terephtalate, cobutylene terephtalate	Co-polymer	Synthetic	Cement stopper, filler	Tunability of degradation and mechanical properties,

				bioactivity
Polyphosphazene	Polymer	Synthetic	Drug delivery	Erosion/degradation favourable for long term implantation
Polyanhydride	Polymer	Synthetic	Drug delivery, tissue repair	Erosion/degradation favourable for long term implantation
Polyorthoesters	Polymer	Synthetic	Drug delivery, tissue repair	
Polyethyleneglycol	Polymer	Synthetic	Drug delivery, tissue repair	Water-based gel, degradable
Coral	Mineral	Natural	Bone filler	Similar composition to host bone
Bone	Composite mineral / organic	Natural	Bone filler	Similar composition to host bone
Demineralized bone matrix	Organic	Natural	Bone filler	Biodegradable, natural source of osteoinductive agents
Collagen	Organic	Natural	Hard and soft tissue repair	Biodegradable
Hyaluronic acid	Organic	Natural	Soft tissue repair	Biodegradable, water-based gel, injectable
Alginate	Organic	Natural	Soft tissue repair	Drug delivery capabilities, degradable
Agarose	Organic	Natural	Soft tissue repair	Drug delivery capabilities, degradable
Chitosan	Organic	Natural	Soft tissue repair	Biodegradable
Fibrin	Organic	Natural	Soft tissue repair	Sealing capacity

Tissue engineering applications and materials for tissue engineering

The recent years have witnessed a surge of creative ideas and technologies that induced a paradigm change in the problematic of tissue repair/regeneration, specifically within hard tissues regeneration. Accordingly, a new field of healthcare technology, substantiated by developments in basic and clinical sciences, have emerged and has now been referred as tissue engineering. The classic definition of tissue engineering has been established by Langer and Vacanti as "an interdisciplinary field that applies principles and methods of engineering and the life sciences towards

the development of biological substitutes that restore, maintain and improve the function of damage tissues and organs" [75].

The fundamentals of tissue engineering rely on the body's natural biological response to tissue damage in conjunction with engineering principles. The basic approach for bone tissue relies on the harvest and *ex vivo* expansion of selected cell populations – in the presence of adequate biomodulators - that are following seeded onto a scaffold where cell proliferation and/or differentiation events occur, previously to the surgical implantation into the defined bone defect (Figure 7).

As the role of cell signalling and subsequent functionality emerges with greater clarity, the quest for the ideal scaffold continues, specifically for one presenting a physicochemical biomimetic environment, while biodegrading as native tissue integrates and actively promotes or prevents desirable or undesirable physiological responses, respectively [76]. To address these biomimetic requirements, a bone scaffold for tissue engineering applications should [77]:

- provide temporary mechanical support to the affected anatomical location;
- allow for osteoid deposition;
- be highly porous in order to facilitate vascular and bone tissue ingrowth;
- facilitate the homing of osteoprogenitor cells;
- support and promote the osteogenic differentiation (osteoinduction);
- enhance cellular activity towards scaffold-tissue integration (osteointegration);
- degrade in a controlled and timely fashion in order to facilitate load transfer to de new developing tissue;
- generate non-toxic degradation products;
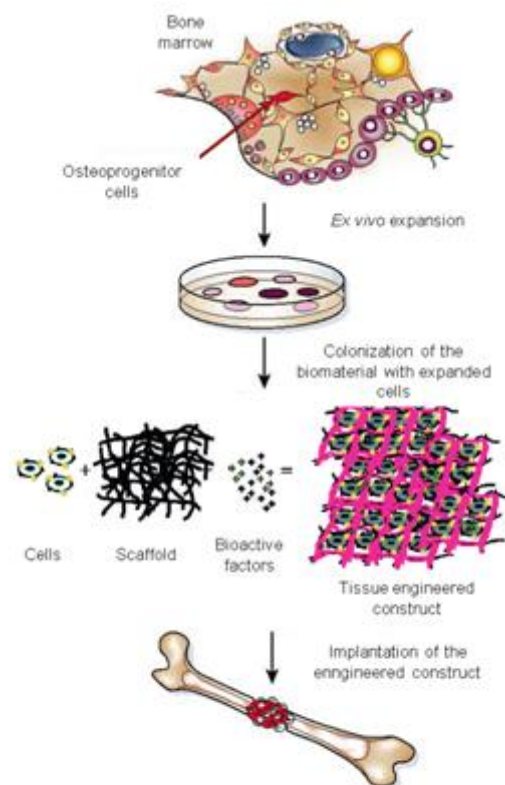- do not induce adverse biological reactions following implantations, e.g. chronic inflammatory response, foreign body reaction;

Figure 7 – Schematic representation of a tissue engineering approach for bone regeneration. Adapted from [78].

- be easily sterilizable without loss of biomechanical properties;

and

- allow the controlled release of bioactive molecules or drugs to facilitate tissue healing or prevent pathology establishment.

Materials aiming to be used in tissue engineering applications must adequately interact with cells and culture media *in vitro*, prior to their clinical implantation. Additionally, prepared scaffolds (solid porous structures) and matrices (gel-like structures) must assure the hostage of enough cells and support their viability for an adequate period of time [78].

Several natural-based materials have been assayed as potential sources of scaffolds/matrices for tissue engineering applications. Nonetheless they were able to support cell viability and in the adequate microenvironment, cell proliferation and differentiation, natural matrices such as hyaluronic acid, fibrin, alginate, chitosan and collagen seem to be unable to endure body's loading conditions although the attributed satisfactory biocompatibility [79]. Furthermore, in determined clinical applications, the defect borders may degrade if the defect is not filled with a material with mechanical properties similar to those of the host tissue [80] and, even more, some materials – namely esterified hyaluronic acid and fibrin – have sporadically demonstrated undesirable effects over the host tissue and its repair processes [81]. Natural minerals such as demineralized bone matrix, coral- and bovine bone-derived materials are also used in tissue engineering applications, providing efficient porosity and interconnectivity for cell growth and differentiation, as well as suitable mechanical properties for load bearing applications [82, 83].

Apart from natural derived materials, several synthetic matrices and scaffolds have been developed for tissue engineering purposes. Synthetic materials based on calcium phosphate constituents and bioactive glasses exhibit excellent bone-bonding properties and processes of biological degradation that have contributed to the clinical success of more than 40 years [84]. Several materials have been developed and successfully used in clinical environment, including: hydroxyapatite, tricalcium phosphate, bicalcium phosphate brushite and octacalcium phosphate. As porous structures, they are suitable candidates as scaffolds. Additionally, synthetic polymer hydrogels have shown promise behaviour nonetheless the limited biocompatibility issues and general low mechanical stability [85]. Among polymers, most of the assayed materials for these applications belong to the poly(α-hydroxy esters) family, including polyglycolic acid, polylactic acid and their copolymers that have shown to adequately support cell guided growth and differentiation. However, some biocompatibility issues

have arise from the produced acidic degradation that is expected to induce an adverse biological response [86].

Notwithstanding the relative simplicity of the (re-)construction of a single-cell type tissue, it is clear that currently used technologic advances for the repair of the skeletal tissues are generally unsatisfactory and require the development and implementation of new approaches for the achievement of the desired clinical objectives. Among the currently developed techniques to the repair of damage tissues, the immobilization and transplantation of cells on carried scaffolds, or tissues grown *in vivo* or *ex vivo*, have been assayed. To this end, extensive research has been developed in evaluating the range of cell sources, materials for cell transplantation, as well as material design that can be used to immobilize cells and support gradual neo-tissue formation, at the same time that a programmed degradation occurs. In this regard, the assessment of a biomaterial biocompatibility outputs a two-way approach: in one hand allows the fundamental assessment of a biomaterial behaviour in contact with cells and/or tissues in order to make assumptions of its applicability in clinical scenario; on the other hand, *in vitro* cell culture studies allow to preliminary access the results of candidate tissue engineering applications, since orthotopic cells are generally used for biocompatibility testing and provide data regarding cell proliferation and differentiation events.

Biocompatibility assessment in bone regenerative strategies

Materials used in medical devices and tissue engineering constructs, namely those which aim to contact, be inserted or permanently implanted in the body, are broadly described as biomaterials and have unique design requirements. The National Institute of Health Consensus Development Conference defined a biomaterial as "any substance (other than a drug) or combination of substances, synthetic or natural in origin, which can be used for any period of time, as a whole or as a part of a system which treats, augments, or replaces any tissue, organ, or function of the body" [87].

The individual and specific requirements of each biomaterial are determined by the selected application and functionality of the device. In a generic approach, biomaterials can be used in: 1) blood-contacting applications, e.g. external devices that remove and return blood from the body, devices that are inserted into a blood vessel, or devices that are permanently implanted; 2) soft-tissue device applications, e.g., materials aiming the augmentation of soft-tissues; 3) hard-tissue device applications, e.g., applications for joint, bone, and tooth replacement and repair; 4) specific organ

applications, e.g., neural, pancreatic and liver; and 5) scaffolds for tissue engineering aiming tissue and organ replacement/regeneration [88].

The material's form and size, the close interface with body fluids and/or tissues, and the duration of use will also determine its required properties. Overall, one material property alone is unlikely to lead to a successful and durable device, whereas a lack of inadequacy regarding a single key property, can lead to a disastrous failure. Accordingly, materials aiming biological functions need to meet basic biocompatibility requirements, generally substantiated in the ISO 10993 standards (Table 2). This is, to be nontoxic, non-thrombogenic, non-carcinogenic, non-antigenic, and non-mutagenic [89].

Table 2 - International ISO standards for biological evaluation of medical devices [90].

Reference	Title
ISO 10993-1: 2009	Evaluation and testing within a risk management process
ISO 10993-2: 2006	Animal welfare requirements
ISO 10993-3: 2003	Tests for genotoxicity, carcinogenicity, and reproductive toxicity
ISO 10993-4: 2002	Selection of tests for interactions with blood
ISO 10993-5: 2009	Tests for in vitro cytotoxicity
ISO 10993-6: 2007	Tests for local effects after implantation
ISO 10993-7: 2008	Ethylene oxide sterilization residuals
ISO 10993-8	Withdrawn: Clinical investigation of medical devices – updated by ISO 14155 - Clinical investigation of medical devices for human subjects
ISO 10993-9: 2009	Framework for identification and quantification of potential degradation products
ISO 10993-10: 2010	Tests for irritation and skin sensitization
ISO 10993-11: 2006	Tests for systemic toxicity
ISO 10993-12: 2007	Sample preparation and reference materials
ISO 10993-13: 2010	Identification and quantification of degradation products from polymeric medical devices
ISO 10993-14: 2001	Identification and quantification of degradation products from ceramics
ISO 10993-15: 2000	Identification and quantification of degradation products from metals and alloys
ISO 10993-16: 2010	Toxicokinetic study design for degradation products and leachables
ISO 10993-17: 2002	Establishment of allowable limits for leachable substances

ISO 10993-18: 2005	Chemical characterization of materials
ISO 10993-19: 2006	Physico-chemical, morphological and topographical characterization of materials
ISO 10993-20: 2006	Principles and methods for immunotoxicology testing of medical devices

In vitro testing

The assessment of the biocompatibility of a product and/or its components based on ISO 10993 offers a "horizontal" approach that, for practical use, offers different starting points, potential applicable to the vast majority of the developed and developing medical devices. *In vitro* testing is highly regarded within cytocompatibility assessment, offering the opportunity to test early in product development since potential toxicity can be assayed and therefore expensive and undesirable development work can be circumvented. Moreover, it allows for a rapid biological evaluation, uses standardized protocols and produces quantitative and comparable data [91]. Additionally, marketed products can be regularly tested with regards to cytotoxicity, monitorization in the production process and identification of breaches in disinfection and sterilization procedures.

In vitro characterization methodologies, based on established cell cultures, allow for a strict controlled environment which has shown some advantages and limitations in its application to biotechnology (Table 3).

Table 3 – Advantages and limitations of cell culture. Adapted from [92].

	Category	Issue
Advantages	Physicochemical environment	Control of pH, temperature, osmolality, etc
	Physiological conditions	Control of nutrients and biomodulators concentrations
	Microenvironment	Regulation of the cell-cell and cell-matrix interaction Regulation of the gaseous diffusion
	Cell line homogeneity	Cloning capability which enhances reproducibility of the assay
	Characterization	Quantitative and qualitative data can be assessed
	Replicates and variability	Specific characterization techniques like cytology and immunostaining are easily performed
	Preservation	High life span in adequate freezing conditions
	Validation and accreditation	Origin, history, purity can be authenticated and recorded
Limitations	Necessary expertise	Sterile handling

		Risk of chemical and microbial contamination
		Cross-contamination
	Environmental control	Workplace
		Incubation, pH control
		Containment and disposable of biohazards
	Quantity and cost	Capital equipment
		Disposable plastics
		Cell culture reagents, specific media, serum, molecular biology assays
	Genetic instability	Heterogeneity, variability
	Phenotypic instability	Dedifferentiation
		Adaptation
		Selective overgrown
	Cell type identification	Markers are not always expressed
		Morphology and microenvironment changes cytological responses

Nonetheless the stated advantages and limitations, the development of adequate standards regarding *in vitro* models of cytocompatibility has been conducted not without associated precincts which broadly include the discernment of the relevant biological reactions for which simulation assays can be devised; and the critical design of tests and assays that are moderately easy to perform in laboratory and allow for consistent data gathering throughout time, and among repeated procedures. Accordingly, moreover than a basic cytotoxic evaluation, *in vitro* testing ought to allow data assessment of a wide range of biological processes which converge to substantiate the cytocompatibility characterization. Experimental studies have demonstrated the good correlation between *in vitro* and *in vivo* tests, thus confirming the usefulness of the *in vitro* test as systems to biologically evaluate materials aiming clinical application.

Cells, *in vitro,* are generally more sensitive to toxic materials than *in vivo* tissues. In this line of thought, a material toxic *in vitro* may result not particularly toxic for the tissues *in vivo*, while a material harmless to the cells, even in long-lasting assays, is likely to be also toxically inert *in vivo*. A different picture is seen when a material releases wear debris or corrosion particles; reactive processes can be triggered, with the risk of loosening the implant and progress to a complete failure of the regenerative process [91].

Methods for direct and/or indirect cell contact can be used depending on the nature and duration of the device contact with the biological systems. Either way, a

combined execution of direct and indirect cell contact tests can more adequately substantiate the biological characterization process [93]. An adequate selection of the test series to be performed, oriented to the product particularities, and taking into account the specificities of sample preparation, are of the utmost relevance. Moreover, positive and negative controls are ought to be used, wherever possible, to assess the effect of the candidate material compared to controls.

Three fundamental cell culture assays are used for evaluating cytocompatibility: direct contact, agar diffusion and elution - extract dilution - (Table 4). The three testing methodologies vary in the manner in which the material contacts with the *in vitro* system as it can be placed directly in close contact with cells or extracted in an appropriate solution that is subsequently placed in contact with the cultured cells.

Table 4 – Advantages and disadvantages of cell culture methods for biocompatibility assessment. Adapted from [94].

	Advantages	Disadvantages
Direct contact	- Eliminates extraction preparation - Allows the assessment of a zone of diffusion - Target cells are able to directly contact the material - Mimics physiological conditions - Standardize amount of test material or test indeterminate shapes - The exposure time can be controlled	- Cellular trauma if the material moves - Cellular trauma with high density materials - Decreased cell populations with potential highly soluble toxicants
Agar diffusion	- Eliminates extraction preparation - Allows the assessment of a zone of diffusion - Better concentration gradient of potential toxicants - Independent of the material density	- Requires flat surfaces - Risk of thermal shock during agar preparation - Limited exposure time - Risk of water absorption from agar
Elution	- Separates extraction from testing - Dose response effect - Extend exposure time - Control of the extract conditions - Choice of the solvents	- Additional time and steps

In order to allow reproducible and comparable results between assays, several variables, namely the number of seeded cells, growth phase of the cells, cell type and population, duration of exposure, test sample size, geometry, thickness, shape and surface area, must be carefully controlled. Bearing in mind these particularities, and within the quantitation range of the selected assays, varying slopes of the dose-

response curve or exposure-effect relationship are expected to occur with different cytotoxic agents, in a manner hopefully related to animal bioassays [95].

In a preliminary approach, cell lines that have been developed for facilitated growth *in vitro* are preferably used in detriment of primary or serial passage cell cultures established from biological tissues, since cell lines improve the reproducibility of the data gathered and the variability among laboratories [96]. Cell lines maintain their genetic, metabolic and morphological characteristics throughout the extended life span. For instance, L-929 mouse fibroblasts have been used most extensively for biomaterials testing due to the easy maintenance in culture and the ability to output results that are highly correlated with specific *in vivo* bioassays [97]. Moreover, fibroblasts have been broadly chosen since they are one of the early cells to populate the wound healing location and are often the major cell population in tissues that contact to the implanted devices.

In the screening stage, the functions shared by all types of cells are investigated, which generally include the assessment of the metabolic activity (e.g., MTT and Alamar blue assay), cell viability (e.g., neutral red uptake, propidium iodine staining) and cell proliferation (e.g., cell counting, total protein content, DNA assay, ^{3}H-TDR uptake) [96]. Moreover, morphology assessment is also generally conducted by reaching hand of scanning electron microscopy or confocal laser scanning microscopy, following adequate cell staining [91, 96].

In the supplementary tests for the assessment of the specific cell functionality in the presence of the medical device, cell lines from other tissues may also be used and generally, cell populations of the tissues that the medical device aims to contact with, are selected [96]. In which relates to the assessment of the biocompatibility of bone-related materials and medical devices, not only osteoblastic, but also osteoclastic and endothelial cells are broadly used to study the specific biomaterial/cell interaction.

A sufficient amount of bone cells is easily available, most of them being osteoblast-like cell lines derived from mouse, rat or human osteosarcomas (UMR-106, MC3T3-E1, ROS17/2.8, SAOS-2, HOS and MG-63) [98]. Osteogenic sarcoma cells retain many markers of the osteoblastic phenotype but differ from physiological bone cells in their functional activity, responsiveness to external agents and expression of surface molecules [99, 100]. The choice to use a continuous cell line, in spite of finite cell line derived from tissue-established primary cultures, should be carefully deliberated bearing in mind the specificities and the objectives of the test. Properties of both cell populations are presented on Table 5.

Table 5 – Properties of finite and continuous cell lines. Adapted from [101].

Properties	Cell line derived from a biological tissue-established primary culture (finite)	Transformed cell line (continuous)
Ploidy	Euplod, diploid	Aneuploid, heteroploid
Transformation	Normal	Immortal, alterations in growth control and chance of tumorogenicity
Anchorage dependence	Yes	No
Contact inhibition	Yes	No
Density limitation of the cell proliferation	Yes	Reduced or lost
Mode of growth	Monolayer	Monolayer or suspension
Maintenance	Cyclic	Steady state possible
Serum requirements	High	Low
Cloning efficiency	Low	High
Markers	Tissue specific	Chromosomal, enzymatic, antigenic
Special functions (e.g., virus susceptibility, differentiation)	May be retained	Often lost
Growth rate	Slow (TD of 24 – 96h)	Rapid (TD of 12 – 24h)
Yield	Low	High

Tissues broadly used to obtain osteoblastic cells for a large variety of experimental set-ups include cancellous bone specimens from human or animal origin, as well as calvaria bone from foetal or neonatal animals. Bone cells can be obtained from bone by enzymatic digestion or from outgrowth of bone explants [102]. Human first passage cells derived from cancellous bone have been characterised and shown to possess a phenotype that is clearly distinct from that of fibroblastic cells derived from the dermis [103]. Early characterisation revealed that cultured bone-derived cells presented a flattened, multiple morphology and an abundance of cytoplasmic stress fibres, while skin-derived fibroblasts showed an elongated bipolar morphology. Bone-derived cells, in the presence of a glucocorticoid, change their morphology to a more polygonal shape – situation that has been associated with the transition to a more differentiation stage [104, 105]. Comparing to fibroblasts grown in culture, bone-derived cells proliferate less rapidly, reach lower saturation densities and express high levels of the non-specific isoform of alkaline phosphatase. Both cell populations synthesize a collagen-rich extracellular matrix but the cells derived from the bone express greatly collagen type I, less than 10% of collagen type III and small quantities of collagen type

V [103, 106]. These cells also synthesize several non-collagenous proteins, including bone sialoprotein, osteocalcin – known late stage markers of the osteoblastic lineage. The level of expression of these proteins, and alkaline phosphatase as well, is markedly influenced by the cell culture stage of maturation – which in turn is a function of the initial cell density and the absence or presence of specific biomodulators such as glucocorticoids, vitamin D3, ascorbic acid, beta-glycerophosphate, among others [104]. In addition to established supplements, members of the bone morphogenetic protein (BMP) family of growth factors are also routinely used for osteoinduction. BMP-2 alone appears to increase bone nodule formation and the calcium content of osteogenic cultures *in vitro*, while concomitant application of BMP-2 and basic fibroblast growth factor increases osteogenesis both *in vivo* and *in vitro* [107]. Either way, the most compelling evidence for the presence of cells of the osteogenic lineage in culture is the demonstration of extracellular matrix mineralization, and the formation of well-organized mineralised nodules that, through an histological and histochemical approach, resemble the mineralised organisation of the woven bone tissue [108].

Additionally, cells with osteoblastic phenotype can also be differentiated from selected precursors from the bone marrow [102]. There are three main cellular systems in the bone marrow: haemopoietic, endothelial and stromal, which are histogenetically distinct with no common precursor in the post-natal development. Marrow cells prepared as a single cell suspension and cultured *in vitro* with foetal calf serum form fibroblastic colonies, each derived from a single cell or colony forming unit-fibroblastic (CFU-F) [109]. These colonies are heterogeneous in size, morphology and potential of differentiation but when these cells are grown in osteogenic inducing conditions – including foetal calf serum, an appropriate level of glucocorticoid, a source of phosphate and vitamin C – phenotypical characteristics of the osteoblastic lineage develop, including the formation of discrete three-dimensional mineralising nodules within focal areas of the cell layer [109]. Nonetheless a single cell, or colony forming unit-osteogenic (CFU-O) is sufficient for the production of one mineralised nodule, these CFU-O have limited capacity for self-renewal [109].

In recent years, a thoroughly characterization of the origin and properties of stromal cell populations revealed that within this population, cells initially isolated from the bone marrow of adult organisms and initially characterized as plastic adherent, fibroblastoid cells with the capacity to generate heterotopic osseous tissue when transplanted *in vivo*, correspond in fact, to a defined stem cell population - mesenchymal stem cells (MSCs) - shown to reside within the connective tissue of most organs, and with a surface phenotype well defined [110]. By using flow cytometry, MSCs have been shown to be negative for hematopoietic markers CD14, CD34 and

CD45. The cells stain positive for a number of surface markers including SH2, SH3, CD29, CD44, CD71, CD73, CD90, CD 105, CD106, CD120a, CD124 and CD166 [24, 111]. The progeny of *ex vivo* expanded MSCs reveal that they share a similar gene expression profile for a variety of transcriptional regulators, extracellular matrix proteins, growth factors/receptors, cell adhesion molecules, and some but not all, lineage makers characteristic of fibroblasts, endothelial cells, smooth muscle cells, and osteoblasts [111].

Apart from the differentiation of MSC into the osteoblastic lineage with the aim of establishing a homogeneous cell population for biocompatibility assessment, MSCs also provide an exciting progenitor cell source for tissue engineering and regenerative medicine applications. Developing strategies may include direct implantation and/or *ex vivo* tissue engineering approaches, in combination with biocompatible/biomimetic biomaterials and/or biomodulators. MSCs may also be considered for gene therapy applications for the delivery of genes or gene products. Another intriguing prospect for the future is the use of MSCs to create 'off-the-shelf' tissue banks.

Practical, biological and technological issues still need to be fixed in order to fully harness the potential of these cells, their cellular and molecular characteristics, in order to establish an optimal identification, isolation, and expansion, and to understand the natural, endogenous role(s) of MSCs in normal and abnormal tissue functions.

In vivo testing

In the biological assessment of the biocompatibility between a medical device and the biological tissues, *in vitro* procedures are used as a first stage test for acute toxicity and cytocompatibility to avoid unnecessary use of animals in the testing of inappropriate materials. The term biocompatibility is often inaccurately used within *in vitro* applications, as biocompatibility can be only assessed within the range of testing in living organisms – animals or humans – with the correct term for *in vitro* tests being cytocompatibility [112]. Accordingly, *in vitro* testing gives information regarding cytotoxicity, genotoxicity, cell proliferation and differentiation and is more easily standardised and quantifiable than *in vivo* testing [113]. *In vitro* studies are also used for screening new materials for product quality and the release of potentially harmful additives or components [96]. Conversely, *in vitro* testing is not able to demonstrate the tissue response to materials – instead is restricted to the response of cell lines. Additionally, cell culture testing may also overestimate the intensity of material toxicity and is limited to acute studies, due to the relative short lifespan of the culture systems [96]. Moreover, and regarding bone related testing, no cell culture system is able to mimic or reproduce loading that stimulates the *in vivo* behaviour, only approachable in

few *ex vivo* systems [114]. For these reasons animal models are necessary for biocompatibility assessment, tissue response and mechanical function of a medical device, moreover in the regards of bone-related applications, prior to clinical set up of the devices.

Animal models allow the evaluation of medical devices, in loaded or unloaded conditions, potentially for long durations and in different biological conditions (for instance, in the absence or presence of associated pathology) and ages [112]. In this way, the tissues in the neighbouring area of the implant can be assessed, as well as remote locations, which is relevant in the evaluation of the effect of potential released particles of wear debris [115]. For this purpose, a wide range of models for implant testing, ranging from the evaluation of protein adsorption to soft tissue adherence or bone integration, are widely available. Nonetheless, one may keep in mind that each model possesses unique advantages and disadvantages and while it may closely represent the biomechanical and physiological particularities of the human organism, it must be remembered that it is only an approximation.

When selecting the required animal species for a particular model, several factors must be addressed. Following the clear establishment of the research question, animal selection factors generally include: cost on the acquisition and maintenance of the animals, availability, social and ethical acceptance, easy of housing and handling, inter-individual uniformity, susceptibility to disease, biological characteristics in similarity with humans, availability of background data, tolerance to surgery, and team expertise (regarding facilities and support staff) [112, 116]. Additionally, the lifespan of the species should be adequate to the duration and objectives of the study and, for studies dealing with bone-implant interactions, specific bone characteristics of the species (within the regards of macro and microstructure, bone composition and modelling/remodelling properties) should be particularly considered.

Overall, no single animal model will be completely appropriate for all testing purposes, nor a model can be dismissed as inappropriate for all purposes. In fact, multiple animal models are likely required to establish a broadly body of data that supports biocompatibility assessment [117]. International standards established regarding the use of species suitable for testing implantation of medical devices, state that mice, rats, guinea pigs, rabbits, dogs, sheep, goats and pigs are all suitable – a comparative approach of the bone tissue characteristics of different species is presented on Table 6. The number of animals required, surgical procedures and implantation time are also issues addressed on the ISO 10993-6: 2007 Tests for local effects after implantation [90].

Table 6 – Overview of the key attributes in terms of similarity between animal and human bone. Adapted from [112].

Properties	Rodents (mice and rat)	Rabbit	Sheep/goat	Canine	Pig
Macrostructure	+	+	+++	++	++
Microstructure	+	+	+	++	++
Bone composition	+	++	++	+++	+++
Bone remodelling	+	+	++	++	+++

+ least similar, ++ moderately similar, +++ most similar.

Animal models play an important role in bone tissue-related research by providing methodological approaches to study detailed events and regenerative advances, which aim to establish adequate translational knowledge to substantiate clinical research in the following phase of biocompatibility assessment of a developed medical device. As a result, the never-ending scientific questions related to bone physiology and pathological conditions, and disease and regenerative approaches demand the availability of a wide range of animal models and the continue innovation of new model systems. Opportunities for advancement in animal models are identified in four general domains: 1) the development of new models to address new questions and relevant variables (e.g., cell transplantation survival in tissue engineering approaches, mass transport, *in vivo* biomodulator delivery, signal transduction modifications); 2) application of new methodologies of quantitative analysis (e.g., imaging techniques, immunohistochemical and histological evaluations that validate features of existing models that have not been previously accessible); 3) improved validation and standardization, as well as rigorous use of models in competitive testing that enhance the predictability of the clinical performance of the assay; 4) the design and implementation of models that more adequately represent the clinical settings [118].

Many authors converge to the fact that demonstration of similarities with humans – both in what relates to physiological and pathological events, as well as the capability to address numerous events and subjects within a relatively reduced time frame, are advantageous characteristics of an animal model, providing most relevant information for the successive testing in clinical scenario [116, 119, 120].

References

1. Kirschvink J, Walker M, Diebel C. Magnetite-based magnetoreception. Curr Opin Neurobiol 2001;11:462-467.

2. Burg K, Porter S, Kellam J. Biomaterial developments for bone tissue engineering. Biomaterials 2000;21:2347-2359.

3. Turner C. Biomechanics of bone: determinants of skeletal fragility and bone quality. Osteoporos Int 2002;13:97-104.

4. Weiner S, Wagner H. The material bone: structure-mechanical function relations. Annu Rev Mater Sci 1998;28:271-298.

5. Institute NC. Compact bone and spongy (cancellous bone). Online. Accessed on 16/09/2010.Available from http://training.seer.cancer.gov/anatomy/skeletal/tissue.html

6. Athanasiou K, Zhu C, Lanctot D, Agrawal C, Wang X. Fundamentals of biomechanics in tissue engineering of bone. Tissue Eng 2000;6:361-381.

7. Su X, Sun K, Cui F, Landis W. Organization of apatite crystals in human woven bone. Bone 2003;32(150-62).

8. Paschalis E, Verdelis K, Doty S, Boskey A, Mendelsohn R, Yamauchi M. Spectroscopic characterization of collagen cross-links in bone. J Bone Miner Res 2001;16:1821-1828.

9. Knott L, Bailey A. Collagen cross-links in mineralizing tissues: a review of their chemistry, function, and clinical relevance. Bone 1998;22:181-187.

10. Marie P. Bone cell-matrix protein interactions. Osteoporos Int 2009;20:1037-1042.

11. Kazanecki C, Uzwiak D, Denhardt D. Control of osteopontin signaling and function by post-translational phosphorylation and protein folding. J Cell Biochem 2007;102:912-924.

12. Baht G, Hunter G, Goldberg H. Bone sialoprotein-collagen interaction promotes hydroxyapatite nucleation. Matrix Biol 2008;27:600-608.

13. Hauschka P, Wians FJ. Osteocalcin-hydroxyapatite interaction in the extracellular organic matrix of bone. Anat Rec 1989;224:180-188.

14. Lamoureux F, Baud'huin M, Duplomb L, Heymann D, Rédini F. Proteoglycans: key partners in bone cell biology. Bioessays 2007;29:758-771.

15. Alford A, Hankenson K. Matricellular proteins: Extracellular modulators of bone development, remodeling, and regeneration. Bone 2006;38:749-757.

16. Cazalbou S, Combes C, Eichert D, Rey C. Adaptative physico-chemistry of bio-related calcium phosphates. J Mater Chem 2004;14:2148-2153

17. Boskey A. Biomineralization: conflicts, challenges, and opportunities. J Cell Biochem Suppl 1998;30-31:83-91.

18. Pasteris J, Wopenka B, Valsami-Jones E. Bone and Tooth Mineralization: Why Apatite? Elements 2008;4:97-104.

19. Ozawa H, Hoshi K, Amizuka N. Current Concepts of Bone Biomineralization. J Oral Bioscience 2008;1:1-14.

20. Schmidt-Rohr K. The apatite-collagen interface in bone. Ames Laboratory. Online. Accessed on 08/09/2010. Available from URL: http://www.matchem.ameslab.gov/high_Bone.htm

21. Schulz J, Pretzsch M, Khalaf I, Deiwick A, Scheidt H, Salis-Soglio G, et al. Quantitative monitoring of extracellular matrix production in bone implants by 13C and 31P solid-state nuclear magnetic resonance spectroscopy. Calcif Tissue Int 2007;80:275-285.

22. Jaeger C, Groom N, Bowe E, Horner A, Davies M, Murray R, et al. Investigation of the Nature of the Protein−Mineral Interface in Bone by Solid-State NMR. Chem Mater 2005;17:3059–3061.

23. Jaiswal N, Haynesworth S, Caplan A, Bruder S. Osteogenic differentiation of purified, culture-expanded human mesenchymal stem cells in vitro. J Cell Biochem 1997;64:295-312.

24. Pittenger M, Mackay A, Beck S, Jaiswal R, Douglas R, Mosca J, et al. Multilineage potential of adult human mesenchymal stem cells. Science 1999;284:143-147.

25. Jiang Y, Jahagirdar B, Reinhardt R, Schwartz R, Keene C, Ortiz-Gonzalez X, et al. Pluripotency of mesenchymal stem cells derived from adult marrow. Nature 2002;418:41-49.

26. Caplan A, Bruder S. Mesenchymal stem cells: building blocks for molecular medicine in the 21st century. Trends Mol Med 2001;7:259-264.

27. Klein-Nulend J, Nijweide P, Burger E. Osteocyte and bone structure. Curr Osteoporos Rep 2003;1:5-10.

28. Lanyon L. Osteocytes, strain detection, bone modeling and remodeling. Calcif Tissue Int 1993;53 Suppl:S106-107.

29. Everts V, Delaissé J, Korper W, Jansen D, Tigchelaar-Gutter W, Saftig P, et al. The bone lining cell: its role in cleaning Howship's lacunae and initiating bone formation. J Bone Miner Res 2003;17:77-90.

30. Parfitt A. The bone remodeling compartment: a circulatory function for bone lining cells. J Bone Miner Res 2001;16:1583-1585.

31. Dallas S, Bonewald L. Dynamics of the transition from osteoblast to osteocyte. Ann N Y Acad Sci 2010;1192:437-443.

32. Alberts B, Johnson A, Lewis J, Raff M, Roberts K, Walter P. http://www.ncbi.nlm.nih.gov/bookshelf/br.fcgi?book=mboc4&part=A4177&rendertype=figure&id=A4191. Online. Accessed on 08/09/2010.

33. Teitelbaum S. Bone resorption by osteoclasts. Science 2000;289:1504-1508.

34. Boyle W, Simonet W, Lacey D. Osteoclast differentiation and activation. Nature 2003;423:337-342.

35. Ross F, Christiano A. http://www.biology-online.org/kb/article.php?p=skin_bone/figures. Online. Accessed on 10/09/2010.

36. Hadjidakis D, Androulakis I. Bone remodeling. Ann N Y Acad Sci 2006;1092:385-396.

37. Leibbrandt A, Penninger J. RANK/RANKL: regulators of immune responses and bone physiology. Ann N Y Acad Sci 2008;1143:123-150.

38. Deal C. Potential new drug targets for osteoporosis. Nat Clin Pract Rheumatol 2009;5:20-27.

39. Borle A. Calcium and phosphate metabolism. Annu Rev Physiol 1974;36:361-390.

40. Weitzmann M, Pacifici R. Estrogen deficiency and bone loss: an inflammatory tale. J Clin Invest 2006;116:1186-1194.

41. Brennan O, Kennedy O, Lee T, Rackard S, O'Brien F. Estrogen depletion and zoledronic acid therapy: effects on osteocyte apoptosis and microdamage J Biomech 2008;41 Suppl 1:S127.

42. Lieberman J, Daluiski A, Einhorn T. The role of growth factors in the repair of bone. Biology and clinical applications. J Bone Joint Surg Am 2002;84-A:1032-1044.

43. van Straalen J, Sanders E, Prummel M, Sanders G. Bone-alkaline phosphatase as indicator of bone formation. Clin Chim Acta 1991;14:27-33.

44. Kimmel D. A paradigm for skeletal strength homeostasis. J Bone Miner Res 1993;8 Suppl 2:S515-522.

45. Mullender M, Huiskes R. Osteocytes and bone lining cells: which are the best candidates for mechano-sensors in cancellous bone? Bone 1997;20:527-532.

46. Burchardt H. The biology of bone graft repair. Clin Orthop 1983;174:28-42.

47. Cypher T, Grossman J. Biological principles of bone graft healing. J Foot Ankle Surg 1996;35:413-417.

48. McAllister B, Haghighat K. Bone Augmentation Techniques. J Periodont 2007;78:377-396.

49. Younger E, Chapman M. Morbidity at bone graft donor sites. J Orthop Trauma 1989;3:192-195.

50. Deutsch H, Haid R, Rodts GJ, Mummaneni P. The decision-making process: allograft versus autograft. Neurosurgery 2007;60:S98-102.

51. Guillaume B, Gaudin C, Georgeault S, Mallet R, Baslé M, Chappard D. Viability of osteocytes in bone autografts harvested for dental implantology. Biomed Mater 2009;4:015012.

52. Arrington E, Smith W, Chambers H, Bucknell A, Davino N. Complications of iliac crest bone graft harvesting Clin Orthop 1996;329:300-309.

53. Oakley M, Smith W, Morgan S, Ziran N, Ziran B. Repetitive posterior iliac crest autograft harvest resulting in an unstable pelvic fracture and infected non-union: case report and review of the literature. Patient Saf Surg 2007;1:6.

54. Kurz L, Garfin S, Booth R. Harvesting autogenous iliac bone grafts: a review of complications and techniques. Spine 1989;14:1324–1331.

55. Boyce T, Edwards J, Scarborough N. Allograft bone. The influence of processing on safety and performance. Orthop Clin North Am 1999;30:571-581.

56. Pinkowski J, Reiman P, Chen S. Human lymphocyte reaction to freeze-dried allograft and xenograft ligamentous tissue. Am J Sports Med 1989;17:595–600.

57. Greenwald A, Boden S, Goldberg V, Khan Y, Laurencin C, Rosier R. Bone-graft substitutes: facts, fictions, and applications. J Bone Joint Surg Am 2001;83-A:98-103.

58. McAllister D, Joyce M, Mann B, Vangsness CJ. Allograft update: the current status of tissue regulation, procurement, processing, and sterilization. Am J Sports Med 2007;35:2148-2158.

59. Friedlaender G. Immune responses to osteochondral allografts. Current knowledge and future directions. Clin Orthop Relat Res 1983;174:58-68.

60. Wang J, Alanay A, Mark D, Kanim L, Campbell P, Dawson E, et al. A comparison of commercially available demineralized bone matrix for spinal fusion. Eur Spine J 2007;16:1233-1240.

61. Glowacki J, Zhou S, Mizuno S. Mechanisms of osteoinduction/chondroinduction by demineralized bone. J Craniofac Surg 2009;20 Suppl 1:634-638.

62. Malinin T, Temple H. Comparison of frozen and freeze-dried particulate bone allografts. Cryobiology 2007;55:167-170.

63. Holtzclaw D, Toscano N, Eisenlohr L, Callan D. The safety of bone allografts used in dentistry: a review. J Am Dent Assoc 2008;139:1192-1199.

64. Palmer S, Gibbons C, Athanasou N. The pathology of bone allograft. J Bone Joint Surg Br 1999;81:333-335.

65. Mellonig J. Human histologic evaluation of a bovine-derived bone xenograft in the treatment of periodontal osseous defects. Int J Periodontics Restorative Dent 2000;20:19-29.

66. Bannister S, Powell C. Foreign body reaction to anorganic bovine bone and autogenous bone with platelet-rich plasma in guided bone regeneration. J Periodont 2008;79:1116-1120.

67. Sogal A, Tofe A. Risk asssment of bovine spongiform Encenphalopathy transmission through bone graft material derived from bovine bone used for dental applications. J Periodont 1999;70:1053-1063.

68. Barrère F, Mahmood T, de Groot K, van Blitterswijk C. Advanced biomaterials for skeletal tissue regeneration: Instructive and smart functions. Mater Sci Eng R Rep 2008;59:38-71.

69. Breme H, Biehl V, Helsen J. Metals and implants. In: Breme H, Helsen J, editors. Metals as Biomaterials. Chichester: John Wiley & Sons, Ltd, 1988.

70. Habibovic P, de Groot K. Osteoinductive biomaterials--properties and relevance in bone repair. J Tissue Eng Regen Med 2007;1:25-32.

71. Williams D. The Williams Dictionary of Biomaterials. Liverpool: Liverpool University Press, 1988.

72. Ryan G, Pandit A, Apatsidis D. Fabrication methods of porous metals for use in orthopaedic applications. Biomaterials 2006;27:2651-2670.

73. Roach P, Eglin D, Rohde K, Perry C. Modern biomaterials: a review - bulk properties and implications of surface modifications. J Mater Sci Mater Med 2007;18:1263-1277.

74. Hutmacher D, Schantz J, Lam C, Tan K, Lim T. State of the art and future directions of scaffold-based bone engineering from a biomaterials perspective. J Tissue Eng Regen Med 2007;1:245-260.

75. Langer R, Vacanti J. Tissue engineering Science 1993;260:920-926.

76. Mistry A, Mikos A. Tissue engineering strategies for bone regeneration. Adv Biochem Eng Biotechnol 2005;94:1-22.

77. Porter J, Ruckh T, Popat K. Bone tissue engineering: a review in bone miomimetics and drug delivery strategies. Biotechnol Prog 2009;25:1539-1560.

78. Bianco P, Robey P. Stem cells in tissue engineering. Nature 2001;414:118-121.

79. Dang J, Leong K. Natural polymers for gene delivery and tissue engineering. Adv Drug Deliv Rev 2006;58:487-499.

80. Saris D. Joint Homeostasis in Tissue Engineering for Cartilage Repair. Utrecht: Utrecht University; 2002.

81. Lowe N, Maxwell C, Patnaik R. Adverse reactions to dermal fillers: review. Dermatol Surg 2005;31:1616-1625.

82. Yang S, Leong K, Du Z, Chua C. The design of scaffolds for use in tissue engineering. Part I. Traditional factors. Tissue Eng 2001;7:679-689.

83. Hollister S. Porous scaffold design for tissue engineering. Nat Mater 2005;4:518-524.

84. LeGeros R. Properties of osteoconductive biomaterials: calcium phosphates. Clin Orthop Relat Res 2002;395:81-98.

85. Drury J, Mooney D. Hydrogels for tissue engineering: scaffold design variables and applications. Biomaterials 2003;24:4337-4351.

86. Gunatillake P, Adhikari R. Biodegradable synthetic polymers for tissue engineering. Eur Cell Mater 2003;20:1-16.

87. Boretos J, Eden M. Contemporary Biomaterials, Material and Host Response, Clinical Applications, New Technology and Legal Aspects Park Ridge, NJ: Noyes Publications; 1984.

88. Helmus M, Gibbons D, Cebon D. Biocompatibility: Meeting a Key Functional Requirement of Next-Generation Medical Devices. Toxicol Pathol 2008;36:70-80.

89. Helmus M. Biomaterials in the design and reliability of medical devices. New York and George Town, Tx: Kluwer Academic/Plenum Publishers and Landes Bioscience, 2003.

90. ISO. TC 194 - Biological evaluation of medical devices. Online. Accessed on 19/09/2010. Available from URL: http://www.iso.org/iso/iso_catalogue/catalogue_tc/catalogue_tc_browse.htm?commid=54508

91. Cenni E, Ciapetti G, Granchi D, Arciola C, Savarino LS, S, Montanaro L, et al. Established cell lines and primary cultures in testing medical devices in vitro. Toxicol In Vitro 1999;13:801-810.

92. Freshney R. Introduction. In: Freshney R, editor. Culture of animal cells: a manual of basic technique. Hoboken, NJ: John Wiley & Sons, 2005.

93. Muller U. In Vitro Biocompatibility Testing of Biomaterials and Medical Devices. Online. Accessed on 20/09/2010. Available from URL: http://www.emdt.co.uk/article/vitro-biocompatibility-testing-biomaterials-and-medical-devices

94. Anderson J, Bianco R, Grehan J, Grubbs B, Hanson S, Hauch K, et al. Biological testing of biomaterials. In: Ratner B, Hoffman A, Schoen F, Lemons J, editors. Biomaterials Science: Elsevier Inc, 2004.

95. Klaasen C. Principles of toxicology. In: Klaasen C, AMdur M, Doull J, editors. Casarett and Douell's Toxicology: McGraw-Hill Professional, 2001.

96. Pizzoferrato A, Ciapetti G, Stea S, Cenni E, Arciola C, Granchi D, et al. Cell culture methods for testing biocompatibility. Clin Mater 1994;15:173-190.

97. Eibl D, Eibl R, Pörtner R. Mammalian Cell Culture Technology: An Emerging Field. In: Eibl R, Eibl D, Pörtner R, Catapano G, Czermak P, editors. Cell and Tissue Reaction Engineering: Principles and Practice: Springer, 2008.

98. Ahmad M, Mc Carthy M, Gronowicz G. An in vitro model for mineralization of human osteoblast-like cells on implant materials. Biomaterials 1999;20:211-220.

99. Rifas L, Halstead L, Scott M, Fedarko N, Avioli L, Gehron R. Comparison of secretory products of normal rat osteoblasts and osteogenic sarcoma cells in vitro. J Bone Miner Res 1989;4:S409.

100. Miller M, Puzas J. Differential growth factor effects on normal and transformed rat bone cells. J Bone Miner Res 1988;3:S201.

101. Freshney R. Subculture and cell lines. In: Freshney R, editor. Culture of animal cells: a manual of basic techniques John Wiley & Sons, 2005.

102. Aubin J, Herbertson A. Osteoblast lineage in experimental animals. In: Beresford J, Owen M, editors. Marrow stromal cell culture: Cambridge University Press, 1998.

103. Gallagher JG, R, Beresford J. Isolation and culture of bone-forming cells (osteoblasts) from human bone. In: Jones G, editor. Methods in Molecular Medicine: Human Cell Culture Protocols. Totowa, NJ: Humana Press Inc, 1996.

104. Coelho M, Fernande M. Human bone cell cultures in biocompatibility testing. Part II: effect of ascorbic acid, beta-glycerophosphate and dexamethasone on osteoblastic differentiation. Biomaterials 2000;21:1095-1102.

105. Shalhoub V, Conlon D, Tassinari M, Quinn C, Partridge N, Stein G, et al. Glucocorticoids promote development of the osteoblast phenotype by selectively modulating expression of cell growth and differentiation associated genes. J Cell Biochem 1992;50:425-440.

106. Stein G, Lian J, Owen T. Relationship of cell growth to the regulation of tissue-specific gene expression during osteoblast differentiation. FASEB J 1990;4:3111-3123.

107. Hanada K, Dennis J, Caplan A. Stimulatory effects of basic fibroblast growth factor and bone morphogenetic protein-2 on osteogenic differentiation of rat bone marrow-derived mesenchymal stem cells. J Bone Miner Res 1997;12:1606-1614.

108. Tenenbaum H, Heersche J. Differentiation of osteoblasts and formation of mineralized bone in vitro. Calcif Tissue Int 1982;34:76-79.

109. Owen M. The marrow stromal system. In: Beresford J, Owen M, editors. Marrow stromal cell culture: Cambridge University Press, 1998.

110. Phinney D, Prockop D. Concise review: mesenchymal stem/multipotent stromal cells: the state of transdifferentiation and modes of tissue repair - current views. Stem Cells 2007;25:2896-2902.

111. Baksh D, Song L, Tuan R. Adult mesenchymal stem cells: characterization, differentiation, and application in cell and gene therapy. J Cell Mol Med 2004;8:301-316.

112. Pearce A, Richards R, Milz S, Schneider E, Pearce S. Animal models for implant biomaterial research in bone: a review. Eur Cell Mater 2007;13:1-10.

113. Nahid M, Bottenberg P. Importance of cell cultures in biocompatible dental materials research. Rev Belge Med Dent 2003;58:189-196.

114. Davies C, Jones D, Stoddart M, Koller K, Smith E, Archer C, et al. Mechanically loaded ex vivo bone culture system "Zetos": system and culture preparation. Eur Cell Mater 2006;11:57-75.

115. Urban R, Jacobs JT, MJ, Gavrilovic J, Black J, Peoc'h M. Dissemination of wear particles to the liver, spleen, and abdominal lymph nodes of patients with hip or knee replacement. J Bone Joint Surg Am 2000;82:457-476.

116. Schimandle J, Boden S. Spine update. The use of animal models to study spinal fusion. Spine 1994;19:1998-2006.

117. Hazzard D, Bronson R, McClearn G, Strong R. Selection of an appropriate animal model to study aging processes with special emphasis on the use of rat strains. J Gerontol 1992;47:B63-B64.

118. Muschler G, Raut V, Patterson T, Wenke J, Hollinger J. The design and use of animal models for translational research in bone tissue engineering and regenerative medicine. Tissue Eng Part B Rev 2010;16:123-145.

119. Liebschner M. Biomechanical considerations of animal models used in tissue engineering of bone. Biomaterials 2004;25:1697-1714.

120. Egermann MG, Schneider, E. Animal models for fracture treatment in osteoporosis. Osteoporos Int 2005;16 Supple 2:S129-S138.

Chapter 2

Biocompatibility evaluation of DLC-coated Si$_3$N$_4$ substrates for biomedical applications

Biocompatibility evaluation of DLC-coated Si$_3$N$_4$ substrates for biomedical applications

E. Salgueiredo[1], M. Vila[1], M.A. Silva[2], M.A. Lopes[2,3], J.D. Santos[2,3], F.M. Costa[4], R.F. Silva[1], P.S. Gomes[5] , M.H. Fernandes[5]

1 - CICECO, Glass and Ceramics Eng. Department, University of Aveiro, 3810-193 Aveiro, Portugal
2 - Instituto de Engenharia Biomédica (INEB), Lab. Biomateriais, Porto, Portugal
3 - Dep. Eng. Metalúrgica e Materiais, Faculty of Engineering, U. Porto, Portugal
4 - Physics Department, University of Aveiro, Portugal
5 - Laboratory of Pharmacology and Cellular Biocompatibility, Faculty of Dental Medicine, U. Porto, Portugal

Abstract

DLC coatings are of enormous interest for biotribological applications due to their biocompatibility, auto-lubricious, and non-stick properties. The most demanding implant is the hip joint. Alternative materials to metal alloys are being increasingly investigated aiming low wear debris volume, in any case innocuous wear particles. Silicon nitride (Si_3N_4) ceramics are light, tough, mechanical resistant, inert materials, turning them suitable for high-load medical applications. In this study, Si_3N_4 polished substrates were coated with adherent DLC coatings grown by DC magnetron sputtering to reduce of the friction forces against any antagonist material. Surface characterization results showed that the developed material is quite hydrophobic, with a total surface tension of 45.7 mN/m (polar component: 9.1 mN/m; dispersive component: 36.6 mN/m), and a zeta potential of -35.0 ± 1.3 mV. In vitro testing using an acellular simulated body fluid (SBF) showed no apatite layer formation ability, as confirmed by SEM observation and analysis of the solution ions concentration with immersion time. MG63 osteoblast-like cells showed poor adhesion on the DLC films but the adherent cells displayed a normal morphology and, as compared to standard polystyrene tissue culture plates, exhibited a higher cell growth rate, suggesting no indication of cytotoxicity. Results suggested that the novel DLC-coated Si_3N_4 biomaterial should be adequate to be used for articular prostheses medical application.

Introduction

Some medical applications require materials with a non cell-adhesive surface, such as devices in contact with human blood (e.g., artificial heart valves), while others need a cell-adhesive surface to assure complete tissue integration of the implanted material in the human body. In orthopaedic applications, the osteointegration is promoted by the formation of an apatite layer on the surface of the biomaterial upon implantation. The biomaterial surface properties can be defined aiming to control its bioactivity and biocompatibility. For applications such as replacement of the hip joint, which is composed of a stem, a femoral head and an acetabulum, the formation of an apatite layer is desired on the stem, but not at femur head or acetabulum surface since it would compromise the tribo-system performance. There are many different shapes, sizes, and designs of artificial components of the hip joint, made of several materials such as chrome, cobalt, titanium, polymeric or ceramic materials. Nevertheless, on going problems with wear and particulate debris still exist, causing metallosis, and eventually periprosthetic osteolysis and aseptic loosening [1].

Silicon nitride (Si_3N_4) based ceramics are well known for their superior combination of fracture toughness and hardness [2]. These are key properties for an excellent wear resistance, which, combined with Si3N4 chemical inertness, turns this material a suitable candidate for high-load medical applications, namely for metal prostheses replacement. In order to diminish the friction forces in such kind of bio-tribological systems, the Si_3N_4 surfaces must be modified. Diamond-like carbon (DLC) coatings are of enormous interest for biomedical applications due to their biocompatible, auto-lubricious, and non-stick properties [3-5]. Therefore, DLC is a very good candidate for coating the hip joint tribosystem, especially when combined with the adequate bio-mechanical properties of the Si_3N_4 ceramic [6].

Surface properties such as surface chemistry, surface energy and surface topography can be critical for biomaterials biocompatibility, together with bulk properties characteristics. Protein adsorption, which is a virtually instantaneous process during an implantation procedure, is a dynamic and a very complex phenomenon that precedes any cell-mediated effects either in vitro or in vivo. Biomaterial surface properties, important in protein adsorption, that can be readily quantified, include interfacial free energy, hydrophobicity and surface charge density.

In this study, Si_3N_4 polished substrates were coated with adherent DLC coatings grown by DC magnetron sputtering. An intermediate Si layer promotes the adhesion between the ceramic and the DLC film. Wettability and zeta potential studies were performed to characterize the hydrophobicity, surface tension and surface charge of the DLC Si_3N_4 coated material. In vitro bioactivity was assessed through an acellular

simulated body fluid (SBF) testing assay and biocompatibility evaluation using MG63 osteoblast-like cells.

Materials and methods

Silicon nitride ceramic discs (empty set 10 mm × 3 mm), whose preparation is described elsewhere [6], were coated with continuous, homogeneous and adherent DLC films, by DC magnetron sputtering from a graphite target of 3 mm thickness. Before deposition of the amorphous carbon, an intermediate layer of Si was deposited by the same technique from a silicon wafer target, in order to promote adhesion between the substrates and the DLC films.

Zeta potential measurements were performed in Anton Paar EKA — Electro Kinetic Analyser equipment, using a rectangular cell in which the solution passes along a channel formed by two layers of the sample separated by an inert spacer. AgCl electrodes at each end of the channel were used to determine the potential generated by the flow. The measurements were performed using 0.001 M KCl as electrolyte solution, at pH 7.4 ± 0.2. The zeta potential, ζ, is calculated from:

$$\zeta = (V_S/\Delta p) \times (\eta/\varepsilon\varepsilon_0) \times (L/A) \times (1/R) \qquad (1)$$

where VS is the streaming potential, Δp the hydrodynamic pressure difference across the sample, η is the viscosity and ε the permittivity of the liquid, ε_0 the permittivity of free space, L and A are the length and cross sectional area of the sample and R is the electrical resistance across it. Fairbrother and Mastin's [7] approach was used to determine the term L/A.

For surface tension and contact angle determinations, water, glycerol and diiodomethane (Merk Schuchardt, > 99%) were the test liquids. Water was distilled and deionised, while diiodomethane was doubly distilled under vacuum. Contact angles were measured on the DLC coated surfaces using the sessile drop technique in a video-base system DATA Physics Contact Angle System OCA 15. The drop is deposited directly on the surface of the material from a micrometric syringe with a metallic needle. The ellipse method was used to fit a mathematical function (Laplace–Young Fitting) to the measure drop contour line. For each experiment, were analysed no less than 12 drops. The measurements were carried out at 25 °C inside a refrigerated stainless steel chamber, with glass windows of optical quality and saturated with the liquid in analysis. Young's equation establishes the contact angle of a liquid drop resting on a solid surface, θ, from the relation between the surface tension of a liquid in equilibrium with its vapour, γLV, the solid-vapour surface tension, γSV,

and the solid–liquid interfacial tension, γSL:γLVcosθ = γSV − γSL. The Owen and Wendt's approach [8] postulates that the total surface tension can be expressed as the sum of the dispersive, γd, and the polar, γp, components. The solid–liquid interfacial tension can be rewritten as:

$$\gamma_{SL} = \gamma_{SV} + \gamma_{LV} - 2\sqrt{\gamma_{SV}^d \gamma_{LV}^d} - 2\sqrt{\gamma_{SV}^p \gamma_{LV}^p} \qquad (2)$$

Using Young's equation and Eq. (2), γSV and γSL can be determined taking the values of contact angles measured with some testing liquids whose surface tension components are known.

A simulated body fluid (SBF) solution was prepared as reported in literature [9] for in vitro testing, by dissolving reagent-grade $NaCl$, $NaHCO_3$, KCl, $K_2HPO_43H_2O$, $MgCl_26H_2O$, $CaCl_2$ and Na_2SO_4 into deionised water, and buffered at pH 7.40 with tris(hydroxymethyl)amminomethane (($CH_2OH)_3CNH_3$) and hydrochloric acid (HCl) at 37 °C. Triplicate samples were soaked into SBF solution in sterile polystyrene bottles for 7, 21 and 35 days. A ratio of solution volume to surface area of the specimen was kept at 0.1 ml/mm^2. After soaking, samples were analyzed using SEM to detect apatite layer formation, and changes in ionic concentrations were evaluated by inductive plasma coupled atomic emission spectrometry (ICP-AES). Changes in the pH of the fluid were also registered.

MG63 osteoblast-like cells were cultured in α-Minimal Essential Medium containing 10% fetal bovine serum, 50 µg ml^{-1} ascorbic acid, 50 µg ml^{-1} gentamicin and 2.5 µg ml^{-1} fungizone, at 37 °C in a humidified atmosphere of 5% CO_2 in air. For subculture, adherent cells were enzymatically released (0.05% trypsin, 0.25% EDTA) and cultured (10^4 cell cm^{-2}) for 3 days in control conditions (absence of materials, standard polystyrene tissue culture plates) and on the DLC coated Si_3N_4 material surface. Control cultures and seeded DLC films were evaluated for cell adhesion and morphology (SEM) and cell viability/proliferation (MTT assay). For SEM observation, samples were fixed with 1.5% glutaraldehyde in 0.14 M sodium cacodylate buffer (pH 7.3), dehydrated in graded alcohols, critical-point dried, sputter-coated with gold and analysed in a JEOL JSM 6301F scanning electron microscope. Cultures were observed at 1, 5, 24 and 72 h. In the MTT assay, cultures were incubated with 0.5 mg ml^{-1} of MTT (3-[4,5-dimethylthiazol-2-yl]–2,5-diphenyltetrasodium bromide) during the last 4 h of the culture periods tested (24 and 72 h); the medium was then decanted, formazan salts were dissolved with 200 µL of dimethylsulphoxide and the absorbance was measured at 600 nm in an ELISA reader. The results were normalized in terms of macroscopic area and expressed as A cm^{-2}.
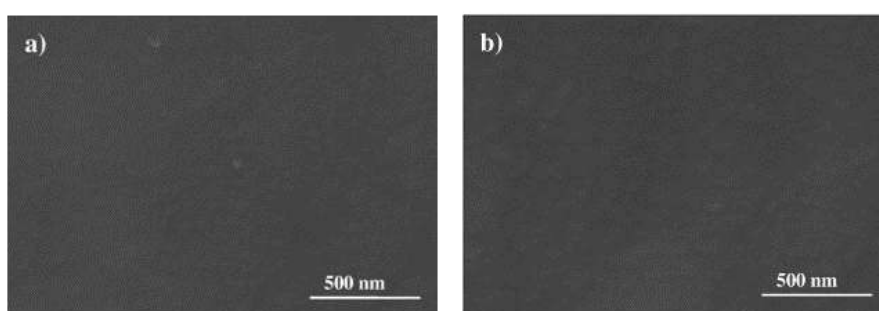
Results and discussion

Figure 1 shows the surface of DLC coated Si_3N_4 samples before (a) and after 35 days of immersion in SBF solution (b), as observed by SEM. No apatite layer or any other type of deposits can be seen on these ultra-high smooth surfaces. Also, ICP measurements showed no significant changes on the ionic concentration levels of calcium, phosphorous, magnesium and sodium with immersion time. The DLC coated surface is only slightly negative charged, as denoted by the zeta potential value of − 35.0 ± 1.3 mV at pH 7.4 ±0.2, which explains the low Ca^{2+} ions adsorption that would be imperative for further nucleation of an amorphous apatite layer.

Figure 1 – Surface of DLC coated Si_3N_4 samples before (a) and after 35 days of immersion in SBF solution (b), as observed by SEM.

The surface tension of DLC coated samples was found to be 45.7 mN/m (Table 1). The dispersive component of the surface tension is predominant (36.6 mN/m), corresponding to a contribution of about 80% to the total surface tension. Values in Table 1 were calculated from the measurements of contact angles on DLC (65.8° ± 5.8° for water; 55.4° ± 4.7° for glycerol; and 40.9° ± 3.8° for diiodomethane), which are in the range of the values published in the literature, obtained for samples coated with DLC by other methods [11].

Table 1 - Surface tension of testing liquids [10] and the values determined for the DLC-coated Si3N4 biomaterial.

	Surface tension (mN/m)	Dispersive component (mN/m)	Polar component, (mN/m)
Water	71.5	21.4	50.1
Glycerol	63.4	37.0	26.4
Diiodomethane	50.5	50.5	0
DLC coatings	45.7	36.6	9.1

MG63 osteoblast-like cells were used for a quick screening biocompatibility assay of the prepared DLC coated Si_3N_4 samples. After cell plating, few cells were able to attach to DLC films, as evident in Figure 2a, showing the appearance of the surface at 1 h. After 24 h, adherent cells presented a normal morphology (Figure 2b). Neighbouring cells have connection with each other through cytoplasmic extensions and proliferated with culture time (Figure 2b and c). As compared to control cultures (performed in standard polystyrene tissue culture plates), MTT reduction was very low at 24 h, but results at 72 h showed that cell growth rate was significantly higher on the seeded DLC surface (Figure 3).
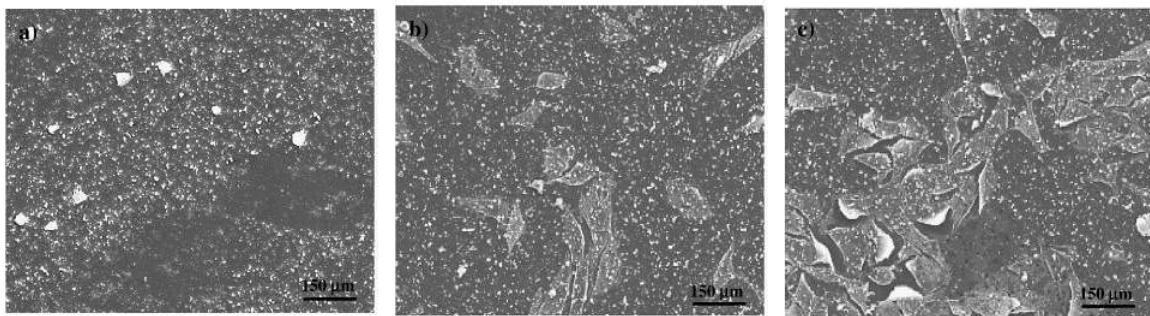
Figure 2 – Surface of DLC coated Si_3N_4 samples seeded with MG63 osteoblastic-like cells. SEM appearance at 1 h (a), 24 h (b) and 72 h (c).
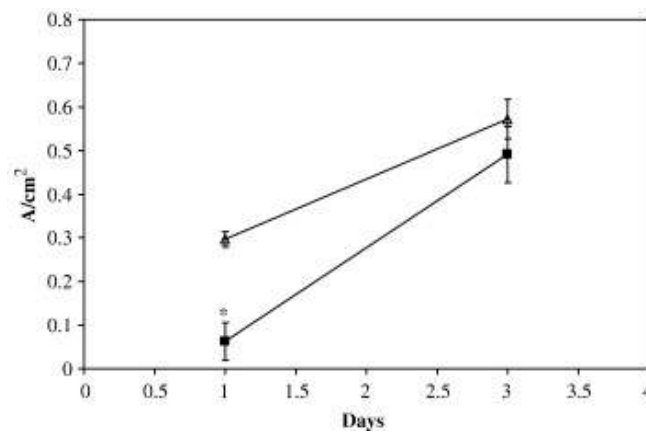
Figure 3 - Cell viability/proliferation. Control (▲) and DLC surface (■). *Significantly different from control.

It is well known that surface charge, along with wettability, plays an important role in the biological response to implant materials and, despite the widely varied observations reported in the literature, some generalizations may be made from in vitro

published studies [12]. Given that virtually all interfaces are charged in aqueous solution, and that biomolecules carry a net charge, it is intuitive that electrostatic interactions will play a role in the cell response. Moderately hydrophilic surfaces appear to induce more favourable cell responses than hydrophobic materials, by favouring adsorption of proteins and better preserving their bioactivity. Both positively- and negatively-charged surfaces are able to bind adhesion proteins and support cell adhesion. However, the mode of cell adhesion is distinct for positive and negative charges, since cell membranes, that carry a negative charge, adhere very closely to positively charged surfaces, whereas contact occurs only at distinct points on near-neutral and negatively charged surfaces [13-15]. These differences can be attributed primarily to electrostatic attraction and repulsion, respectively, but also demonstrated quantitative and qualitative patterns in protein adsorption and functionality. The results of the present work regarding the interaction of MG63 osteoblastic cells with the DLC coated Si3N4 material during the first 24 h do not suggest an optimum surface for cell adhesion. Although with an optimized experimental design favouring the cell adhesion process (plating of a cell suspension over a plane surface), only few cells were able to attach to the DLC films, as evident by SEM observation and also from the MTT reduction values measured at 24 h. The negative value of ZP of the surface may have contributed, in synergy with its wettability properties, to the poor cell adhesion observed. However, it is worth to mention that attached cells presented a normal pattern of cell spreading displaying the typical morphology at 24 h without no evidence of cytotoxicity. In addition, compared to the cell behaviour observed in standard polystyrene culture plates, the DLC adherent cells showed a significantly higher cell growth rate, as suggested by the MTT assay. These observations are in line with previous biocompatibility studies performed in several cell culture systems, namely mouse peritoneal macrophages, mouse fibroblasts, murine macrophage cell line IC-21, human synovial fibroblasts, osteoblast-like SaOS-2 cells and glial and fibroblast cell lines with no indication of cytotoxicity in vitro and cell growth kinetics studies reporting that cells generally grew faster on DLC [[16], for a review].

Conclusions

The excellent set of intrinsic characteristics of Si3N4 (bioinertness, low density, high fracture toughness) ceramics can be further improved by adherent, biocompatible, auto-lubricious, DLC coatings, regarding hip replacement medical applications. The DLC films are slightly negative surface charged, exhibiting a zeta potential of − 35.0 ± 1.3 mV. The total surface tension is 45.7 mN/m, with a minor polar component (9.1 mN/m), which turns the DLC coating quite hydrophobic. As a result of this, DLC

showed no apatite layer formation ability in vitro testing using an acellular simulated body fluid (SBF). Also, no evidence of cytotoxicity was demonstrated by cells normal morphology and higher cell growth rate compared to standard culture plates, although with low cell adhesion. These properties render DLC-coated Si3N4 attractive to be used as femoral head and the acetabulum hip joint components, in which cell adhesion is not desirable.

References

1. Sargeant A, Goswami T. Hip implants: Paper V. Physiological effects. Mater Des 2006;27:287-307.

2. Petzow G, Herrmann M, in: M. Janson (Ed.), High Performance Non-Oxide Ceramics II, Structure and Bonding, vol. 102, Springer-Verlag, Berlin, 2002.

3. Narayan RJ. Nanostructured diamondlike carbon thin films for medical applications. Mater Sci Eng C 2005;25:405-416.

4. Cui FZ, Li DJ. A review of investigations on biocompatibility of diamond-like carbon and carbon nitride films. Surf Coat Technol 2000;131:481-487.

5. Zhao Q, Liu Y, Abel EW. Effect of temperature on the surface free energy of amorphous carbon films. J Colloid Interface Sci 2004;280:174-83.

6. Vila M, Abreu CS, Salgueiredo E, Almeida FA, Fernandes AS, Costa FM, Gomes JR, Silva RF. Reciprocating sliding behaviour of self-mated amorphous diamond-like carbon coatings on Si3N4 ceramics under tribological stress. Thin Solid Films 2006;515:2192-6.

7. Fairbrother F, Mastin H. Studies in electro-endosmosis. Part I. J Chem Soc 1924;75: 2319-30.

8. Owens DK, Wendt RC. Estimation of the surface free energy of polymers. J Appl Polym Sci 1969;13:1741-7.

9. Kokubo T, Takadama H. How useful is SBF in predicting in vivo bone bioactivity? Biomaterials 2006;27:2907-15.

10. Strom G, Fredriksson M, Stenius P. Contact angles, work of adhesion, and interfacial tensions at a dissolving Hydrocarbon surface. J Colloid Interface Sci 1987;119:352-61.

11. Schulz H, Leonhardt M, Scheibe HJ, Schultrich B. Ultra hydrophobic wetting behaviour of amorphous carbon films. Surf Coat Technol 2005;200:1123-6.

12. Wilson CJ, Clegg RE, Leavesley DI, Pearcy MJ. Mediation of biomaterial-cell interactions by adsorbed proteins: a review. Tissue Eng 2005;11:1-18.

13. Haynes CA, Norde W. Globular proteins at solid/liquid interfaces. Colloids Surf B 1994:2:517-566.

14. Shelton RM, Rasmussen AC, Davies JE. Protein adsorption at the interface between charged polymer substrata and migrating osteoblasts. Biomaterials 1988;9:24-9.

15. Dames JE, Causton B, Bovell Y, Davy K, Sturt CS. The migration of osteoblasts over substrata of discrete surface charge. Biomaterials 1986;7:231-3.

16. Dearnaley G, Arps JH. Biomedical applications of diamond-like carbon (DLC) coatings: A review. Surf Coat Technol 2005;200:2518-2524.

Chapter 3

Cell adhesion and proliferation over Zinc-glass reinforced hydroxyapatite composites

Cell adhesion and proliferation over Zinc-Glass Reinforced Hydroxyapatite Composites (Zn-GRHA)

N. Sooraj Hussain[1,2], P. S. Gomes[3], M.A. Lopes[4], M.H. Fernandes[3] and J. D. Santos[4]

1 - INESC Porto, Rua do Campo Alegre, 687, 4169-007 Porto, Portugal.

2 - Departamento de Física, Faculdade de Ciências, Universidade do Porto, Rua do Campo Alegre, 687, 4169-007 Porto, Portugal

3 - Laboratório de Farmacologia e Biocompatibilidade Celular, Faculdade de Medicina Dentária, Universidade do Porto, Rua Dr. Manuel Pereira da Silva, 4200-393 Porto, Portugal.

4 - Departamento de Engenharia Metalúrgica e Materiais, Faculdade de Engenharia, Universidade do Porto, Rua Dr. Roberto Frias, 4200-465 Porto, Portugal.

Abstract

Hydroxyapatite (HA), $Ca_{10}(PO_4)_6(OH)_2$, and tricalcium phosphate (TCP) bioceramics have been used as a graft materials in vivo. However, zinc is a biosafe, biocompatible element, and incorporation of Zn could favor for specific proliferative effect on osteoblastic cells and inhibitory effect on osteoclastic bone resorption. Therefore, this paper investigates the preliminary results and potential impact on zinc glass reinforced hydroxyapatite (Zn-GRHA) on cell proliferation studies. The biological behaviour of Zn-GRHA samples was assessed by confocal laser scanning microscopy and material characterization performed by SEM-EDX and XRD analysis. From these results, an increased proliferation and a confluent cell layer were verified in some areas of the material surface, at day 2. Cells were spread all over the material surface and established multiple cell-to-cell interactions relying on prominent cytoplasmic processes. At day 6, a confluent cell monolayer was verified on the Zn-GRHA material's surface.

Introduction

In tissue engineering strategies, there is a great effort into the development of degradable tridimensional scaffolds since they allow for improved cell transport and viability, both for soft and hard tissue regenerative approaches. After implantation, they should allow for cell proliferation and maintenance of the local phenotype, at the same time that should be gradually resorbed and substituted by natural formed tissue [1]. Scaffold constructs made of natural and synthetic polymers have limited applications, since they are mechanically weak and report an inadequate degradation profile [2]. On the other hand, bioceramics are widely used, especially within hard tissue regeneration, due to their physicochemical and mechanical properties [3].

Bone tissue engineering strategies may reach hand from a diverse range of bioactive ceramic materials that have been employed to repair bone associated defects, namely because of their adequate biocompatibility and ability to bond with mineralized tissues. Synthetic hydroxyapatite (HA), with the chemical composition of $Ca_{10}(PO_4)_6(OH)_2$, is one of the most widely available and clinically used biomaterials, although it differs from the biological apatite (the mineral content of the bone extracellular matrix) regarding composition, crystalinity, stoichiometry, and reports a low dissolution rate, limited physical and mechanical properties, when implanted in vivo [4]. Biological apatite results from crystal nucleation and mineralization events that occur naturally in mammals' biological systems, both in physiological (i.e., bone tissue remodeling and teeth formation) and pathological (i.e., hyperostosis and ossifying cartilage) conditions. Deposited crystals have been shown to adapt (both in terms of crystalinity and orientation), according to mechanical strength and turnover characteristics of the local tissue. Several ionic substitutions within the lattice are reported and seem to modulate these processes [5, 6]. These substitutions include carbonate, fluoride, chloride, sodium, magnesium, potassium and zinc, among others, and although the exact role of many of these ions has not been established yet, most of them seem to play an important role in the physiological process of bone remodeling [7], as well as during bone healing [8].

Zinc has been recognized to be essential for animals' and humans' metabolic processes since the mid-20th century. It is known to be an essential trace element during fetal growth and development [9-10] and it plays an important biological role since it is a cofactor for more than 200 enzymes and is a constituent of nearly every cell type in the human body [11]. It contributes to the immune response, wound healing and participates actively on the bone metabolic process, namely by inducing osteoblastic proliferation, biomineralization and bone formation [12, 13]. Including, it is a co-factor of the alkaline phosphatase (ALP) enzyme, which is known to play an

important role in the initiation of the mineralization process of the extracellular matrix, during in vitro and in vivo bone formation [12, 14]. Selected concentrations of Zn increase ALP activity on osteoblastic cells [12, 15]. On the other hand, Zn deficiencies led to the activation of the monocyte-macrophage lineage affecting the cell-mediated immune response [16] and, in the elders, it has been associated with the development of osteoporosis [17].

In order to assure a local delivery of adequate amounts of Zn, several attempts have been assayed including the development of Zn-containing bone-regenerative bioceramics. Webster et al. showed that Zn-doped HA improved osteoblast adhesion when compared to undoped HA [18]. Ramaswamy et al. report that the incorporation of Zn into a Ca-Si system, forming Hardystonite ($Ca_2Zn-Si_2O_7$) improved the mechanical properties of the ceramic, as well as its bioactivity, by inducing the attachment, proliferation and differentiation of human bone marrow-derived osteoblastic cells, comparing to $CaSiO_3$ [19]. Further, this ceramic allowed the differentiation of mature and functional osteoclasts, reflected by the presence of resorption imprints, while $CaSiO_3$ failed to allow the differentiation of osteoclasts from their hematopoietic precursors [19]. Ikeuchi et al. reported an increased osteogenic differentiation (assessed by ALP activity and matrix mineralization) both in human- and rat-derived bone marrow cells, cultured on the surface of Zn-releasing Ca-P ceramics [20].

In vivo anabolic effects have also been achieved with Zn-containing bioceramics that reported a quantitative stimulation in bone formation around implants and bone mineral density (BMD), in a model of femoral implants in rabbits [21]. Furthermore, Zn has been shown to induce bone remodeling and regeneration in experimental models of systemic pathological conditions. For instance, the controlled release of Zn has been shown to increase BMD in osteoporotic rats [22], while a composite ceramic of Zn-tricalcium phosphate and HA has shown increased stability at the bone-implant interface in osteopenic rabbits, comparing to control (composite ceramic of TCP and HA) [23]. Further, the intramuscular injection of ZnTCP powders increased the BMD in the vicinity of the injection site, in a Zn^{2+}-deficient osteopenic rat model [24].

Zn has also proven to be a useful antibacterial agent in bone associated infections. When associated with glass-based cements and coatings for bone regeneration, Zn has proven activity against Staphylococcus aureus and other bacteria associated with acute or chronic bone infections [25, 26].

In this work, the authors report the preparation, characterization and biological assessment of two compositionally different novel Zn-glass reinforced hydroxyapatite

composites obtained by a liquid phase sintering process, via the combination of ZnO-P_2O_5-CaO-Na_2O-CaF_2 glass with a HA matrix. Biological assessment was conducted in vitro by the direct culture of MG63 human osteoblast-like cells over the composites. HA was used as control.

Previously, the present group has developed and characterized, both in vitro and in vivo, the osteogenic potential of a CaO-P_2O_5-Na_2O-CaF_2 glass reinforced hydroxyapatite, without ZnO, and patented the composite as Bonelike®. When compared to HA, Bonelike® reports enhanced bioactivity and improved mechanical properties resulting from the addition of the phosphate based bioactive glasses. During the sintering process, these glasses induce HA decomposition into β-tricalcium phosphate, which in turn, at higher sintering temperatures, is decomposed into α-tricalcium phosphate [27, 28]. Bonelike® appears to induce bone formation through specific activation of osteoblasts with the regulated release of ionic species, namely F^-, Mg^{2+}, Na^+, among others. The incorporation of ZnO is expected to further improve the composite bioactivity.

Materials and Methods

Preparation of ZnO glasses

Two ZnO based glasses (5ZnO or 10ZnO), with a chemical composition of $xZnO$–(70-x) P_2O_5–15CaO- 5Na_2O- 10CaF_2 (%mol), where x = 5 or 10, have been prepared by employing conventional glass making techniques as described in Chap. 6 of this book. Briefly, reagent analytical graded chemicals, i.e., ZnO, P_2O_5, $CaHPO_4$, Na_2CO_3 and CaF_2 were mixed and placed in a platinum crucible for about an hour, in an electrical furnace at 1450 °C. Following, the prepared glasses were crushed and sieved to granules (≤ 75 μm).

Preparation of the Hydroxyapatite (HA)

HA, with the chemical composition of $Ca_{10}(PO_4)_6(OH)_2$, has been prepared in accordance with the following chemical equation: $10Ca(OH)_2 + 6H_3PO_4 \rightarrow Ca_{10}(PO_4)_6(OH)_2 + 18 H_2O$, as described in Chap. 6 of this book.

In brief, analytical grade calcium hydroxide - $Ca(OH_2)$ - and ortho phosphoric acid - H_3PO_4 - have been independently mixed with deionised water and subsequently, $Ca(OH_2)$ has been slowly transferred into H_3PO_4, during 4 hours, in constant mixing conditions (100 rpm) and with maintenance of the pH at 10.50. After 24 hours, the material was filtered to remove the excess of water and dried, at 60°C, for approximately 48 hours. The dried product was finally crushed and sieved to granules (≤ 75 μm). Following, they were isostatically pressed at 200 MPa and the obtained

disks were sintered at 1300°C for 1 hour. After cooling, specimens were polished down to 1 mm finishing using silicon carbide paper, ultrasonically degreased with ethanol and cleaned with deionised water. Prior to cell seeding, HA discs were sterilized in a steam autoclave. HA was used as control.

Preparation of Zn-GRHA Composites

The Zn-GRHA composites were obtained by mixing 2.5%wt of either 5ZnO- or 10ZnO-based glasses with HA, in isopropanol. Composites were designated, respectively, as 5Zn-GRHA and 10Zn-GRHA. The obtained composites were dried at 60°C for 24 hours and sieved to less than 75 μm. Composite disks were prepared following isostatic pressure and sintering, as previously reported for HA. Zn-GRHA discs were sterilized in a steam autoclave.

Materials' Characterization

X-ray diffraction (XRD) was performed on powder samples of 5ZnO and 10ZnO glasses, as well as on 5Zn-GRHA, 10Zn-GRHA and HA, by using Siemens D 5000 diffractometer with Cu-Kα radiation (λ= 1.5418Å). The scans were made in the range of 25-40° (2θ) with a step size of 0.02° and a count time of 2 sec/step. A scanning electron microscopy (JEOL JSM 630IF), equipped with an energy dispersive analyzer, was used to investigate the microstructure of the samples.

In vitro testing with osteoblastic cells

MG63 cells, human osteosarcoma-derived osteoblastic cells, were cultured in a standard culture medium, α-Minimal Essential Medium, supplemented with 10% foetal bovine serum, ascorbic acid (50 μg.ml^{-1}), penicillin-streptomicin (100 IU.ml^{-1} and 10 mg.ml^{-1}, respectively) and fungizone (2.5 μg.ml^{-1}), at 37ºC, in a humidified atmosphere of 5% CO_2 in air. For subculturing, adherent cells were enzymatically released (5 minutes at 37ºC - 0.05% trypsin - 0.25% EDTA) and resuspended in complete medium for reseeding.

Cells were cultured at a density of 10^4 cells.cm^{-2}, for 6 days, on the surface of HA, 5Zn-GRHA and 10Zn-GRHA discs, that had been previously immersed in complete culture medium for 1h. Seeded material samples were evaluated throughout the incubation time at days 1, 2 and 6, for cell morphology and cell growth, by confocal laser scanning microscopy (CLSM), following the subsequent technique. Briefly, cells grown over the samples were fixed in 3.7% methanol-free formaldehyde and permeabilized with 0.1% Triton. Cell cytoskeleton filamentous actin (F-actin) was visualized by treating the fixed cells with Alexa Fluor® 488-conjugated phalloidin dye

(1:100 in PBS, 20 minutes), after initial incubation with bovine serum albumin (10mg.ml-1 in PBS 1 hour), in order to block non-specific interactions. Cells were counterstained with propidium iodide (10 mg.ml^{-1}) for cell nuclei labelling, for 10 minutes. Labeled cultures were mounted in Vectashield® and examined with a Leica SP2 AOBS (Leica Microsystems®) microscopy.

Results and Discussion

Physicochemical and morphological analysis of the Zn-GRHA composites

      The EDX analysis of 5ZnO and 10ZnO glasses are reported on Figure 1, while the microstructure of the glasses' surface is shown on Figure 2, where representative SEM micrographs are presented at 150x and 1000x magnification.
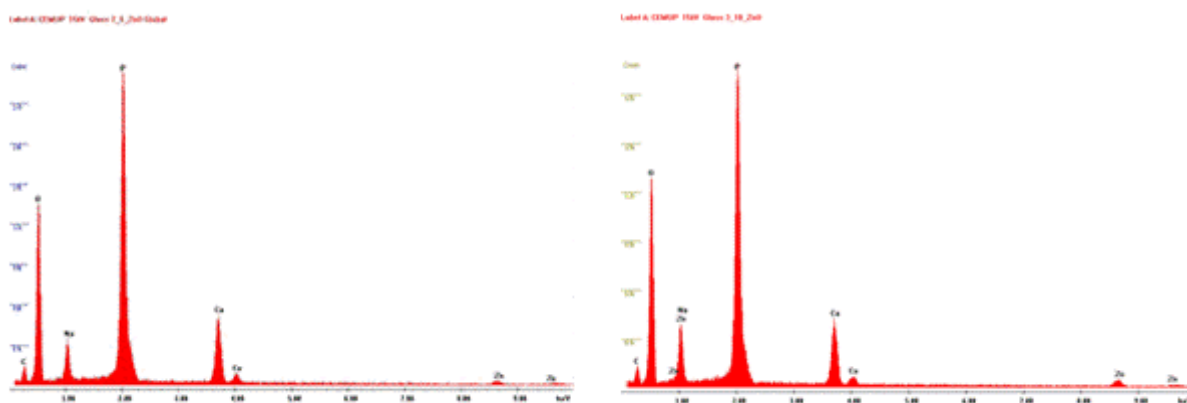
Figure 1 - EDX analysis of ZnO-based glass materials: 5ZnO (left) and 10ZnO (right).
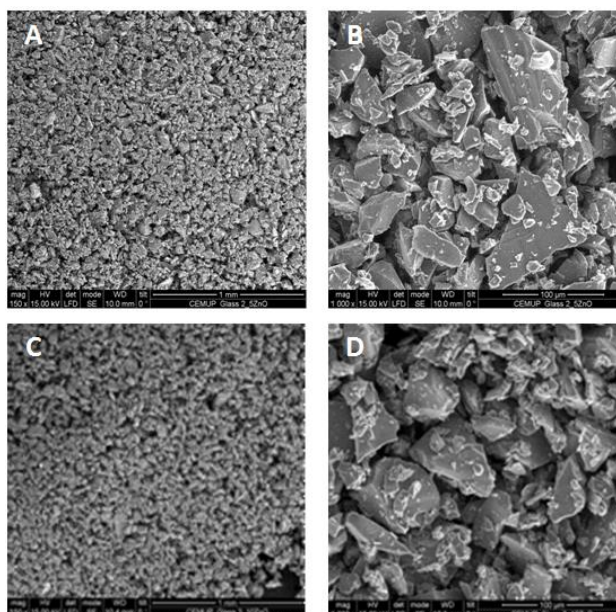
Figure 2 - SEM micrographs of 5ZnO (A and B) and 10ZnO-based glasses (C and D). A and C - 150x magnification. B and D – 1000x magnification.

Similarly, Figure 3 shows the EDX analysis of 5Zn-GRHA and 10Zn-GRHA composites, while Figure 4 reports high magnification SEM images of the composites' surface.
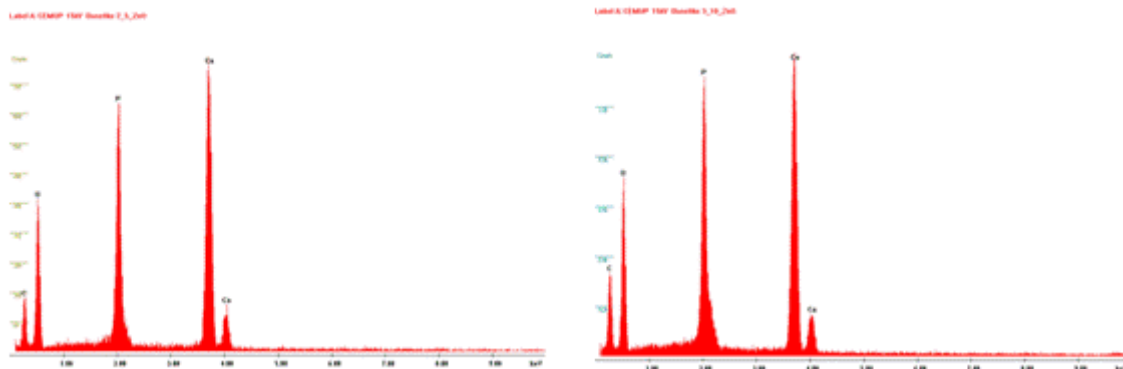
Figure 3 - EDX analysis of 5Zn-GRHA (left) and 10Zn-GRHA composites (right).

When observing the microstructure of the Zn-GRHA composites by EDX (Figure 3), Zn was not detected although this element was identified by the same analysis, conducted on the prepared glasses (Figure 1). This might be related to the fact that the composites contain only a small amount of added glass (2.5%wt). In addition, Zn also might be expected to become widely distributed throughout the crystallographic structure of the composite, following the sintering process.

SEM evaluation of the composites' surface showed that both 5Zn-GRHA and 10Zn-GRHA are almost fully dense materials (Figure 4).
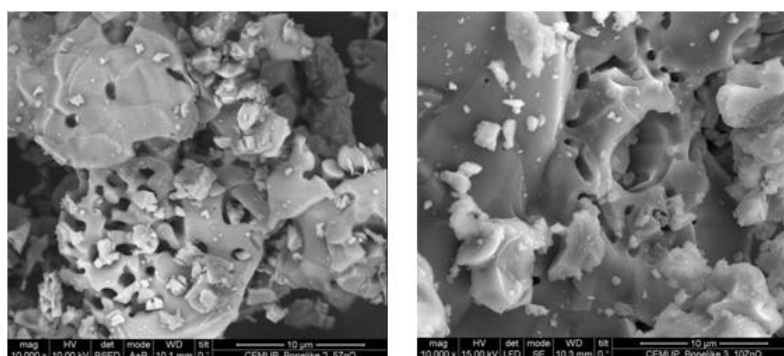
Figure 4 - SEM micrographs of 5Zn-GRHA (left) and 10Zn-GRHA (right) composites, with a magnification of 10000x.

Figure 5 shows the XRD phase analysis of prepared HA, which reveals a pure phase material. The XRD of 10Zn-GRHA composite is shown in Figure 6. From this diffractogram, the following phases can be identified: HA - $Ca_{10}(PO_4)_6(OH)_2$, β- and α-TCP - $Ca_3(PO_4)_2$. No zinc containing phases were detected. It means that the zinc ions

are expected to be incorporated in the tridimensional lattice of HA or TCP phases. Further, Rietveld analysis of the XRD spectrum obtained should be done to confirm this incorporation by quantifying the lattice parameters and the distortion index.

The presence of TCP phases in the composition of the Zn-GRHA were expected, since previous reports of this research team have already demonstrated that the liquid sintering process leads to the reaction of HA with the added glass, resulting in a partial conversion of HA into TCP phases [27, 28].
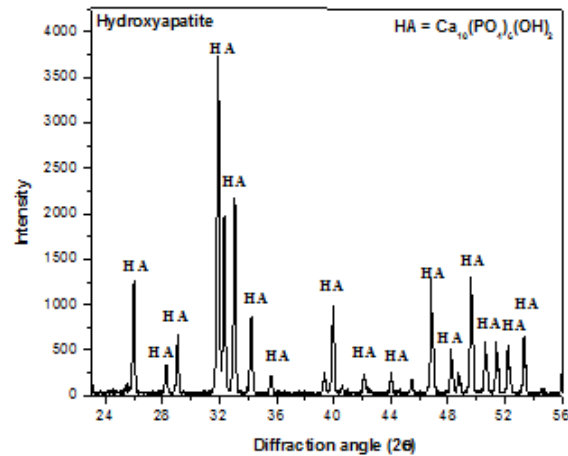
Figure 5 - XRD diffraction pattern of the prepared Hydroxyapatite.
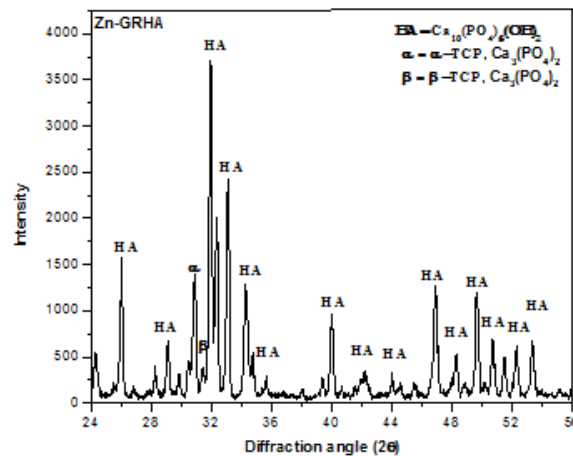
Figure 6 - XRD diffraction pattern of the 10Zn-GRHA composite.

In vitro biocompatibility of the Zn-GRHA composites

MG63 human osteoblast-like cells were cultured on the surface of 5Zn-GRHA, 10Zn-GRHA and HA samples for 6 days. The biological assessment of the seeded materials was established by confocal laser scanning microscopy, following staining for

F-actin cytoskeleton and nucleus counterstaining. Representative micrographs of the colonized surfaces are shown in Figures 7 – 9.

CLSM images of seeded HA samples, at day 2 of culture (Figure 7A), revealed that the materials' surface was colonized with well-spread MG63 cells, establishing multiple cell-to-cell contacts. Cells proliferated actively throughout the culture time and, at day 6, a significant percentage of the materials' surface allowed the organization of high cell density areas (Figure 7D). Comparing to HA, both 5Zn-GRHA (Figure 7B) and 10Zn-GRHA (Figure 7C) reported improved adhesion and early proliferation events, since an increased cell number was visualized on both composites' surface, at day 2. Comparatively, and in a qualitative way, significant more cells could be visualized over the 10Zn-GRHA surface. Following, at day 6 of culture, multiple cell layers could be visualized over both composites (Figure 7E and 7F).

Attained differences might be associated with the composition of the tested materials as well as with differences regarding surface microstructure, which can be assessed on Figure 8, by CLSM, following immersion in complete culture medium for 6 days.
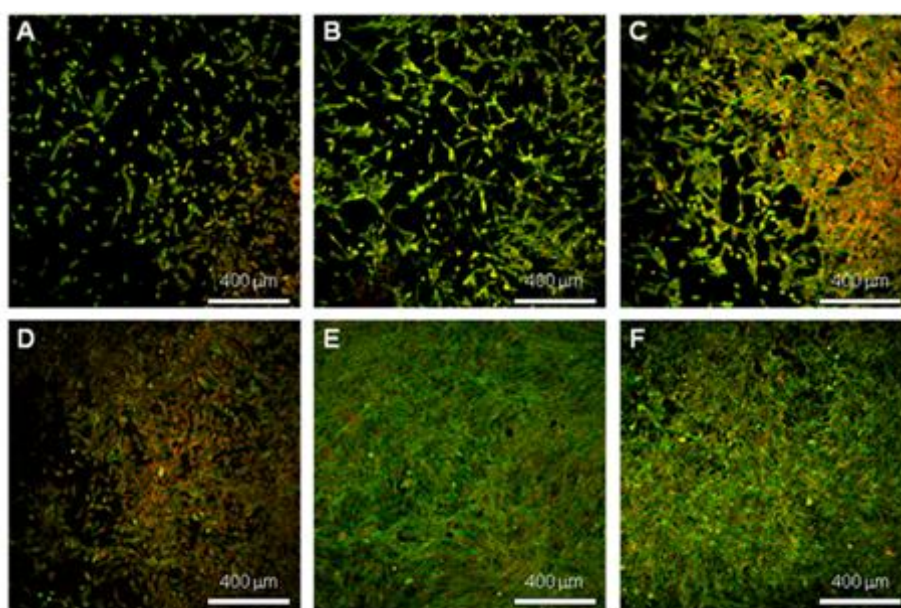
Figure 7 - Proliferation of MG63 cells seeded on HA (A, D), 5Zn-GRHA (B, E) and 10Zn-GRHA (C, F), at 2 (A, B and C) and 6 (D, E and F) days of culture. CLSM observation following actin filaments (green) and nucleus (red) staining.
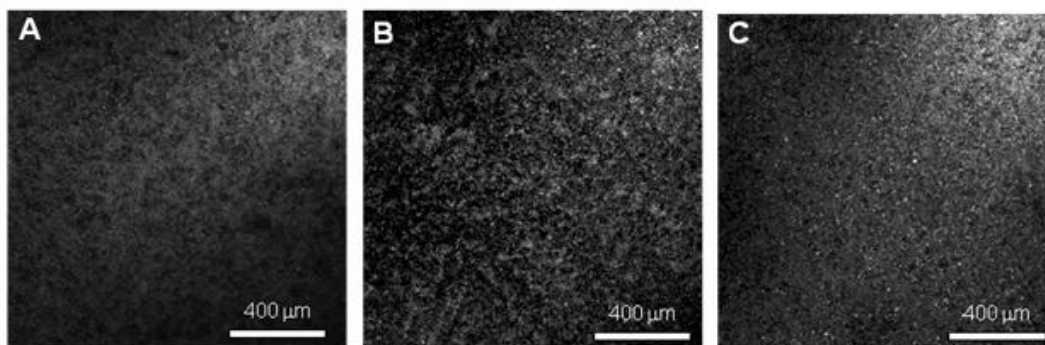
Figure 8 - Surface characteristics of HA (A), 5Zn-GRHA (B) and 10Zn-GRHA (C) samples. CLSM observation of the materials, following 6 days of incubation with fully supplemented culture medium.

Regarding morphological analysis, all the biomaterials allowed the display of normal cell morphology, with adequate cytoplasmic spreading, prominent nucleus and nucleoli, as well as numerous filipodia that contributed to the extensive cell-to-cell contact. Representative data is presented in high magnification micrographs of Figure 9, regarding the seeded materials at 24 hours of culture.
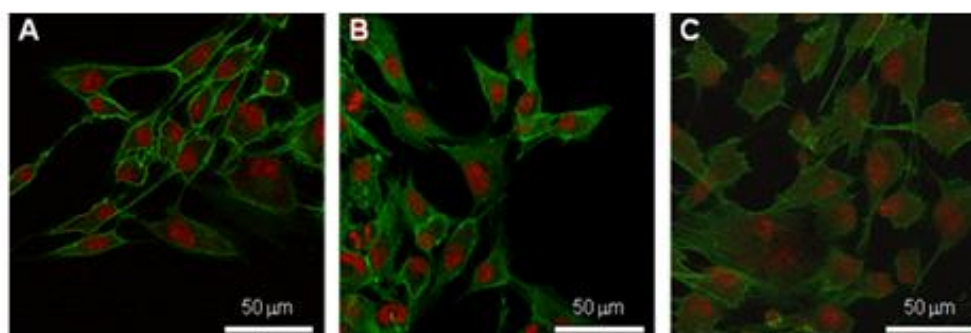
Figure 9 - High-magnification morphologic appearance of MG63 cells seeded on HA (A), 5Zn-GRHA (B) and 10Zn-GRHA (C), at 24 hours of culture. CLSM observation following actin filaments (green) and nucleus (red) staining.

The acquisition of normal morphology following adhesion is in agreement with the adequate reorganization of the cytoskeleton during the first 12-24 hours. The cytoskeleton is a dynamic structure that maintains cell shape, enables cellular motion and plays an important role, both in intracellular transport and cellular division. Further, the dynamic regulation of cytoskeleton is very sensitive to substrates' characteristics and early disturbances, associated with chemical or physical properties may compromise adhesion, proliferation and differentiation events [29]. In this way, early cytoskeleton re-organization events might be of relevance to the cell long term fate on the biomaterials' surface.

Obtained results converge to an improved biological performance of Zn-GRHA composites, comparing to HA. Both formulations (5Zn-GRHA and 10Zn-GRHA) increased cell proliferation at days 2 and 6 of the established culture system. Also, in all experimental conditions, seeded cells presented an adequate cytoskeleton organization, compatible with adhesion to a non cytotoxic substrate. These results are in line with previous reported in vitro and in vivo studies carried out on various Zn-containing or Zn-releasing ceramic substrates [12, 18-26].

Some mechanisms have been purposed to justify the anabolic effect of Zn over bone metabolism, including the increased activity of aminoacyl-tRNA synthetase, an enzyme associated with the initiation of protein synthesis [30]. This initial event is connected to the production of ALP and type I collagen by osteoblastic cells [31]. Even so, although Zn may be adequate to treat bone-associated diseases, a high concentration of this ion may induce significant cytotoxicity over cells [32]. Yamamoto evaluated the cytotoxicity of zinc salts and reported that the IC50 of zinc for MC3T3-E1 osteoblastic cells was about 5.85 mg/l [33]. In addition, the releasing conditions of Zn may also determine its biological role: for instance, an eventual initial burst, which is obtained in many delivery systems, may be adverse for biological tissues. In this way, it is clear that the therapeutic index for Zn is very narrow and that a strictly controlled slow and sustained release rate must be assured for the establishment of an eventual anabolic effect over the biological tissues.

Conclusions

The novel Zn-glass reinforced hydroxyapatite composites have reported adequate biocompatibility, further enhancing adhesion and proliferation of human osteoblastic-like cells. Regarding biological evaluation by confocal laser scanning microscopy, increased cell adhesion was verified in Zn-GRHA materials compared to pure phase HA. Also, Zn-GRHA composites induced cell proliferation in a more effective way than HA and, at 6 days of culture, multiple cell layers were visualized on the surface of both composites.

Although further in vitro and in vivo studies must be accomplished to assess the osteoblastic response of these materials, composites of the Zn-GRHA system may be adequate scaffolds for bone tissue engineering applications.

References

1. Sachlos E, Czernuszka J. Making tissue engineering scaffolds work. Review: the application of solid freeform fabrication technology to the production of tissue engineering scaffolds. Eur Cell Mater 2003;30:29-40.

2. Sheridan M, Sheaa L, Peters M, Mooney D. Bioabsorbable polymer scaffolds for tissue engineering capable of sustained growth factor delivery. Journal of Controlled Release 2000;64:91-102.

3. Karageorgiou V, Kaplan D. Porosity of 3D biomaterial scaffolds and osteogenesis. Biomaterials 2005;26:5474-91.

4. Suchanek W, Yoshimura M. Processing and properties of hydroxyapatite-based biomaterials for use as hard tissue replacement implants. Journal of Materials Research 1998;13:94-117.

5. Driessens F. Formation and stability of calcium phosphate in relation to the phase composition of the mineral in calcified tissue. In: DeGroot K, editor. Bioceramics of calcium phosphate. Florida: CRC Press; 1983.

6. LeGroz R. Calcium phosphates in oral biology and medicine. In: Myers H, editor. Monographs in oral sciences. Basel: Karger; 1991.

7. Daculsi G, Bouler J, LeGroz R. Adaptative crystal formation in normal and pathological calcifications in synthetic calcium phosphate and related biomaterials. Int Rev Cytol 1997;172:129-91.

8. Buckwalter J, Glimcher M, Cooper R, Becker R. Bone biology, part I: structure, blood supply, cells, matrix, and mineralization. Instr Course Lect 1996;45:376-86.

9. Spadaro JA, Becker RO, Bachman CH. The distribution of Trace Metal ions in Bone and Tendon. Calc TissRes 1970;6:49-54.

10. Prasad AS. Zinc in human health: an update. J Trace Elem Exp Med 1998;11:63–87.

11. Williams R. Zinc: What is its role in biology? Endeavour 1984;8:65-70.

12. Hall S, Dimai H, Farley J. Effects of zinc on human skeletal alkaline phosphatase activity in vitro. Calcif Tissue Int 1999;64:163-72.

13. Ovesen J, Moller-Madsen B, Thomsen J, Danscher G, Mosekilde L. The positive effects of zinc on skeletal strenght in growing rats. Bone 2001;29:565-70.

14. Yoon K, Golub E, Rodan G. Alkaline phosphatase cDNA transfected cells promote calcium and phosphate deposition. Connect Tissue Res 1989;22:17-25.

15. Storrie H, Stupp S. Cellular response to zinc-containing organoapatite: an in vitro study of proliferation, alkaline phosphatase activity and biomineralisation. Biomaterials 2005;26:5492-9.

16. Prasad AS. Effects of Zinc Deficiency on Immune Functions. J Trace Elem Exp Med 2000;13:1-20.

17. Szathmari M, Steczek K, Szucs J, Hollo I. Zinc excretion in osteoporotic women. Orv Hetil 1993;134:911-4.

18. Webster T, Ergun C, Doremus R, Bizios R. Hydroxyapatite with substituted magnesium, zinc, cadmium and yttrium. II. Mechanisms of osteoblast adhesion. J Biomed Mat Res A 2002;59:312-7.

19. Ramaswamy Y, Wu C, Zhou H, Zreiqat H. Biological response of human bone cells to zinc-modified Ca-Si based ceramics. Acta Biomaterialia 2008;in press.

20. Ikeuchi M, Ito A, Dohi Y, Ohgushi H, Shimaoka H, Yonemasu K, et al. Osteogenic differentiation of cultured rat and human bone marrow cells on the surface of zinc-releasing calcium phosphate ceramics. J Biomed Mat Res A 2003;67:1115-22.

21. Kawamura H, Ito A, Miyakawa S, Layrolle P, Ojima K, Naito H, et al. Stimulatory effect of zinc on bone formation around zinc-releasing calcium phosphate ceramics implanted in rabbits femora. J Biomed Mat Res 2000;50:184-90.

22. Otsuka M, Marunaka S, Matsuda Y, Ito A, Naito H, Ichinose N, et al. Effect of particle size on zinc release from zinc containing tricalcium phosphate (Zn-TCP) in Zn-deficient osteoporosis rats. Biomed Mater Eng 2003;13:103-13.

23. Kawamura H, Ito A, Muramatsu T, Miyakawa S, Ochiai N, Tateish T. Long-term implantation of zinc-releasing calcium phosphate ceramics in rabbit femora. J Biomed Mat Res A 2003;65:468-74.

24. Otsuka M, Ohshita Y, Marunaka S, Matsuda Y, Ito A, Ichinose N, et al. Effect of controlled zinc release on bone mineral density from injectable Zn-containing b-tricalcium phosphate suspension in zinc-deficient diseased rats. J Biomed Mat Res A 2004;69:552-60.

25. Osinaga P, Grande R, Ballester R, Simionato M, Delgado-Rodrigues C, Muench A. Zinc sulfate addition to glass-ionomer-based cements: influence on physical and antibacterial properties, zinc and fluoride release. Dent Mater 2003;19:212-7.

26. Bright K, Gerba C, Rusin P. Rapid reduction of Staphylococcus aureus populations on stainless steel surfaces by zeolite ceramic coating silver and zinc ions. J Hosp Infect 2002;52:307-0.

27. Lopes M, Monteiro F, Santos J. Glass reinforced hydroxyapatite: a comprehensive study of the effect of glass composition on the crystallography of the composite. J Biomed Mat Res 1998;39:244-50.

28. Lopes M, Monteiro F, Santos J. Glass-reinforced hydroxyapatite composites: secondary phase proportions and densification effect on biaxial bending strength. J Biomed Mat Res 1998;48:734-40.

29. Stamenovic D. Effects of cytoskeletal prestress on cell rheological behaviour. Acta Biomaterialia 2005;1:255-62.

30. Yamaguchi M, Oishi H, Suketa Y. Zinc stimulation of bone protein synthesis in tissue culture: activation of aminoacyl-tRNA synthetase. Biochem Pharmacol 1988;37:4075-80.

31. Yamaguchi M, Gao Y, Ma Z. Synergistic effect of genistein and zinc on bone components in the femoral-metaphyseal tissues of female rats. J Bone Miner Metab 2000;18:77-83.

32. Aina V, Perardi A, Bergandi L, Malavasi G, Menabue L, Morterra C, Ghigo D. Cytotoxicity of zinc-containing bioactive glasses in contact with human osteoblasts. Chem Biol Interact 2007;167:207-218.

33. Yamamoto A, Honma R, Sumita M. Cytotoxicity evaluation of 43 metal salts using murine fibroblasts and osteoblastic cells. J Biomed Mat Res 1998;39:331-40.

Chapter 4

Cytotoxicity evaluation of nanocrystalline diamond coatings by fibroblast cell cultures

Cytotoxicity evaluation of nanocrystalline diamond coatings by fibroblast cell cultures

M. Amaral[1], P. S. Gomes[2], M. A. Lopes[3,4], J. D. Santos[3,4],R. F. Silva[1], M. H. Fernandes[2]

1 - CICECO, Department of Ceramics and Glass Engineering, University of Aveiro, 3810-193 Aveiro, Portugal

2 - Laboratório de Farmacologia e Biocompatibilidade Celular, Faculdade de Medicina Dentária, Universidade do Porto (FMDUP), Rua Dr. Manuel Pereira da Silva, 4200-393 Porto, Portugal

3 - Faculdade de Engenharia da Universidade do Porto (FEUP), Secção de Materiais (DEMM), Rua Dr. Roberto Frias, 4200-465 Porto, Portugal

4 - Instituto de Engenharia Biomédica (INEB), Laboratório de Biomateriais, Rua do Campo Alegre, 823, 4150-180 Porto, Portugal

Abstract

The cytotoxicity profile of nanocrystalline diamond (NCD) coatings on a Si3N4 ceramic was investigated. This material is envisaged to have biomedical dental applications such as burrs and surgical instruments. Two fibroblast cell culture systems were used to address the cytotoxicity of NCD-coated samples: L929 cells (a mouse permanent cell line) and human gingival fibroblasts. Cell behavior was evaluated in terms of cell adhesion, cell viability/proliferation (mitochondrial function, MTT assay) and the pattern of cell growth. Fibroblast cell behavior on standard polystyrene culture plates was used as control, as Si3N4 substrates have previously been shown to be biocompatible. NCD coatings provided a suitable surface for cell attachment, spreading and proliferation. Human gingival cells showed a homogeneous cytoplasm spreading, a flattened elongated morphology and a typical parallel alignment on confluent cultures. In comparison, L929 cells denoted a lower cytoplasm expansion, a heterogeneous spreading but a higher proliferation rate. For both cells, after few days, the NCD coating was completely covered with continuous cell layers. As compared to standard polystyrene culture plates, no deleterious or cytotoxic responses were observed with L929 and human fibroblast cell cultures, and in both a slight enhancement in cell proliferation was observed. In addition, the seeded NCD film allowed reproduction of the typical features of the two cell culture systems tested, further suggesting the lack of cytotoxicity of this coating.

Introduction

Nanocrystalline diamond (NCD) films have attracted the attention of researchers from different areas, and have therefore been the object of several studies in recent years. NCD is a unique material presenting the exceptional properties of diamond combined with smoother surfaces, higher toughness, lower friction coefficient, wide band gap and higher electron emission efficiency [1]. Thus, a wide range of applications is anticipated for NCD, particularly in the biomedical field. Implants and surgical instruments for dentistry, cardiology, orthopedics, ophthalmology, arterial and venous disorder repair, as well as biosensors and scaffolds for tissue engineering, are just some examples where the use of NCD is particularly innovative [2-9]. In addition, NCD films exhibit the highest resistance to bacterial colonization when compared to medical steel and titanium [10], a relevant issue since bacterial infection associated with the use of biomaterials is still a significant clinical problem.

Dental applications may take advantage of NCD films. In particular, NCD coating of surgical and dental instruments, such as scalpels and dental burrs, may improve the performance and lifetime of tools, as well as their biocompatibility. Diamond-coated dental burrs are an excellent option to substitute the conventional ones [11-12], which are made by embedding synthetic diamond particles into the working surfaces using a binder matrix material containing metallic ions. Those ions are responsible for contaminating of oral tissues, inflammatory responses, tissue disturbance and metal artifacts on magnetic resonance images [5], [11-13]. The deposition of a diamond coating without metallic binder between the crystals would be extremely helpful in terms of reducing contamination-related problems. Furthermore, diamond-coated burrs can work with no signs of deterioration in more than 1000 operations, while the conventional burrs are ineffective after 30–60 operations [12]. To date, only chemical vapor deposition of microcrystalline diamond (MCD) has been reported in the literature [11-12], and, to the best of our knowledge, there are no references about the use of NCD on dental burrs. Clinical application of MCD-coated dental burrs, mounted on an ultrasonic handpiece, allow for a more precise cavity preparation in hard tissue ablation, resulting in a greater conservation of sound tooth structure [14]. Further, this system allows a higher angulation during tissue ablation and this makes interproximal preparation and finishing safer, reducing the chances of hitting adjacent structures [14]. In addition, patient discomfort, which is usually associated with mechanical vibrations, is greatly reduced [14]. Even with the early satisfactory clinical results with MCD diamond burrs, NCD may additionally improve the burr performance due to its lower surface roughness and higher toughness when compared to MCD [1].

NCD films can be deposited in several types of substrates used in biomedical applications, such as silicon [7, 8], stainless steel [10, 15], cobalt–chromium alloys [16], titanium alloys [6, 17, 18] and WC–Co cement carbide substrates [19]. An advantageous substrate is the silicon nitride (Si_3N_4) ceramic because it presents a thermal expansion coefficient very close to that of diamond [20], ensuring good film adhesion, a crucial requirement for biomedical applications. In addition, Si_3N_4 substrates possess the mechanical resistance necessary to work as a substrate for coated materials for biomedical applications [21] and were previously shown to elicit positive responses on cultured cells [22, 23].

This work aims to evaluate the cytotoxicity profile of a NCD-coated Si3N4 ceramic, as part of ongoing projects regarding the use of this material combination in biomedical dental applications, namely burrs and surgical tools. The few reported publications on the biological behavior of NCD coatings are very specific regarding the cell type/application [3, 24, 25, 26]; in the present work, two fibroblast cell culture systems were used to address the cytotoxicity of NCD-coated Si_3N_4 samples: L929 cells (a mouse permanent cell line) and human gingival fibroblasts. Cell behavior was evaluated in terms of cell adhesion on the NCD films, cell viability/proliferation (mitochondrial function, MTT assay) and pattern of cell growth.

Materials and methods

Materials preparation and characterization

Disc-shaped Si_3N_4 substrates (diameter = 10 mm, thickness = 3 mm) were manufactured according to a processing route described in detail in a previous work [20]. Before deposition, the 15 µm lapped substrates were scratched in an ultrasonic bath for 1 h in a 1 µm diamond powder suspension in n-hexane and then ultrasonically cleaned in ethanol for 10 min. The Si_3N_4 discs were coated by NCD using the hot filament chemical vapor deposition (HFCVD) method. A Ar–CH_4–H_2 gas mixture was used with volume ratios of Ar/H_2 = 0.1 and CH_4/H_2 = 0.04. Other deposition parameters were as follows: P = 5 kPa (total gas pressure); F = 50 ml min^{-1} (total gas flow); Ts = 750 °C (substrate temperature); Tf = 2300 °C (filament temperature); td = 2 h (deposition time).

The as-grown NCD films were observed by atomic force microscopy (AFM, Digital Instrument Multimode IIIa) and micro-Raman spectroscopy (Jobin-Yvon T64000, Ar^+ 514.5 nm line).

Before being seeded with the fibroblast cells, the NCD-coated Si3N4 samples were washed with ethanol in an ultrasonic cleaner and sterilized by autoclaving.

Cell cultures

Fibroblast cell line L929

The fibroblast cell line L929 was cultured in α-minimal essential medium (α-MEM) containing 10% fetal bovine serum, 50 μg ml^{-1} ascorbic acid, 50 μg ml^{-1} gentamicin and 2.5 μg ml^{-1} fungizone, at 37 °C, in a humidified atmosphere of 5% CO_2 in air. For subculture, the cell monolayer was washed twice with phosphate-buffered saline (PBS) and incubated with trypsin–EDTA solution (0.05% trypsin, 0.25% EDTA) for 5 min at 37 °C to detach the cells. Cells were resuspended in culture medium and cultured (10^4 cells cm^{-2}) for 8 days in standard plastic culture plates and on the surface of the NCD films in the "as-prepared" condition. The medium was changed every 2–3 days. Cultures were evaluated for cell viability/proliferation at days 1, 4 and 8 (MTT assay) and observed by scanning electron microscopy (SEM) and confocal laser scanning microscopy (CLSM), to assess cell morphology during cell adhesion to the substrate (1, 6, 12 and 24 h) and throughout the culture period.

Human gingival fibroblast cells

Gingiva was collected from a patient undergoing a third molar extraction for orthodontic reasons. Informed consent to use this biological tissue, which would be otherwise discarded, was obtained. Primary cultures were obtained by culturing explants of gingiva, following established procedures [27, 28, 29]. Briefly, the tissue was washed in PBS, cut into small pieces and cultured in the same experimental conditions as those used in the culture of L929 cells. Cell outgrowth from the tissue explants was observed 1–2 weeks after the beginning of the incubation. Cultures showed a high proliferation rate and reached confluence in approximately 1 week, with cells oriented along parallel lines, a typical feature of this culture system [27, 28, 29]. Primary cultures were subcultured (trypsin–EDTA solution) after reaching 70–80% confluence. First-passage human gingival (HG) cells were cultured (10^4 cells cm^{-2}) for 14 days in standard plastic culture plates and on the surface of the NCD films in the "as-prepared" condition. The medium was changed every 2–3 days. Cultures were characterized for cell morphology and proliferation, as described above.

Biochemical and microscopy assays

Cell viability/proliferation

MTT assay (reduction of 3-[4,5-dimethylthiazol-2-yl]–2,5-diphenyltetrasodium bromide (MTT) to a purple formazan reaction product by living cells) was used to estimate cell viability/proliferation. Cultures were incubated with 0.5 mg ml^{-1} of MTT for the last 4 h of the culture period tested. Subsequently, formazan salts were dissolved

with dimethylsulfoxide (the seeded material samples had previously been transferred to a new plate) and the absorbance (A) was measured at 600 nm in an ELISA reader. The results were normalized in terms of macroscopic area and expressed as A cm^{-2}.

SEM and CLSM microscopy

For SEM/EDS observation (JEOL JSM 6301F; Voyager XRMA System, Noran Instruments), samples were fixed with 1.5% glutaraldehyde in 0.14 M sodium cacodylate buffer (15 min, pH 7.3), then dehydrated in graded alcohols, critical-point dried, and sputter-coated with gold.

For CLSM assessment, samples were fixed in 3.7% paraformaldehyde (10 min). Cell cytoskeleton filamentous actin (F-actin) was visualized by treating the cells with Alexa Fluor® 488 Phalloidin (1:20 dilution in PBS, 1 h). Cultures were counterstained with propidium iodide (1 µg ml^{-1}, 10 min) for cell nuclei labelling. Labelled cultures were mounted in Vectashield® and examined with a Leica SP2 AOBS (Leica Microsystems) microscope.

Statistical analysis

Three experiments were performed for each period of culture evaluation. The results are shown as the arithmetic mean ± SD. Analysis of the results was carried out using the non-parametric Kruskall–Wallis test, with a significance level of P < 0.05.

Results

Characterization of the as-grown NCD coating

The HFCVD deposition method enabled a NCD growth rate of about 1 µm h^{-1}, allowing the coating of Si_3N_4 discs with a 2 µm film formed by tiny agglomerates of diamond nanocrystals (Figure 1A and B). The AFM 100 × 100 µm scans on the surface assessed a root mean square (RMS) roughness value of 68 ± 5 nm. The NCD signature is demonstrated by the micro-Raman spectrum in Fig. 1C. Here, a set of typical bands are visible: (i) the 1332 cm^{-1} diamond band; (ii) the graphitic D (1360 cm^{-1}) and G (1560 cm^{-1}) bands; (iii) the transpolyacetylene 1140 and 1480 cm^{-1} shoulders; (iv) the 1228 cm^{-1} nanophase diamond band.
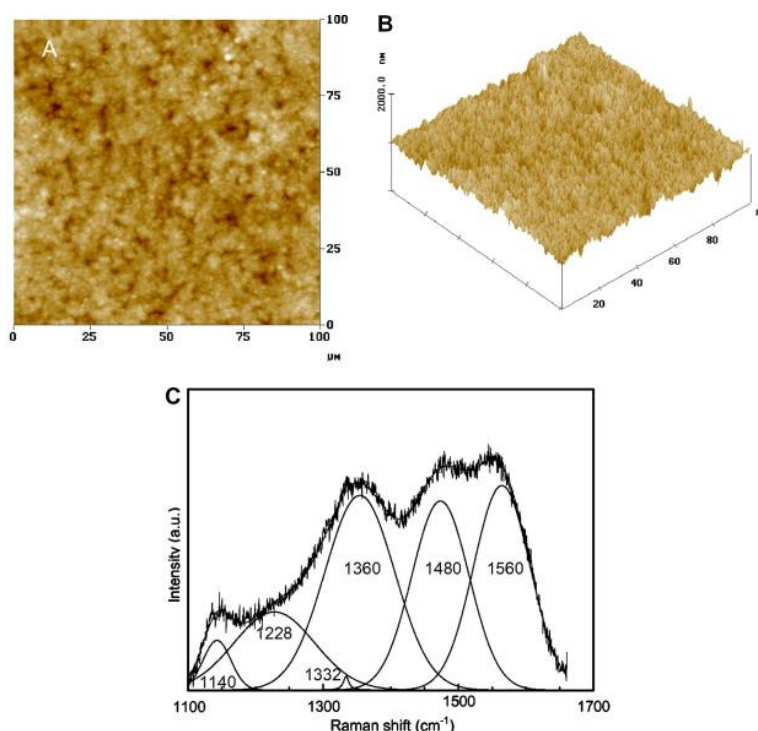
Figure 1 – AFM scan (A and B) and micro-Raman spectrum (C) of the as-grown NCD films.

Cytotoxicity assessment of the NCD coating

Cell morphology and pattern of cell growth

Upon seeding, L929 and HG fibroblast cells contacted with the NCD film within minutes. Morphological changes occurring during cell adhesion and spreading (first 24 h) were observed by SEM and CLSM and are presented in Fig. 2. For both cell types, expansion of the cytoplasm was already evident after 1 h of culture time (Figure 2A and D, inset). After a few hours (12 h), the nucleus was evident and cells already presented an elongated morphology, although coexistence of cells in different stages of spreading could be observed (Figure 2A and D). In 24 h cultures, cells showed a fibroblast-like appearance with cytoplasmic expansions and cell–cell contact (Figure 2B, C, E and F). HG cells presented a higher degree of spreading and a more elongated appearance than L929 cells, as evident in Figure 3 which compares the cell morphology at 24 h. Observation of the seeded materials at longer incubation times showed a high proliferation rate, as suggested by the presence of a flattened sheet of continuous multilayers after approximately 1 and 2 weeks, respectively, for L929 and HG cells (Fig. 4), with HG cells presenting a typical parallel alignment on confluence (Figure 4D and E) and abundant fibrillar matrix (Figure 4F).
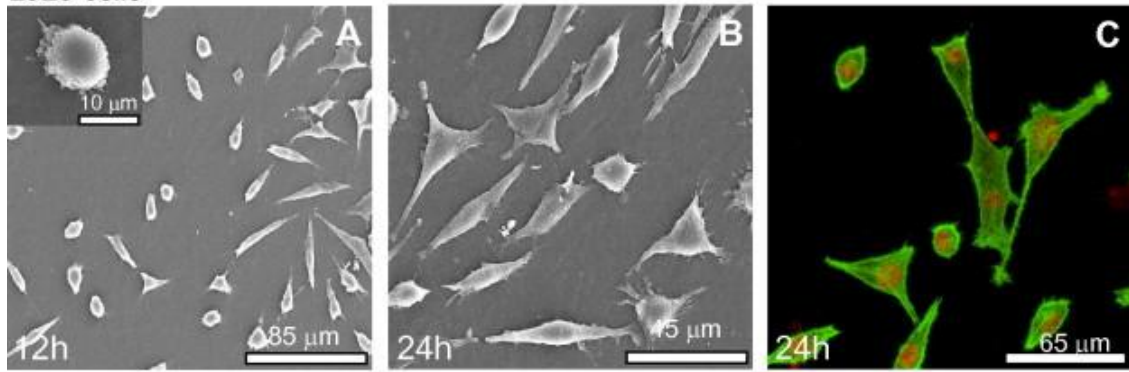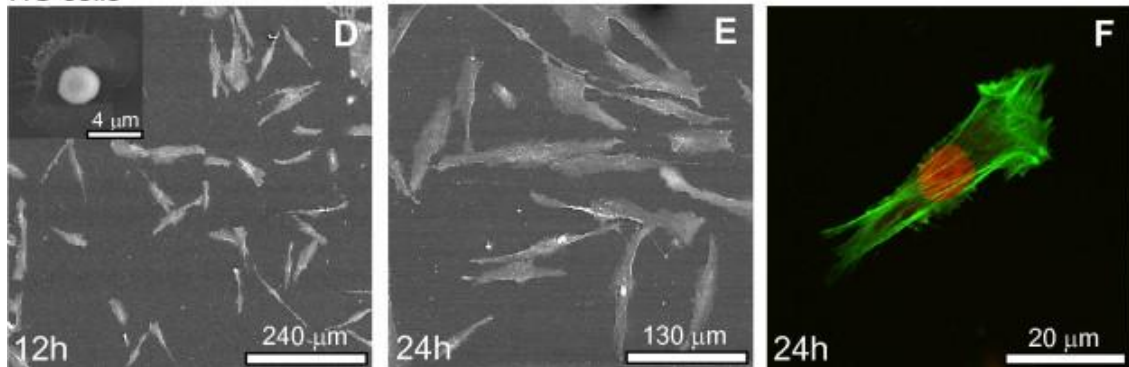
Figure 2 – Morphological appearance of fibroblast cells cultured on the NCD coating, at 12 and 24 h of culture. A, B, D and E: SEM (inset in A and D: 1 h); C and F: CLSM, actin filaments and nucleus staining.
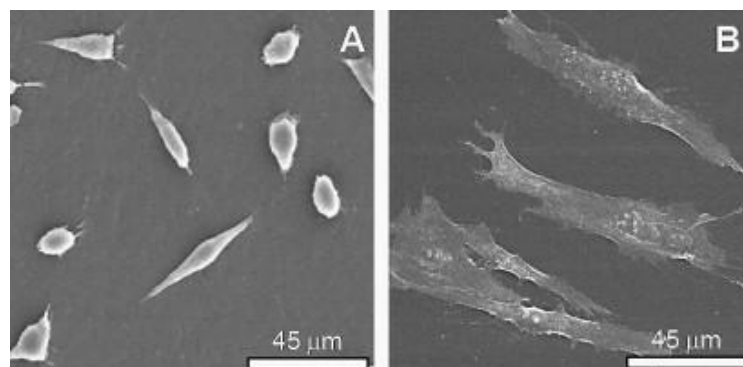

Figure 3 – Comparison of the morphological features of L929 (A) and human gingival fibroblast cells (B) cultured on the NCD coating, at 24 h (SEM images).
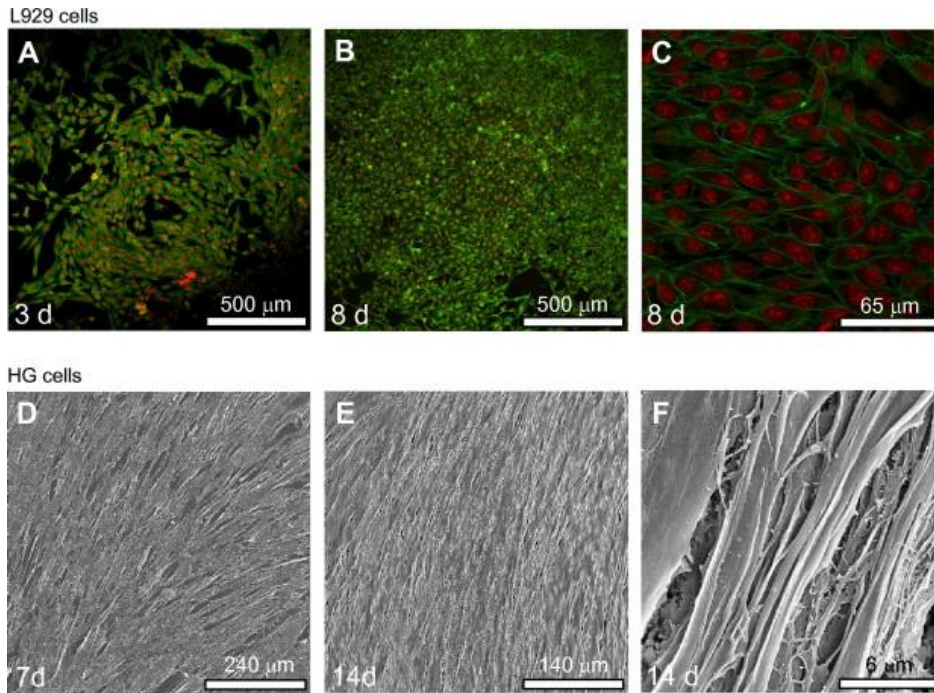
Figure 4 – Time-behavior appearance of fibroblast cells cultured on the NCD coating. (A–C) CLSM, actin filaments and nucleus staining; (D–F) SEM.

The morphological events observed during cell adhesion and spreading on the NCD coating and the subsequent pattern of cell growth described above were similar to those found in the cultures performed on the standard tissue culture plates (Figure 5).
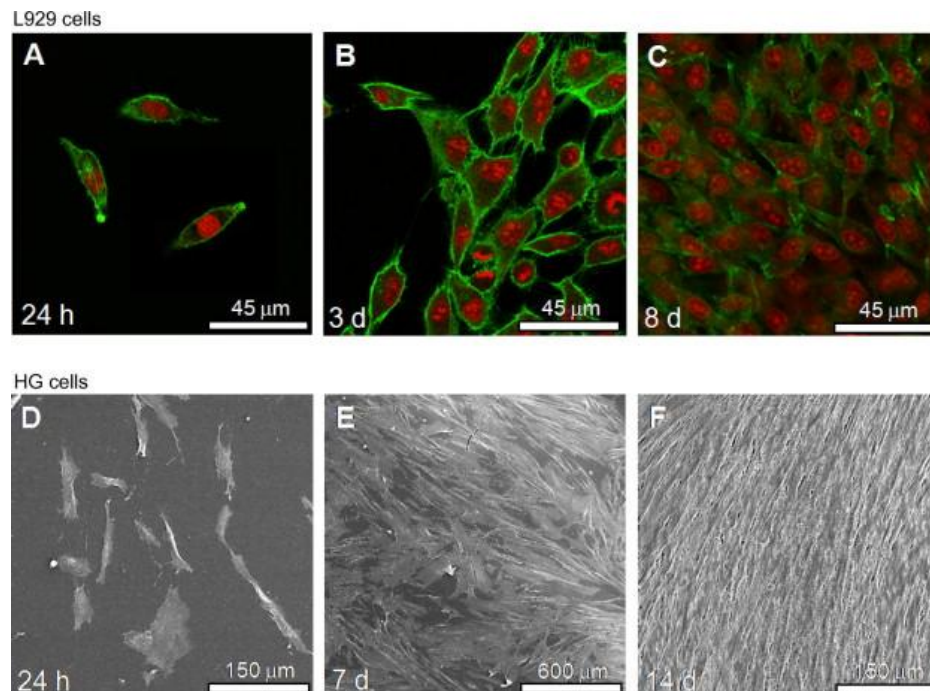

Figure 5 – Time-behavior appearance of fibroblast cells cultured on standard polystyrene culture plates. (A–C) CLSM, actin filaments and nucleus staining; (D–F) SEM.

Cell viability/proliferation

Results regarding cell viability/proliferation (MTT assay) of cultures performed in standard tissue culture plates and on NCD films are shown in Figure 6. L929 cells presented a high proliferation rate throughout the culture time (Figure 6A). HG cells showed a lag phase during the first week, followed by an exponential cell growth, although with a lower growth rate than that exhibited by L929 cells (Figure 6B). At early incubation times, i.e., day 1 (L929 cells) and day 3 (HG cells), values of MTT reduction were similar in standard tissue culture plates and seeded NCD films, suggesting an identical number of attached cells. Subsequently, cells growing in the NCD samples presented a slightly higher proliferation rate, but differences did not attain statistical significance.
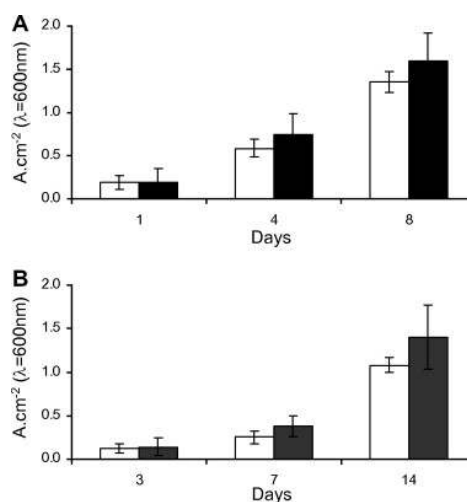

Figure 6 – Cell viability/proliferation of fibroblast cells cultured on the NCD coating (MTT assay). (A) L 929 cells; (B) HG cells. Control cultures (open bars) and seeded NCD coating (black bars).

Discussion

Diamond is one of the allotropic forms of carbon, the element that is the basis of all plant and animal tissue. For this reason, carbon is likely to exhibit excellent biocompatibility and be capable of close binding with human cells [30]. Diamond coatings, particularly NCD, can be obtained by CVD. Raman spectroscopy analysis of the present hot filament-grown NCD films (Fig. 1C) revealed their composite nature, attested by the occurrence of the diamond peak combined with the graphitic peak and the typical bands of nanometric diamond (v = 1228 cm^{-1} [31]; v = 1140 and 1480 cm^{-1} [32, 33]). In addition, NCD films are formed by diamond crystals of nanometric size, usually between 10 and 100 nm [34, 35]. The crystallite size of the present NCD films has an average value of 28 nm, as estimated by X-ray diffraction in a previous work [36]. The higher value of the surface roughness of the NCD films (RMS not, vert,

similar 68 nm) reveals the overlapping effect of the substrate surface finishing with the intrinsic value of the NCD agglomerates.

In the present study, the continuous fibroblast cell line L929 and HG cells were used to assess the cytotoxicity profile of NCD films deposited on a Si3N4 ceramic. F-actin staining and SEM observation showed that, upon seeding, cell adhesion and spreading on the NCD coating followed a similar pattern, compared to that found on standard tissue culture plates. Morphological changes occurring during these initial events correspond to the reorganization of the cytoskeleton, a process reflected by a cytoplasmic expansion and acquisition of phenotypic morphological features after 12–24 h. The cytoskeleton is a key structure that controls cellular shape and surface movements modulating cellular mechanics subjacent to the proliferation and differentiation events [37]. Thus, cytoskeleton dynamics is very sensitive to the material surface properties, and early induced disturbances may compromise adequate cell growth and phenotype expression [37, 38]. Regarding this, L929 and HG cells presented a pattern of cell growth on the NCD coating similar to control, with HG cells exhibited phenotypic features, i.e., a parallel alignment on confluence which is typical of human fibroblastic cell populations derived from adult tissues and abundant fibrillar matrix [27, 28, 29]. In addition, assessment of mitochondrial function (MTT assay) further suggested the lack of cytotoxicity of the NCD coating. Mitochondria are vulnerable targets for toxic injury because of their crucial role in maintaining cellular structure and function via aerobic ATP production. L929 and HG cells presented a profile of cell viability/proliferation representative of the two cell populations: a permanent cell line (high growth rate from the beginning of the incubation) and normal cells in culture (initial lag phase followed by an exponential cell growth) [29, 39].

The biocompatibility of diamond, and more specifically of CVD diamond, has already been proved in the literature [5, 40-46]. Regarding NCD coatings, it has been suggested that this feature can be extrapolated from the behavior of nanometric powders [2, 15, 47], but the purity, defect concentration, amorphous carbon content, specific surface area and morphology is quite different from those of a NCD coating. Only few publications have report on the biocompatibility of NCD coatings, some of them addressing very specific cell responses. Okrój et al. [3] demonstrated that NCD-coated medical steel exhibits a higher level of resistance to blood platelet adhesion and thrombus formation than the bare material. Popov et al. [24] showed that a composite of NCD and amorphous carbon was not cytotoxic to osteoblastic SaOS-2 cells cultured for 3 days, as observed by SEM. Recently, Chong et al. [25] investigated the adhesion properties of human dermal fibroblasts on photochemically functionalized ultrananocrystalline diamond surfaces, and Bajaj [26] reported that for several cell lines

ultrananocrystalline diamond exhibited superior cell adhesion and proliferation compared to silicon and platinum film substrates. The present work addresses the biological profile of NCD coatings regarding the response of fibroblastic cells, namely the permanent cell line L929 and early passage gingival cells, in agreement with the standard ISO guidelines for in vitro cytotoxicity evaluation of medical devices [48, 49]. The cell line L929 is constituted by a highly proliferative population allowing rapid screening assays, mainly regarding acute toxicity testing towards cellular vitality and proliferation, whereas early passage fibroblast cell cultures, established from normal tissues, provide a more representative model of the in vivo fibroblast cell population being very sensitive to external environmental changes, allowing the detection of subtle cell responses. Fibroblast cells are the most common cells of all types of connective tissues, being actively engaged in the synthesis and upkeep of the collagenous extracellular matrix, and, in this context, biological evaluation with fibroblast cell cultures is regarded as a general bioassay providing information on acute and long-term cell responses [48, 49].

Results showed that the present NCD coating provided a suitable surface for normal cellular attachment, morphology and growth. In addition, the seeded NCD coating reproduced the expected features of the two tested cell culture systems [29, 39], suggesting the lack of cytotoxicity of this coating. It is known that nanophase materials are able to simulate surface properties of the constituents of living systems. Proteins, nucleic acids, lipids and carbohydrates possess unique properties determined by the size, folding and patterns at the nanoscale [50]. Therefore, *in vivo*, cells interact with surfaces with a large degree of nanometric roughness. In addition, the unique surface properties of nanophase materials, namely a higher number of atoms at the surface compared to bulk, greater areas of surface defects (such as edge/corner sites and particle boundaries) and larger proportions of surface electron delocalization [51] have been shown to influence initial protein interactions that control cell adhesion [52, 53], a determinant event for the subsequent cell proliferation and function [37]. In general, nanophase materials present improved biocompatibility [54-57] and the present results are in line with the published studies.

Conclusions

The HFCVD deposition technique allows the growth of dense, homogeneous NCD coatings at a moderate rate (1 μm h^{-1}) on bioinert Si_3N_4 ceramic substrates. NCD coatings provide a suitable surface for cell attachment, spreading and proliferation, as assessed by the behavior of a continuous fibroblast cell line (L929 cells) and normal human gingival fibroblast cells. Compared to standard polystyrene culture plates, cell

proliferation is slightly enhanced in both L929 and HG cells. In addition, the seeded films allow reproduction of the typical features of the two cell populations, further suggesting the lack of cytotoxicity of this coating. The cellular biocompatibility of the NCD coatings, allied with the excellent physicochemical performance, anticipates a wide range of applications in the dental biomedical field.

References

1. Griffin J, Ray PC. Role of inert gas in the low-temperature nano-diamond chemical vapour deposition process. Nanotechnology 2006:17;1225–1229.

2. Mitura S, Mitura K, Niedzielski P, Louda P, Danilenko V. Nanocrystalline diamond, its synthesis, properties and applications. J Achievements Mater Manuf Eng 2006:16;9–16.

3. Okrój W, Kamińska M, Klimek L, Szymański W, Walkowiak B. Blood platelets in contact with nanocrystalline diamond surfaces. Diamond Relat Mater 2006:15; 1535–1539.

4. Xiao X, Wang J, Liu C, Carlisle JA, Mech B, Greenberg R, et al. In vitro and in vivo evaluation of ultrananocrystalline diamond for coating of implantable retinal microchips. J Biomed Mater Res B: Appl Biomater 2006:77B;273–281.

5. Tang L, Tsai C, Gerberich WW, Kruckeberg L, Kania DR. Biocompatibility of chemical-vapour-deposited diamond. Biomaterials 1995;16:483–488.

6. Steinmueller-Nethl D, Kloss FR, Haq MU, Rainer M, Larsson K, Linsmeier C, et al. Strong binding of bioactive BMP-2 to nanocrystalline diamond by physisorption. Biomaterials 2006;27:4547–4556.

7. Wenmackers S, Christiaens P, Daenen M, Haenen K, Nesládek M, Ven M, et al. DNA attachment to nanocrystalline diamond films. Phys Status Solidi 2005;202: 2212–2216.

8. Retama JR, Hernando J, Lopez-Ruiz B, Härtl A, Steinmüller D, Stutzmann M, et al. Synthetic nanocrystalline diamond as a third-generation biosensor support. Langmuir 2006;22:5837–5842.

9. Siew PS, Loh KP, Poh WC, Zhang H. Biosensing properties of nanocrystalline diamond film grown on polycrystalline diamond electrodes. Diamond Relat Mater 2005;14:426–431.

10. Jakubowski W, Bartosz G, Niedzielski P, Szymanski P, Walkowiak B. Nanocrystalline diamond surface is resistant to bacterial colonization. Diamond Relat Mater 2004;13:1761–1763.

11. Trava-Airoldi VJ, Corat EJ, Leite NF, Nono M, Ferreira NG, Baranauskas V. CVD diamond burrs—development and applications. Diamond Relat Mater 1996;5:857–860.

12. Amar M, Ahmed W, Sein H, Jones AN, Rego C. Chemical vapour deposition of diamond coatings onto molybdenum dental tools. J Phys Condens Matter 2003;15:S2977–S2982.

13. Tetsumura A, Honda E, Sasaki T, Kino L. Metallic residues as a source of artifacts in magnetic resonance imaging of the temporomandibular joint. Dentomaxillofac Radiol 1999;28:186–190.

14. Carvalho CA, Fagundes TC, Barata TE, Trava-Airoldi VJ, Navarro ML. The use of CVD diamond burrs for ultraconservative cavity preparations: a report of two cases. J Esthet Restor Dent 2007;19:19–29.

15. Mitura K, Niedzielski P, Grzegorz B, Moll J, Walkowiak B, Pawlowska Z, et al. Interactions between carbon coatings and tissue. Surf Coat Technol 2006;201:2117–2123.

16. Fries MD, Vohra YK. Microcrystalline and nanocrystalline diamond film deposition on cobalt chrome alloy. In: Vinci R, Kraft O, Moody N, Besser P, Shaffer II E, Editors. Thin films—stresses and mechanical properties VIII, MRS Publications, Boston MA, 1999.

17. Fries MD, Vohra YK. Properties of nanocrystalline thin films grown by MPCVD for biomedical implant purposes. Diamond Relat Mater 2004;13:1740–1743.

18. Papo MJ, Catledge SA, Vohra YK. Mechanical wear behavior of nanocrystalline and multilayer diamond coatings on temporomandibular joint implants. J Mater Sci: Mater Med 2004;15:773–777.

19. Sun FH, Zhang ZM, Ma YP, Chen M. Synthesis of nanocrystalline diamond films on smooth WC–Co cemented carbide substrates. Int J Abrasive Technol 2007;1:161–172.

20. Belmonte M, Fernandes AS, Costa FM, Oliveira FJ, Silva RF. Adhesion behaviour assessment on diamond coated silicon nitride by acoustic emission. Diamond Relat Mater 2003;12:733–737.

21. Petzow G, Herrmann M. Silicon nitride ceramics. Struct Bond 2002;102: 47–167.

22. Amaral M, Costa MA, Lopes MA, Silva RF, Santos JD, Fernandes MH. Si3N4–bioglass composites stimulate the proliferation of MG63 osteoblast-like cells and osteogenic differentiation of human bone marrow cells. Biomaterials 2002;23:4897–4906.

23. Kue R, Sahrabi A, Nagle D, Frondonza C, Hungerford D. Enhanced proliferation and osteocalcin production by human osteoblast-like cells on silicon nitride ceramic discs. Biomaterials 1999;20:1195–1201.

24. Popov C, Kulisch W, Jelinek M, Bock A, Strnad J. Nanocrystalline diamond/amorphous carbon composite films for applications in tribology, optics and biomedicine. Thin Solid Films 2006;494:92–97.

25. Chong KF, Loh KP, Vedula SR, Lim CT, Sternschulte H, Steinmüller F, et al. Cell adhesion properties on photochemically functionalized diamond. Langmuir 2007;23:5615–5621.

26. Bajaj P, Akin D, Gupta A, Sherman D, Shi B, Auciello O, et al. Ultra-nanocrystalline diamond film as an optimal cell interface for biomedical applications. Biomed Microdevices 2007;9: 787-794.

27. Arnold LF, Baram B. In vitro culture of periodontal ligament cells. J Dent Res 1972:51;953–959.

28. Piche JE, Carnes Jr DL, Graves DT. Initial characterization of cells derived from human periodontia. J Dent Res 1989;68:761–767.

29. Trigo-Cabral C, Costa MA, Fernandes MH. In vitro models of periodontal cells: a comparative study of long-term gingival, periodontal ligament and alveolar bone cell cultures in the presence of β-glycerophosphate and dexamethasone. J Mater Sci: Mater Med 2007;18:1079–1088.

30. Bajpai PK, Billote WG. Ceramic biomaterials. In: Bronzino JD, Editor. The biomedical engineering handbook, CRC Press, Boca Raton, FL (1995), pp. 552–580.

31. Nishitani-Gamo M, Ando T, Watanabe K, Sekita M, Dennig PA, Yamamoto K, et al. Interfacial structures of oriented diamond on Si (1 0 0) characterized by confocal Raman spectroscopy. Diamond Relat Mater 1997;6:1036–1040.

32. Ferrari AC, Robertson J. Origin of the 1150 cm^{-1} Raman mode in nanocrystalline diamond. Phys Rev B 2001; 63:121405-9.

33. Pfeiffer R, Kuzmany H, Knoll P, Bokova S, Salk N, Günther B. Evidence for trans-polyacetylene in nano-crystalline diamond films. Diamond Relat Mater 2003;12:268–271.

34. Zimmermann T, Janischowsky K, Denisenko A, Guillén FH, Kubovic M, Gruen DM, et al. Nanocrystalline diamond pn-structure grown by hot-filament CVD. Diamond Relat Mater 2005;15:203–206.

35. Krauss AR, Auciello O, Gruen DM, Jayatissa A, Sumant A, Tucek j, et al. Ultrananocrystalline diamond thin films for MEMS and moving mechanical assembly devices. Diamond Relat Mater 2001;10:1952–1961.

36. Amaral M, Fernandes AS, Vila M, Oliveira FJ, Silva RF. Growth rate improvements in the hot-filament CVD deposition of nanocrystalline diamond. Diamond Relat Mater 2006;15:1822–1827.

37. Alberts B, Johnson A, Lewis J, Raff M, Roberts K, Walter P. The cytoskeleton. In: Alberts B, Johnson A, Lewis J, Raff M, Roberts K, Walter P, Editors. Molecular biology of the cell (4th ed.), Garland Publishing, New York (2002), pp. 907–972.

38. Stamenovic D. Effects of cytoskeletal prestress on cell rheological behavior. Acta Biomater 2005;1:255–262.

39. Freshney TI. Biology of cultured cells, Culture of animal cells. A manual of basic technique, Wiley-Liss, New York (2000), pp. 9–18.

40. Garguilo JM, Davis BA, Buddie M, Köck FM, Nemanich RJ. Fibrinogen adsorption onto microwave plasma chemical vapor deposited diamond films. Diamond Relat Mater 2004;13:595–599.

41. Ariano P, Baldellia P, Carbonea E, Gilardino A, Giudicea AL, Lovisolo D, et al. Cellular adhesion and neuronal excitability on functionalised diamond surfaces. Diamond Relat Mater 2005;14:669–674.

42. Heinrich G, Grijgler T, Rosiwal SM, Singer RF. CVD diamond coated titanium alloys for biomedical and aerospace applications. Surf Coat Technol 1997;94–95:514–520.

43. Müller R, Adamschik M, Steidl D, Kohn E, Thamasett S, Stiller S, et al. Application of CVD-diamond for catheter ablation in the heart. Diamond Relat Mater 2004;13:1080–1083.

44. Nordsletten L, Hogasen AM, Konttinen YT, Santavirta S, Aspenberg P, Aasen AO. Human monocytes stimulation by particles of hydroxyapatite, silicon carbide and diamond: in vitro studies of new prosthesis coatings. Biomaterials 1996;17:1521–1527.

45. Aspenberg P, Antilla A, Konttinen YT, Lappalainen R, Goodman SB, Nordsletten L, et al. Benign response to particles of diamond and SiC: bone chamber studies of new joint replacement coating materials in rabbits. Biomaterials 1996;17:807–812.

46. Specht CG, Williams OA, Jackman RB, Schoepfer R. Ordered growth of neurons on diamond. Biomaterials 2004;25:4073–4078.

47. Schrand AM, Huang H, Carlson C, Schlager JJ, Omacr E, Hussain M, et al. Are diamond nanoparticles cytotoxic? J Phys Chem B 2007;111:2–7.

48. International Organization for Standardization, ISO 10993-5: biological evaluation of medical devices. Part 5. Tests for cytotoxicity: in vitro methods. Geneva; 1992.

49. International Organization for Standardization, ISO 7405: dentistry—preclinical evaluation of biocompatibility of medical devices used in dentistry—test methods for dental materials. Geneva; 1997.

50. Kaplan FS, Hayes WC, Keaveny TM, Boskey A, Einhorn TA, Iannotti JP. Form and function of bone. In: Simon SP, Editor. Orthopedic basic science, American Academy of Orthopedic Surgeons, Columbus, OH (1994), pp. 127–185.

51. Webster TJ. Proteins: structure and interactions patterns to solid surfaces. In: Schwarz JA, Contescu C, Putyera K, Editors. Encyclopedia of nanoscience and nanotechnology, Marcel Dekker, New York (2004), pp. 3079–3095.

52. Webster TJ. Enhanced functions of osteoblasts on nanophase ceramics. Biomaterials 2000;21:1803–1810.

53. Webster TJ, Ergun C, Doremus RH, Siegel RW, Bizios R. Specific proteins mediate enhanced osteoblast adhesion on nanophase ceramics. J Biomed Mater Res 2000;51:475–483.

54. Shane AC, Marc DF, Yogesh KV, William RL, Jack EL, Shanna W, et al. Nanostructured ceramics for biomedical implants. J Nanosci Nanotechnol 2002;2: 1–20.

55. Price RL, Haberstroh KM, Webster TJ. Enhanced functions of osteoblasts on nanostructured surfaces of carbon and alumina. Med Biol Eng Comput 2003;41:372–375.

56. Webster TJ, Siegel RW, Bizios R. Osteoblast adhesion on nanophase ceramics. Biomaterials 1999;20:1221–1227.

57. Perla V, Webster TJ. Better osteoblast adhesion on nanoparticulate selenium—A promising orthopedic implant material. J Biomed Mater Res 2005;75A:356–364.

Chapter 5

Nanocrystalline diamond: *in vitro* **biocompatibility assessment by MG63 and human bone marrow cells cultures**

Nanocrystalline diamond: *in vitro* biocompatibility assessment by MG63 and human bone marrow cells cultures

M. Amaral[1], A. G. Dias[2,3], P. S. Gomes[4], M. A. Lopes[2,3], R. F. Silva[1], J. D. Santos[2,3], M. H. Fernandes[4]

1 - CICECO, Department of Ceramics and Glass Engineering, University of Aveiro, 3810-193 Aveiro, Portugal
2 - Faculdade de Engenharia da Universidade do Porto (FEUP), Secção de Materiais (DEMM), Rua Dr. Roberto Frias, 4200-465 Porto, Portugal
3 - Instituto de Engenharia Biomédica (INEB), Laboratório de Biomateriais, Rua do Campo Alegre, 823, 4150-180 Porto, Portugal
4 - Laboratório de Farmacologia e Biocompatibilidade Celular, Faculdade de Medicina Dentária, Universidade do Porto (FMDUP), Rua Dr. Manuel Pereira da Silva, 4200-393 Porto, Portugal

Abstract

Nanocrystalline diamond (NCD) has a great potential for prosthetic implants coating. Nevertheless, its biocompatibility still has to be better understood. To do so, we employed several materials characterization techniques (SEM, AFM, micro-Raman spectroscopy) and cell culture assays using MG63 osteoblast-like and human bone marrow cells. Biochemical routines (MTT assays, Lowry's method, ALP activity) supported by SEM and confocal microscopy characterization were carried out. We used silicon nitride (Si_3N_4) substrates for NCD coatings based on a previous demonstration of the superior adhesion and tribological performance of these NCD coated ceramics. Results demonstrate an improved human osteoblast proliferation and the stimulation of differentiated markers, like ALP activity and matrix mineralization, compared with standard polystyrene tissue culture plates. The nanometric featuring of NCD, associated to its chemical affinity are key points for bone regeneration purposes.

Introduction

Nowadays, the hip and the knee are the most replaced joints. The life span for these artificial joints is 10–15 years and their failure is normally associated to the generation of wear debris which causes periprosthetic osteolysis and aseptic loosening, incomplete osseointegration, and severe stress shielding [1,2]. When considering the young patients' joint replacement, this is a very short life time and the need for long-lasting prosthesis that allow reducing the number of revision surgeries is therefore evident [2].

Recently, the research of novel materials for orthopaedic implants had been focused on the incorporation of a certain degree of nanostructured surface features that mimic the nanometric structures and molecules found in bones. In particular, these appear to reduce the chances of rejection of the hip or knee prosthesis [3,4]. Most of the studies reported that nanophase topography fosters cell adhesion on polymers, ceramics and metals, and suggested a positive effect on osteoblasts metabolic activities [5–8].

The deposition of nanocrystalline diamond (NCD) coatings on implant surfaces is likely to improve the durability of orthopaedic prosthesis. NCD mimics the bone surface roughness, and it is very hard, simultaneously presenting a suitable fracture toughness. Moreover, diamond is biocompatible [9–16] and possesses a high chemical resistance. This set of properties envisages a high potential of NCD for biotribological purposes. Aspenberg et al. [11] showed that diamond particles are harmless when compared with UHMWPE, bone cement and chromium-cobalt particles that cause inflammatory reaction and a marked decrease in the amount of bone ingrowth. Furthermore, Nordsletten et al. [12] showed that diamond particles are inert in serum-free monocyte culture and the cell morphology did not change after the ingestion of diamond. Histopathological studies revealed excellent biotolerance of AISI 316L stainless steel disks coated with NCD layers [13,14] and some investigations proved the haemocompatibility of diamond [13,15–17]. Other studies revealed that CVD diamond is as biocompatible as titanium and 316 stainless steel, which have been proved to have good biocompatibility and are frequently used in implantable devices [16]. Recently, it has been reported that NCD and NCD/amorphous carbon composite films were not cytotoxic to human osteoblast-like SaOS-2 cells [18,19].

NCD coatings can be grown on a great variety of possible substrates, however, exceptional film adhesion is one of the crucial requirements for the NCD use in biomedical implants. Silicon nitride (Si_3N_4) based ceramics are able to provide an excellent film adhesion due to the small thermal expansion coefficient mismatch with diamond, among other advantages [20]. The intrinsic mechanical resistance and

biocompatibility of Si_3N_4 ceramics envisage their superior behaviour as substrate bodies of the coated prosthesis. Some reports showed that human osteoblastic cells proliferated on polished surfaces of Si3N4 [21] and porous intramedullary Si_3N_4 rods implanted in rabbit femurs supported bone ingrowth [22]. Furthermore, Si_3N_4-bioglass composites proved to have an inductive effect on the proliferation of MG63 osteoblast-like cells and were able to allow the complete expression of the osteoblastic phenotype [23]. The main purpose of the present work is to evaluate the NCD biocompatibility by in vitro cytotoxicity testing using the human cell system characteristic of the tissue, which the biomaterials it will confront in vivo. Highly adherent NCD films were grown on suitable Si_3N_4 ceramics. In the first stage of this study, NCD coatings were exposed to MG63 osteoblast-like cells for screening toxicity. Then, in the second stage, the NCD films were seeded with human bone marrow cells to assess the effects of the material in cell growth and expression of the osteoblastic phenotype, that is, the formation of a mineralized extracellular matrix.

Material and Methods

Materials preparation and characterization

Details on composition and preparation of silicon nitride ceramics substrates can be found elsewhere [24]. Dense Si_3N_4 disc shaped substrates (diameter = 10 mm, thickness = 3 mm) were ground and submitted to hard cloth polishing with 15 ☐m diamond slurry. Before deposition, the Si_3N_4 substrates were scratched for 1 h in an ultrasonic suspension with 1 ☐m diamond powder in n-hexane (1 g/100 mL), followed by ultrasonic cleaning with ethanol for 10 min. NCD films were grown by the HFCVD technique using a Ar-CH_4-H_2 gas mixture and four linear tungsten filaments (ø= 0.25 mm) precarburised for 30 min under 2% CH_4 in H_2. The filament and substrate temperatures (T_f and T_s, respectively) were monitored by a two-colour pyrometer and a K-type thermocouple in the substrate underside, respectively. NCD films were deposited using the following conditions: Ar/H_2 = 0.1, CH_4/H_2 = 0.04, total gas pressure (P) = 5 kPa, total gas flow (F) = 50 mL min^{-1}, substrate temperature (T_s) = 750ºC, filament temperature ($T_f)$ = 2300ºC and deposition time (t_d) = 2 h.

Before being seeded with cells, the NCD coated Si_3N_4 samples were washed with ethanol in an ultrasonic cleaner and sterilized by autoclaving.

The NCD films were characterized by scanning electron microscopy (SEM; Hitachi S4100), atomic force microscopy (AFM, Digital Instrument Multimode IIIa) and micro-Raman spectroscopy (Jobin-Yvon T64000, Ar$^+$ 514.5 nm line) to assess the morphologic features and quality of the films.

Cell cultures

MG63 osteoblast-like cells

MG63 cells were cultured in a-Minimal Essential Medium (α-MEM) containing 10% fetal bovine serum, 50 μg mL^{-1} ascorbic acid, 50 μg mL^{-1} gentamicin and 2.5 μg mL^{-1} fungizone, at 37ºC in a humidified atmosphere of 5% CO_2 in air. For subculture, the cell monolayer was washed twice with phosphate-buffered saline (PBS) and incubated with trypsin – EDTA solution (0.05% trypsin, 0.25% EDTA) for 5 min at 37ºC to detach the cells. The effect of trypsin was then inhibited by adding the complete culture medium at 37ºC. Cells were resuspended in culture medium and cultured (10^4 cells cm^{-2}) for 7 days in standard polystyrene culture plates (control) and on the surface of the NCD films in the ''as-prepared'' condition. The medium was changed every 2–3 days. Control cultures and seeded material samples were evaluated at days 1, 3, and 7 for cell viability/proliferation and observed by SEM and confocal laser scanning microscopy (CLSM; Leica SP2 AOBS).

Human bone marrow cells

Human bone marrow, obtained from orthopaedic surgery procedures after patient's (male, 27 years) informed consent, was cultured in the same experimental conditions as those used in the culture of MG63 cells. Primary cultures were maintained until near confluence (10–15 days) and, at this stage, adherent cells were enzymatically released (trypsin – EDTA solution) and seeded at a density of 10^4 cells cm^{-2} in standard polystyrene culture plates (control) and on the surface of the ''as-prepared'' NCD films. Control and seeded material samples were cultured for 28 days in similar experimental conditions but the culture medium was further supplemented with 10 mM β-glycerophosphate and 10 nM dexamethasone. All the experiments were performed in the first subculture, since the sequential passage of bone marrow cells fallout in a progressive loss of the osteoblast phenotype [25].

Control cultures and seeded material samples were characterized at days 2, 7, 14, 21, and 28 for cell viability/proliferation, total protein content, alkaline phosphatase (ALP) activity, and observation by SEM and CLSM to evaluate cell morphology and matrix mineralization.

Biochemical and microscopy assays

Cell viability/proliferation

MTT assay (reduction of 3-[4,5-dimethylthiazol-2-yl]–2,5diphenyltetrasodium bromide (MTT) to a purple formazan reaction product by living cells) was used to estimate cell viability/proliferation [26,27]. Cultures were incubated with 0.5 mg mL^{-1} of

MTT in the last 4 h of the culture period tested; the medium was then decanted, formazan salts were dissolved with 200 μL of dimethylsulphoxide and the absorbance was measured at 600 nm in an ELISA reader. The results were normalized in terms of macroscopic area and expressed as A cm^{-2}.

Total protein content and alkaline phosphatase activity

Culture samples were washed twice in PBS, frozen at -20ºC and evaluated at the end of the culture time. The total amount of protein present in the material surface was assayed by the Lowry's method with bovine serum albumin used as a standard. The results are expressed as μg cm^{-2}. ALP activity was determined in cell-layer lysates (obtained by treatment of the cultures with 0.1% triton in water) and assayed by the hydrolysis of p-nitrophenyl phosphate in alkaline buffer solution, pH 10.3, and colorimetric determination of the product (p-nitrophenol) at 405 nm. Hydrolysis was carried out for 30 min at 37ºC (NaOH (1M) was added to stop the reaction). Results are expressed in nanomoles of p-nitrophenol produced per min per μg of protein (nmol min^{-1} μg protein^{-1}).

SEM and confocal microscopy

For SEM observation, samples were fixed with 1.5% glutaraldehyde in 0.14M sodium cacodylate buffer (pH 7.3), then dehydrated in graded alcohols, critical-point dried, sputter-coated with gold and analyzed in a JEOL JSM 6301F scanning electron microscope equipped with a X-ray energy dispersive spectroscopy (EDS) microanalysis capability (voyager XRMA System, Noran Instruments).

Cultures were labeled with calcein for the visualization of calcium-containing deposits. At each testing-point, the cultures were incubated with calcein (25 μg/mL) for the last 3 h at 378C, washed several times in PBS and fixed in 3.7% paraformaldehyde (10 min). Cell cytoskeleton filamentous actin (F-actin) was visualized treating the cells with Alexa Fluor® 488 Phalloidin (1:20 dilution in PBS, 1 h). Cultures were counterstained with propidium iodide for cell nuclei labeling. Labeled cultures were mounted in Vectashield® and examined with a Leica SP2 AOBS (Leica Microsystems) microscopy.

Statistical analysis

Triplicate experiments were performed. The results are shown as the arithmetic mean ± the standard deviation (± SD). Analysis of the results was carried out using the Student's t-test, with a significance level of $p < 0.05$.

Results

Materials characterization

Representative SEM micrographs of the NCD films before being seeded are presented in Figure 1. The film, with ≈2 μm of thickness, is composed by agglomerates of diamond nanocrystals (Figure 1a and b). The NCD coatings surface topography can be observed in Fig. 1c. The root-mean-square value (RMS) from AFM scans over 100 μm x 100 μm regions was 68 ± 5 nm. A representative μ-Raman spectrum is given in Fig. 1d. The 1140 and 1480 cm^{-1} shoulders, usually attributed to trans-polyacetylene, are an indirect proof of the presence of NCD [28,29]. A band at 1228 cm^{-1} is also visible that appeared to be conjugated with vibration modes of C-H chains characteristic of nano- and ultrananocrystalline diamond [30]. Furthermore, it is also visible the 1332 cm^{-1} diamond band as well as the D (1360 cm^{-1}) and G (1560 cm^{-1}) graphite bands.
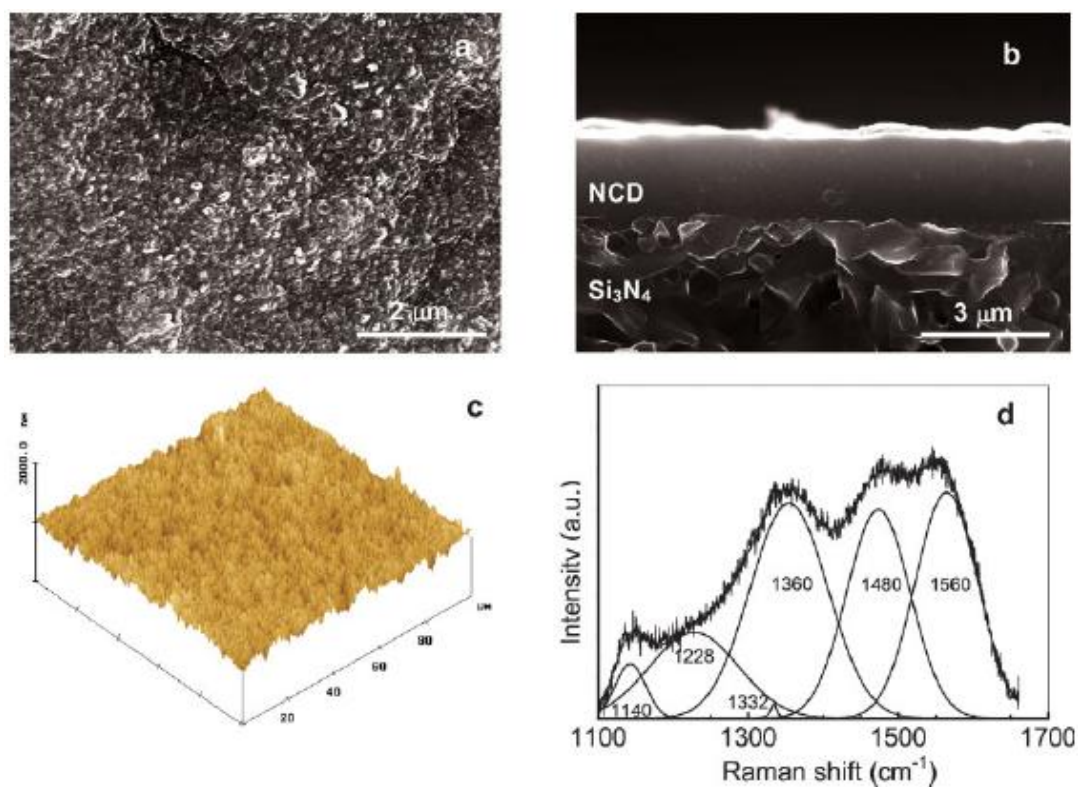

Figure 1 – SEM plan (a) and cross-sectional (b) views, AFM scan (c) and μ-Raman spectrum (d) of the as grown NCD films.

Biological performance

Behavior of MG63 osteoblast-like cells

The results of viability/proliferation (MTT assay) are represented in Figure 2. MTT is metabolized to a purple formazan salt by mitochondrial enzymes in living cells and the absorbance is proportional to the number of viable cells. Comparing to

standard polystyrene culture plates, MTT reduction values for the seeded material samples were similar at day 1 and significantly higher at days 3 and 7. Both in control and in NCD films, cultures reached confluence by day 3 and soon after formed a dense cell layer that was easily lost during routine medium change, explaining the significant decrease in the MTT reduction values observed from day 3 to day 7.
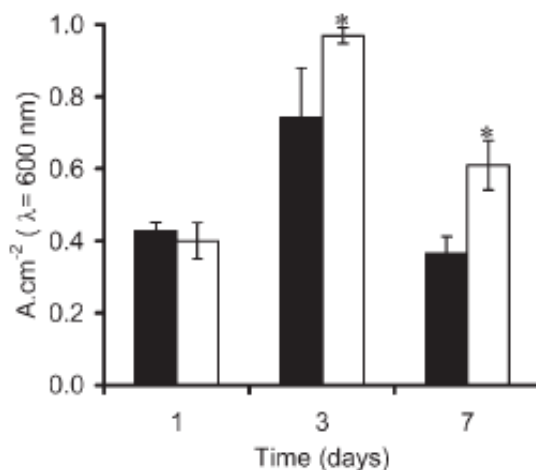

Figure 2 - Cell viability/proliferation of MG63 cells cultured on NCD coated Si_3N_4 substrates for 7 days, estimated by the MTT assay. Open bars, material samples; solid bars, control. (*: statistically different from the control).

As can be seen in Figure 3a and b, at 1 day of culture, MG63 osteoblast-like cells were already well attached and completely spread, displaying a flat configuration and a typical morphology (central spherical body with the cytoplasm extending away from the central area in all directions and adhering to the material surface). Neighbouring cells have an extensive connection with each other through cytoplasmic extensions. After 3 days of culture, the cells formed multilayers of flattened sheets, covering completely the material surface (Figure 3c and d). For this time of culture, CLSM appearance was suggestive of a proliferative cell population (Figure 3d, circled cells). No deleterious or cytotoxic responses were observed for the entire time of culture. Cultures grown on standard polystyrene culture plates showed a similar behavior (not shown).
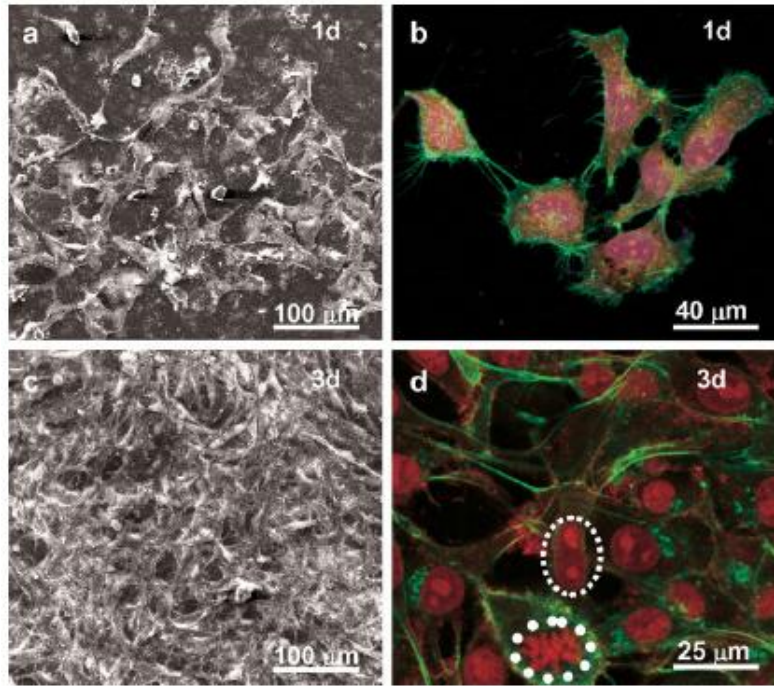
Figure 3 - SEM and CLSM (phalloidin and propidium iodide labeling) photographs of MG63 cells cultured on NCD coated Si_3N_4 substrates for 1 (a, b) and 3 (c, d) days. ■■■ - mitosis; ••• - chromosome duplication.

Behaviour of human bone marrow cells

Human bone marrow cells attached to the NCD films and MTT reduction values increased especially in the first week, remaining approximately constant afterward. As compared to control cultures, MTT values were similar at day 3 and higher at longer incubation times (Figure 4a). Both in control and seeded material, confluence was attained by the second week and after that, cell proliferation decreased slowly, as a result of extracellular matrix accumulation and cell-to-cell contact inhibition. Total protein content is also a measure of cell proliferation and the pattern was similar to that observed for the MTT reduction (Figure 4b). ALP activity (Figure 4c) increased during the first 2 weeks, attaining maximal values around day 14 and decreased afterward, both on the polystyrene plates and seeded NCD. However, the enzyme levels were higher in the NCD films.
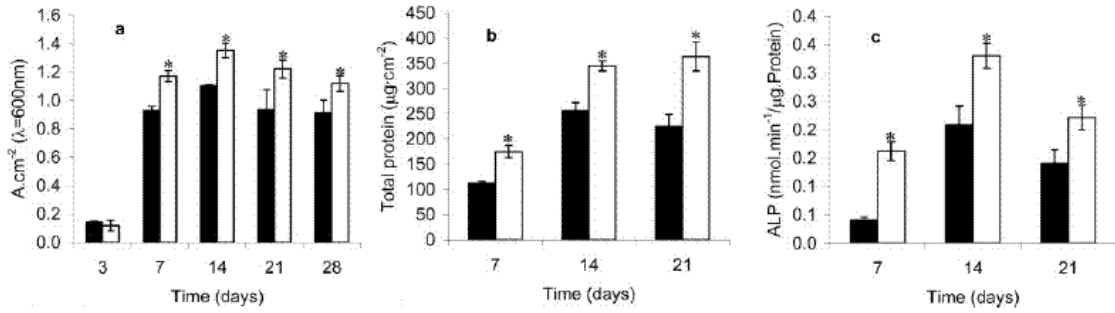
Figure 4 - Cell viability/proliferation (a), total protein content (b), and ALP activity (c) of human bone marrow cells grown on NCD coated Si_3N_4 for 28 days. Open bars, material samples; solid bars, control (*statistically different from the control).

SEM (Figure 5a) and CLSM (Figure 6a) observations of seeded NCD samples showed that cells were well spread and completely covered the surface after 7 days. Cell growth was accompanied by the production of fibrillar matrix, as well evidenced in the observation at day 14 (Figure 5b). In addition, 21-day cultures presented mineralized globular structures intimately associated with the fibrous cell layer (Figure 5c and b). The same sequence of events took place on the standard polystyrene culture plates, although with, apparently, less fibrillar matrix production (Figure 5e), and lower abundance of mineral deposition (Figure 5f).
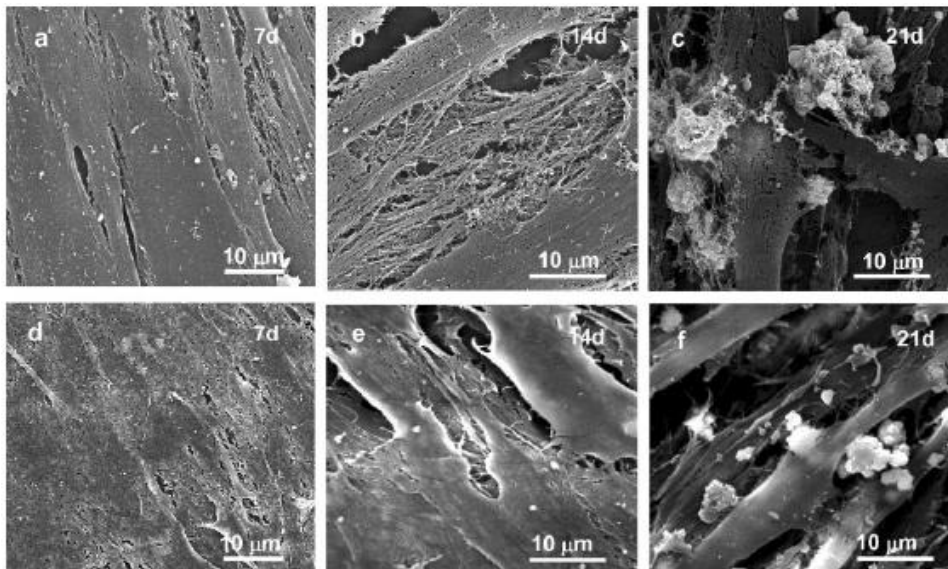

Figure 5 - SEM observation of human bone marrow osteoblastic cells cultured on NCD films at days 7 (a), 14 (b), and 21 (c). For comparison, cell behavior observed on standard polystyrene culture plates at days 7 (d), 14 (e), and 21 (f) is also shown.
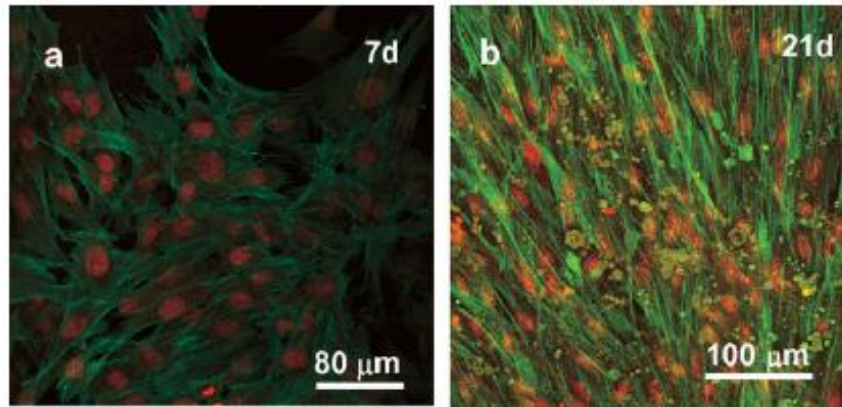
Figure 6 - CLSM observation of human bone marrow osteoblastic cells cultured on NCD films at days 7 (a) and 21 (b) (calcein, phalloidin, and propidium iodide labeling).

The low SEM magnification in Figure 7a corresponding to the 21 days bone marrow cells cultures on NCD films, denotes the abundant presence of the referred mineralized deposits. The X-ray spectrum in Figure 7c from EDS analysis (labeled with an asterisk in Figure 7b), proves the inorganic nature of these structures by showing strong Ca and P peaks.
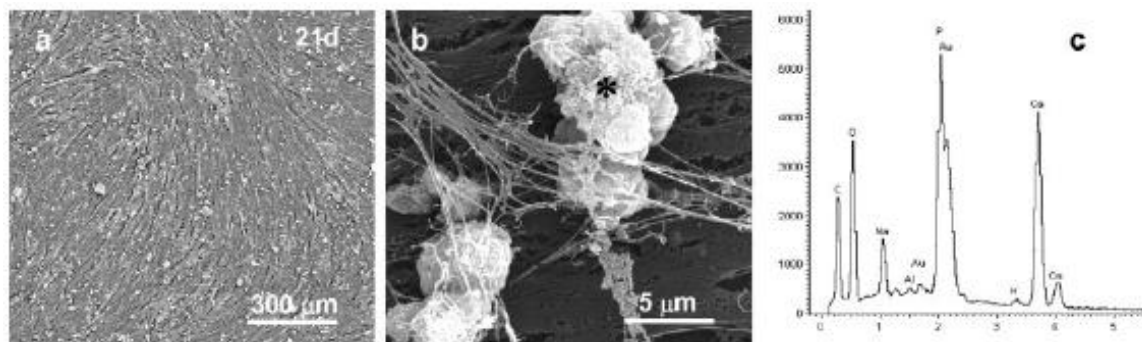

Figure 7 - Formation of calcium phosphate deposits in human bone osteoblastic cell cultures grown on the NCD films at day 21. (a) low magnification SEM appearance; (b) detail of the mineralized structures; (c) representative EDS spectrum of the mineralized structures.

Discussion

The clinical success of any implant depends on the cellular behaviour at the host\biomaterial interface, and if coated, on the coating/substrate reliability, besides the osteointegration of the implant. In our recent works [31–33] it was demonstrated that NCD is highly adherent to Si_3N_4 substrates, presenting an interfacial crack resistance of ≈6 N μm^{-1} in static indentation testing and a delamination threshold load of 60 N (≈3.5 GPa) in self-mated tribological experiments. Also, Si_3N_4 substrates did not induce

cytotoxic responses and were able to allow the complete expression of the osteoblastic phenotype [23].

The present article deals with the NCD chemistry and morphology that can affect the biological response including cell attachment, cell growth, and functional activity. Cell cultures on the materials surface are a reliable, suitable, and reproducible screening method to detect cell death and negative effects on cellular functions and represent the starting point to assess the biological response to foreign materials [1]. The biological performance of NCD coated Si_3N_4 ceramics was evaluated using cell cultures of MG63 osteoblast-like cells for a preliminary and quick screening and human bone marrow cells for assessment of osteoblastic cell growth and osteogenic differentiation.

The results of the study with the MG63 osteoblast-like cells indicate excellent proliferation on NCD surface while keeping a normal cellular morphology (Figure 2 and 3). Also, human bone marrow cells grown in experimental conditions that favor osteoblastic proliferation and differentiation [34,35] presented a high cell growth rate with the formation of abundant fibrillar matrix, production of high ALP levels and matrix mineralization following the maximal ALP activity (Figure 4–7). This behavior is representative of that reported for the development of the osteoblastic phenotype in several bone cell systems including human bone marrow cell cultures [34]. In addition, compared with cultures performed in standard polystyrene culture plates, NCD films induced osteoblastic cell proliferation, as shown by the higher growth rate presented by MG63 and bone marrow cells growing in the material surface, and stimulated metabolic differentiated activities, namely ALP activity and production of a mineralized matrix. These observations are suggestive of a bioactive behaviour of the NCD films. Recent studies on the in vitro osteoblastic biocompatibility of NCD coated surfaces also reported favourable results on osteosarcoma SaOS-2 cells, namely absence of cytotoxicity of a composite of NCD and amorphous carbon as observed by SEM [18] and upregulation of ALP on a BMP-2 treated NCD-coating of titanium disks [19].

NCD is a nanostructured material composed by agglomerates of diamond nanocrystals surrounded by an amorphous matrix (Figure 1) with surface roughness within the nanoscale range. These nanofeatures are likely the responsible for the increased osteoblast proliferation and function, when compared with the control cultures. A variety of studies reports that cells respond differently to nanostructured compared with conventional structured material topographies in terms of cell adhesion, proliferation, and function [3,4]. Nanophase materials simulate surface properties of the constituents of living systems as biomolecules such as proteins, nucleic acids, lipids, and carbohydrates possess unique properties determined by the size, folding, and

patterns at the nanoscale [36]. Regarding the bone constituents, hydroxyapatite, the major inorganic component, is between 2 and 5 nm in width and 50 nm in length. Collagen type I, the major organic component of the bone tissue, is 300 nm in length, 0.5 nm in width, and has a periodicity of 67 nm [36]. In this way, the osteoblasts interact with surfaces with a large degree of nanometric-scale morphological features. Webster et al, in a variety of studies investigating cellular reaction against orthopaedic and dental nanomaterials, found increased osteoblastic activity compared with conventional ceramics, polymers, carbon nanofibers, metals, and composites of these materials [5,6,37–40]. Improved cell performance appears to be related to the unique surface properties of nanophase materials, namely a higher number of atoms at the surface compared to bulk, greater areas of surface defects (such as edge/corner sites and particle boundaries) and larger proportions of surface electron delocalizations [41,42]. Such greater surface reactivity has been shown to influence initial protein adsorption in terms of concentration, conformation, and bioactivity, events that control cell adhesion and proliferation [43–46]. Also, the quantitative increase in the total length of particle boundaries and total number of pores between surface particles of nanophase materials provide a significantly extended surface area for osteoblast proliferation, compared with micron-structured surfaces.

Results obtained under this study suggest that the prepared NCD coating presents excellent biocompatibility and bioactivity features, as shown by the improved human osteoblast proliferation and function. The ultimate biological assessment must now be performed in an animal model to evaluate the interfaces behaviour and the osteointegration through push-out strength measurements and histological studies.

Conclusions

NCD films induced human osteoblast proliferation and stimulated specific metabolic activities such as ALP activity and matrix mineralization. These biocompatibility and bioactivity features suggest the potential of NCD as a coating for orthopedic applications. The high chemical resistance and unique mechanical properties of NCD associated with its ability in simulating the nanometric features of the bone tissue might offer exciting possibilities in the design and efficacy regarding bone regeneration strategies.

References

1. Ratner BD, Hoffman AS, Schoen AS, Lemons JE. Biomaterials Science: An Introduction to Materials in Medicine. New York: Academic Press; 1996.

2. Emery DFG, Clarke HJ, Grover ML. Stanmore total hip replacement in younger patients: Review of a group of patients under 50 years of age at operation. J Bone Joint Surg 1997;79:240–246.

3. Shane AC, Monique C, Yogesh KV, Erick MS, Michelle DM, David Moore K. Surface crystalline phases and nanoindentation hardness of explanted zirconia femoral heads. J Mater Sci: Mater Med 2003;14:863–867.

4. Shane AC, Marc DF, Yogesh KV, William RL, Jack EL, Shanna W, Ramakrishna V. Nanostructured ceramics for biomedical implants. J Nanosci Nanotechnol 2002;2:293–312.

5. Palin E, Liu H, Webster TJ. Mimicking the nanofeatures of bone increases bone-forming cell adhesion and proliferation. Nanotechnology 2005;16:1828–1835.

6. Webster TJ, Siegel RW, Bizios R. Osteoblast adhesion on nanophase ceramics. Biomaterials 1999;20:1221–1227.

7. Price RL, Haberstroh KM, Webster TJ. Enhanced functions of osteoblasts on nanostructured surfaces of carbon and alumina. Med Biol Eng Comput 2003;41:372–375.

8. Perla V, Webster TJ. Better osteoblast adhesion on nanoparticulate selenium—A promising orthopedic implant material. J Biomed Mater Res 2005;75A:356–364.

9. Fries MD, Vohra YK. Nanostructure diamond film deposition on curved surfaces of metallic temporomandibular joint implant. J Phys D: Appl Phys 2002;35:L105–L107.

10. Papo MJ, Catledge SA, Vohra YK. Mechanical wear behavior of nanocrystalline and multilayer diamond coatings on temporomandibular joint implants. J Mater Sci: Mater Med 2004;15:773–777.

11. Aspenberg P, Antilla A, Konttinen YT, Lappalainen R, Goodman SB, Nordsletten L, Santavirta S. Benign response to particles of diamond and SiC: Bone chamber studies of new joint replacement coating materials in rabbits. Biomaterials 1996; 17:807–812.

12. Nordsletten L, Hogasen AKM, Konttinen YT, Santavirta S, Aspenberg P, Aasen AO. Human monocytes stimulation by particles of hydroxyapatite, silicon carbide and diamond: In vitro studies of new prosthesis coatings. Biomaterials 1996;17:1521–1527.

13. Mitura S, Mitura A, Niedzielski P, Couvrat P. Nanocrystalline diamond coatings. Chaos Solitons Fractals 1999;10:2165–2176.

14. Mitura K, Niedzielski P, Grzegorz B, Moll J, Walkowiak B, Pawlowska Z, Louda P, Kiec-Swierczynska M, Mitura S. Interactions between carbon coatings and tissue. Surf Coat Technol 2006;201:2117–2123.

15. Garguilo JM, Davis BA, Buddie M, Ko¨ck FAM, Nemanich RJ. Fibrinogen adsorption onto microwave plasma chemical vapour deposited diamond films. Diamond Relat Mater 2004; 13:595–599.

16. Tang L, Tsai C, Gerberich WW, Kruckeberg L, Kania DR. Biocompatibility of chemical-vapour deposited diamond. Biomaterials 1995;16:483–488.

17. Narayan RJ, Wei W, Jin C, Andara M, Agarwal A, Gerhardt RA, Shih C, Shih C, Lin S, Su Y, Ramamurti R, Singh RN. Microstructural and biological properties of nanocrystalline diamond coatings. Diamond Relat Mater 2006;15:1935–1940.

18. Popov C, Kulisch W, Jelinek M, Bock A, Strnad J. Nanocrystalline diamond/amorphous carbon composite films for applications in tribology, optics and biomedicine. Thin Solid Films 2006;494:92–97.

19. Nethl DS, Kloss FR, Haq MNU, Rainer M, Larsson K, Linsmeier C, Ko¨hler G, Feher C, Lepperdinger G, Liu X, Memmel N, Bertel E, Huck CW, Gassner R, Bonn G. Strong binding of bioactive BMP-2 to nanocrystalline diamond by physisorption. Biomaterials 2006;27:4547–4556.

20. Silva VA, Costa FM, Fernandes AJS, Nazaré MH, Silva RF. Influence of SiC particle addition on the nucleation density and adhesion strength of MPCVD diamond coatings on Si3N4 substrates. Diamond Relat Mater 2000;9:483–488.

21. Kue R, Sahrabi A, Nagle D, Frondonza C, Hungerford D. Enhanced proliferation and osteocalcin production by human osteoblast-like cells on silicon nitride ceramic discs. Biomaterials 1999;20:1195–1201.

22. Howlett C, McCartney E, Ching W. The effects of silicon nitride ceramic on rabbit skeletal cells and tissues. Clin Orthop 1989;244:296–301.

23. Amaral M, Costa MA, Lopes MA, Silva RF, Santos JD, Fernandes MH. Si3N4-bioglass composites stimulate the proliferation of MG63 osteoblast-like cells and support the osteogenic differentiation of human bone marrow cells. Biomaterials 2002;23:4897–4906.

24. Belmonte M, Fernandes AJS, Costa FM, Oliveira FJ, Silva RF. Adhesion behaviour assessment on diamond coated silicon nitride by acoustic emission. Diamond RelatMater 2003;12:733–737.

25. Coelho MJ, Trigo Cabral A, Fernandes MH. Human bone cell cultures in biocompatibility testing, Part 1: Osteoblastic differentiation of serially passaged human bone marrow cells cultured in a-MEM and in DMEM. Biomaterials 2000;21:1087–1094.

26. Clifford CJ, Downes S. A comparative study of the use of colorimetric assays in the assessment of biocompatibility. J Mater Sci: Mater Med 1996;7:637–643.

27. Ciapetti G, Cenni E, Pratelli L, Pizzoferrato A. In vitro evaluation of cell/biomaterial interaction by MTT assay. Biomaterials 1993;14:359–364.

28. Ferrari AC, Robertson J. Origin of the 1150 cm-1 Raman mode in nanocrystalline diamond. Phys Rev B 2001;63:121405–1–4.

29. Pfeiffer R, Kuzmany H, Knoll P, Bokova S, Salk N, Gunther B. Evidence for trans-polyacetylene in nano-crystalline diamond films. Diamond Relat Mater 2003;12:268–271.

30. Fernandes AJS, Neto MA, Almeida FA, Silva RF, Costa FM. Nano- and micro-crystalline diamond growth by MPCVD in extremely poor hydrogen uniform plasmas. Diamond Relat Mater 2007;16:757–761.

31. Almeida FA, Amaral M, Oliveira FJ, Fernandes AJS, Silva RF. Nano to micrometric HFCVD diamond adhesion strength to Si3N4. Vacuum 2007;81:1443–1447.

32. Abreu CS, Amaral M, Oliveira FJ, Fernandes AJS, Gomes JR, Silva RF. Enhanced performance of HFCVD nanocrystalline diamond self-mated tribosystems by plasma pretreatments on silicon nitride substrates. Diamond Relat Mater 2006;15: 2024–2028.

33. Abreu CS, Amaral M, Fernandes AJS, Oliveira FJ, Silva RF, Gomes JR. Friction and wear performance of HFCVD nanocrystalline diamond coated silicon nitride ceramics. Diamond Relat Mater 2006;15:739–744.

34. Stein GS, Lian JB. Molecular mechanisms mediated proliferation-differentiation interrelationships during progressive development of the osteoblast phenotype. Endocr Rev 1993;14:424–442.

35. Coelho MJ, Fernandes MH. Human bone cell cultures in biocompatibility testing, Part 2: Effect of ascorbic acid, b-glycerophosphate and dexamethasone on osteoblastic differentiation. Biomaterials 2000;21:1095–1102.

36. Kaplan FS, Hayes WC, Keaveny TM, Boskey A, Einhorn TA, Iannotti JP. Form and function of bone. In: Simon SP, editor. Orthopedic Basic Science. Columbus, OH: American Academy of Orthopedic Surgeons; 1994. p 127–185.

37. Webster TJ, Ejiofor JU. Increased osteoblast adhesion on nanophase metals: Ti, Ti6A14V, and CoCrMo. Biomaterials 2004;25:4731–4739.

38. Kay S, Thapa A, Haberstroh KM, Webster TJ. Nanostructured polymer/nanophase ceramic composites enhance osteoblast and chondrocyte adhesion. Tissue Eng 2002;8:753–761.

39. Webster TJ, Smith TA. Increased osteoblast function on PLGA composites containing nanophase titania. J Biomed Mater Res A 2005;74:677–686.

40. Balasundaram G, Sato M, Webster TJ. Using hydroxyapatite nanoparticles and decreased crystallinity to promote osteoblast adhesion similar to functionaizing with RGD. Biomaterials 2006;27:2798–2805.

41. Webster TJ. Proteins: Structure and interactions patterns to solid surfaces. In: Schwarz JA, Contescu C, Putyera K, editors. Encyclopedia of Nanoscience and Nanotechnology. New York: Marcel Dekker. 2004;1–16.

42. Siegel RW. Creating nanophase materials. Sci Am (Int Ed) 1996;275:74–79.

43. Webster TJ. Enhanced functions of osteoblasts on nanophase ceramics. Biomaterials 2000;21:1803–1810.

44. Webster TJ. Enhanced osteoclast-like cell functions on nanophase ceramics. Biomaterials 2001;22:1327–1333.

45. Webster TJ, Ergun C, Doremus RH, Siegel RW, Bizios R. Specificproteins mediate enhanced osteoblast adhesion on nanophase ceramics. J Biomed Mater Res 2000;51:475–483.

46. Webster TJ, Schadler LS, Siegel RW, Bizios R. Mechanisms of enhanced osteoblast sdhesion on nanophase alumina involvevitronectin. Tissue Eng 2001;7:291–301.

Chapter 6

New titanium and titanium/hydroxyapatite coatings on ultra-high-molecular-weight polyethylene - *in vitro* **osteoblastic performance**

New titanium and titanium/hydroxyapatite coatings on ultra-high-molecular-weight polyethylene - *in vitro* osteoblastic performance

M. A. Silva[1], P. S. Gomes[2], M. Vila[3], M. A. Lopes[1], J. D. Santos[1], R. F. Silva[3], M. H. Fernandes[2]

1 - Department of Metallurgical and Materials Engineering, Materials Section—Faculty of Engineering,
University of Porto, Portugal
2 - Laboratory of Pharmacology and Cellular Biocompatibility—Faculty of Dental Medicine,
University of Porto, Portugal
3 - Department of Ceramics and Glass Engineering, University of Aveiro, CICECO, Portugal

Abstract

The development of optimized hip joint materials is one of the most challenging opportunities in prosthetic technologies. In current approaches, ultra-high-molecular-weight polyethylene (UHMWPE) has been a favorite material for the acetabular component and, regarding the cementless technique, several coating options may be considered to contain and stabilize bearing surfaces and establish an improved interface with bone. In this work, newly developed constructs of UHMWPE coated with either commercially pure titanium (cpTi-UHMWPE), by DC magnetron sputtering, or with commercially pure titanium and hydroxyapatite (cpTi/HA-UHMWPE), by DC/RF magnetron co-sputtering, have been prepared and biologically characterized with human bone marrow-derived osteoblastic cultures. The cpTi-UHMWPE samples allowed a high cell growth and the expression of the complete osteoblastic phenotype, with high alkaline phosphatase activity, expression of osteogenic-associated genes and evident cell-mediated mineralization of the extracellular matrix. In comparison, the cpTi/HA-UHMWPE samples reported lower cell proliferation but earlier cell-mediated matrix mineralization. Accordingly, these newly developed systems may be suitable candidates to improve the osteointegration process in arthroplastic devices; nevertheless, further biological evaluation should be conducted.

Introduction

The increase in life expectancy, due to the advancements in the field of medical sciences, contributes to increasing number of the elderly demanding replacement of failed tissues with regenerative strategies, which embraces the implantation of biomaterials and artificial implants [1]. In the case of the hip joint, which is subjected to high levels of cyclic mechanical stress, it is expected that the aging process, in close association with the eventual development of degenerative or rheumatologic diseases, establishes a localized tissue destruction, outputting the need of tissue replacement [2]. In this way, the selection of adequate components for joint replacement must consider biological, as well as physical and mechanical issues [3].

Ultra-high-molecular-weight polyethylene (UHMWPE) has gained widespread support as a material of choice for bearing surfaces routinely used in several arthroplastic applications (including total shoulder, knee and hip replacements), due to its adequate elastic properties, corrosion resistance and ability to achieve a smooth surface through machining techniques [4, 5]. Despite the clinical success attained with this material in hip arthroplasty, definitive long-term function has not been established yet, especially within cemented applications [6]. Major limitations include deleterious biological effects due to the exothermic reaction occurring during the cement curing process [7], and mechanical failure of the bone–cement interface, cement–implant interface or the cement mantle itself, generally leading to implant revision due to aseptic loosening [8]. In fact, the long-term failure rate of cemented polyethylene cups has been reported in the range of 22 to 49% [9–11]. Consequently, cementless acetabular components were developed with the introduction of a modular metal liner, aiming to contain and stabilize UHMWPE bearing surfaces and establish a direct interface with the bone tissue. This direct union has the ability to provide a dynamic and durable interface which is expected to be resistant to late aseptic loosening [11]. Even so, the metal-backed system has been reported to generate new complications including liner dissociation, expansile osteolysis and late debonding of the coatings [11], most of the time associated with reduced polyethylene thickness required by component modularity and suboptimal designs related to locking mechanisms and three-dimensional geometry [12, 13].

In this way, the development of a new approach that allows the control of surface properties and maintains the thickness and design of the UHMWPE component, at the same time favoring its long-time integration with the bone tissue, may improve the clinical outcome of total hip replacements [14]. Several coating options may be considered in order to control the physical and mechanical properties of the bulk material, enhancing, at the same time, the biological response. Either way,

depending on the strategy, the coatings should either provide a stable, non-dissolving interface with tissues (achieved, for instance, with a titanium coating) or should dissolve gradually being substituted by newly formed bone (which can be achieved with a calcium phosphate-based coating) [14]. Titanium is a bioinert material that does not induce adverse reactions following tissue implantation [15]. In fact, titanium and titanium alloys have reported adequate biocompatibility both for in vitro and in vivo functions and are currently used in diverse arthroplastic fixative surfaces, mainly due to their apatite-inducing ability [16–18]. Furthermore, bioactive calcium phosphate coatings have also been used to provide a superficial environment that induces bone growth at the materials' surface, promoting a high strength interfacial bonding between the implant and the tissue [19–21]. Accordingly, and to the best of the authors' knowledge, the development and comparison of titanium and titanium plus hydroxyapatite (HA) coatings over UHMWPE substrates have not been previously reported, although these novel approaches are expected to significantly enhance the biological and biomechanical behavior of total arthroplastic applications.

In this way, the purpose of this study consists in the evaluation of the biological behavior of two newly developed coatings onto UHMWPE substrates, i.e. UHMWPE coated with commercially pure titanium (cpTi) and UHMWPE coated with cpTi and HA. The coatings were applied by DC magnetron sputtering and DC/RF magnetron co-sputtering, respectively, techniques which allow the deposition of thin, dense, fine-grained and uniform coatings with strong adhesion and compact structure that can survive without delamination in body fluids and are able to withstand high surface pressures [14, 22].

Materials and methods

Materials preparation

UHMWPE polished disks (diameter of 16.1 mm and thickness of 5.1 mm) were used as substrates. cpTi and phase pure HA were used as sputtering target materials. UHMWPE substrates were coated with cpTi byDC magnetron sputtering (cpTi-UHMWPE) and with cpTi/HA by DC/RF magnetron co-sputtering. HA preparation, as well as cpTi-UHMWPE and cpTi/HA-UHMWPE samples' preparation and physicochemical characterization, was studied in detail in a previous report [23]. Briefly, cpTi and cpTi/HA coatings exhibited slight differences in the wettability (contact angle of 93.5◦ ± 7.4 and 84.0◦ ± 14.4 for water, respectively), estimated surface tension (38.2 mN m^{-1} and 26.6 mN m^{-1}, respectively) and zeta potential (−55.1±5.2mV and −45.4± 3.7 mV, respectively). On scanning electron microscopy (FEIQuanta 400FEG scanning electron microscope equippedwith X-ray EDS microanalysis capability, EDAX Genesis

X4M), both coatings presented a homogeneous coverage of the substrate surface, although distinct morphologies were observed, as shown in Figure 1. Regarding the cpTi/HA samples, the presence of calcium, phosphorus and titanium was analyzed by x-ray mapping, which reported a homogeneous distribution of these elements. Representative maps are shown in Figures 1D, E and F and represent the distribution, in weight percentage, of these three elements in the cpTi/HA samples [23].

Evaluation of samples' cross section allowed the determination of the thickness of the coating. cpTi-UHMWPE coatings presented a uniform thickness of 1.61 ± 0.35 µm, while cpTi/HA-UHMWPE presented a thickness of 0.22 ± 0.04 µm [23]. A representative cross-section image of cpTi-UHMWPEis shown in figure 1(C). As a result of the deposition process, by DC/RF magnetron co-sputtering, the ceramic material deposited presented an amorphous structure rather than a crystalline one, which impaired XRD quantification.
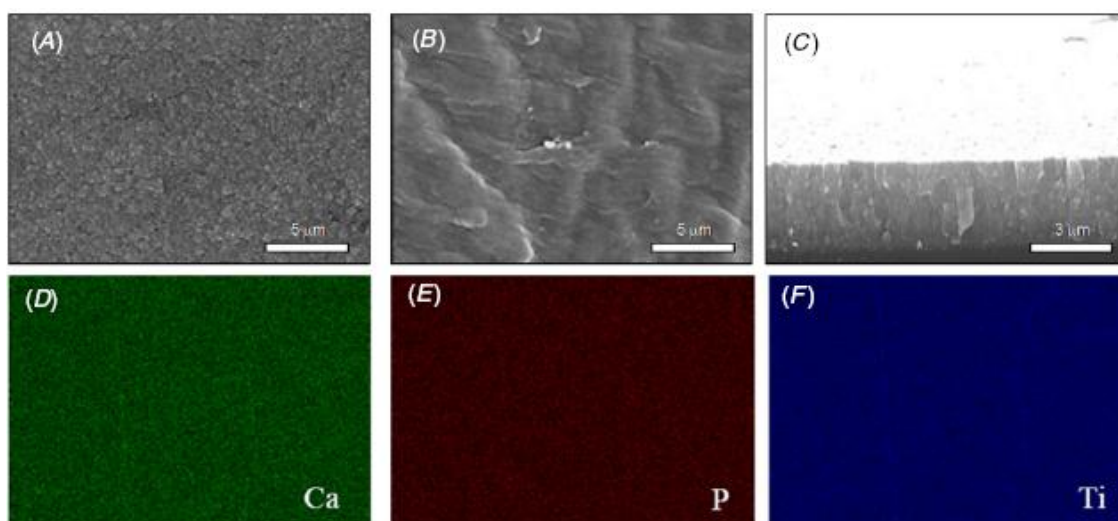

Figure 1 - SEM morphology of the surface of cpTi-UHMWPE (A) and cpTi/HA-UHMWPE (B) samples. Cross section of a cpTi-UHMWPE sample (C). X-ray mapping of the surface of the cpTi/HA-UHMWPE samples for calcium (D), phosphorus (E) and titanium (F).

Adhesion measurement was performed using a Sebastian V tester, which has the same functional principle as the pull-off test. The cpTi-UHMWPE samples presented inferior adhesion compared to that of the cpTi/HA-UHMWPE samples (3.26 ± 1.19 MPa and 5.00 ± 1.61 MPa, respectively) [23].

Prior to the in vitro biological study, all samples were sterilized with ethylene oxide gas.

Cell cultures

Human bone marrow cells were collected from orthopedic surgical procedures of traumatic reconstruction, after patients gave their informed consent. The patients were males, between 25 and 40 year old, and reported the absence of systemic associated pathologies. The bone marrow cells were cultured in an α-minimal essential medium (α-MEM) supplemented with 10% of fetal bovine serum, 50 μg.ml^{-1} of ascorbic acid, 100 IU.ml^{-1} of penicillin, 100 μg.ml^{-1} of streptomycin and 2.5 μg.ml^{-1} of fungizone, at 37 ◦C and 5% CO_2 in air. The culture medium was changed twice a week. The primary culture was maintained until near confluence, and first subcultured cells were seeded (10^4 cells cm^{-2}): (i) under control conditions (standard polystyrene culture plates) and (ii) onto the cpTi-UHMWPE and cpTi/HA-UHMWPE coated samples, both under the 'as-prepared' condition (A samples) and after pre-incubation treatment with a fully supplemented culture medium over 24 h (B samples). The cells were cultured, for 21 days, under the same conditions as used in the primary culture, but the culture medium was further supplemented with 10 mM β-glycerophosphate and 10 nM dexamethasone—conditions known to induce the osteogenic phenotype [24]. Cultures were characterized throughout the incubation time for proliferation and osteoblastic function, as follows.

Cell viability/proliferation.

Evaluation of the cellular viability/proliferation was performed through the MTT assay at days 7, 14 and 21. MTT is reduced, by living cells, to purple formazan crystals. Cultures were incubated with 0.5 mg.ml^{-1} of MTT (37 ºC, 5% CO_2 in air, 4 h), following which the medium was decanted, the formazan crystals dissolved with dimethylsulphoxide and the absorbance determined (600 nm) with an ELISA reader (Denley Wellscan). The results were expressed as absorbance per square centimeter (A.cm^{-2}).

Protein content and alkaline phosphatase activity

At days 7, 14 and 21, the cultured samples were washed twice with PBS and the total protein content was determined according to the Lowry method, using bovine serum albumin as a standard. The activity of alkaline phosphatase (ALP) was determined in cell lysates (obtained by treatment of the cultures with 0.1% triton) and assayed through the hydrolysis of p-nitrophenyl phosphate, (30 min, 37 ºC), in an alkaline buffer solution (pH 10.3), followed by colorimetric determination of the product, p-nitrophenol, at 405 nm. The results were expressed as nanomoles of p-nitrophenol produced per minute per microgram of total protein (nmol.min^{-1}/μg protein).

Total RNA extraction and RT-PCR analysis

RT-PCR was used to access the expression of ALP, bone morphogenic protein-2 (BMP-2) and collagen type I (Col I) genes by bone marrow-derived osteoblastic cells, grown for 21 days on the surface of control, cpTi-UHMWPE and cpTi/HA-UHMWPE samples. Total RNA was extracted using the RNAeasy® Mini Kit from Qiagen, according to the manufacturer's instructions and was quantified by measuring the absorbance of the samples at 260 nm. RT-PCR was done using the TitanOne TubeRT-PCR System from Roche Applied Science, according to the manufacturer's instructions. Briefly, 0.5 µg of total RNA from each sample was reverse transcribed into cDNA (30 min at 50 ºC), while PCR was performed with an annealing temperature of 55 ºC, for 25 cycles. The used primers are reported in Table 1.

Table 1. Specific PCR primers.

Gene	Forward primer	Reverse primer
ALP	ACGTGGCTAAGAATGTCATC	CTGGTAGGCGATGTCCTTA
BMP-2	GACGAGGTCCTGAGCGAGTT	GCAATGGCCTTATCTGTGAC
Collagen I	TCCGGCTCCTGCTCCTCTTA	ACCAGCAGGACCAGCATCTC
GADPH	GGAAGGTGAAGGTCGGAGTCAAC	GTGGCAGTGATGGCATGGACTGT

Following, the PCR products were electrophoresed in a 1% agarose gel, stained with ethidium bromide. Densitometric analysis was performed with the ImageJ software (version 1.41o, National Institutes of Health, USA) after normalization to the housekeeping gene GADPH.

Immunostaining of F-actin cytoskeleton.

At days 3 and 14 of the culture, the cells were fixed (4% formaldehyde, 15 min), permeabilized with 0.1% triton and incubated in 10 mg.ml^{-1} bovine serum albumin with 100 µg.ml^{-1} RNAse. F-actin filaments were stained with Alexa Fluor-conjugated phalloidin (1:100) and nuclei were counterstained with 10 µg.ml^{-1} propidium iodide. Images were obtained using aLeica TCP SP2 AOBS confocal microscope.

Matrix mineralizarion

At days 14 and 21, the cultures were fixed (1.5% of glutaraldehyde in 0.14 M of sodium cacodilate buffer, 10 min), dehydrated in graded alcohols (70, 80, 2 × 90 and 99.8%), dried at critical point and sputter-coated with gold. The samples were observed by SEM and analyzed by x-ray spectroscopy (EDS), under a FEI Quanta 400FEG

scanning electron microscope equipped with EDS microanalysis capability, EDAX Genesis X4M.

Statistical analysis.

The results are presented as arithmetic means ± standard deviation of five replicates. Analysis of the results was carried out with the use of Student's t-test, with a significance level of $P < 0.05$.

Results

Cell viability/proliferation

Cell viability/proliferation, evaluated through the MTT assay, is presented in Figure 2. The cells grown on the surface of the culture plate (control cultures) proliferated through the culture time, with a stationary phase during the third week.

Regarding the cpTi-UHMWPE samples, MTT reduction was lower at days 7 and 14, and similar at day 21. The pre-incubation treatment did not have a significant effect on the cell viability/proliferation of the seeded cpTi/UHMWPE samples. Comparatively, seeded cpTi/HA-UHMWPE presented lower MTT reduction values through the culture time. The outcomesof the pre-incubation revealed to be significant for this material. At days 7, 14 and 21, the values were significantly higher than those observed in the non-pre-incubated samples.
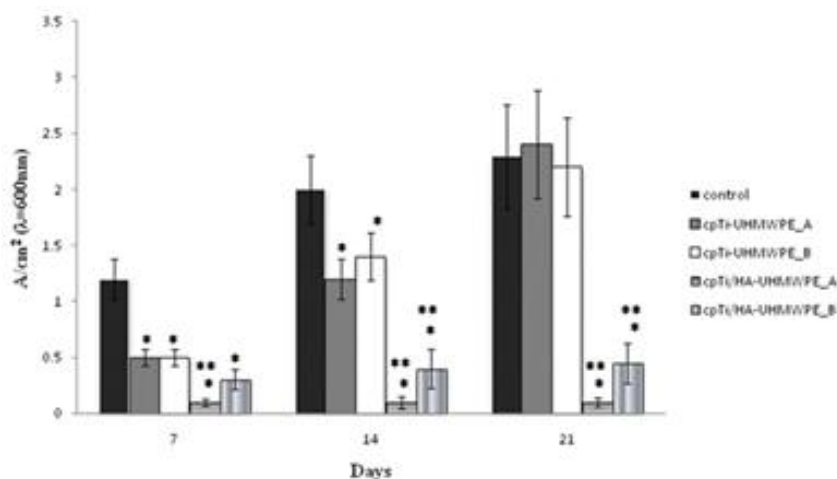

Figure 2 - Cell viability/proliferation of human bone marrow osteoblastic cells cultured for 21 days on the culture plate (control), and on the surface of cpTi-UHMWPE and cpTi/HA-UHMWPE. A: 'as prepared' samples; B: pre-incubated samples. *Significantly different from control. **Significantly different from cpTi-UHMWPE.

Immunostaining of the cytoskeleton

Confocal laser scanning microscopy (CLSM) appearance of the material samples labeled for F-actin and nuclei is shown in Figure 3. On cpTi-UHMWPE (both on 'as-prepared' and pre-incubated samples), at day 3, the cells were well distributed on the material surface and presented an elongated morphology and cell-to-cell contact (Figures 3A, B); at day 14, the cell layer covered a significant area of the material surface (Figures 3E, F). 'As-prepared' cpTi/HA-UHMWPE presented a poor performance; the few cells attached to the surface displayed a disrupted morphology, which further deteriorated throughout the culture time (Figures 3C, G). However, on the pre-incubated samples, the cells appeared well spread and, at day 14, disperse cell aggregates were found throughout the materials' surface (Figures 3D, H). At a high magnification, the organization of the actin cytoskeleton of both pre-incubated cpTi-UHMWPE and cpTi/HA-UHMWPE samples appeared similar to that of control, Figures 3I–K.
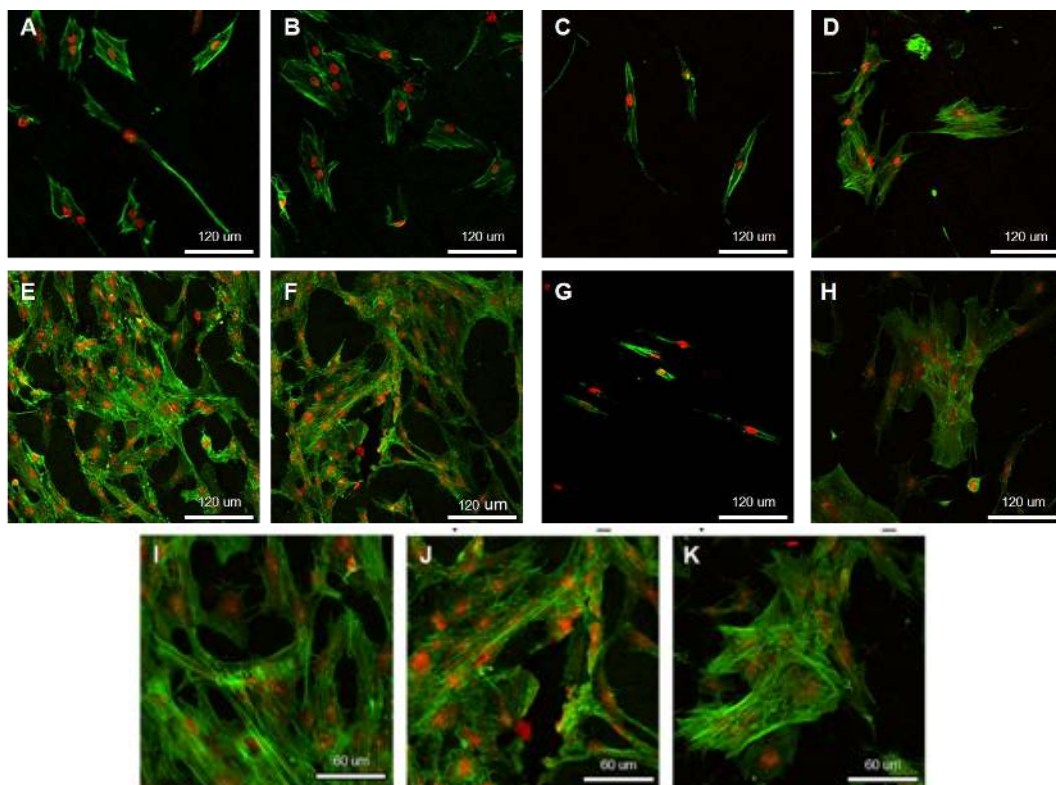

Figure 3 - CLSM appearance of the cpTi-UHMWPE and cpTi/HA-UHMWPE samples cultured with human bone marrow osteoblastic cells for 3 days (A)–(D) and 14 days (E)–(H). cpTi-UHMWPE A (A, E) and cpTi/HA-UHMWPE A (C, G): 'as prepared' samples; cpTi-UHMWPE B (B, F) and cpTi/HA-UHMWPE B (D, H): pre-incubated samples. High magnification of control cultures (I); pre-incubated cpTi-UHMWPE (J) and pre-incubated cpTi/HA-UHMWPE (K), at 14 days.

Cell function

Figure 4 shows that, regarding ALP activity, both 'as-prepared' and pre-incubated cpTi-UHMWPE samples, as well as the pre-incubated cpTi/HA-UHMWPE materials, presented a profile similar to that of the control cultures, i.e. a significant increase in the enzyme activity during the third week of culture. By contrast, ALP was practically absent on the seeded 'as-prepared' cpTi/HA-UHMWPE samples.
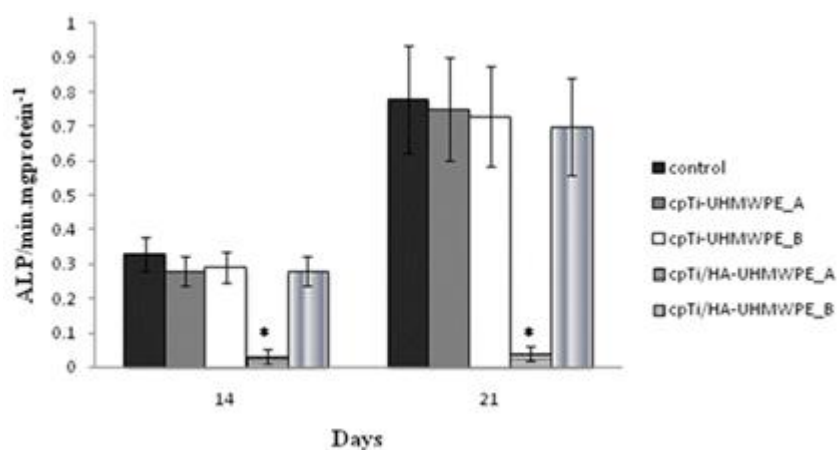

Figure 4 - ALP activity of human bone marrow osteoblastic cells cultured for 21 days on the culture plate (control) and on the surface of cpTi-UHMWPE and cpTi/HA-UHMWPE. A: 'as prepared' samples; B: pre-incubated samples. *Significantly different from control.

Regarding the assessment of osteogenic-related gene expression by RT-PCR, following 21 days of culture over both control and material samples pre-incubated with the culture medium, there were no significant differences found regarding the expression of ALP, BMP-2 and Col I, as shown in Figure 5.
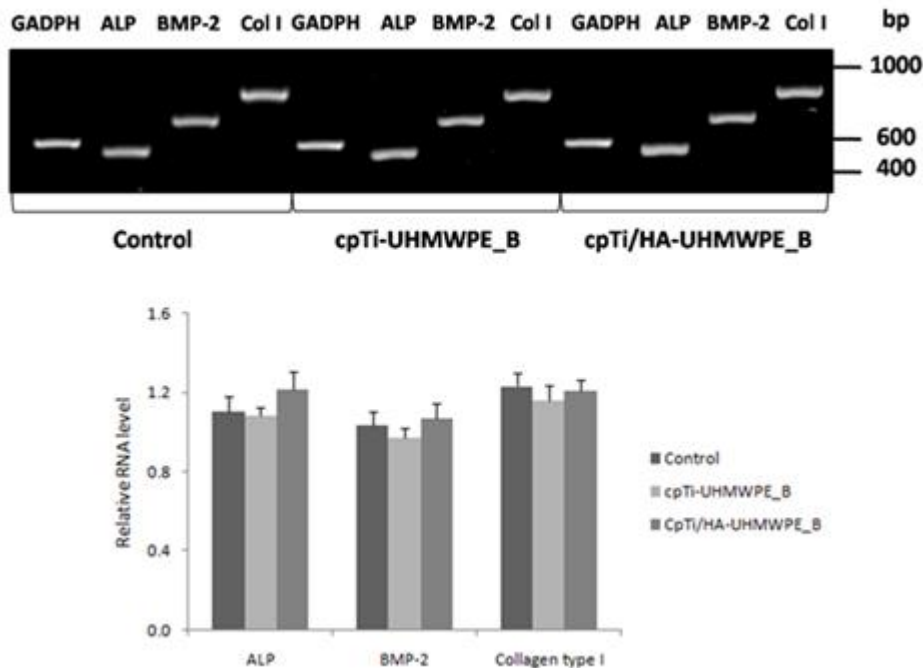
Figure 5 - Results from the RT-PCR of osteogenic-associated genes (ALP, BMP-2 and Col I) in cultures established for 21 days on the surface of control and pre-incubated samples. Representative agarose gel and densitometric analysis.

SEM observation of the cpTi-UHMWPE samples at days 14 and 21 (Figure 6) showed an excellent proliferation profile with the surface completely covered by a cell layer, at day 21. In addition, the 21 day cultures displayed discrete mineralized deposits which contained calcium and phosphorus. The pre-incubation treatment did not affect the cell behavior. On the other hand, cpTi/HA-UHMWPE seeded under the 'as-prepared' condition showed few attached cells with a disrupted structure (Figures 7A and D, 14 day cultures). However, the pre-incubated cpTi/HA-UHMWPE samples presented cell clusters with evident formation of cell-mediated mineralized deposits at day 14 (Figures 7B, C and E). For comparison, Figure 8 shows the SEM appearance of human bone marrow cells cultured on the tissue culture plate (control cultures), at days 14 and 21. The presence of calcium phosphate deposits was observed by day 21.
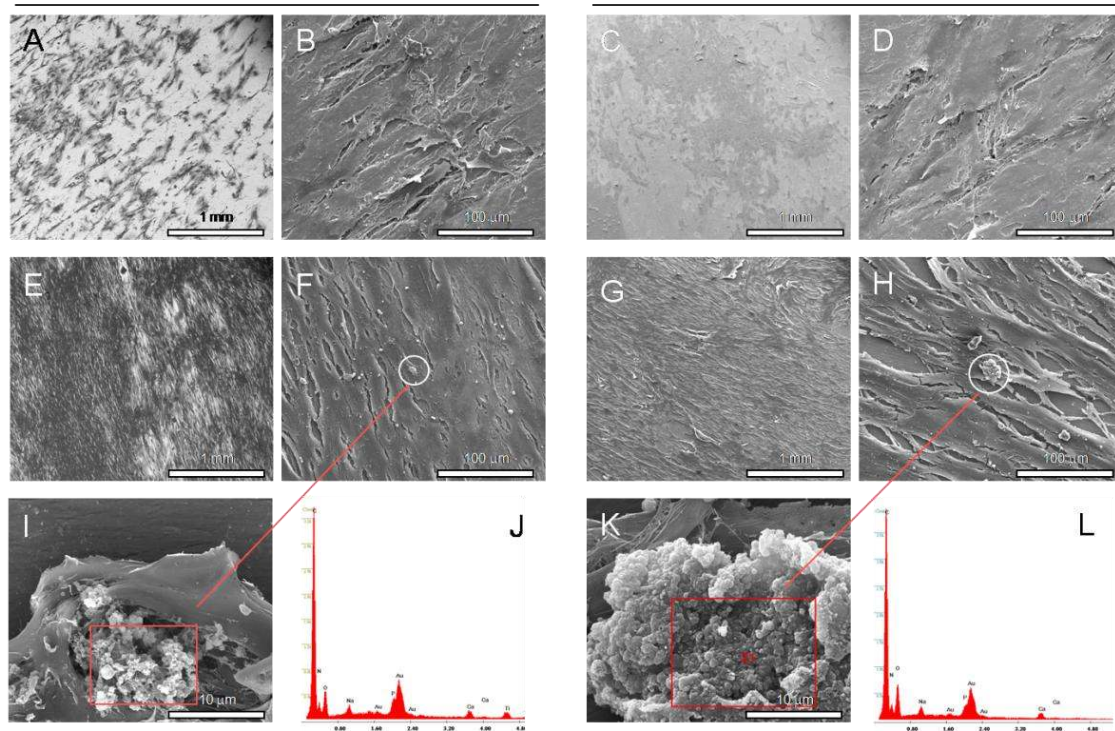
Figure 6 - SEM appearance of the cpTi-UHMWPE samples cultured with human bone marrow osteoblastic cells for 14 days (A)–(D) and 21 days (E)–(H). High magnification of the mineralized deposits in 21 day samples (I) and (K) and the respective EDS spectra (J) and (L). cpTi-UHMWPE A (A, B, E, F, I, J): 'as prepared' samples; cpTi-UHMWPE B (C, D, G, H, K, L): pre-incubated samples.
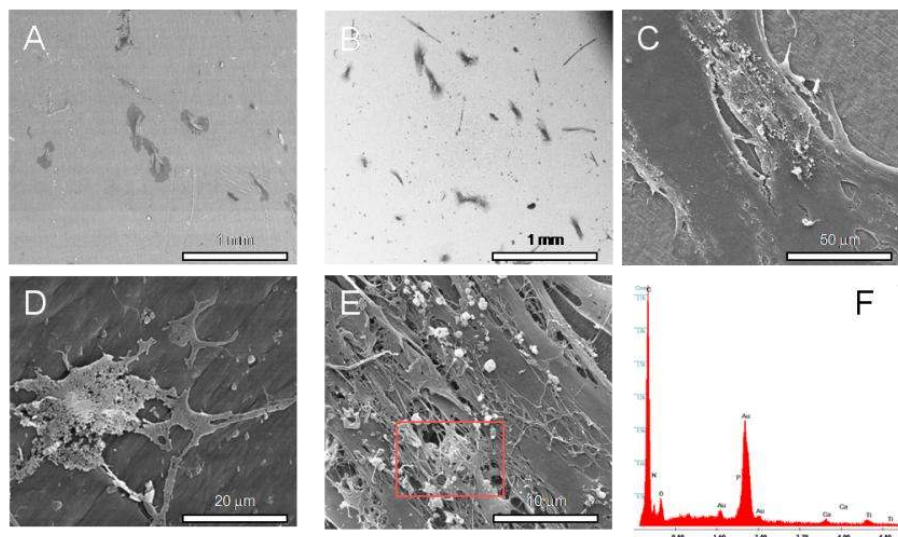

Figure 7 - SEM appearance of the cpTi/HA-UHMWPE samples cultured with human bone marrow osteoblastic cells for 14 days (A)–(E). (F) EDS spectrum of the mineralized deposits present on pre-treated cp-Ti/HA-UHMWPE. cpTi/HA-UHMWPE A (A, D): 'as prepared' samples; cpTi/HA-UHMWPE B (B, C, E, F): pre-incubated samples.
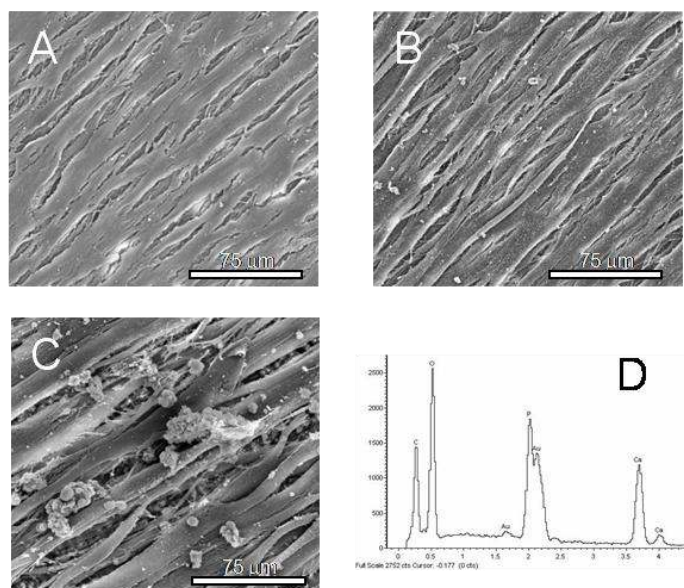
Figure 8 - SEM appearance of human bone marrow osteoblastic cells cultured on standard tissue culture plates (control cultures) for 14 days (A) and 21 days (B), (C). (D) EDS spectrum of the mineralized deposits.

Discussion

The development of UHMWPE samples coated with cpTi (cpTi-UHMWPE) or cpTi and HA (cpTi/HA-UHMWPE), by DC magnetron sputtering and DC/RF magnetron cosputtering, respectively, aimed the conception of a novel acetabular component made of just one piece, in which the metallic shell is substituted by a coating material. The cellular biocompatibility of the coated UHMWPE samples was assessed with human bone marrow cells cultured under experimental conditions known to favor osteoblastic differentiation [24]. The material samples were tested 'as-prepared' and after a pre-incubation treatment with fully supplemented culture medium for 24 h.

The seeded cpTi-UHMWPE samples exhibited the complete proliferation/differentiation sequence of human bone osteoblastic cells,with a high cell growth, the synthesis of high ALP levels, expression of osteogenic-related genes, and the formation of a calcium-phosphate-containing mineralized matrix by day 21. Compared to control, fewer cells attached to the material surface, as suggested by the lower values in the MTT assay, at day 7. This is most probably related to the seeding procedure in which a cell suspension was poured over the surface of a disk and, as expected, a significant percentage of cells slipped off to the bottom of the culture plate. This event was further enhanced by the smooth features of the material surface. However, subsequently, the attached cells presented a high proliferation rate forming a cell sheet over the surface, from 2 weeks onward. At day 21, the MTT reduction values

were similar to control suggesting a good performance of this material. Pre-incubation treatment revealed to have no significant influence on the biological behavior of the cpTi- UHMWPE samples. The present results are in agreement with the known behavior of titanium surfaces, which are reported to be biocompatible, supporting osteoblast proliferation and differentiation, as well as adequate osteointegration in vivo [16].

The results regarding the cpTi/HA-UHMWPE samples showed that the performance of this coating was very sensitive to the pre-incubation treatment. The 'as-prepared' samples reported few attached cells with disrupted morphology and low viability. This behavior might be related to the leaching of the HA component leading to an altered ionic concentration on the surface microenvironment impairing cell anchorage and adhesion which compromises the subsequent proliferation event. These limitations are favored by the in vitro stationary system used, which does not allow the renewal of the medium, resulting in accumulation of the leaching material on the coating surface. In vivo, the impairment of the cell response due to these surface events is expected to be attenuated by the permanent flow of body fluids at the cell/biomaterial interface. In addition, the material surface is conditioned by bioactive molecules present in the extracellular fluid, providing a suitable environment for the adhesion of the available osteoprogenitor cells. In this way, pre-incubation of the cpTi/HA-UHMWPE samples with a complete culture medium, before cell seeding, should decrease the deleterious effects resulting from the accumulation of leaching products on the material surface and also provide some biological conditioning of the surface. Accordingly, results showed that pre-incubation of the cpTi/HA-UHMWPE samples improved cell behavior, i.e. the cells exhibited a normal morphology and organized into small cell clusters that expressed high levels of ALP and showed earlier exuberant cell-mediated matrix mineralization compared to cpTi-UHMWPE coating. Several works in the literature using CaP-sputtered coatings support these results. For instance, Hulshoff et al stated that proliferation of mouse osteoblastic cells was significantly higher on noncoated samples compared to CaP-coated Ti samples, although increased matrix mineralization was established on the coated surfaces. Also, TEM analysis showed that the cells were embedded by crystallized needle-shaped CaP structures, entrenched in collagen fibers [25]. Further, Perozzolo et al reported that osteogenic cells from a newborn rat calvaria presented significantly more 'bone-like nodules' when cultured over HA-coated surfaces compared to titanium-coated ones [26]. One of the mechanisms associated with the increased differentiation process may be related to the early dissolution of the CaP coating, increasing the availability of calcium and phosphate in the microenvironment, followed by the

formation of a bonelike mineral layer by re-precipitation. This mineral layer may favor early protein adhesion that enhances cell behavior, namely the differentiation process of osteoblastic cells [27]. The surface characteristics of cpTi-UHMWPE and cpTi/HAUHMWPE might also contribute to the different cell behavior on the material samples. In regard to surface topography, as visualized by high magnification SEM micrographs, the observed differences may contribute to the distinct biological behavior. In addition, the characterization of the adhesion values of the deposited coatings on the substrate was considered to be among those which are strong enough to be used in the envisaged applications. Unlike HA coatings on metallic implants, there are no minimum requirements for this kind of coating in the medical field. The association of HA with cpTi led to a slight increase of the coatings' hydrophilicity, as was determined by contact angle measurements with water, and to a less negative zeta potential, as was determined by streaming potential measurements. However, the biological significance of these differences is most probably negligible considering that the behavior of the cpTi/HA-UHMWPE coating, under cell culture conditions, was highly conditioned by material leaching, hampering a correlation with surface charge and hydrophobicity effects. Additional biological characterization should be conducted, reaching the level of dynamic in vitro cell culture models or preliminary in vivo experiments, in order to further address and compare the biological profile of both developed systems.

Conclusion

The cpTi-UHMWPE and cpTi/HA-UHMWPE systems, prepared by DC magnetron sputtering and DC/RF magnetron co-sputtering, respectively, might constitute useful approaches to the development of novel acetabular components made of just one piece, in which the coating material establishes a direct interface with the bone tissue. The cpTi-UHMWPE samples allowed a high cell proliferation and ALP expression, while the cpTi/HA-UHMWPE system induced earlier cell-mediated matrix mineralization—the final event of the in vitro osteogenic differentiation. These newly developed systems may be suitable candidates to improve the osteointegration process in arthroplastic devices; nevertheless, further biological evaluation should be conducted.

References

1. Niinomi M. Recent research and development in titanium alloys for biomedical applications and healthcare goods Sci Technol Adv Mater 2003;4:445–54.

2. Ratner BD, Hoffman AS, Schoen FJ, Lemons JE, editors. Biomaterials Science: An Introduction to Materials in Medicine 2004, (Amsterdam: Elsevier).

3. Liang H, Shi B, Fairchild A, Cale T. Applications of plasma coatings in artificial joints: an overview. Vacuum 2004;73:317–26.

4. Kurtz S, Muratoglu O, Evans M, Edidin A. Advances in the processing, sterilization, and crosslinking of ultra-high molecular weight polyethylene for total joint arthroplasty. Biomaterials 1999;20:1659–88.

5. Kurtz S, editor.The UHMWPE Handbook (New York: Academic) pp 71–92

6. Berry D, Harmsen W, Cabanela M, Morrey B. 25-year survivorship of 2000 consecutive primary Charnley total hip arthroplasties J Bone Joint Surg Am 2002;84:171–7.

7. Dunne N, Orr J. Curing characteristics of acrylic bone cement. J Mater Sci: Mater Med 2002;13:17–22.

8. Webb J, Spencer R. The role of polymethylmethacrylate bone cement in modern orthopaedic surgery. J Bone Joint Surg Br 2007;89:851–7.

9. Callaghan JJ, Templeton JE, Liu SS, Pedersen DR, Goetz DD, Sullivan PM, Johnston RC. Results of Charnley total hip arthroplasty at a minimum of thirty years. A concise follow-up of a previous report. J Bone Joint Surg Am 2004;86 690–5.

10. Berry DJ, Harmsen WS, Cabanela ME, Morrey BF. Twenty-five-year survivorship of two thousand consecutive primary Charnley total hip replacements: factors affecting survivorship of acetabular and femoral components. J Bone Joint Surg Am 2002;84:171–7.

11. Hamilton W, Calendine C, Beykirch S, Hopper R, Engh C. Acetabular fixation options—first-generation modular cup curtain calls and caveats. J Arthroplasty 2007;22:75–81.

12. Nashed R, Becker D, Gustilo R. Are cementless acetabular components the cause of excess wear and osteolysis in total hip arthroplasty? Clin Orthop Relat Res 1995;317:19-28.

13. Hamilton W, Hopper R, Ginn S, Hammell N, Engh C Jr, Engh C. The effect of total hip arthroplasty cup design on polyethylene wear. J Arthroplasty 2005;20:63–72.

14. Lappalainen R, Santavirta SS. Potential of coatings in total hip replacement: materials and tribology on total hip replacement. Clin Orthop Relat Res 2005;430:72–9.

15. Brånemark R, Brånemark PI, Rydevik B, Myers RR. Osseointegration in skeletal reconstruction and rehabilitation: a review. J Rehabil Res Dev 2001;38:175–81.

16. Rodriguez J. Acetabular fixation options: notes from the other side. J Arthroplasty 2006;21:93–6.

17. Chen X, Nouri A, Li YC, Lin JG, Hodgson PD, Wen CE. Effect of surface roughness of Ti, Zr, and TiZr on apatite precipitation from simulated body fluid. Biotechnol Bioeng 2008;101:378–87.

18. Wang XJ, Li YC, Lin JG, Hodgson PD, Wen CE. Apatite-inducing ability of titanium oxide layer on titanium surface: the effect of surface energy. J Mater Res 2008;23:1682–8.

19. Yang Y, Kim K, Ong J. A review on calcium phosphate coatings produced using a sputtering process: an alternative to plasma spraying. Biomaterials 2005;26:327–37.

20. Leeuwenburgh S, Wolke J, Siebers M, Schoonman J, Jansen J. In vitro and in vivo reactivity of porous, electrosprayed calcium phosphate coatings. Biomaterials 2006;27:3368–78.

21. Xiong J, Li Y, Hodgson PD, Wen C. Nanohydroxyapatite coating on a titanium–niobium alloy by a hydrothermal process. Acta Biomater 2010;6:1584–90.

22. Massaro C, Baker M, Cosentino F, Ramires P, Klose S, Milella E. Surface and biological evaluation of hydroxyapatite-based coatings on titanium deposited by different techniques. J Biomed Mater Res 2001;58:651–7.

23. Silva MA, Vila M, Tavares C, Gomes PS, Fernandes MH, Santos JD, Silva R, Lopes MA. Physicochemical characterization of cpTi and cpTi/HA coatings onto UHMWPE material. J Mater Sci:Mater Med 2010, submitted.

24. Coelho M, Fernandes MH. Human bone cell cultures in biocompatibility testing: part II. Effect of ascorbic acid b-glycerophosphate and dexamethasone on osteoblastic differentiation. Biomaterials 2000;21:1095–102.

25. Hulshoff J, van Dijk K, van der Waerden J, Wolke J, Ginsel L, Jansen J. Biological evaluation of the effect of magnetron sputtered Ca/P coatings on osteoblast-like cells in vitro. J Biomed Mater Res 1995;29:967–75.

26. Perozzollo D, Lacefiled W, Brunette D. Interaction between topography and coating in the formation of bone nodules in culture for hydroxyapatite- and titanium-coated micromachine surfaces. J Biomed Mater Res 2001;56:494–503.

27. LeGeros R, Orly I. The Bone Biomaterial Interface. Ed, J Davies (Toronto: Toronto University Press) pp 76–88.

Chapter 7

Growth and phenotypic expression of human endothelial cells cultured on a glass-reinforced hydroxyapatite

Growth and phenotypic expression of human endothelial cells cultured on a glass-reinforced hydroxyapatite

J.M. Silva Marques[1], P.S. Gomes[2], M.A. Silva[3], A.M. Silvério-Cabrita[4], J.D. Santos[3], M.H. Fernandes[2]

1 - Cooperativa de Ensino Superior Egas Moniz, Monte de Caparica, Portugal

2 - Laboratório de Farmacologia e Biocompatibilidade Celular, Faculdade de Medicina Dentária, Universidade do Porto (FMDUP), Rua Dr. Manuel Pereira da Silva, 4200-393 Porto, Portugal

3 - Faculdade de Engenharia da Universidade do Porto (FEUP), Secção de Materiais (DEMM), Rua Dr. Roberto Frias, 4200-465 Porto, Portugal

4 - Instituto de Patologia Experimental, Faculdade de Medicina, Universidade de Coimbra, Coimbra, Portugal

Abstract

Glass-reinforced hydroxyapatite composites (GR–HA) are bone regenerative materials that are characterized by their increased mechanical properties, when compared to synthetic hydroxyapatite. Bonelike® is a GR–HA that is a result of the addition of a $CaO–P_2O_5$ based glass to a HA matrix. This biomaterial has been successfully applied in clinical bone regenerative applications.

This work aims to evaluate the ability of Bonelike® to support the adhesion, proliferation and phenotypic expression of human endothelial cells, aiming to establish new bone tissue engineering pre-endothelialization strategies. Bonelike® discs, regardless of being submitted to a pre-immersion treatment with culture medium, were seeded with first passage human umbilical vein endothelial cells, and characterized regarding proliferation and differentiation events. Pre-immersed Bonelikeallowed the adhesion, proliferation and phenotype expression of endothelial cells. Seeded materials presented positive immunofluorescent staining for PECAM-1 and a tendency for the formation of cord-like arrangements under angiogenesis-stimulating conditions, although, compared to standard culture plates, a slight decreased cell growth was observed. In this way, Bonelike® may be a suitable candidate for pre-endothelialization approaches in bone tissue engineering applications.

Introduction

The current interest about the process of angiogenesis—the formation of new blood vessels from pre-existing ones—is growing in all research and clinical fields, aiming to solve several pathological conditions, including the impaired tissue regeneration. The interaction between the bone and the vascular system has long been known [1] although, for a long time, research focused on the osteogenic process. More recently, a paradigm shift was driven into the establishment of adequate vasculature given that insufficient or inappropriate tissue irrigation is associated with decreased bone formation [2]. Also, inhibition of the angiogenic process leads to the formation of fibrous tissue in animal models of bone fracture repair [3] and distraction osteogenesis [4]. It is also established that poor blood supply is a risk factor for bone healing and that several other risk factors may act negatively over the vasculature, impairing an adequate biological response [5–7].

Upon implantation of a bone graft, the first days are critical, with inflammation and revascularization occurring. Current evidence reflects that the establishment of adequate vascularisation, right after the implantation, is essential for the development of the repair process and wound healing [7, 8]. An adequate vascular network allows the nutritional support and removal of metabolic waste products from the regenerating area, and provides a continuous availability of precursor cells to the target area, along with a large variety of biological mediators involved in cell-to-cell communication [9, 10]. In this way, endothelial cells play an essential role in the wound healing as they constitute the inner surface of the blood vessels and are the primary cells involved in the process of angiogenesis. They are also actively engaged in the release of cytokines and the expression of cell adhesion molecules, thus participating in the inflammatory response and contributing to the intercellular cross-talk. This process is particularly relevant when established within cells of the osteoblastic lineage, which are responsible for the bone formation events at the material's surface [7].

Accordingly, several approaches have emerged to enhance the rate of vascularization from the surrounding tissues into the implanted bone grafts. These include the incorporation of angiogenic factors into the materials [11,12], deposition of an angiogenic extracellular matrix on the materials' surface [13, 14] and delivery of genes encoding angiogenic factors [15–17], all aiming to induce the endothelial function. Other promising approach is the materials' pre-vascularization with autologous endothelial cells which, upon implantation with the host's vascular system, would allow a rapid vascular supply throughout the biomaterial. Regarding this, recent in vitro studies addressed the potential of several bone regenerative materials to

perform as appropriate substrates for endothelial cell growth and differentiation, to be used on tissue regeneration applications [18, 19].

New approaches on biomaterial's production for tissue engineering strategies include natural and synthetic materials, designed in a biomimetic approach regarding the bone tissue composition. Biological apatite (which comprises the mineral phase of the calcified tissues) contains mainly Ca^{2+}, PO_4^{3-} and OH^- ions, although several trace ions like Mg^{2+}, F^- and CO_3^{2-} are also present and contribute to an important biological purpose. Synthetic hydroxyapatite (HA), with the chemical composition of $Ca_{10}(PO_4)_6(OH)_2$, differs from the biological one regarding the stoichiometry, composition, crystallinity and other physical and mechanical properties [20]. Bonelike® is a glass-reinforced HA with the ability to mimic bone's inorganic chemical composition, with a microstructure composed by HA, α-tricalcium phosphate (α-TCP) and β-TCP phases spread throughout the material, creating fully interpenetrated matrices of HA and TCP [21, 22]. Bonelike® supports the proliferation and differentiation of human osteoblastic cells [23, 24] and allows fast bone formation at the bone/material interface in animal models [25, 26]. Regarding clinical application, Bonelike® grafts have been successfully applied in several areas of regenerative surgery, namely, in oral and maxillofacial surgery, implantology and orthopaedics, in a particulated form [27–30], as well as in a tridimensional macroporous scaffold, prepared by a biomodelling technique [31]. Clinical data clearly shows that Bonelike® presents appropriate features to perform as a bone graft [27–31].

Considering the relevance of angiogenic strategies in bone tissue engineering applications, the present work evaluates the ability of Bonelike® to support the adhesion, growth and differentiation of human endothelial cells. This aims to access the potential suitability of this biomaterial for pre-endothelialization approaches in order to improve graft vascularization, in bone tissue regenerative applications.

Material and Methods

Preparation of Bonelike®

For the production of Bonelike®, a glass was prepared with the chemical composition of $65P_2O_5$–$15CaO$–$10CaF_2$–$10Na_2O$ in mol% from reagent-grade chemicals using conventional glass making techniques. The composite was obtained by adding the milled glass to HA powder (Plasma Biotal; Tideswell UK) in 2.5% (wt/wt), using isopropanol as a solvent. The powders were mixed, dried and sieved to less than 75 m and disc samples were prepared by uniaxial pressing at 200 MPa, using steel dies to obtain 8 mm diameter discs. The discs were then sintered at 1300ºC (using a ramp rate of 4ºC/min), with the temperature being maintained for 1 h, followed by

natural cooling inside the furnace. Detailed description of Bonelike® preparation has been previously reported [22]. Phase identification and quantification was assessed by X-ray diffraction and Rietveld analysis.

For in vitro testing, the discs were mechanically polished to the same final topology of 1 μm using silicon carbide paper, ultrasonically degreased, cleaned with ethanol followed by deionized water and sterilized by autoclaving. Before cell seeding, Bonelike® samples were observed by scanning electron microscopy (SEM) for the assessment of the surface topography.

Culture of human endothelial cells on Bonelike®

Primary cultures of endothelial cells were established from human umbilical veins, from umbilical cords, following a standard procedure [13]. This biological material, that would be otherwise discarded, was obtained through local hospitals under the approval of the appropriate Ethical Committee, with patient informed consent.

Briefly, umbilical cords were perfused with isotonic solution to remove blood and cellular debris. Following, endothelial cells were released from the umbilical vein with 0.1% collagenase in medium M199 (7 min, 37ºC, 5% CO_2/air) and the resultant cell suspension was centrifuged (1,500 rpm, 5 min). Cells were resuspended and seeded in culture plates pre-coated with 0.2% gelatine (1 h, 37ºC). Cultures were established (37ºC, 5% CO_2/air) in medium M199 supplemented with 20% foetal bovine serum, penicillin–streptomycin (100 UI/ml and 100 lg/ml, respectively) and 1% L-glutamine. At 70–80% confluence, primary cultures were enzymatically released (0.04% trypsin in 0.25% EDTA solution), and the obtained cell suspension was seeded (2 x 10^4 cells/cm^2) in standard 48-well plates (control cultures) and on the surface of Bonelike® discs, both previously coated with 0.2% gelatine. Bonelike® samples were assayed with or without being submitted to a preimmersion treatment of 3 h, in complete culture medium. Cultures were maintained for 7 days in the medium described above, further supplemented with 1% sodium heparin and 1 μg/ml endothelial cell growth supplement (ECGS). Control and seeded Bonelike® samples were characterized throughout the culture time for cell viability/proliferation, cytoskeleton organization, expression of platelet endothelial cell adhesion molecule-1 (PECAM-1) and ability to form tube-like networks upon the addition of a collagen type I gel.

Cell viability/proliferation: visualization of cell growth

MTT assay - reduction of 3-(4,5-dimethylthiazol-2-yl)-2,5-diphenyltetrazolium bromide to a purple formazan product by viable cells - was used to estimate endothelial cell viability/proliferation, during the 7 day culture period. At determined time points, samples were incubated with 0.5 mg/ml of MTT for the last 4 h of the culture period; the medium was then decanted, formazan salts were dissolved with dimethylsulphoxide and the absorbance (A) was determined at $\square$ = 600 nm on a microplate reader. Results were expressed as A/cm^2.

Also, at days 3 and 6 of the culture period, cells were incubated with 0.1 $\square$M calcein-acetoxymethylester (calcein-AM) for 30 min at 37ºC. Calcein-AM is taken up by viable cells and converted by intracellular esterases into the membrane- impermeable fluorescent calcein that spreads throughout the entire cytoplasm of the cell. Fluorescence was visualized by confocal laser scanning microscopy (CLSM).

Immunofluorescent staining of F-actin cytoskeleton filaments and PECAM-1

At days 3 and 6, immunodetection of F-actin and PECAM-1 was conducted by CLSM. Briefly, samples were fixed with 4% formaldehyde (methanol free), permeabilized with 0.1% Triton (5 min, RT) and incubated in 10 mg/ml bovine serum albumin (BSA, 1 h, RT) with 100 μg/ml RNAse. Following, samples were either stained for F-actin or PECAM-1.

F-actin filaments were stained with Alexa-Fluor-conjugated phalloidin® (1:100, 1 h, RT) and nuclei were counterstained with 10 μg/ml propidium iodide (10 min, RT). Alternatively, samples were incubated overnight with primary PECAM-1 antibody (1:100, 48ºC), followed by the addition of the secondary antibody (1:1000, anti-mouse Alexa-Fluor®; 1 h, RT), and then counterstained with 10 μg/ml propidium iodine (10 min, RT).

Culture under angiogenesis-inducing conditions

At adequate confluence (around 80% at 5 days of culture), control cultures and seeded Bonelike® discs were covered with a 1.5 mg/ml solution of collagen type I in M199 (pH ≈ 7.2–7.4). Within 30 min, the collagen mixture formed a gel. Complete culture medium was carefully overlayed on top of the gel and incubation was continued. Samples were analysed for cell viability/growth by calcein-AM staining, 24 h after the addition of the collagen gel.

Statistical analysis

Three independent experiments were performed using cell cultures from different patients. On the MTT assay, each point represents the mean ± standard deviation of three replicates. Statistical differences between control and Bonelike® seeded discs were analyzed by Student's t-test. P-values ≤ 0.05 were considered significant. Qualitative assays were performed in triplicate.

Results

Human endothelial cells, cultured on the surface of Bonelike® discs and on standard polystyrene culture plates, were characterized for cell viability/proliferation and differentiation events.

Bonelike® XRD data revealed a microstructure with a main crystalline phase of HA, with α- and β-TCP as secondary phases (Figure 1a). SEM observation of the polished discs, prior to cell culture, revealed a uniform and smooth surface (Figure 1b).
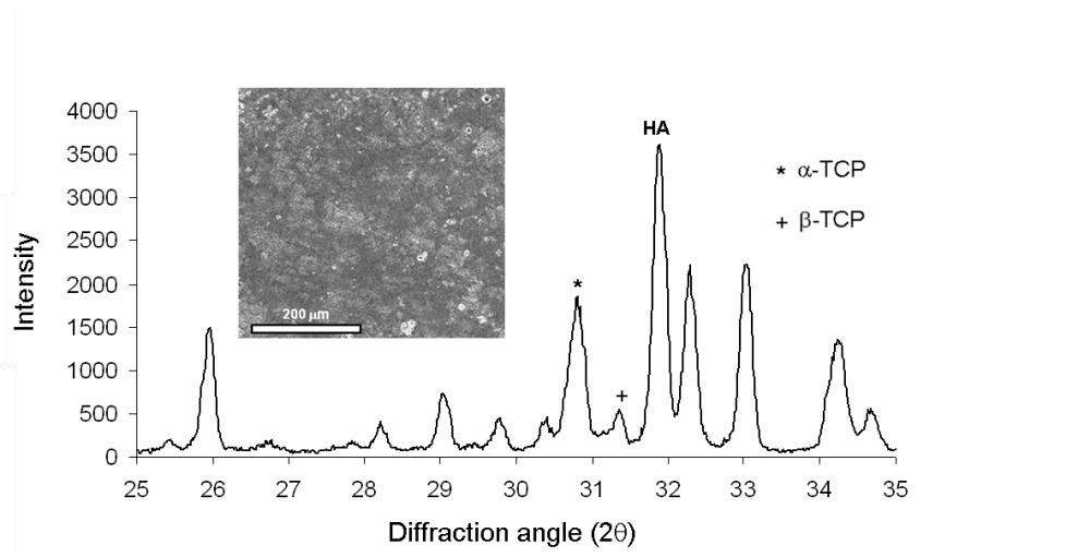

Figure 1 - X-ray diffraction pattern of Bonelike®, showing the presence of HA and α-and β-TCP phases and SEM appearance of the polished material samples (inset).

Cell viability/proliferation. Pattern of cell growth

Bonelike® samples pre-coated with gelatine, but not submitted to the pre-immersion treatment with culture medium, presented a poor performance. Cells were able to attach to the material's surface, as demonstrated by the micrograph taken at 24 h, but few cells were visible at 48 h and evident cytoskeleton modifications were visualized by F-actin staining (Figure 2). In addition, distributed cellular debris could be observed at 24 and 48 h of culture, on the material's surface.
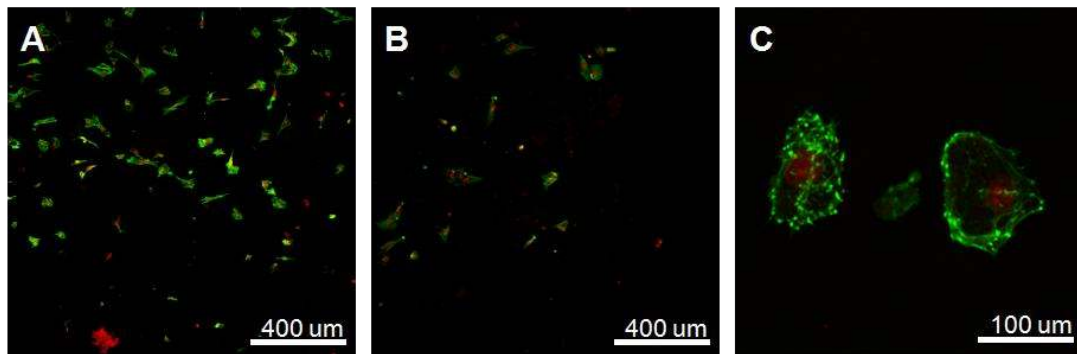
Figure 2 - Life span of human endothelial cells cultured on the surface of Bonelike® discs not submitted to the pre-immersion treatment with culture medium. Cells were able to attach to the material surface (A, 24 h) but died within few hours (B, 48 h). Also, morphological alterations were visualized by F-actin staining (C, 48 h).

CLSM observation revealed that endothelial cells attached to the pre-immersed Bonelike® samples and proliferated throughout culture time. Seeded materials, stained for F-actin cytoskeleton and nucleus, presented a tendency for a circular orientation during the proliferative phase, at 3 days of culture (Figure 3A). Calcein-AM staining demonstrated the viability of these circular arrangements (Figure 3B). In addition, cells presented a normal morphology, with a well defined nucleus, several cytoplasmicspreading and cell-to-cell contacts (Figure 3C). Pattern of cell growth and cell morphology were similar to those observed on standard tissue culture plates (Figure 3D – F).
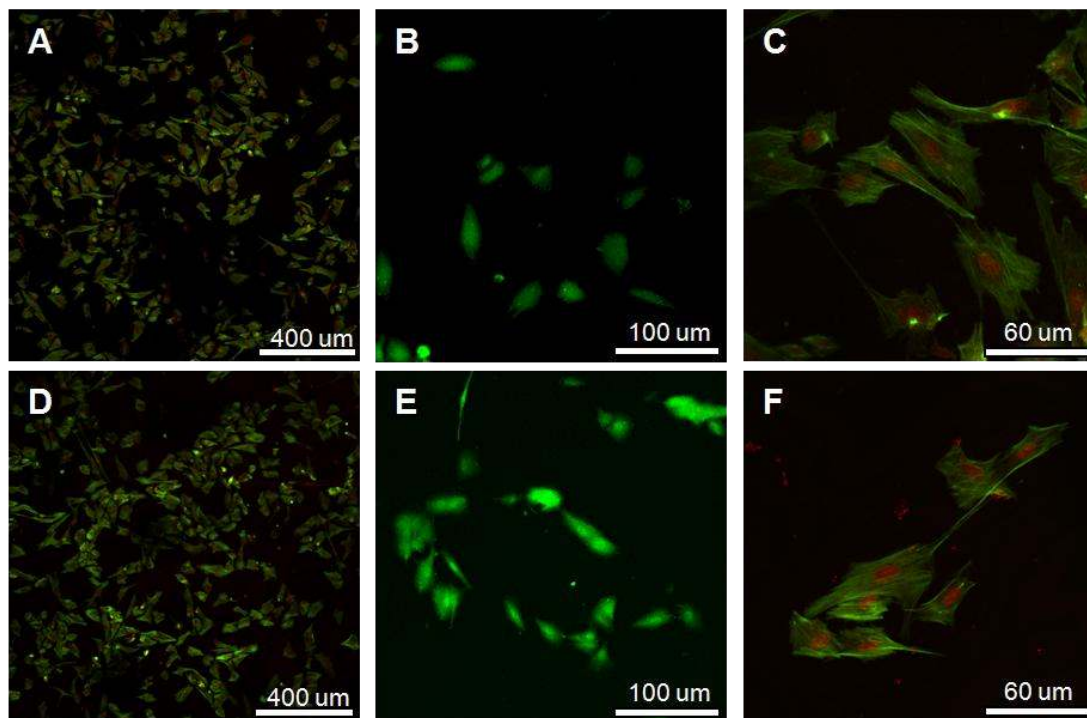
Figure 3 - Organization and morphology of human endothelial cells cultured on Bonelike® discs (A-C) and polystyrene culture plates (D-F) for 3 days. On Bonelike®, cells presented a trend for a circular organization (A, B) and a normal morphology with well-defined nucleus, cytoplasmic spreading and cell-to-cell contact. Pattern of cell organization and cell morphology were similar to those on standard culture plates (D–F). CLSM images: F-actin and nucleus staining (A, C, D, F); Calcein-AM assay (B, E).

Regarding the MTT assay (Figure 4), cultures grown on Bonelike® samples presented an initial lag phase (during approximately 2 days) and proliferated afterwards. Compared to control cultures, MTT reduction values were lower throughout the culture time, with statistical significance at days 3 and 5.
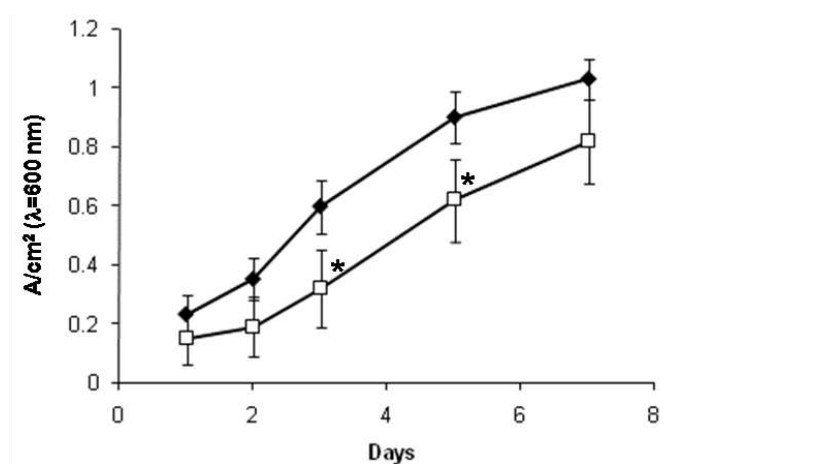

Figure 4 - Cell viability/proliferation (MTT assay) of human endothelial cells cultured on Bonelike® discs (□) and polystyrene tissue culture plates (♦).

143

Expression of the endothelial phenotype

Endothelial cells grown on Bonelike® samples exhibited a positive staining for the presence of PECAM-1 at the junction of adjacent cells, similar to that observed in control cultures, respectively Figure 5A,B and Fig. 5D,E, regarding 6-day cultures.

Addition of a collagen type I gel to the cultures growing on Bonelike® induced a trend for a reorganization of the cell layer with the formation of viable cord-like arrangements after 24 hours, as observed in calcein-AM stained cultures (Figure 5C). In the same experimental conditions, control cultures presented a better organization of the collagen-induced tubular structures (Figure 5F).
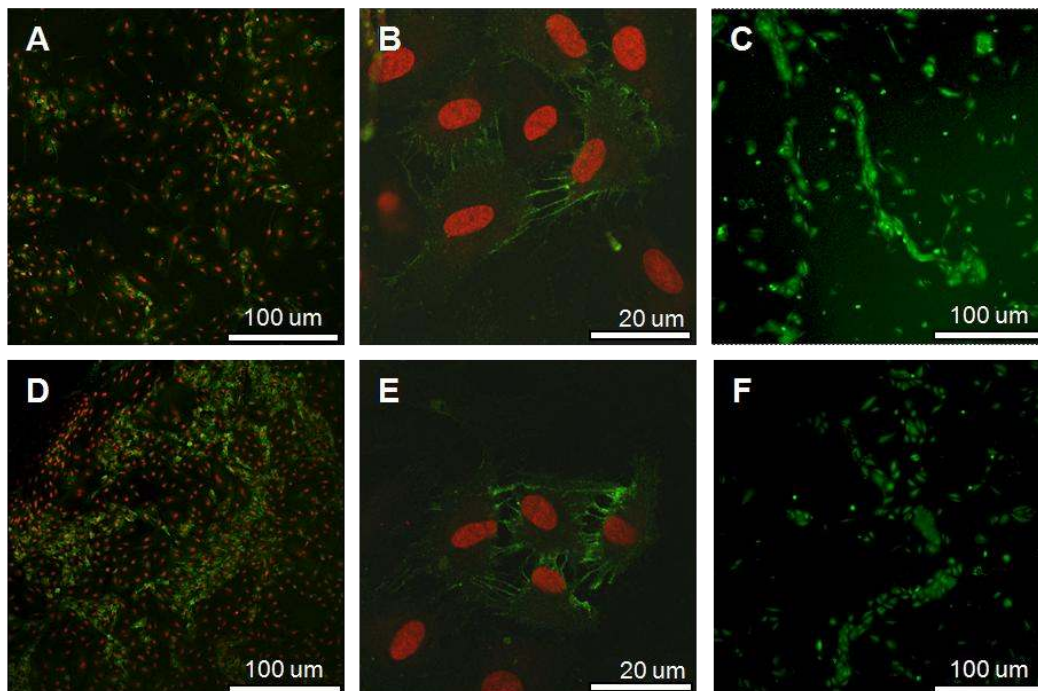

Figure 5 - Expression of functional parameters by human endothelial cells cultured on Bonelike® discs (A–C) and polystyrene culture plates (D–F), at day 6. On Bonelike®, cells exhibited a positive staining for the presence of PECAM-1 at the junction of adjacent cells (A, B) and formed cord-like arrangements upon the addition of a collagen type I gel (C, 24 h after the adhesion of the gel). This behavior was similar to that observed on control cultures (D–F). CLSM images: PECAM-1 staining (A, B, D, E); Calcein-AM assay (C,F).

Discussion

Endothelial cell cultures are a valid in vitro assay in the study of vascular system/biomaterials interactions since they are able to mimic most steps of the complex angiogenic cascade, including endothelial cell proliferation, migration and differentiation [32, 33]. In addition, with the intimate association of the vascular system

with bone and osteogenic cells being stressed, endothelial cell cultures are now considered as a valuable tool in the implementation of bone tissue engineering strategies, namely regarding the possibility of developing pre-vascularization approaches for biomaterials prior to implantation [33, 34]. In the present study, Bonelike® was seeded with first passage human endothelial cells (derived from umbilical veins) and grown for appropriate time periods and conditions for optimal cell proliferation and differentiation [35].

Bonelike® samples assayed in the present work presented a XRD spectrum representative of this material [22]. All materials tested were coated with a gelatine solution. It has been previously reported that several biomaterials require prior coating with adhesion molecules e.g. collagen, gelatin, laminin or fibronectin, in addition to those present in the serum component of culture medium. In their absence, endothelial cell attachment is not efficient and determines an unpredictable cellular spread and growth [36-38]. In this way, cell adhesion and proliferation was first assayed on samples pre-coated with gelatine, but not submitted to a pre-immersion treatment with culture medium (i.e. in the "as-prepared" condition). A reduced biological performance was verified with few cells attached to the material's surface, at 48 hours of culture, with significant cytoskeleton modifications being visualized by F-actin staining. F-actin is highly concentrated just beneath the plasma membrane, forming an organized layer which controls cellular shape and surface movement and is expected to modulate cellular mechanics subjacent to the proliferation and differentiation events [39]. Early cytoskeleton modifications may compromise adequate cell growth and phenotypic expression. Further, cellular debris can be visualized by CLSM at 24 and 48 hours of culture, which is in accordance with the impaired biological behaviour of non-pre-immersed samples.

Bonelike® is a glass-reinforced HA with a HA stable phase and the more soluble phases of α- and β-TCP, and the contact with the culture medium causes an initial superficial leaching [22] resulting in a significant increase in the concentration of ionic species on the material surface difficulting the anchorage of the adhering cells and having deleterious effects on the subsequent cellular events. Accordingly, improved cell behaviour was observed when Bonelike® samples were pre-immersed in the culture medium. Endothelial cells attached to the material surface, exhibiting a normal morphology with cytoplasmic spreading and cell-to-cell contact, and showed a trend for a circular orientation during the proliferative phase, as evident by CLSM observation of the stained samples – either with calcein-AM or F-actin. Pre-immersion of the material with culture medium causes a superficial ionic leaching and, simultaneously, deposition of bioactive molecules from the medium, apparently,

145

rendering the surface more compatible to cell attachment and growth. These dynamic events are more significant at early incubation times and tend to a progressive equilibrium leading to a stabilization of the material surface [22], which probably explains the initial delay in the cell growth and the following improved cell behaviour.

Immunofluorescent staining of PECAM-1 on seeded Bonelike® and control cultures throughout the incubation time was performed in order to access the expression of the endothelial phenotype in culture. PECAM-1 is a 130-KDa transmembrane glycoprotein found in large amounts on endothelial cells, that plays a major role in several cellular interactions, namely in the adhesion cascade between endothelial cells and other cell types involved in the inflammatory process and, also, between adjacent endothelial cells during the process of angiogenesis [40]. These cellular junctions are crucial to maintain the integrity of the endothelial layer and play an essential role in the process of vessel sprouting and elongation [40]. According to some studies, the distribution of PECAM-1 represents a very sensitive marker of endothelial cell functionality [34]. Both seeded standard culture plates and Bonelike® exhibited a positive localized staining at the junction of adjacent endothelial cells. Under culture conditions, the cells are spread flatly and the PECAM-1 concentration along the borders highlights the established cell-cell contacts. In addition, phenotypic characterization was conducted at angiogenesis-stimulating conditions, i.e. upon the addition of a collagen type I gel. Cells growing on standard tissue culture plates showed an evident trend for reorganization with the formation of cord-like structures, in agreement with that reported for the behaviour of cultured endothelial cells in these conditions [41, 42]. Seeded Bonelike® presented a similar trend, an effect independent of the subjacent surface topography, considering the SEM appearance of the material surface before cell seeding. In both situations, these structures maintained their viability, as shown by calcein-AM assay. However, Bonelike® showed a poorer definition of these arrangements which might be related with the surface reactive properties of this material, mentioned above.

Results showed that the in vitro performance of Bonelike® regarding endothelial cell culture was similar to that occurring in standard tissue culture plates, although with an initial impairment regarding cell proliferation. The behaviour of human endothelial cells on ceramic-based biomaterials, aiming at vascularization strategies, was addressed in few recent studies. Choong et al showed that hydroxyapatite-coated polycaprolactone substrates were superior for human bone marrow endothelial cell line (HBMEC-60) attachment and proliferation, compared to untreated substrates [19]. Hunger et al reported that human dermal microvascular endothelial cells (HDMEC), growing on three-dimensional porous hydroxyapatite and calcium phosphate

substrates, did not migrate to form microcapillary-like structures as they did on cell culture plastic [19]. In the present work, rudimental cord-like arrangements could be observed on the Bonelike® samples. Established differences to the reported studies might account for these observations, namely those related to the in vitro system, i.e. endothelial cell type, cell passage, cell plating density, and also, differences regarding the biomaterials tested and pre-treatments carried out. Endothelial cells are very sensitive to the surface properties and chemistry, structure and porosity of the materials, characteristics known to affect cell adhesion, spreading, growth and function [43-45].

The present results provide information regarding the ability of Bonelike® to support the adhesion, proliferation and differentiation of endothelial cells. However, due to the known complex interactions between endothelial and osteoblastic cells in the regeneration environment [7, 33, 34], which has been clearly evidenced in co-culture systems [34, 35], the suggestive suitability of Bonelike® for endothelialization strategies needs to be addressed in more complex and representative models.

Conclusion

Bonelike® allowed the adhesion and spreading of human endothelial cells. Also, this bone graft supported the subsequent proliferation and phenotype expression, with growing cells showing positive immunofluorescent staining for PECAM-1 at cell-cell interfaces and a trend for the formation of cord-like arrangements under angiogenesis-stimulating conditions. The surface reactive properties of Bonelike® are compatible with the proliferation and differentiation of endothelial cells, a relevant cell type involved in the bone regenerative process, suggesting the potential suitability of this bone graft for pre-endothelialization strategies in bone tissue engineering.

References

1. Haller A. Experimentorum de ossiem formatione. In: Grasset F, editor. Opera minora, 1763.

2. Glowacki J. Angiogenesis in fracture repair. Clin Orthop 1998;355S:S82-S89.

3. Hausman M, Schaffler M, Majeska R. Prevention of fracture healing in rats by an inhibitor of angiogenesis. Bone 2001;29:560-564.

4. Fang T, Salim A, Xia W, Nacamuli R, Guccione S, Song H, et al. Angiogenesis is required for successful bone induction during distraction osteogenesis. J Bone Miner Res 2005;20:1114-1124.

5. Einhorn T. The cell and molecular biology of fracture healing. Clin Orthop 1998;355S:S7-S21.

6. Gerstenfeld L, Cullinane D, Barnes G, Graves D, Einhorn T. Fracture healing as a post-natal development process: molecular, spatial and temporal aspects of its regulation. J Cell Biochem 2003;88:873-884.

7. Carano R, Filvaroff E. Angiogenesis and bone repair. Drug Discovery Today 2003;8:980-989.

8. Kirkpatrick C, Unger R, Krump-Konvalinkova V, Peters K, Schmidt H, Kamp G. Experimental approaches to study vascularization in tissue engineering and biomaterial applications. J Mater Sci - Mater Med 2003;14:677-681.

9. Folkman J. Angiogenesis and apoptosis. Semin Cancer Biol 2003;13:159-167

10. Ko H, Milthorpe B, McFarland C. Engineering thick tissues - the vascularisation problem Eur Cell Mater 2007;14:1-19.

11. Huang Y, Kaigler D, Rice K, Krebsbach P, Mooney D. Combined angiogenic and osteogenic factor delivery enhances bone marrow stromal cell-driven bone regeneration. J Bone Miner Res 2005;20:848-857.

12. Leach J, Kaigler D, Wang Z, Krebsbach P, Mooney D. Coating of VEGF-releasing scaffolds with bioactive glass for angiogenesis and bone regeneration. Biomaterials 2006;27:3249-3255.

13. Kidd K, Nagle R, Williams S. Angiogenesis and neovascularisation associated with extracellular matrix-modified porous implants. J Biomat Mar Res 2002;59:366-377.

14. Kidd K, Williams S. Laminin-5-enriched extracellular matrix accelerates angiogenesis and neovascularisation in association with ePTFE. J Biomed Mat Res A 2004;69:294-304.

15. Moldovan N, Ferrari M. Prospects for microtechnology and nanotechnology in bioengineering of replacement microvessels. Arch Pathol Lab Med 2002;126:320-324.

16. Soker S, Machado M, Atala A. Systems for therapeutics angiogenesis in tissue engineering. World J Urol 2000;18:10-18.

17. Alessandri G, Emanueli C, Madeddu P. Genetically engineered stem cell therapy for tissue regeneration. Ann N Y Acad Sci 2004;1015:271-284.

18. Choong C, Hutmacher D, Triffitt J. Co-culture of bone marrow fibroblasts and endothelial cells on modified polycaprolactone substrates for enhanced potential in bone tissue engineering. Tissue Engineering 2006;12:2521-2531.

19. Santos M, Fuchs S, Gomes M, Unger R, Reis R, Kirkpatrick C. Response of micro- and macrovascular endothelial cells to starch-based fiber meshs for bone tissue engineering. Biomaterials 2007;28:240-248.

20. Hench L. Bioactive materials: the potential for tissue regeneration. J Biomed Mater Res 1998;15:511-518.

21. Santos J, Hastings D, Knowles J. Sintered hydroxyapatite compositions and method for the preparation thereof - European Patent WO 0068164, 1999.

22. Hussain S, Lopes M, Maurício A, Ali N, Fernandes M, Santos J. Bonelike® graft for bone regenerative application. In: Ahmed W, Jackson M, editors. Surface Engineered Surgical Tools and Medical Devices. New York: Springer Publications, 2007. p. 477-512.

23. Lopes M, Knowles J, Santos J, Monteiro F, Olsen I. Direct and indirect effects of P2O5-glass reinforced hydroxyapatite on the growth and function of osteoblast-like cells. Biomaterials 2000;21:1165-1172.

24. Costa M, Gutierres M, Almeida R, Lopes M, Santos J, Fernandes M. In vitro mineralization of human bone marrow cells culture on Bonelike®. Key Eng Mat 2004;254-256:821-824.

25. Lobato J, Hussain N, Botelho C, Maurício A, Afonso A, Ali N, et al. Assessment of Bonelike® graft with a resorbable matrix using an animal model. Thin Solid Films 2006;515:362-367.

26. Lopes M, Santos J, Monteiro F, Ohtsuki C, Osaka A, Kaneko S, et al. Push-out testing and histological evaluation of glass reinforced hydroxyapatite composites implanted in the tibia of rabbits. J Biomed Mat Res A 2001;54:463 - 469.

27. Gutierres M, Hussain N, Lopes M, Afonso A, Cabral A, Almeida L, et al. Histological and scanning electron microscopy analyses of bone/implant interface using the novel Bonelike® synthetic bone graft. J Orthop Res 2006;24:953 - 958.

28. Lobato J, Hussain N, Botelho C, Maurício A, Lobato J, Lopes M, et al. Titanium dental implants coated with Bonelike®: Clinical case report. Thin Solid Films 2006;515:279-284.

29. Sousa R, Lobato J, Maurício A, Hussain N, Botelho C, Lopes M, et al. A Clinical Report of Bone Regeneration in Maxillofacial Surgery using Bonelike ® Synthetic Bone Graft. J Biomat Appli 2008;22:373 - 385.

30. Gutierres M, Lopes M, Hussain N, Lemos A, Ferreira J, Afonso A, et al. Bone ingrowth in macroporous Bonelike® for orthopaedic applications. Acta Biomaterialia 2008;4:370-377.

31. Gutierres M, Dias A, Lopes M, Hussain N, Cabral A, Almeida L, et al. Opening wedge high tibial osteotomy using 3D biomodelling Bonelike macroporous structures: case report. J Mater Sci Mater Med 2007;18:2377-2382.

32. Kirkpatrick C, Otto M, Van Kooten T, Krump V, Kriegsmann J, Bittinger F. Endothelial cell cultures as a tool in biomaterial research. J Mat Sci: Mat Med 1999;10:589-594.

33. Fuchs S, Hofmann A, Kirkpatrick C. Microvessel-Like Structures from Outgrowth Endothelial Cells from Human Peripheral Blood in 2-Dimensional and 3-Dimensional Co-Cultures with Osteoblastic Lineage Cells. Tissue Engineering 2007;13:2577-2588.

34. Kirkpatrick C, Fuchs S, Hermanns M, Peters K, Unger R. Cell culture models of higher complexity in tissue engineering and regenerative medicine. Biomaterials 2007;28:5193-5198.

35. Unger R, Krump-Konvalinkova V, Peters K, Kirkpatrick C. In Vitro Expression of the Endothelial Phenotype: Comparative Study of Primary Isolated Cells and Cell Lines, Including the Novel Cell Line HPMEC-ST1.6R. Microvasc Res 2002;64:384-397.

36. Anderson J, Price T, Hanson S, Harker L. In vitro endothelialization of small-caliber vascular grafts. Surgery 1987;101:577–586.

37. Kaehler J, Zilla P, Fasol R, Deutsch M, Kadletz M. Precoating substrate and surface configuration determine adherence and spreading of seeded endothelial cells on polytetrafluoroethylene grafts. J Vasc Surg 1989;9:535–541.

38. Unger R, Peters K, Huang Q, Funk A, Paul D, Kirkpatrick C. Vascularization and gene regulation of human endothelial cells growing on porous polyethersulfone (PES) hollow fiber membranes. Biomaterials 2005;26:3461–3469.

39. Stamenovic D. Effects of cytoskeletal prestress on cell rheological behaviour. Acta Biomaterialia 2005;1:255-262.

40. Michiels C. Endothelial cell functions. J Cell Physiol 2003;196:430 - 443.

41. Kubota Y, Kleinman H, Martin G, Lawley T. Role of laminin and basement membrane in the morphological differentiation of human endothelial cells into capillary-like structures. J Cell Biol 1988;107:1589-1598.

42. Bach T, Barsigian C, Chalupowicz D, Busler D, Yaen C, Grant D, et al. VE-Cadherin Mediates Endothelial Cell Capillary Tube Formation in Fibrin and Collagen Gels. Exp Cell Res 1998;238:324-334.

43. Hirschi K, Skalak T, Peirce S, Little C. Vascular Assembly in Natural and Engineered Tissues. Ann N Y Acad Sci 2002;961:223-242.

44. McLucas E, Moran M, Rochev Y, Carroll W, Smith T. An investigation into the effect of surface roughness of stainless steel on human umbilical vein endothelial cell gene expression. Endothelium 2006;13:35-41.

45. Zhu Y, Gao C, Guan J, Shen J. Promoting the biocompatibility of polyurethane scaffolds via surface photo-grafting polymerization of acrylamide. J Mat Sci: Mat Med 2004;15:283-289.

Chapter 8

Osteoblastic response to tetracyclines in seeded hidroxyapatite and Bonelike®

Cell-induced response by tetracyclines on human bone marrow colonized hydroxyapatite and Bonelike®

P.S. Gomes[1], J.D. Santos[2,3], M. H. Fernandes[1]

1 – Laboratório de Farmacologia e Biocompatibilidade Celular - Faculdade de Medicina Dentária, Universidade do Porto (FMDUP). Rua Dr. Manuel Pereira da Silva, s/n 4200-392 Porto, Portugal
2 – Faculdade de Engenharia, Universidade do Porto (FEUP), - Secção de Materiais, DEMM, Rua Dr. Roberto Frias, 4200-465, Porto, Portugal
3 - Instituto de Engenharia Biomédica (INEB), Laboratório de Biomateriais, Rua do Campo Alegre, 823, 4150-180, Porto, Portugal

Abstract

Semi-synthetic tetracyclines are commonly used antibiotics that also seem to play an important role in the modulation of the immuno-inflammatory imbalance, verified in several bone diseases. The association of a therapeutic agent (that prevents bacterial infection and induces tissue formation) to a biomaterial aiming to repair/regenerate bone defects could contribute to a more predictable clinical outcome. The present study intends to evaluate the proliferation and functional activity of osteoblastic-induced human bone marrow cells, cultured on the surface of hydroxyapatite (HA) and Bonelike®, in the presence of therapeutic concentrations of doxycycline and minocycline.

First passage bone marrow cells were cultured for 35 days on the surface of HA and Bonelike® discs, in the absence or presence of 1 μg/ml doxycycline and minocycline. Cultures performed in standard tissue culture plates were used as control.

Doxycycline or minocycline induced cell proliferation and increased extent of matrix mineralization in osteoblastic cell cultures established in the three substrates. Also, an improved biological behavior was verified in seeded Bonelike® comparing to HA. Results suggest that the local delivery of tetracyclines might associate the antimicrobial activity in implant-related bone infection with an eventual induction of osteoblastic proliferation and maintenance of the characteristic biological activity of these cells.

Introduction

Tetracyclines are commonly used bacteriostatic antibiotics active against a wide range of both aerobic and anaerobic gram-positive bacteria. Their antimicrobial activity is due to the inhibition of bacterial protein synthesis, by binding to the 30S ribosome subunit, blocking the bond to the tRNA, on the mRNA-ribosome complex [1].

In the last years, several observations converge to justify the therapeutic effectiveness of tetracycline (as well as its semi-synthetic derivatives, minocycline and doxycycline) in the modulation of the immuno-inflammatory imbalance verified in several animal and human bone diseases [2-4]. Different mechanisms, distinct from the antimicrobial action, have been proposed to justify the pro-anabolic activity of these pharmacological agents regarding bone metabolism. These include enhancing of bone formation, decreasing of connective tissue breakdown and diminishing of bone resorption [5-10]. Clinical application of these agents targeting bone might also be favored by their cation quelation activity and consequent avidity for mineralized tissue [11].

Currently, ceramic-based biomaterials have been used in bone tissue repair strategies for their adequate mechanical properties and chemical composition – similar to those of the bone tissue. Among them, HA has generated a great deal of interest in the last years [12]. This synthetic bone graft substitute, although lacking osteogenic properties that can only be found on autologous grafts, still offer advantages that include a reduced local tissue morbidity, absence of complications at donor site and unlimited material availability [13]. This biomaterial, being similar to the mineral component of natural bone revealed good osteoconductivity and bone bonding ability [14]. However, HA presents low load bearing capacity [15] and the introduction of phosphate based glasses as a sintering aid is known to reinforce HA mechanically [16]. Glass-reinforced HA with bioactive properties has been applied with success in medical and dental clinical applications aiming to regenerate the bone tissue [17, 18]. Bonelike® is a registered and patented glass-reinforced HA with improved mechanical properties and enhanced bioactivity that result from the addition of CaO - P_2O_5 based glasses during the liquid phase sintering process of HA, leading to several ionic substitutions in the lattice that are responsible for the reduction of porosity and grain size [19, 20]. Recently, it has been successfully applied in regenerative procedures aiming to restore bone structure and function in oral, maxillofacial and orthopedic procedures [21, 22].

Although the wide application of synthetic biomaterials in order to repair/regenerate the bone tissue, several clinical complications are established and prove difficult to remedy. Among them, osteomyelitis, septic arthritis and prosthetic joint infection are specially caused by Gram-positive organisms and known to contribute to a

heavy clinical and economic burden [23]. Treatment is often complicated at sites of reduced vascularization, requiring prolonged antimicrobial use, usually associated with surgical drainage or debridement [24]. In this way, the selection of the most effective therapeutic approach, based on several parameters that include the specificity of the pathogenic agents, their sensitivity profile, pharmacokinetics of the drug, local vascular supply, presence or absence of a biomaterial and individual factors, is essential in order to minimize tissue and function loss, as well as to reduce discomfort and need of further medical/surgical intervention [24]. Also, it is known that local and systemic measures to control the colonization of the surgical wound at the early healing phase, associated with reduction of the infections' spreading, may increase the predictability of the results [25]. Tetracyclines have been proven to be effective in several bone and joint related infections [26-28].

Regarding bone regeneration strategies, the association of a biomaterial and a therapeutic agent that might induce bone formation at the same time that prevents bacterial infection could, undoubtedly, contribute to a more predictable clinical outcome. In this way, the objective of this research was to evaluate the proliferation and functional activity of osteoblastic-induced human bone marrow cells, cultured on the surface of HA and Bonelike®, in the presence of therapeutic concentrations of doxycycline and minocycline.

Materials and Methods

Preparation of samples

Bonelike® was prepared with the chemical composition of $65P_2O_5$-$15CaO$-$10CaF_2$-$10Na_2O$ in mol% from reagent grade chemicals using conventional glass making techniques. The composite was obtained by adding the milled glass to HA powder in 2.5% (wt/wt), using isopropanol as a solvent. The powders were then dried and sieved to less then 75 μm under nitrogen atmosphere. Disc samples were therefore prepared for *in vitro* testing by uniaxial pressing at 200 MPa, using steel dies to obtain 12 mm diameter discs. The discs were then sintered at 1300ºC (using a ramp rate of 4ºC/min), with the temperature maintained for 1 hour, followed by natural cooling inside the furnace. Phase identification and quantification was assessed by X-ray diffraction and Rietveld analysis. XRD was performed on Bonelike® samples using a Siemens D5000 diffractometer with Cu-K$_\alpha$ radiation (λ=1.5418 Å). The scans were made in the range of 25–35º (2θ) with a step size of 0.02º and a count time of 2 s/step. Detailed description of Bonelike® preparation has been previously reported (20).

For *in vitro* testing, discs were mechanically polished to the same final topology of 1 μm using silicon carbide paper, ultrasonically degreased, cleaned with ethanol followed by deionised water and finally sterilized, prior to cell culture.

HA samples were also prepared as 12 mm diameter discs in order to compare to the biological behavior of Bonelike®.

Cell culture

Human bone marrow was obtained from orthopedic surgical procedures conducted in adult patients (aged between 25 and 45 years). Informed consent was obtained to use this biological material that would be otherwise discarded. Bone marrow was cultured in α-MEM culture medium containing 10% foetal bovine serum, 50 µg/ml gentamicin, 2.5 µg/ml fungizone and 50 µg/ml ascorbic acid. Primary cultures were maintained in a humidified atmosphere (5% CO_2 in air at 37 ºC) for 10-15 days until sub-confluence condition. At this stage, cells were enzymatically released (0.05% trypsin and 0.025% collagenase) and the resultant suspension was cultured at a density of 10^4 cell/cm^2, in the previous described culture medium further supplemented with 10 mM β-glycerophosphate and 10 nM dexamethasone. Cell cultures were established for 35 days and maintained in the surface of the culture plate (control cultures), HA or Bonelike® in the absence or presence of doxycycline or minocycline (1 µg/ml). Tetracyclines were both renewed at every medium change that occurred twice a week.

Culture characterization

Cell viability/proliferation and total protein content

MTT assay was used to estimate cell viability/proliferation. This assay is based on the reduction of 3-(4,5-dimethylthiazol-2-yl)-2,5-diphenyltetrazolium bromide to a purple formazan product by viable cells. Cultured cells were incubated with 0.5 mg/ml of MTT during the last 4 hours of each test time. The medium was then decanted, the stained product dissolved with dimethylsulphoxide and absorbance determination was conducted at 600 nm in an ELISA reader. Results were expressed as absorbance per square centimeter (A/cm^2).

Total protein content was determined by Lowry method after treatment of the cell layer with 0.1 M NaOH for 1 hour. Bovine serum albumin was used as a standard and absorbance determination was conducted at 750 nm.

Alkaline phosphatase (ALP) activity

Activity of ALP was determined in cell lysates (obtained after treatment of cultured cells with 0.1% triton) by the hydrolysis of p-nitrophenyl phosphate (30 minutes at 37º C) in an alkaline buffer solution (pH 10.3). Colorimetric determination of p-nitrophenol was established at 405 nm. Enzyme activity was normalized by total protein content and results were expressed as nanomoles of p-nitrophenol produced per minute per µg of protein (nmol/min/µg protein).

Cai loss from the culture medium

Culture medium from cultures in control and experimental conditions was collected every 2-3 days (and cultures reefed with fresh medium) between days 10 and 35 of the culture. Analysis of Cai content was conducted using Sigma Diagnostics Kit, procedure number 587. Results were expressed as milimoles per litre of ionized calcium loss from medium (Cai mmol/L).

Scanning electron microscopy (SEM)

Glutaraldehyde (3%) fixed cultures were dehydrated in graded alcohols (70, 80, 2 x 90 and 99.8%), critical-point dried, sputter-coated with gold and analyzed in a JeoL JSM 6301F scanning electron microscope equipped with a X-ray energy dispersive spectroscopy (EDX) microanalysis capability (Voyager XRMA System, Noran Instruments).

Statistical Analyses

Results presented in this study are from three separate experiments using cell cultures from different patients. In each experimental situation, three replicas were accomplished. Groups of data were evaluated using a two-way analysis of variance (ANOVA) and no significant differences in the pattern of the cell behaviour were found. Statistical differences found between control and experimental conditions were determined by Bonferroni's method. P-values ≤0.05 were considered significant.

Results

Human bone marrow stromal cells were characterized for proliferation and differentiation events, on the surface of the culture plate, HA and Bonelike®, in the presence of an osteogenic inducing medium, further supplemented with 1 µg/ml doxycycline or minocycline.

XRD analysis revealed that due to the reaction between the HA matrix and P_2O_5-based glass during the sintering process, the Bonelike® microstructure had a

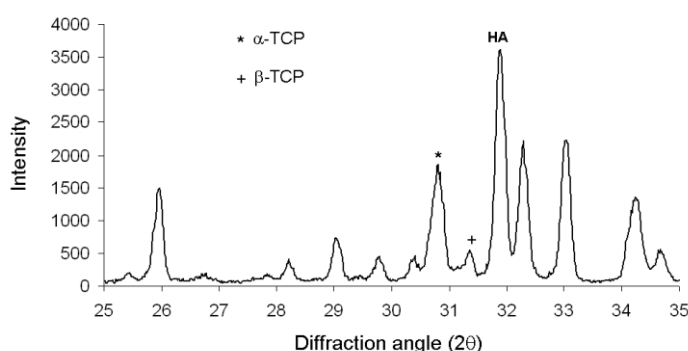main crystalline phase of HA with β- and α-tricalcium phosphate as secondary phases (Figure 1).

Figure 1 – X-ray diffraction pattern of Bonelike®. Bonelike® is composed of HA and α- and β-TCP phases.

Cell viability/proliferation

The results regarding the evaluation of cell proliferation by the MTT assay are reported on Figure 2A.

Cultures grown on the surface of the culture plate proliferated gradually till day 21, followed by a decrease in the remaining time of culture. Seeded Bonelike® presented a similar behavior to control, while cultures established on the surface of HA showed an initial lag phase of approximately two weeks and maximal MTT reduction values were only achieved by day 28. The presence of doxycycline or minocycline (1 μg/ml) increased cell proliferation in control cultures and on seeded sample materials. Results were statistically significant ($p \leq 0.05$) at days 21, 28 and 35 for cultures grown on the culture plate, and at maximal MTT reduction values for cultures established on the surface of the materials – day 21 for Bonelike® and 28 for HA. The stimulatory effect was evident after an initial lag stage (during approximately the first week) and maximal MTT values were around 30% and 40% higher in the presence of minocycline and doxycycline, respectively, comparing to those obtained on non-treated cultures.
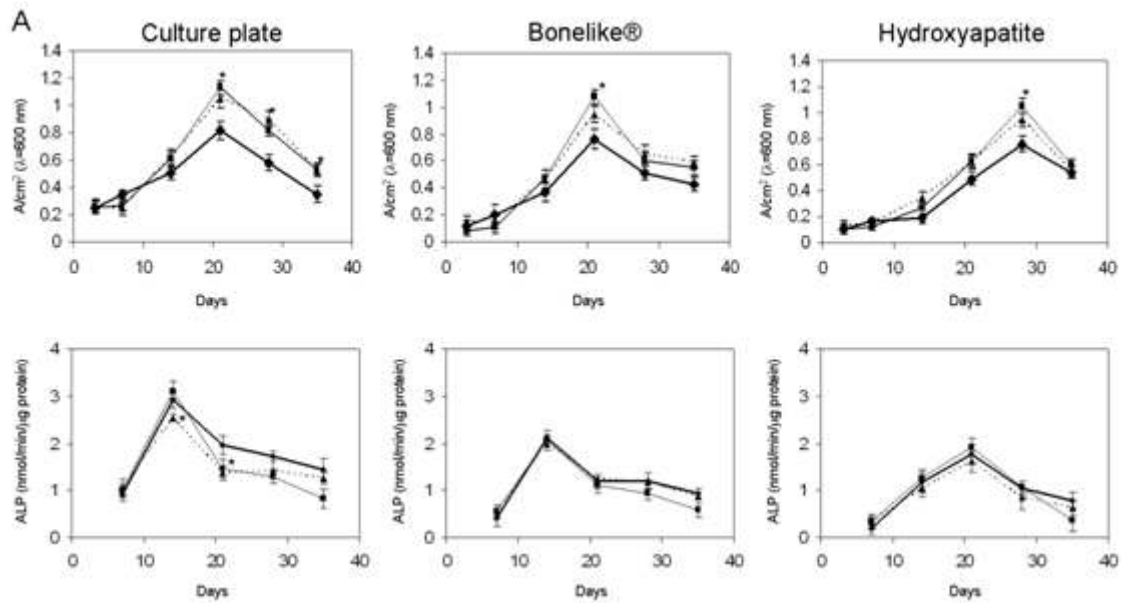
Figure 2. Cell viability/proliferation (A) and alkaline phosphatase activity (B) of human bone marrow osteoblastic cells cultured for 35 days on the surface of culture plate, Bonelike® and HA in the absence (♦) and presence of 1 μg/ml Doxycycline (■) or Minocycline (▲). * Significantly different from control cultures (p≤0.05).

Alkaline phosphatase activity

Results regarding the activity of alkaline phosphatase are presented on Figure 2B.

ALP activity was low during the first week of culture and increased significantly afterwards achieving maximal values by day 14 in control and cultures established on the surface of Bonelike® and, later, by day 21, on seeded HA. Subsequently, ALP activity decreased throughout the remaining culture time. Comparing to control cultures, reduced enzymatic activity was verified in seeded Bonelike® and HA.

No significant differences were found in ALP activity in the presence of doxycycline, although, in minocycline-treated cultures, a tendency for a reduction in the enzyme activity was verified and statistically significant (p≤0.05), comparing to cultures grown on the surface of the culture plate.

Mineralized deposits in the extracellular matrix

The presence of mineralized deposits (calcium phosphate) in the cell layer was evaluated by the analysis of ionized calcium (Cai) loss from the culture medium throughout days 10 to 35 and by SEM observation.

160

Cai loss from the culture medium

The Cai (in association with Pi) is consumed in the formation of calcium phosphate deposits in the extracellular matrix, reflecting the mineralization process. In the present work, the Cai consumption reflects the changes occurring between every medium change (intervals of 2-3 days), since the medium was totally replaced at every change, outputting values that are not cumulative. Results are presented on Figure 3.

Levels of Cai were determined in the absence of cultured cells and a relatively steady value of 1.7 mmol/L was verified in the absence of materials. A higher variation of Cai levels (between 1.6 and 1.8 mmol/ml) occurred in incubated Bonelike$^®$ and HA samples.

Cultures grown on the surface of the culture plate revealed almost no Cai loss from the culture medium, between day 10 and 17. Since this day onwards, a significant and progressive increase of the Cai loss was verified and, at day 30, values around 1.35 mmol/L were attained. Medium collected from cultures established on the surface of Bonelike$^®$ revealed a similar behavior. Cai loss regarding cultures grown on the surface of HA, was significant from day 20 onwards, achieving approximately 1.15 mmol/L around day 30.

In the presence of doxycycline and minocycline, levels of Cai followed a similar pattern. However, in cultures established on the surface of culture plate and Bonelike$^®$, the initial rate of calcium deposition (between days 17 and 23) was higher compared to non-treated cultures, especially in the presence of doxycycline (results statistically significant, p≤0.05).
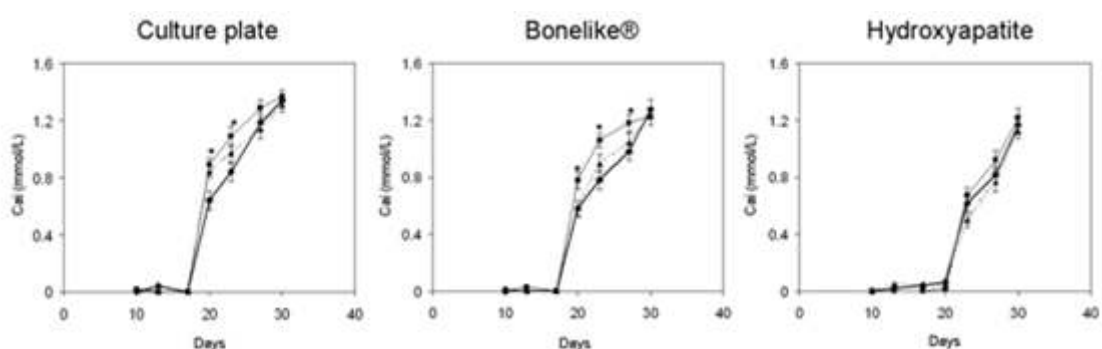

Figure 3. Levels of ionized calcium (Cai) loss from the culture medium regarding human bone marrow osteoblastic cell cultures performed on the surface of the culture plate, Bonelike® and HA. Cai loss was not cumulative, as the medium was totally replaced at each medium change (twice a week), and levels measured reflect changes occurring in intervals of 2-3 days throughout the culture period. Cultures were grown in the absence (♦) and presence of 1 μg/ml Doxycycline (■) or Minocycline (▲). * Significantly different from control cultures (p≤0.05).

SEM

Representative scanning electron micrographs of the cell layer, at day 21, are presented on Figure 4 corresponding to different experimental conditions.

Control cultures and seeded HA and Bonelike® revealed a continuous cell layer with distributed globular mineral deposits in close association with the matrix (Figure 4A-C). Treatment with doxycycline (Figure 4D-F) or minocycline (Figure 4G-I) increased mineral deposition. Regarding cultures established on the surface of HA, significantly less mineral deposits were visualized both in the absence (Figure 4C) and presence of doxycycline (Figure 4F) and minocycline (Figure 4I).
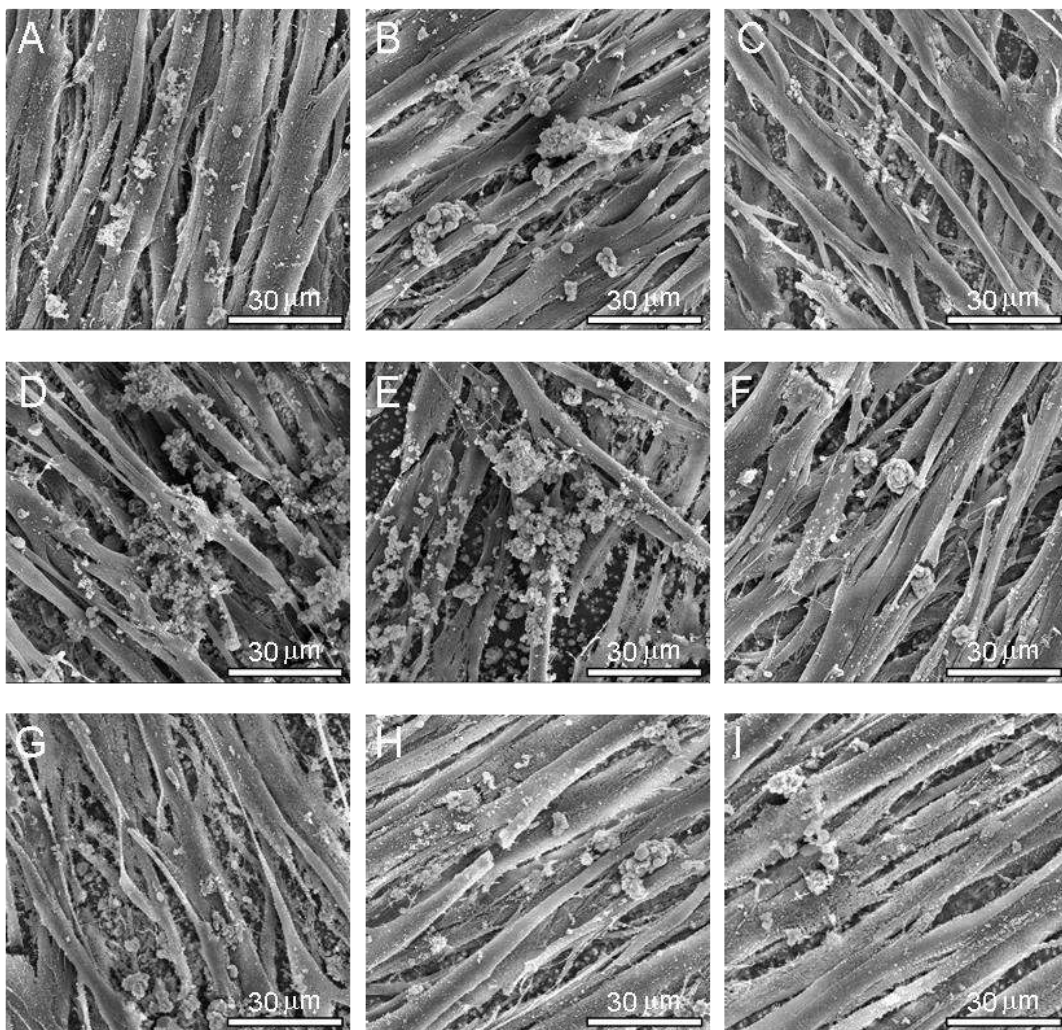

Figure 4. SEM appearance of human bone marrow osteoblastic cell cultures grown in the absence (A-C) or the presence of 1 μg/ml Doxycycline (D-F) and 1 μg/ml Minocycline (G-I), at day 21, in the surface of the culture plate (A, D and G), Bonelike® (B, E and H) and HA (C, F and I).

Discussion

Each year, almost two million patients worldwide undergo bone graft surgery in order to repair skeletal lesions resulting from trauma, tumor resection or degenerative diseases [29] and several synthetic graft materials, with osteoconductive and osteoinductive properties have been designed to fulfill this need [30]. The implantation of a bone graft causes an inflammatory reaction and, frequently, an infectious process [31]. The direct contact of the material surface with blood and/or tissue fluid enhances the formation of an adsorbed protein film. Several of the adsorbed proteins (including fibronectin, vitronectin and fibrinogen) provide anchoring sites for bacteria via the expression of adhesion molecules from the pathogenic agents. When the adhesion process is established, the bacteria proliferate and create an infectious process in close association with the implanted material [32]. In order to control the infection, several methodologies have been proposed. Local control offers many advantages over systemic antibiotic chemotherapy [25, 32] and, in addition, the association of antimicrobial activity with a positive modulation of the host response contributes to a more predictable and rapid clinical outcome in bone regeneration therapies [33].

Tetracyclines are broad spectrum antibiotics important in the treatment of bone and joint infections [26-28] which have been associated with a positive effect in bone metabolism [5-10]. In previous studies, performed in standard tissue culture plates, we reported that therapeutic levels of doxycycline and minocycline were able to induce proliferation of osteoblastic bone marrow cells while maintaining their specific phenotype [34]. In the present study, HA and Bonelike®, a glass-reinforced HA, were cultured with human bone marrow cells in a medium known to induce osteogenic differentiation [35, 36], and cell proliferation and function were assessed in the presence of 1 μg/ml doxycycline or minocycline, representative of the plasmatic levels attained with standard therapeutic systemic dosages [37].

Bone marrow cells grown on standard polystyrene culture plates, in the absence of tetracyclines, presented active proliferation during the first three weeks associated with expression of high levels of ALP. The maximum levels of ALP, achieved on day 14, indicate the subjacent differentiation process being established at this stage. ALP is associated with the availability of high levels of phosphate ions, essential to the onset of the mineralization process, being subsequently down-regulate [38]. Accordingly, the pattern of Cai loss from the culture medium and SEM observation showed that mineral deposition closely associated with the cell layer occurred from day 17 onwards. Over the last two weeks of culture, cell proliferation was greatly reduced by the embedding of the cells in the mineralized extracellular matrix, as in accordance with the established model for the *in vitro* development of the osteoblastic phenotype

[35, 36, 38]. Cell response on the surface of Bonelike® was similar. HA showed a poor performance during the initial stages of the culture, reflected by a long lag phase, which resulted in delayed maximal values in the MTT assay and ALP activity, compared to Bonelike®. Upon cell seeding, surface chemical and topographic changes resulting from the interactions between the material surface and the culture medium are of particular importance to the subsequent cell growth and differentiation events. Appropriate surface features for normal cell behavior seem to take place earlier on Bonelike®, comparing to HA. Bonelike® is composed by an HA matrix with soluble β- and α-tricalcium phosphate phases (Figure 1) and the ongoing release/deposition events of Ca and P ionic species leads to a rapid formation of an apatite layer, according to previous studies [39]. This behavior appears to contribute to the improved biological performance of Bonelike®, both *in vitro* [40, 41] and *in vivo* [22, 42, 43]. Comparatively, formation of an apatite layer on the surface of HA occurs slowly [39] with favorable surface conditions for cell growth being observed later. However, the interfacial reactions tend to an equilibrium rendering the surface of the two materials with similar features. Accordingly, after two weeks, cell behavior on HA surface showed a pattern similar to that observed on Bonelike® samples. Also, the presence of F in the composition of Bonelike® and/or its release may also contribute to the improved initial response, as this ion is reported to stimulate osteoblastic proliferation [44].

Doxycycline or minocycline affected the proliferation of osteoblastic cells in a time-dependent manner. After a small lag phase during the first week, induced cell proliferation was observed in all experimental situations, i.e. control cultures, seeded HA and Bonelike®. ALP activity was similar, although somewhat reduced in minocycline-treated cultures performed in standard culture plates. Rate of mineral deposition, as assessed by the pattern of Cai loss from the culture medium, was slightly higher in tetracycline-treated cultures, which is probably related with the presence of increased cell number of functional active cells in these experimental conditions.

Osteoblastic cell response to tetracyclines was addressed in few previous studies, performed in standard tissue culture plates. Minocycline (up to 3 μg/ml) was reported to increase the efficiency of rat bone marrow stromal cells regarding colony forming capacity [45]. Also, induction of early differentiation events and cell proliferation improvement were observed in osteoblast-like MG63 cells cultured in tetracycline pre-coated dentin [46]. In contrast, doxycycline failed to cause any anabolic effect in murine calvarial osteoblasts and MG63 osteoblast-like cells [47]. A recent study assessed the effect of a variety of antibiotics on human bone trabecullar bone derived cells and on the cell line MG63, exposed during 48 hours, and found a mean IC_{20} of 60 μg/ml for

164

tetracycline [48]. As mentioned above, we reported previously that long-term exposure of osteogenic-induced human bone marrow cells to 1 μg/ml doxycycline and minocycline resulted in increased cell growth, while higher levels caused dose-dependent deleterious effects [34]. Positive effects of tetracyclines over osteoblastic cells were also reported in an in vivo model of normal bone metabolism [10]. Tetracycline administration to squirrel monkeys over a period of 17 days increased osteoblastic activity and osteoid formation in alveolar bone [10], consistent with similar effects of other tetracycline compounds in animal models of bone-deficiency diseases [5-8].

The mechanisms underlying the effects of tetracyclines over osteoblastic cells remain unclear. However, changes in the collagenous extracellular matrix, expected from the well established inhibitory effect of tetracyclines over matrix metalloproteinases (MMPs) [4, 49, 50] might play a role. Tetracyclines can inhibit collagenase and/or the breakdown of collagen under a variety of conditions [51-54]. Also, additional effects on collagen metabolism may occur, particularly increased collagen synthesis after tetracycline administration verified on pathological models of bone-associated diseases and cell population from soft tissues [53, 54]. In addition, it is interesting to refer that progressive consolidation of collagenous connective tissue at the apical portions of periodontal pockets is reported to occur in patients receiving subantimicrobial doses of doxycycline [55, 56]. These events might result in improved osteoblastic behavior, since a stable collagenous matrix is know to play a significant role in the osteoblastic proliferation/differentiation sequence [38, 57, 58].

In the present study, treatment with doxycycline or minocycline, 1 μg/ml, induced cell proliferation and increased extent of matrix mineralization in human osteoblastic cell cultures growing on HA or Bonelike®. Results suggest that the local delivery of tetracyclines might associate the antimicrobial activity in implant-related bone infection with an eventual induction of osteoblastic proliferation and maintenance of the characteristic biological activity of these cells. In this way, tetracyclines may become suitable candidates to drug confinement and delivery applications regarding the use of ceramic matrices for hard tissue regeneration.

References

1. Chambers H. Protein Synthesis Inhibitors and Miscellaneous Antibacterial Agents. In: Brunton L, editor. Goodman & Gilman's - The Pharmacological Basis of Therapeutics: McGraw-Hill; 2006. p. 1173-202.

2. Alkan A, Erdem E, Gunhan O, Karasu Ç. Histomorphometric Evaluation of the Effect of Doxycycline on the Healing of Bone Defects in Experimental Diabetes Mellitus: A Pilot Study. J Oral Maxillofac Surg. 2002;60:898.904.

3. Buchter A, Kleinheinz J, Meyer U, Joos U. Treatment of severe peri-implant bone loss using autogenous bone and a bioabsorbable polymer that delivered doxycycline (AtridoxTM). British Journal of Oral and Maxillofacial Surgery. 2004;42:452-6.

4. Ramamurthy N, Rifkin B, Greenwald R, Xu J-W, Liu Y, Turner G, et al. Inhibition of Matrix Metalloproteinase-Mediated Periodontal Bone Loss in Rats: A Comparison of 6 Chemically Modified Tetracyclines. Journal of Periodontology. 2005;73:726-34.

5. Golub L, Ramamurthy N, Kaneko H, Sasaki T, Rifkin B, McNamara T. Tetracycline administration prevents diabetes-induced osteopenia in the rat: initial observations. Research Communications in Chemical Pathology and Pharmacology. 1990;68:27.

6. Williams S, Wakisaka A, Zeng Q, Barnes J, Martin G, Wechter W. Minocycline prevents the decrease in bone mineral density and trabecular bone in ovariectomized aged rats. Bone. 1996;19:637-44.

7. Williams S, Wakisaka A, Zeng Q, Barnes J, Seyedin S, Martin G, et al. Effect of minocycline on osteoporosis. Advanced Dental Research. 1998;12:71-5.

8. Pytlik M, Folwarczna J, Janiec W. Effects of Doxycycline on Mechanical Properties of Bones in Rats with Ovariectomy-Induced Osteopenia. Calcified Tissue International. 2004;75:225-30.

9. Holmes S, Still K, Buttle D, Bishop N, Grabowski P. Chemically modified tetracyclines act through multiple mechanisms directly on osteoclast precursors. Bone. 2004;35:471-8.

10. Polson A, Bouwsma O, McNamara T, Golub L. Enhancement of Alveolar Bone Formation after Tetracycline Administration in Squirrel Monkeys. The Journal of Applied Research in Clinical Dentistry. 2005:32-42.

11. Yamaguchi A, Udagawa T, Sawai T. Transport of divalent cations with tetracycline as mediated by the transposon Tn10-encoded tetracycline resistance protein. J Biol Chem. 1990;265:4809-13.

12. Li S, de Wijn J, Layrolle P, de Groot K. Synthesis of macroporous hydroxyapatite scaffolds for bone tissue engineering. J Biomed Mater Res. 2002;61:109–20.

13. Giannoudis P, Dinopoulos H, Tsiridis E. Bone substitutes: An update. Int J Care Injured. 2005;365:220.

14. LeGeros R. Properties of osteoconductive biomaterials: calcium phosphates. Clin Orthop. 2002;395:81–98.

15. Suchanek W, Yoshimura M. Processing and properties of hydroxyapatite-based biomaterials for use as hard tissue replacement implants. Journal of Materials Research. 1998;13:94-117.

16. Lopes M, Santos J, Monteiro F, Knowles J. Glass reinforced hydroxyapatite: a comprehensive study of the effect of glass composition on the crystallography of the composite. J Biomed Mater Res. 1998;39:244-50.

17. Hench L. Bioactive materials: the potential for tissue regeneration. J Biomed Mater Res. 1998;41:511-8.

18. Kellomaki M, Niiranen H, Puumanen KA, N, Waris T, Tormala P. Bioabsorbable scaffolds for guided bone, regeneration, and generation. Biomaterials. 2000;21:2495-505.

19. Santos J, Reis R, Monteiro F, Knowles J, Hastings G. Liquid phase sintering of hydroxyapatite by phosphate and silicate glass additions structure and properties of the composites. J Mater Sci Mat Med. 1995;6:348.

20. Santos J, Silva P, Knowles J, Talal S, Monteiro F. Reinforcement of hydroxyapatite by adding P2O5- CaO glasses with Na2O,K2O and MgO. J Mater Sci Mat Med. 1996;7:187.

21. Duarte F, Santos J, Afonso A. Medical applications of Bonelike® in Maxillofacial Surgery. Mater Sci Forum. 2004;370:455-6.

22. Gutierres M, Hussain N, Afonso A, Almeida L, Cabral A, Lopes M, et al. Biological behaviour of Bonelike® graft implanted in the tibia of humans. Key Eng Mater. 2005;1041:284-6.

23. Brause B. Infections with prostheses in bones and joints. In: Mandell G, Bennet J, Dolin R, editors. Mandell, Douglas and Bennett's Principles and Practice of Infectious Diseases. 5th ed. Philadelphia: Churchill Livingstone; 2000. p. 1196-200.

24. Darley E, MacGowan A. Antibiotic treatment of Gram-positive bone and joint infections. Journal of Antimicrobial Chemotherapy. 2004;53:928-35.

25. Zucchelli G, Sforza N, Clauser C, Cesari C, De Sanctis M. Topical and systemic antimicrobial therapy in guided tissue regeneration. Journal of Periodontology. 1999;70:239-47.

26. Yukna R, Sepe W. Clinical evaluation of localized periodontosis defects treated with freeze-dried bone allografts combined with local and systemic tetracyclines. Int J Periodontics Restorative Dent. 1982;2:8-21.

27. Shirtliff M, Mader J. Acute Septic Arthritis. Clinical Microbiology Reviews. 2002;15:527-44.

28. Sunder M, Babu N, Victor S, Kumar K, Kumar T. Biphasic Calcium Phosphates for Antibiotic Release. Trends Biomater Artif Organs. 2005;18:213-8.

29. Lieberman J, Daluiski A, Einhorn T. The Role of Growth Factors in the Repair of Bone : Biology and Clinical Applications. Journal of Bone and Joint Surgery. 2002;84:1032-44.

30. Carson J, Bostrom M. Synthetic bone scaffolds and fracture repair. Injury. 2007;38:S33-S7.

31. Regí-Vallet M, Balas F, Colilla M, Manzano M. Drug Confinement and Delivery in Ceramic Implants. Drug Metabolism Letters. 2007;1:37-40.

32. Lin T-L, Lu F-M, Conroy S, Sheu M-S, Su S-H, Tang L. Antimicrobial coatings: a remedy formedical device-related infections. Med Device Technol. 2001;12:26-30.

33. Beardmore A, Brooks D, Wenke J, Thomas D. Effectiveness of Local Antibiotic Delivery with an Osteoinductive and Osteoconductive Bone-Graft Substitute. Journal of Bone and Joint Surgery. 2005;87:107-12.

34. Gomes P, Fernandes M. Effect of Therapeutic Levels of Doxycycline and Minocycline in the Proliferation and Differentiation of Human Bone Marrow Osteoblastic Cells. Archives of Oral Biology. 2007;52:251-9.

35. Coelho M, Fernandes M. Human bone cell cultures in biocompatibility testing. Part II: effect of ascorbic acid, b-glycerophosphate and dexamethasone on osteoblastic differentiation. Biomaterials. 2000;21:1095-102.

36. Jørgensen N, Henriksena Z, Sørensena O, Civitelli R. Dexamethasone, BMP-2, and 1,25-dihydroxyvitamin D enhance a more differentiated osteoblast phenotype: validation of an in vitro model for human bone marrow-derived primary osteoblasts. Steroids. 2004;69:219-26.

37. Sakellari D, Goodson J, Socransky S, Kolokotronis A, Konstantinidis A. Concentration of 3 tetracyclines in plasma, gingival crevice fluid and saliva. Journal of Clinical Periodontology. 2000;27:53-60.

38. Stein G, Lian J. Molecular mechanisms mediating proliferation/differentiation interrelationships during progressive development of the osteoblast phenotype. Endocr Rev. 1993;14:424-42.

39. Zhang Y, Lopes M, Santos J. CaO-P2O5 Glass Ceramics Containing Bioactive Phases: Crystallization and in vitro Bioactivity Studies. Key Eng Mater. 2001;192:643-6.

40. Lopes M, Knowles J, Santos J, Monteiro F, Olsen I. Direct and indirect effects of P2O5-glass reinforced hydroxyapatite on the growth and function of osteoblast-like cells. Biomaterials. 2000;21:1165-72.

41. Costa M, Gutierres M, Almeida L, Lopes M, Santos J, Fernandes M. In Vitro Mineralisation of Human Bone Marrow Cells Cultured on Bonelike®. Key Eng Mater. 2004;254-256:821-4.

42. Lopes M, Santos J, Monteiro F, Ohtsuki C, Osaka A, Kaneko S, et al. Push-out testing and histological evaluation of glass reinforced hydroxyapatite composites implanted in the tibia of rabbits. J Biomed Mater Res. 2001;54:463-9.

43. Gutierres M, Hussain N, Lopes M, Afonso A, Cabral A, Almeida L, et al. Histological and scanning electron microscopy analyses of bone/implant interface using the novel Bonelike® synthetic bone graft. J Ortho Res. 2006;24:953.

44. Kima H-W, Leea E-J, Kima H-E, Salihb V, Knowles J. Effect of fluoridation of hydroxyapatite in hydroxyapatite-polycaprolactone composites on osteoblast activity. Biomaterials. 2005;26:4395-404.

45. Williams S, Barnes J, Wakisaka A, Ogasa H, Liang C. Treatment of Osteoporosis with MMP Inhibitors. Annals of the New York Academy of Sciences. 1999;878:191-200.

46. Schwartz Z, Lohmann C, Wieland M, Cochran D, Dean D, Textor M, et al. Osteoblast proliferation and differentiation on dentin slices are modulated by pretreatment of the surface with tetracycline or osteoclasts. Journal of Periodontology. 2000;71:586-97.

47. Bettany J, Wolowacz R. Tetracycline Derivatives Induce Apoptosis Selectively in Cultured Monocytes and Macrophages but not in Mesenchymal Cells. Advanced Dental Research. 1998;12:136-43.

48. Duewelhenke N, Krut O, Eysel P. Influence on mythochondria and cytotoxicity of different antibiotics administred in high concentrations on primary human osteoblasts and cell lines. Antimicrobial agents and chemotherapy. 2007;51:54-63.

49. Golub L, Wolff M, Roberts S, Lee H-M, Leung M, Payonk G. Treating periodontal diseases by blocking tissue-destructive enzymes. JADA. 1994;125:163-9.

50. Woessner J, Nagase H. Inhibition of MMPs. In: Woessner J, Nagase H, editors. MMPs and Timps: Oxford University Press; 2000. p. 109-25.

51. Golub L, Ramamurthy N, McNamara T, Gomes B, Wolff M, Casino A, et al. Tetracyclines inhibit tissue collagenase activity. A new mechanism in the treatment of periodontal disease. Journal of Periodontal Research. 1984;19:651-5.

52. Yu Z, Ramamurthy N, Leung M, Chang K, McNamara T, Golub L. Chemically-modified tetracycline normalizes collagen metabolism in diabetic rats: a dose-response study. Journal of Periodontal Research. 1993;28:420-8.

53. Karimbux N, Ramamurthy N, Golub L, Nishimura I. The expression of collagen I and XII on RNAs in porphyromonas gingivalis-induced periodontitis in rats: The effect of doxycycline and chemically-modified tetracycline (CMT-1) Journal of Periodontology. 1998;69:39-40.

54. Ramamurthy N, Pirila E, Lee H-M. Delayed wound healing, altered collagen level and keratinocyte growth factor expression in skin of ovariectomized rat is normalized

by estrogen or chemically modified doxycycline. In: Schneider H, editor. Menopause-The Sate of the Art in Research and Management, The Proceedings of the Tenth World Congress. New York: Parthenon Publishing Group; 2003. p. 236-43.

55. Gurkan A, Çunarcuk S, Huseyinov A. Adjunctive subantimicrobial dose doxycycline: effect on clinical parameters and gingival crevicular fluid transforming growth factor-b1 levels in severe, generalized chronic periodontitis. Journal of Clinical Periodontology. 2005;32:244-53.

56. Caton J. Evaluation of Periostat for patient management. Compendium of Continuing Education in Dentistry. 1999;20:451-6.

57. Salasznyk R, Williams W, Boskey A, Batorsky A, Plopper G. Adhesion to Vitronectin and Collagen I Promotes Osteogenic Differentiation of Human Mesenchymal Stem Cells. Journal of Biomedicine & Biotechnology. 2004;1:24-34.

58. Gerstenfeld L, Chipman S, Kelly C, Hodgens K, Lee D, Landis W. Collagen expression, ultrastructural assembly, and mineralization in cultures of chicken embryo osteoblasts. Journal of Cell Biology. 1988;106:979-89.

Chapter 9

Evaluation of human osteoblastic cell response to plasma sprayed silicon-substituted hydroxyapatite coatings over titanium substrates

Evaluation of human osteoblastic cell response to plasma sprayed silicon-substituted hydroxyapatite coatings over titanium substrates

P.S. Gomes[1], C. Botelho[2], M. A. Lopes[2], J. D. Santos[2], M. H. Fernandes[1]

1 – Laboratório de Farmacologia e Biocompatibilidade Celular, Faculdade de Medicina Dentária, Universidade do Porto. Rua Dr. Manuel Pereira da Silva, 4200-393 Porto, Portugal
2 – Secção de Materiais, Departamento de Engenharia Metalúrgica e de Materiais, Faculdade de Engenharia, Universidade do Porto. Rua Dr. Roberto Frias, 4200-465 Porto, Portugal

Abstract

Silicon-substituted hydroxyapatite (Si-HA) coatings have been plasma sprayed over titanium substrates (Ti-6Al-4V), aiming to improve the bioactivity of the constructs for bone tissue repair/regeneration. X-ray diffraction analysis of the coatings has shown that, previous to the thermal deposition, no secondary phases were formed due to the incorporation of 0.8wt% Si into HA crystal lattice. Partial decomposition of hydroxyapatite, which lead to the formation of the more soluble phases of α- and β-tricalcium phosphate and calcium oxide, and increase of amorphization level, only occurred following plasma spraying.

Human bone marrow-derived osteoblastic cells were used to assess the in vitro biocompatibility of the constructs. Cells attached and grew well on the Si-HA coatings, putting in evidence an increased metabolic activity and alkaline phosphatase expression comparing to control, i.e., titanium substrates plasma sprayed with hydroxyapatite. Further, a trend for increased differentiation was also verified by the up-regulation of osteogenesis-related genes, as well as by the augmented deposition of globular mineral deposits within established cell layers.

Based on the present findings, plasma spraying of Si-HA coatings over titanium substrates demonstrates improved biological properties regarding cell proliferation and differentiation, comparing to HA coatings. This suggests that incorporation of Si into the HA lattice could enhance the biological behavior of the plasma-sprayed coating.

Introduction

Titanium (Ti) and Ti containing alloys have been favorite materials for dental, orthopedic and maxillofacial surgical applications, reporting long-term clinical function with a substantial success rate [1,2]. Even so, in order to maintain mechanical properties of the metallic substrates, and simultaneously improve the implants' bioactivity, coating of the titanium's surface has been assayed with calcium phosphate-based ceramics [3-5]. One of the most widely used biomaterial for bone regenerative coating applications is synthetic hydroxyapatite (HA), with the chemical formulation of $Ca_{10}(PO_4)_6(OH)_2$ and a Ca to P ratio of 5:3, which exhibits a similar chemical and crystallographic structure to the bone's inorganic apatite [6]. However, biological apatite reports calcium, phosphate and hydroxyl deficiencies and several anionic and cationic substituents [7]. In this regard, carbonate (up to 8 wt%), as well as trace elements like sodium (up to 0.8 wt%) and magnesium (up to 0.5 wt%) play an important role along with ultra-trace level substituents including potassium, strontium, zinc, fluorine, chlorine and silicon [7-9].

Accordingly, increasing evidence regarding the enhanced biological response induced by silicon (Si) has been gained since the early 70's by Schwarz [10] and Carlisle [11,12] works', which reported that a deficient diet in silicon retarded the growth and disturbed the development of bone structure, in animal models. More recently, it was established by a cohort study that higher dietary silicon intake is positively correlated with improved bone health in humans, as translated by increased levels of bone mineral density [13]. Also, several authors substantiate the positive effects of Si at molecular and cellular level by reporting increased DNA synthesis [14] and induced osteoblastic proliferation [15], as well as increased alkaline phosphatase (ALP) activity, collagen type I and osteocalcin expression [16,17].

In order to take advantage of the Si-induced bioactivity within the bone tissue, it was thought to incorporate silicon in the composition of diverse biomaterials for bone regeneration. Cumulative data support that the addition of Si to bioceramics and ceramic-glass composites has a direct anabolic effect on bone tissue, namely by inducing osteoblastic proliferation and expression of phenotypic characteristics [18,19]. Overall, silicon-substituted bioceramics have been developed and extensively characterized, especially, in the granule or bulk form, as reviewed by Vallet-Regí et al [20] and Pietak et al [21]. However, few studies report the preparation and characterization of silicon substituted hydroxyapatite in the form of coating, apart from magnetron sputtering [22], electrospraying [23], sol-gel [24] and pulsed laser deposition [25]. Further, fewer of these evaluated the biological behavior of the coatings either by in vitro or in vivo methodologies [22,23].

Although all technologies have attractive features, thermal spraying, especially the conventional atmospheric plasma spraying method, has been studied most extensively and is still the most frequently used technology for producing clinical applications embracing HA-based coatings over metallic implants [26]. These constructs (plasma-sprayed HA over metal substrates) allow for the combination of adequate strength and ductility of the metal with the improved biocompatibility and bioactivity of the HA, essential for load-bearing bone applications [26]. An improved biological behavior may be expected from plasma-sprayed substrates, including earlier and greater fixation to the surrounding tissues and a strong direct bonding to the bone [26,27].

To take advantage of the plasma-spraying technology and the benefits of Si-HA, a new construct was developed, composed of Ti-6Al-4V substrates plasma-sprayed with 0.8%wt Si-HA, obtained by a precipitation chemical route. The Si-substituted HA, in a bulk form, has proven enhanced osteoblastic activity *in vitro* [28], and increased bone apposition in an experimental model of in vivo bone regeneration [29]. In order to access the biological performance of Si-HA plasma sprayed Ti-6Al-4V substrates, the constructs' were assayed in vitro, with human bone marrow-derived osteoblastic cell cultures, and compared to the behavior of Ti-6Al-4V substrates plasma-sprayed with HA.

Materials and Methods

Preparation of samples

HA and 0.8 wt% Si-HA were prepared according to the technique previously described by Gibson et al [30]. Briefly, an aqueous precipitation chemical reaction was established between calcium hydroxide and orthophosphoric acid solutions. In order to produce Si-HA, silicon tetraacetate [$Si(CH_3COOH)_4$] was incorporated into the mixture. Precipitation was carried out at room temperature, with the pH being maintained at 10.5 by the addition of ammonium hydroxide solution. After complete mixing, the suspensions were aged overnight. The obtained powders (HA or Si-HA) were filtered, washed and dried at 80ºC. Following, powders were fine grounded and compacted uniaxially at 18 MPa, and sintered at 1300 ºC for 2 hours, followed by natural cooling inside the furnace. Sintered discs were milled and sieved to obtain a fine powder with a specific particle size distribution between 45 and 125 μm.

Titanium alloy (Ti-6Al-4V) disks with 14 mm of diameter and 3 mm of thickness were pre-treated prior to plasma spraying: samples were grit blasted with Al_2O_3 spheres and chemically degreased. Plasma spray coating was performed with a Plasma Technik® automated equipment at atmospheric conditions. Parameters of the

plasma spraying, including chemical composition and flow rate of used gases are depicted on Table 1.

Table 1 - Plasma spraying parameters, chemical composition and flow rate of gases used for the preparation of the HA and Si-HA coatings.

Parameters, chemical composition and flow rate of gases used for Si-HA and HA plasma-spraying	Values
Plasma arc voltage	66 V
Plasma arc current	450 A
Projection gun	Reference 4 (CATIM)
Beak/electrode distance	6 mm
Injection angle	90°
Length of injector	1.5 mm
Injection distance	6 mm
Flow rate of transportation gas	2 L/min
Powder feedrate	30 g/min
Projection distance	100 mm
Rotation	No
Transverse speed	150 mm/s
Air cooling of the coating and substrate during spraying	Yes
Sweeping	Horizontal
Argon (Ar)	20.1 L/min
Nitrogen (N)	15.0 L/min

For *in vitro* testing, HA and Si-HA coated Ti discs were ultrasonically degreased, cleaned with ethanol followed by deionised water and finally sterilized by autoclaving, prior to cell culture.

Materials' characterization

Phase identification

X-ray diffraction (XRD) analysis was used to identify the crystalline phases present in the Si-HA coating. The coating was removed from Ti-6Al-4V alloy substrates, ground to a fine powder and analyzed using a Bruker D8 Advance X-ray diffractometer. A flat plate geometry and Cu Kα radiation were used. Data was collected using a scintillation counter from 10 to 70 (2θ), with a step size of 0.02 º and a counting time of 5 seconds per step. Quantitative phase analysis was performed by the Rietveld method using TOPAS software.

Ionic release/adsorption of silicon, calcium and phosphorous from Si-HA and HA samples

The assessment of the ionic release of silicon, calcium and phosphorous was evaluated in simulated body fluid (SBF), pH 7.4, for both Si-HA and HA constructs. Specimens were immersed into an acellular SBF (volume of SBF / surface area of specimen $\cong$ 0.1 ml/mm^2), and maintained at 37 ºC, for adequate time. The fluid was prepared accordingly to the specifications reported by Oyane et al [31]. All materials were soaked for periods of 1, 3, 5, 7, 14 and 21 days, and, at the end of each time point, the specimens were removed from the fluid and carefully washed with deionised water and dried in air. The concentration of silicon, calcium and phosphorous ions was measured by inductively coupled plasma emission spectroscopy (ICP: Optima 2000DV), with a detection limit of around 0.2 ppm.

Surface analysis of the Si-HA and HA samples

In order to characterize the surface microstructure of the materials before and after immersion in SBF, a scanning electron microscope [SEM: S-4800, Hitachi, Ltd., Japan coupled to an energy dispersive X-ray microanalyzer (EDS: EMAX ENERGY EX-400, Horiba, Ltd., Japan)] was used.

Coating adhesion to the substrate

A standard testing method (DIN 50161) was used to characterize the adhesion strength of the coating to the substrate. The adhesion test was performed on Si-HA and HA samples, before and after the immersion in SBF, for 21 days, at 37ºC. In the test, compressive stresses were applied, at a rate of 10 mm/min. Results were expressed according to the following equation:

$$F = \frac{Fmax}{\pi * \phi * h}$$

F=shear strength (MPa), Fmax=maximum shear force (N), h=maximum height (mm) and ϕ=diameter of the sample (mm). Additionally, SEM observation was used in order to determine the type of failure mechanism.

Cell cultures

Human bone marrow was obtained from femoral regenerative surgical procedures conducted in adult male individuals (aged between 25 and 45 years), without associated bone metabolic diseases. Informed consent to use this biological material, that would be otherwise discarded, was obtained.

Bone marrow was cultured, for 10-15 days until adequate confluence, in α-MEM culture medium containing 10% fetal bovine serum, 100 IU/ml penicillin, 100 μg/ml streptomycin, 2.5 μg/ml fungizone and 50 µg/ml ascorbic acid. Cultures were maintained in a humidified atmosphere of 5% CO_2 in air, with the temperature being maintained at 37 ºC. At adequate confluence, adherent cells were enzymatically released with 0.05% trypsin - 0.025% collagenase and counted using a hemocytometer. Cells were then seeded over HA and Si-HA coated Ti samples at a density of 2 x 10^4 cells/cm^2 and cultured using the previously described experimental conditions, with the culture medium being further supplemented with 10 mM sodium β-glycerophosphate and 10 nM dexamathasone. Cell cultures were established for 21 days and the culture medium was changed twice a week. Cultures were characterized, at adequate time points, for cell viability/proliferation, total protein content, alkaline phosphatase (ALP) activity, expression of osteogenic-associated genes (ALP, bone morphogenic protein – 2 (BMP-2) and collagen type I (Col I)) by reverse transcription-polymerase chain reaction (RT-PCR), scanning electron microscopy (SEM) and confocal laser scanning microscopy (CLSM). In addition, culture medium was analyzed for ionized calcium, in order to quantify the mineralization process.

Culture characterization

Cell viability/proliferation and total protein content

MTT assay was used to estimate cell viability/proliferation. This assay is based on the reduction of 3-(4,5-dimethylthiazol-2-yl)-2,5-diphenyltetrazolium bromide to a purple formazan product by viable cells. At each endpoint test, cultured cells were incubated with 0.5 mg/ml of MTT during the last 4 h of the culture. Following, the medium was decanted, the stained product dissolved with dimethylsulfoxide and absorbance was determined in an ELISA reader at 600 nm. Results were expressed as absorbance per square centimeter (A/cm2).

Total protein content was determined by the Lowry method after treatment of the cell layer with 0.1 M NaOH for 1 h. Bovine serum albumin was used as a standard and absorbance was determined at 750 nm.

Alkaline phosphatase (ALP) activity

ALP activity was determined in cell lysates which were obtained with the treatment of cultured cells with 0.1% triton. Enzymatic activity was established with the hydrolysis of p-nitrophenyl phosphate (30 min at 37 ºC), in an alkaline buffer solution (pH 10.3), following colorimetric determination, at 405 nm, of p-nitrophenol. The

enzyme activity was normalized by the total protein content and results were expressed as nanomoles of p-nitrophenol produced per minute per microgram of protein (nmol.min-1/μg.protein).

Total RNA extraction and RT-PCR analysis

RT-PCR was used to access the expression of ALP, BMP-2 and Col I genes by bone marrow-derived osteoblastic cells, grown for 14 days on the surface of Si-HA or HA plasma sprayed titanium substrates.

Total RNA was extracted using the RNeasy® Mini Kit from Qiagen, according to manufacturer's instructions. RNA was quantified by measuring the absorbance of the samples at 260nm.

RT-PCR was done using the Titan One Tube RT-PCR System from Roche Applied Science, according to the manufacturer's instructions. Briefly, 0.5 μg of total RNA from each sample was reverse transcribed into cDNA (30 minutes at 50 ºC), while PCR was performed with an annealing temperature of 55ºC, for 25 cycles. To amplify the human ALP transcript, the forward primer (5'-ACGTGGCTAAGAATGTCATC-3') was used in combination with the reverse primer (5´-CTGGTAGGCGATGTCCTTA-3'). To amplify the human BMP-2 transcript, the forward primer (5'-GACGAGGTCCTGAGCGAGTT-3') was used in combination with the reverse primer (5´-GCAATGGCCTTATCTGTGAC-3'). To amplify the human Col I transcript, the forward primer (5'-TCCGGCTCCTGCTCCTCTTA-3') was used in combination with the reverse primer (5´-ACCAGCAGGACCAGCATCTC-3'). To amplify the human GADPH transcript, the forward primer (5'-GGAAGGTGAAGGTCGGAGTCAAC-3') was used in combination with the reverse primer (5´-GTGGCAGTGATGGCATGGACTGT-3'). Following, the PCR products were electrophoresed in a 1% agarose gel, stained with ethidium bromide.

Analysis of RNA levels was performed by densitometry with ImageJ software (Version 1.41, National Institutes of Health, Bethesda, MD), after normalization to the housekeeping gene (GAPDH).

Ionized calcium in culture medium

Culture medium was collected at each medium change and analyzed for ionized calcium (Cai), using an adapted Sigma procedure (Sigma Diagnostics Kit – procedure number 587) based on the interaction between the ion and a cromogenic agent (o-cresolphthalein complexone). This reaction occurs on alkaline medium, with pH 10-12, resulting on the formation of a purple complex. Coloration intensity is proportional to the concentration of Cai and was determined in a spectrophotometer at

575nm, using a calibration curve (standard solution, Sigma nº 360-11). Results were expressed in mmol of Cai per litre of medium (mmol/L).

Confocal Laser Scanning Microscopy (CLSM) and Scanning Electron Microscopy (SEM)

For CLSM observation, cells were fixed with 3.7% formaldehyde (methanol free), permeabilized with 0.1% triton and incubated for 1 hour in a 10 mg/ml bovine serum albumin solution, in order to block non-specific interactions. Following, F-actin filaments were stained with 488 AlexaFluor-conjugated phalloidin (1:100) and nuclei were counterstained with 10 μg/ml propidium iodide. Samples were washed with PBS and mounted in Vectashield®. Images were acquired on a Leica TCP SP2 AOBS.

For SEM observation, cells were fixed with 1.5% glutaraldehyde in 0.14 M sodium cacodylate. The samples were dehydrated in graded series of alcohols (70, 80, 2x90 and 99.8%) and critical point dried. Specimens were mounted and sputter-coated with gold previously to observation in a scanning electron microscope (S-4800, Hitachi Ltd., Japan), coupled to an energy dispersive X-ray microanalyzer (EMAX ENERGY EX-400, Horiba Ltd., Japan).

Statistical analysis

Results presented in this study are from three separate experiments using cell cultures from different patients. Four replicates for each experimental situation were conducted. Groups of data were evaluated using a two-way analysis of variance (ANOVA) and no significant differences in the pattern of the cell behavior were found.

Statistical differences found were determined by Bonferroni's method. Values of p≤0.05 were considered significant.

Results

Materials' characterization

Figure 1 shows representative XRD patterns of Si-HA, before and after plasma-spraying, over metallic substrates. The analysis of the attained pattern, previous to plasma-spraying, reveals that the material is a pure phase HA, since no secondary phases were formed. Due to the high temperature and rapid cooling of plasma-spraying coating process, the material suffered partial phase decomposition which lead to the development of TCP (α-TCP (27%), and β-TCP (26%)) and CaO (13%) phases, besides HA (34%). Simultaneously, the ceramic became more amorphous, as indicated by the broader background.
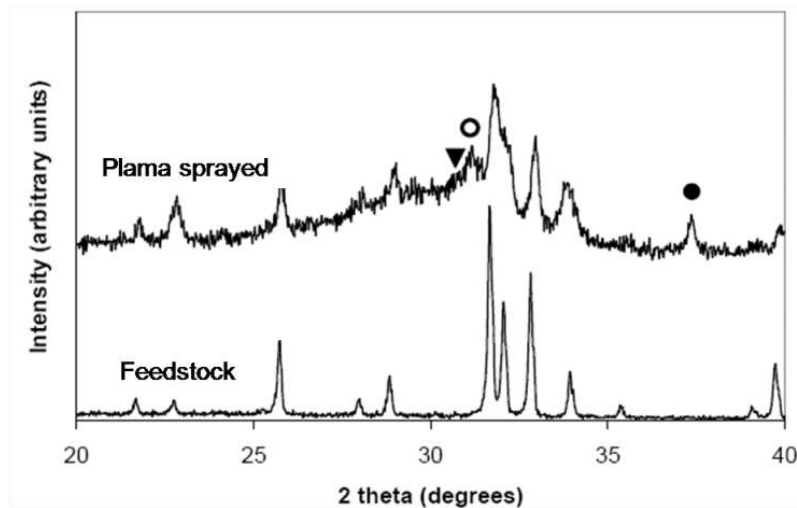
Figure 1 - X-ray diffraction pattern of feedstock and plasma-sprayed Si-HA coatings, showing the presence of a hydroxyapatite phase (unmarked diffraction peaks), with impurities of β-$Ca_3(PO_4)_2$ ($\circ$), CaO ($\bullet$) and indication of a trace of α-$Ca_3(PO_4)_2$ ($\blacktriangledown$). Note the presence of an amorphous phase which is visible as the broader background, regarding the plasma sprayed graphic line.

Regarding the evaluation of the released ions from the Si-HA coatings (Figure 2), it could be seen that there was a small increase in the ionic concentration of silicon in SBF with pH 7.4, throughout the evaluation period. Ionic concentration of Si was around 0.05 mM following 3 days of immersion, and around 0.1 mM following 7 days of immersion. Throughout the remaining test time, a tendency for a stable Si release was verified, with a concentration around 0.12 mM. HA did not report Si release during the evaluated period. In which regards Ca and P ionic concentrations in SBF, a continuous decrease of both ionic species was attained, regarding both tested materials. The decrease in the ionic concentration was high during the first 5-7 days of the test – decreased from around 2.5 mM to 2 mM and from 1.0 mM to 0.5 mM, regarding Ca and P, respectively. Following, a tendency to the maintenance of a stable concentration was verified throughout the remaining test time – around 1.7 mM and 0.5 mM for Ca and P, respectively. Initial decrease of Ca and P concentrations, in SBF, was higher for Si-HA immersed samples, attaining statistical significance at days 1 and 3 of the assayed procedure. In addition, the formation of an apatite layer could be visualized in the surface of both materials, with continuous globular agglomerates, assessed by SEM, following 7 days of immersion (Figure 3).
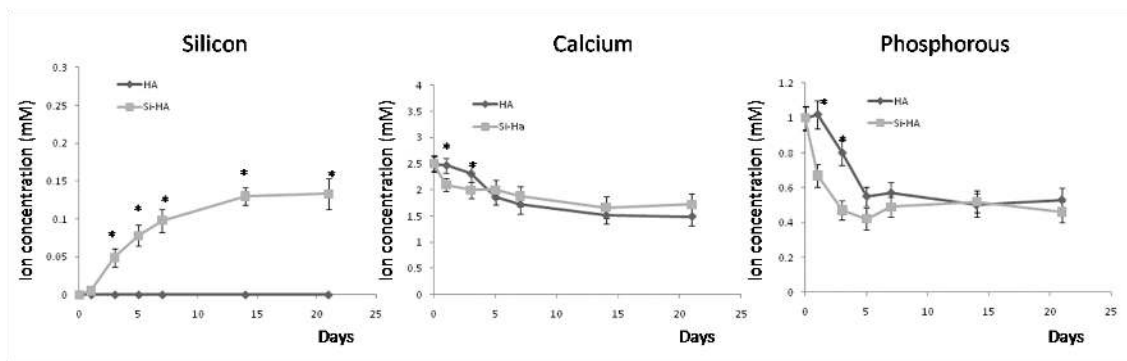
Figure 2 – Ionic release/adsorption of silicon, calcium and phosphorous from Si-HA and HA coated samples following immersion in SBF, for 21 days.
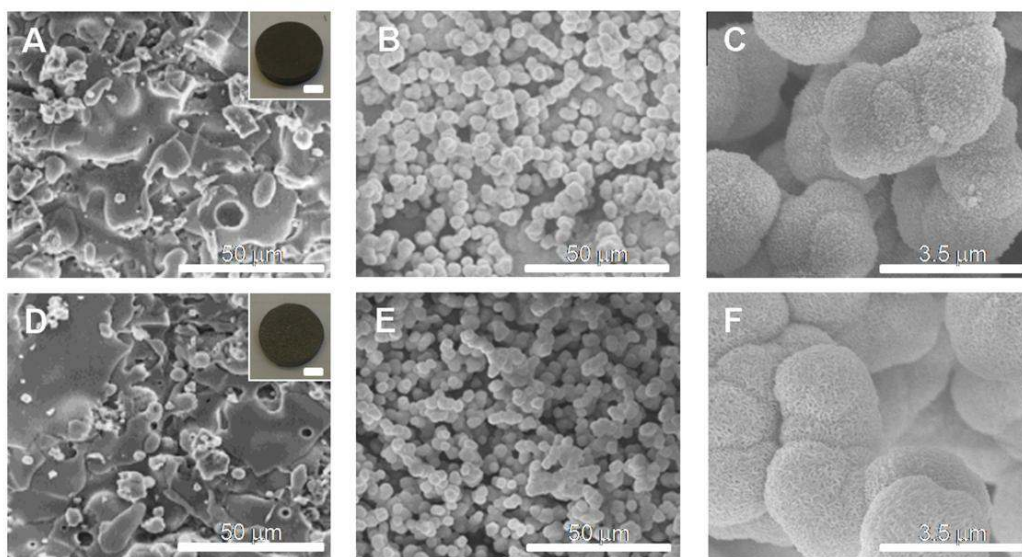

Figure 3 – SEM images of HA (A-C) and Si-HA (D-E) samples in the as-prepared condition (A and D), and following 7 days of immersion in SBF (B, C, E and F). The insets in A and D show the macroscopic appearance of the HA and Si-HA constructs, respectively – scale bar 5 mm.

In which regards to the adhesion test, which was accessed by the DIN 50161 standard, no significant differences were verified between the adhesion strength of both Si-HA and HA coatings, before and after soaking in SBF, for 21 days, at 37ºC (Figure 4A). Adhesion values were around 30 MPa. The SEM characterization of the Si-HA sample surface following test establishment, and before SBF immersion, revealed three distinct zones: the Ti alloy substrate (Z1), the failure zone (Z2) and the coating (Z3) (Figure 4B). High magnification micrographs (Figure 4C and 4D) revealed that the cleavage plans are clearly identified, as well as an irregular surface.

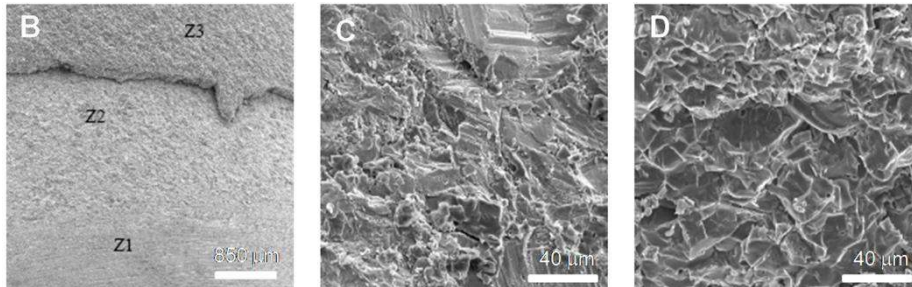| A	Before soaking (MPa)	After soaking (MPa)
Si-HA	29.5 ± 2.4	33.4 ± 5.4
HA	28.7 ± 3.1	32.1 ± 4.2

Figure 4 - Adhesion stress results measured according to DIN 50161 standard, for Si-HA and HA coatings, before and after soaking in SBF, for 21 days (A). SEM images of the samples tested for Si-HA coating, before soaking in SBF (B). Z1 corresponds to the Ti-6Al-4V alloy surface, Z2 to the failure zone and Z3 to the coating. C – high magnification of the Z2 area. D – high magnification of the Z3 area.

Osteoblastic cell response

Cell viability/proliferation

The viability/proliferation of the cells was inferred from the MTT assay, Figure 5A. Both HA and Si-HA coated surfaces were able to support cell growth, as the metabolic activity of human osteoblasts increased from early time points until day 14, decreasing afterwards. Si-HA coated samples reported increased MTT values at every time point and significant differences were attained at days 7 and 14.

Alkaline phosphatase activity

Results regarding the activity of alkaline phosphatase are presented in Figure 5B. ALP activity increased significantly during the second week, achieving maximal values by day 14, in cultures established on the surface of both coatings. Subsequently, ALP activity decreased throughout the remaining culture time. ALP activity was significantly higher in the cultures established on the surface of Si-HA coated titanium samples, at day 14.
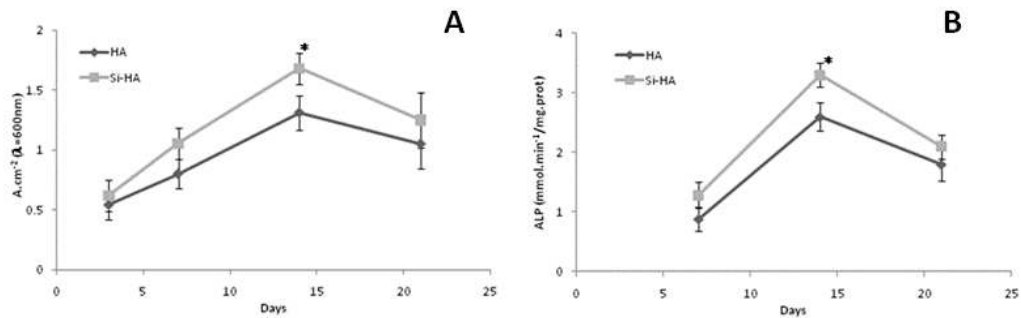
Figure 5 - Cell viability/proliferation (A) and alkaline phosphatase activity (B) of human bone marrow osteoblastic cells cultured, for 21 days, on the surface of HA and Si-HA plasma sprayed titanium substrates. * Significantly different from HA (p≤0.05).

Osteogenic-related gene expression

The differentiation of bone marrow-derived osteoblastic cells was assessed by RT-PCR, following 14 days of culture over both HA and Si-HA constructs. As shown in Figure 6, ALP, BMP-2 and Col I genes were transcribed by the cultures established over both materials, under osteogenic inducing conditions. Additionally, increased expression of the evaluated genes can be visualized in cultures performed over Si-HA.
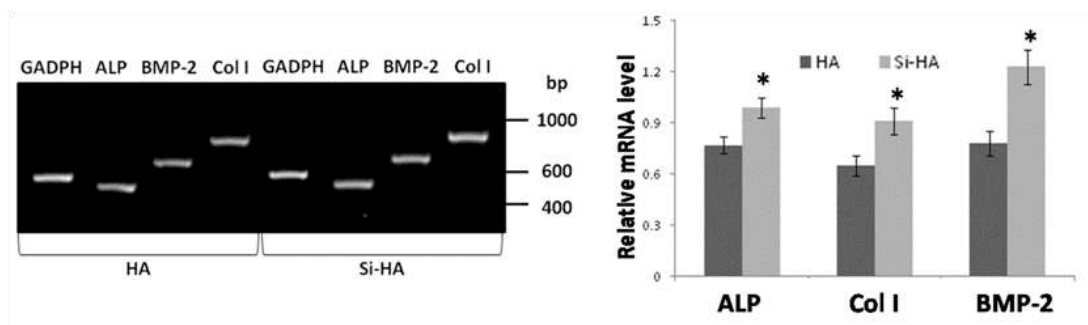

Figure 6 - Results from the RT-PCR showing amplification of osteogenic-associated genes (ALP, BMP-2 and Col I) in cultures established for 14 days on the surface of both HA and Si-HA coatings. Representative agarose gel is shown in the left panel with corresponding densitometric analysis on the right panel. Densitometric analyses of transcription levels were standardized using GAPDH, as a housekeeping gene. * Significantly different from HA.

Ionized calcium (Cai) in culture medium

Results regarding the concentration of Cai in the culture medium are presented on Figure 7. During the first 2 weeks of culture, values for Cai were kept more or less stable in the cultures established over both constructs. Following, at day 14, Cai concentration began to decrease in seeded Si-HA samples, while in which regards to

seeded HA constructs, the decrease in Cai concentration was only attained following day 17.
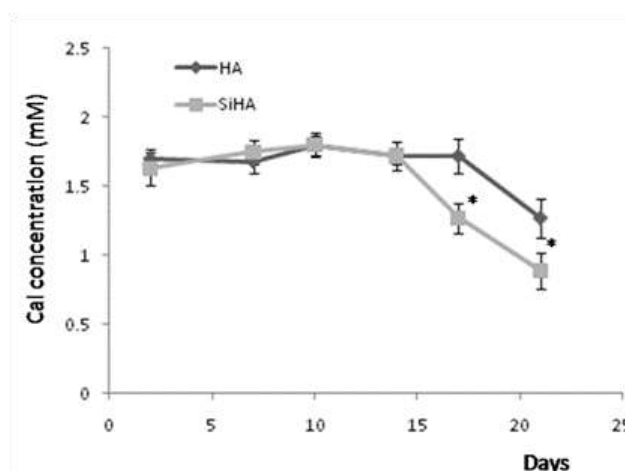

Figure 7 - Ionized calcium (Cai) concentration in culture medium of seeded Si-HA and HA constructs, for 21 days. * Significantly different from HA (p≤0.05).

Confocal Laser Scanning Microscopy (CLSM) and Scanning Electron Microscopy (SEM)

CLSM images of cells cultured over HA and Si-HA coated substrates, after 3, 7, 14 and 21 days are presented in Figures 8 and 9, while representative SEM micrographs of cultures established for 21 days over both materials, are presented on Figure 10.

CLSM images report that cells were able to adhere well to the coated Ti surface since early cytoplasmic spreading was established with several philipodia being visualized contacting with the irregularities found on the materials' surface. As soon as day 3, cells adopted an elongated morphology with a prominent nucleus and multiple cell-to-cell contacts, as it can be observed by the high magnification images of Figure 9. Cells were distributed randomly over both coatings and following, cells proliferated actively throughout culture time, covering a significant area of the materials' surface at days 7 and 14, although, qualitatively, more cells could be visualized on the surface of Si-HA samples, at these time points. At day 21, the surface of the samples was covered by dense and multiple cell layers, over both coatings. Representative images are shown on Figure 8.

Regarding SEM observation, multiple cell layers can be visualized over both materials' surface, interspersed with mineral globular deposits closely associated with the fibrous matrix. The Si-HA coating seems to report increased mineral deposition

comparing to that attained over the HA coating, as more globular mineral deposits can be observed. Representative high magnification images are reported on Figure 10.
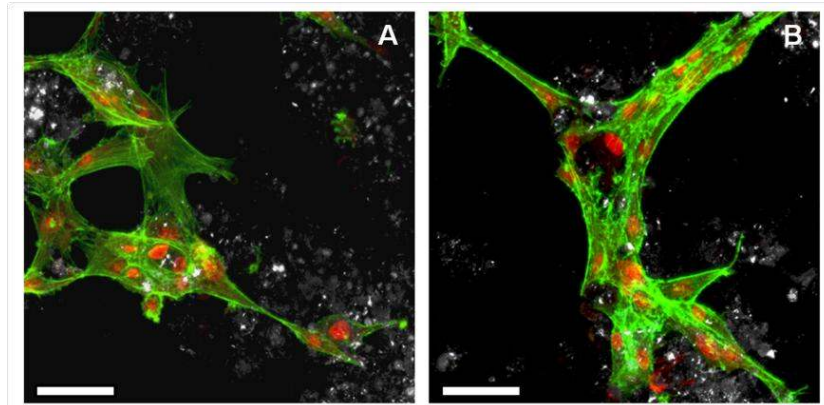
Figure 8 - High magnification CLSM images of the cultures established for 3 days over HA (A) and Si-HA (B). Labeling: phalloidin – green, propidium iodide – red, material's surface – grey. The scale bar represents 50 μm.
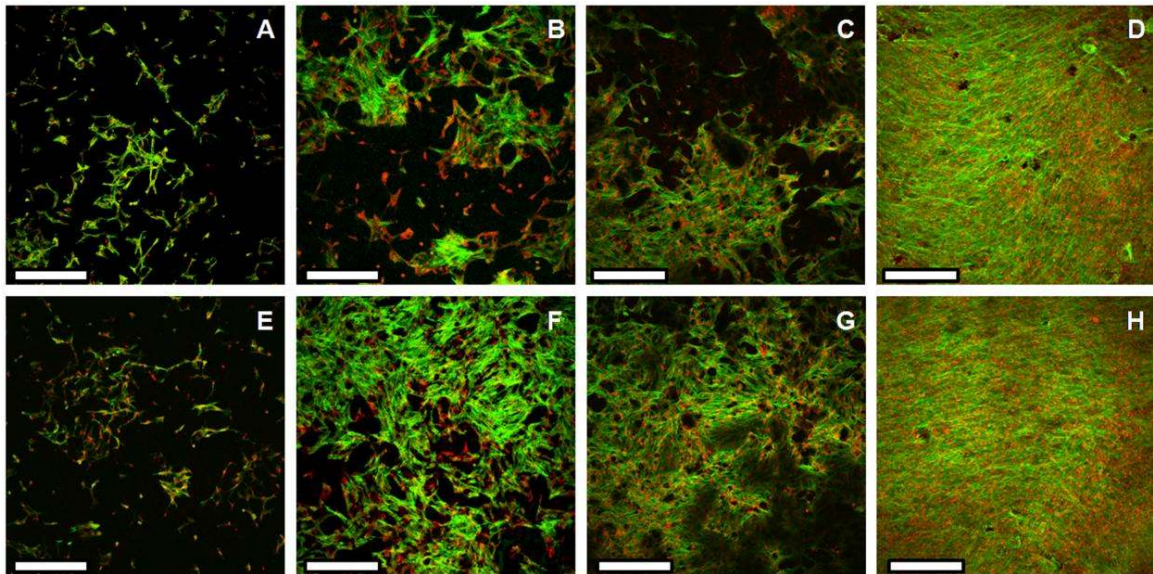

Figure 9 – CLSM images of the time-course behavior of cultures established for 21 days over HA (A to D) and Si-HA (E to H) plasma sprayed substrates. Labeling: phalloidin – green, propidium iodide – red. A and E – 3 days, B and F – 7 days, C and G – 14 days, D and H – 21 days. The scale bar represents 300 μm.
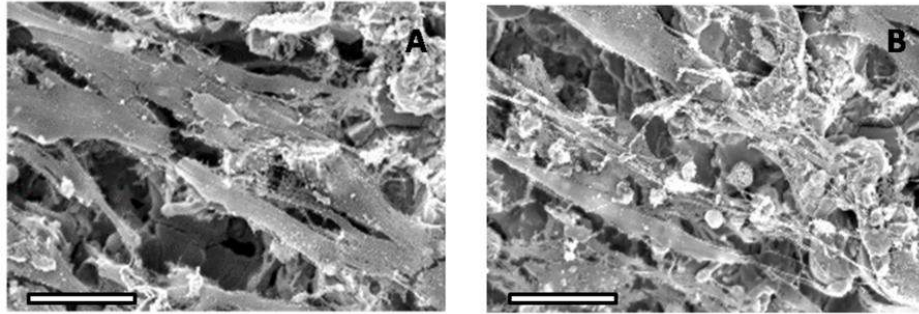
Figure 10 – High magnification SEM micrographs of cultures grown for 21 days over HA (A) and Si-HA (B) coatings. Note the globular mineral deposits interspersed with the thick cell layer. The scale bar represents 100 μm.

Discussion

Titanium based alloys have been widely used for orthopedic and dental applications due to their satisfactory mechanical properties and adequate osseointegration [1,2]. However, since primary fixation is one of the most important factors for establishing adequate clinical function, several approaches have been employed to maximize bone formation and implant fixation, including the deposition of ceramic films and coatings over the surface contacting the biological tissues [32].

Among the available techniques, plasma spraying appears to be the most favorable, and thus, most commonly used for fabricating bioactive ceramic-based coatings on implants [26]. In fact, deposition of plasma-sprayed HA increases surface roughness and porosity of the construct, establishing a favorable microenvironment for cell adhesion and proliferation, and though, promoting osteointegration by direct bone interlocking [33].

Taking advantage of this technique and the benefits of Si-HA, we report the in vitro biological evaluation of Ti-6Al-4V substrates, plasma-sprayed with 0.8 wt% Si-substituted HA, regarding proliferation and differentiation events of human bone-marrow derived osteoblastic cultures, established for 21 days in conditions known to induce the osteoblastic phenotype [34]. Ti-6Al-4V substrates plasma-sprayed with HA were used as control.

The addition of 0.8 wt% Si to the HA lattice did not induce modifications in the phase composition since no secondary phases were detected in the Si-HA powder, regarding XRD analysis. In fact, the substitution of PO_4^{3-} groups by SiO_4^{4-} groups, up to a certain level, introduces only small changes in the cell unit which does not lead to HA's phase decomposition [30,35]. Accordingly, new and more soluble phases (including tricalcium phosphate – α-TCP and β-TCP – and calcium oxide) were only obtained following plasma-spraying of feedstock powders, both regarding HA and Si-

HA materials. As previously published by the research group [36,37], pure phase HA, after plasma spraying, becomes more amorphous and suffers phase decomposition leading to the formation of CaO (6.4%) and β-TCP (6.4%) phases, besides HA (87.2%). Decomposition occurs as a consequence of the high temperature followed by a rapid cooling rate – characteristics of the thermal deposition technique [33]. Additional characterization of the coatings has also shown that the adhesive strength of the plasma sprayed surfaces (around 30 MPa before and following immersion in SBF) satisfies the stress requirements for coated bearing biomedical applications [36,37]. Fracture surfaces of the samples subjected to DIN 50161 have shown that failure occurred by the coating – cohesive failure.

By comparing the phase analysis results of both coating materials, Si-HA material suffered the highest conversion of HA, and showed the presence of α-TCP phase that was not detected in the HA coating. The introduction of Si into HA lattice led to its distortion [38], and therefore the Si-HA feedstock powder was more susceptible to suffer phase transformation than HA feedstock powder, during plasma spraying. Moreover, silicon has been shown to stabilize TCP phases, preventing the fully conversion of α-TCP into β-TCP – as described following the decomposition of HA, after plasma spraying [39,40]. The initial increased Ca and P adsorption associated with Si-HA materials might suggest the early formation of the apatite layer on this material over HA constructs, nevertheless following 7 days of immersion, similar globular agglomerates were assessed by SEM.

In cultures established over Si-HA and HA sprayed substrates, cells showed early attachment and spreading, as well as an elongated fibroblast-like morphology with a close interaction with the materials' surface irregularities and intense cell-to-cell contact. In a general way, Si-HA coatings allowed an increased viability/proliferation, as well as the expression of higher levels of ALP. Maximum values of these parameters, observed at day 14, were significantly higher than those of control – HA coatings. Further, several osteogenic markers like ALP, BMP-2 and Col I were shown to be up-regulated by cultures grown over Si-HA-coated substrates, while assessment of the Cai in the culture medium indicates that calcium deposition began around day 14 for the cultures established over Si-HA constructs and later on regarding seeded HA constructs. These results are in concordance with ALP activity which is expected to reach maximal value just before the beginning of matrix mineralization. SEM observation suggested an increased mineralization of the extracellular matrix in Si-HA, comparing to control. This might converge to substantiate an increased osteogenic differentiation by cultures established on the surface of Si-HA plasma sprayed substrates.

Regarding previous in vitro biological evaluation of Si-containing coatings over titanium substrates, Thian et al. reported improved cell growth on a magnetron sputtered 0.8 wt% Si-containing hydroxyapatite over titanium surfaces, comparing to uncoated ones [22]. Further, a porous CaP layer was observed from day 16 onwards, which grew denser and thicker till day 42. In comparison, uncoated substrates revealed a very porous layer comprising only CaP crystallites, after 42 days of culture [22]. However, these studies compared Si-containing coatings with uncoated titanium substrates and not with the control surfaces, i.e. the deposited ceramic coatings without the addition of Si to the formulation. Therefore, no information is provided regarding the specific role of Si in the evaluated cell response, since other ions are released during the coating incubation with the culture medium, and expected to influence the biological response [41].

In a general way, the results presented in this study regarding the positive effect of Si-HA compared to HA are in accordance with previously reported data from the literature which have shown an improved biological response induced by Si-containing biomaterials [18-21,30]. Although no definitive mechanisms have been established, silicon release may contribute to the attained biological response. In the present work, the ionic release of Si was assessed throughout the cell culture period (21 days) in SBF, at pH 7.4. During the test period, a continuous Si release was established and a concentration of around 0.12 mM (around 3.4 ppm) was attained, after 21 days of immersion. This concentration is within the range of the large interval, between 1 and 100 ppm, which lead to a dose dependent increase in human osteoblast-like cells' proliferation and differentiation, in short-term cultures [15-17].

In humans, the silicon concentration is highly variable according to the biological location. For instance, serum concentration is around 0.6 ppm, while for muscle and lung tissues, it is around 40 and 50 ppm, respectively [42,43]. Other mammals show a similar range of silicon concentrations in multiple tissues [44]. Therefore, the levels of Si released from the Si-HA plasma-sprayed constructs reported in the present work are well within the physiological range of Si levels. In addition, and of particular relevance, an experimental rabbit model of bone regeneration with a Si-rich bioactive glass, revealed that nevertheless the attained high Si concentration neighboring the implant location, this ion was continuously released into the blood and promptly excreted into the urine, with no adverse physiological effects or accumulation in major organs, substantiating the biosafety of Si-releasing biomaterials [45].

Previous work regarding the biological performance of the present material, 0.8% Si-HA, in a bulk form, did not show significant differences on the proliferation profile, ALP activity and matrix mineralization of osteogenic-induced human bone

marrow cells, comparing to HA, although a slight increase in the expression of osteocalcin was noted over Si-HA [46]. This might suggest that the incorporation of Si in the composition of a plasma-sprayed ceramic coating could lead to an improved cell response, compared to that occurring on Si containing bulk ceramic materials. This might be related with the intrinsic properties of plasma-sprayed materials, i.e., increased surface area, porosity and roughness [26,33], as well as with the increased solubility associated with the phase modifications', elicited by the thermal spraying deposition. Both may contribute to an improved pattern of Si release, comparing to that observed in a bulk material with similar composition. In fact, plasma sprayed ceramics report a faster dissolution rate which is known to contribute to the formation of a supersaturated microenvironment that may potentiate the precipitation of physiologically produced apatite over the coatings, enhancing bone ingrowth [47,48]. In agreement, in the present work, a continuous globular apatite layer could be visualized in the surface of both materials, from early time points, following immersion in SBF. Furthermore, it is also reported that bone growth occurs at a faster rate when the coating has a higher content of amorphous phase, as reported in plasma-sprayed substrates [26].

The addition of Si to the HA composition may assemble, along with the plasma spraying characteristics', an optimized microenvironment that is more favorable for cell adhesion, proliferation and differentiation than that achieved with the plasma spraying of non-doped HA.

References

1. Kasemo B. Biocompatibility of titanium implants: surface science aspects. J Prosthet Dent 1983;49:832-7.

2. Carlsson L, Röstlund T, Albrektsson B, Albrektsson T, Brånemark P. Osseointegration of titanium implants. Acta Orthop Scand 1986;57:285-9.

3. Geesink R, de Groot K, Klein C. Bonding of bone to apatite coated implants. J Bone Jt Surg 1988;70-B:17-22.

4. Biesbrock A, Edgerton M. Evaluation of the clinic predictability pf hydroxyapatite-coated endosseus dental implants: a review of the literature. Int J Oral Maxillofac Implants 1995;10:712-20.

5. Lavos-Valereto I, Wolynec S, Deboni M, Konig Jr B. In vitro and In vivo biocompatibility testing of Ti-6Al-7Nb alloy with and without plasma-sprayed hydroxyapatite coating. J Biomed Mater Res (Appl Biomater) 2001;58:727-733.

6. Le Geros R, Le Geros J. Dense hydroxyapatite. In: Hench L, editor. An introduction to bioceramics. Singapore: World Scientific; 1993. p 139-80.

7. Posner A. Crystal chemistry of bone mineral. Physiol Rev 1969;49:760-792.

8. Mc Connel D. Biological apatites. Berlin: Springer; 1973.

9. Elliott J. Structure and chemistry of the apatites and other calcium orthophosphates. Amsterdam: Elsevier; 1994. 389 p.

10. Schwarz K, Milne D. Growth-promoting effects of silicon in rats. Nature 1972;239:333-4.

11. Carlisle E. Silicon: a possible factor in bone calcification. Science 1970;167:279-280.

12. Carlisle E. Essentiality and function of silicon. In: Bendz G, Lindquist I, editors. Biochemistry of Silicon and Related Problems. New York: Plenum; 1977.

13. Jugdaohsingh R, Tucker K, Qiao N, Cupples L, Kiel D, Powell J. Dietary silicon intake is positevely associated with bone mineral density in men and premenopausal women of the framingham offspring cohort. J Bone Miner Res 2004;19:297-307.

14. Darley W, Volcani B. Role of silicon in diatom metabolism. A silicon requirement for deoxyreibonucleic acid synthesis in diatom Cylindrotheca-fusiformis reimann and lewin. Exp Cell Res 1969;58:334.

15. Keeting P, Oursler M, Wiegand K, Bonde S, Spelsberg T, Riggs B. Zeolite A increases proliferation, differentiation, and transforming growth factor beta production in normal adult human osteoblast-like cells in vitro. J Bone Miner Res 1992;7:1281-9.

16. Reffitt D, Ogston N, Jugdaohsingh R, Cheung H, Evans B, Thompson R, Powell J, Hampson G. Orthosilicic acid stimulates collagen type I synthesis and osteoblastic differentiation in human osteoblastic-like cells in vitro. Bone 2003;32:127-35.

17. Arumugam M, Ireland D, Brooks R, Rushton N, Bonfield W. The Effect Orthosilicic Acid on Collagen Type I, Alkaline Phosphatase and Osteocalcin mRNA Expression in Human Bone-Derived Osteoblasts In Vitro. Key Eng Mater 2004;254-256:869-872.

18. Gao T, Aro H, Ylanen H, Vuorio E. Silica-based bioactive glasses modulate expression of bone morphogenic protein-2 mRNA in Saos-2 osteoblasts in vitro. Biomaterials 2001;22:1475-83.

19. Grough J, Jones J, Hench L. Nodule formation and mineralization of human primary osteoblasts cultured on aporous bioactive glass scaffold. Biomaterials 2004;25:2039-2046.

20. Vallet-Regí M, Arcos D. Silicon substituted hydroxyapatites. A method to upgrade calcium phosphate based implants. J Mater Chem 2005;15:1509-16.

21. Pietak A, Reid J, Stott M, Sayer M. Silicon substtitution in the calcium phosphate bioceramics. Biomaterials 2007;28:4023-4032.

22. Thian E, Huang J, Best S, Barber Z, Brooks R, Rushton N, Bonfield W. The response of osteoblasts to nanocrystalline silicon-substituted hydroxyapatite thin films. Biomaterials 2006;27:2692-2698.

23. Huang J, Jayashinghe S, Best S, Edirisinghe M, Brooks R, Rushton N, Bonfield W. Novel deposition of nano-sized silicon substituted hydroxyapatite by electrospraying. Journal of Materials Science:Materials in Medicine 2005;16:1137-1142.

24. Hijón N, Cabanas M, Pena J, Vallet-Regí M. Dip coated silicon-substituted hydroxyapatite films. Acta Biomaterialia 2006;2:567-574.

25. Solla E, Borrajo J, González P, Serra J, Chiussi S, León B, García López J. Study of the composition transfer in the pulsed laser deposition of silicon substituted hydroxyapatite thin films. Applied Surface Science 2007;253:8282-8286.

26. Sun L, Berndt C, Gross K, Kucuk A. Material fundamentals and clinical performance of plasma-sprayed hydroxyapatite coatings: a review. J Biomed Mater Res 2001;58:750-92.

27. Knabe C, Berger G, Gildenhaar R, Klar F, Zreiqat H. The modulation of osteogenesis in vitro by calcium titanium phosphate coatings. Biomaterials 2004;25:4911-4919.

28. Gibson I, Huang J, Best S, Bonfield W. Enhanced In Vitro Cell Activity and Surface Apatite Layer Formation on Novel Silicon-Substituted Hydroxyapatites. In: Ohgushi H, Hasting G, Yoshikawa T, editors. Proceedings of the 12th International Symposium on Ceramics in Medicine. Nara, Switzerlnad: Trans Tech Publications; 1999. p 191.

29. Patel N, Best S, Bonfield W, Gibson I, Hing K, Damien E, Revell P. A Comparative Study on the in vivo Behaviour of Hydroxyapatite and Silicon Substituted Hydroxyapatite Granules. J Mater Sci Mater Med 2002;13:1199-1206.

30. Gibson I, Best S, Bonfield W. Chemical characterization of silicon-substituted hydroxyapatite. J Biomed Mater Res 1999;44:422-428.

31. Oyane A, Kim H-M, Furuya T, Kokubo T, Miyazaki T, Nakamura T. Preparation and assessment of revised simulated body fluid. J Biomed Mater Res 2003;65A:188-195.

32. Friedman R, Black J, Galante J, Jacobs J, Skinner H. Current concepts in orthopaedic biomaterials and implant fixation. Journal of bone and joint surgery. American volume 1993;75:1086-1109.

33. Tsui Y, Doyle C, Clyne T. Plasma sprayed hydroxyapatite coatings on titanium substrates Part 1: Mechanical properties and residual stress levels. Biomaterials 1998;19:2015-2029.

34. Coelho M, Trigo Cabral A, Fernandes M. Human bone cell cultures in biocompatibility testing. Part I: Osteoblastic differentiation of serially passaged human bone marrow cells cultured in α-MEM and in DMEM. Biomaterials 2000;21:1087-1094.

35. Botelho C, Lopes M, Gibson I, Best S, Santos J. Structural analysis of Si-substituted hydroxyapatite: Zeta potential and X-ray photoelectron spectroscopy (XPS). J Mater Sci Mater Med 2002;1123-1127.

36. Silva P, Santos J, Monteiro F, Knowles J. Adhesion and Microstructural characterisation of Plasma Sprayed Hydroxyapatite-Glass Ceramic coatings onto Ti-6Al-4V substrates. Surf Coat Tech 1998;102:191-196.

37. Ferraz M, Fernandes M, Santos J, Monteiro F. HA and Double layer HA-P2O5/CaO Glass coatings: influence of chemical composition on human bone marrow cells osteoblastic behaviour. J Mater Sci Mater Med 2001;12:629-638.

38. Porter A, Botelho C, Lopes M, Santos J, Best S, Bonfield W. Ultrastructural comparison of dissolution and apatite precipitation on hydroxyapatite and silicon-substituted hydroxyapatite in vitro and in vivo. J Biomed Mater Res 2004;69A:670 - 679.

39. Reid J, Tuck L, Sayer M, Fargo K, Hendry J. Synthesis and characterization of single-phase silicon-substituted α-tricalcium phosphate Biomaterials 2006;27:2916-2925

40. Dorozhkin S. Calcium Orthophosphates. J Mater Sci Mater Med 2006;42:1061-1095.

41. Chou L, Marek B, Wagner W. Effects of hydroxylapatite coating crystallinity on biosolubility, cell attachment efficiency and proliferation in vitro Biomaterials 1999;20:977-985

42. Dobbie J, Smith M. The silicon content of body fluids. Scott Med J 1982;27:17-9.

43. Hamilton E, Minski M, Cleary J. The concentration and distribution of some stable elements in healthy human tissues from United Kingdom: an environmental study. Sci Total Environ 1973;1:341-74.

44. LeVier R. Distribution of silicon in the adult rat and rhesus monkey. Bioinorg Chem 1975;4:109-15.

45. Lai W, Garino J, Ducheyne P. Silicon excretion from bioactive glass implanted in rabbit bone. Biomaterials 2002;23:213-217.

46. Botelho C, Brooks R, Best S, Lopes M, Santos J, Rushton N, Bonfield W. Human osteoblast response to silicon-substituted hydroxyapatite. J Biomed Mater Res 2006;79A:723-730.

47. Gross K, Berndt C, Goldschlag D, Iacono V. In vitro changes of hydroxyapatite coatings. Int J Oral Maxillofac Implants 1997;12:589-597.

48. MacDonald D, Betts F, Stranick M, Doty S, Boskey A. Physicochemical study of plasma-sprayed hydroxyapatite-coated implants in humans. J Biomed Mater Res 2000;54:480-490.

Chapter 10

Rodent models in bone-related research – the relevance of calvarial defects in the assessment of bone regeneration strategies

Rodent models in bone-related research – the relevance of calvarial defects in the assessment of bone regeneration strategies

P.S. Gomes, M. H. Fernandes

Laboratory of Pharmacology and Cellular Biocompatibility
Faculty of Dental Medicine, U. Porto
R. Dr. Manuel Pereira da Silva – 4200-393 Porto, Portugal

Abstract

In vivo research with animal models has been a preferred experimental system in bone-related biomedical research since, by approximation, it allows relevant data gathering regarding physiological and pathological conditions that could be of use to establish more effective clinical interventions. Animal models, and more specifically rodent models, have been extensively used and have contributed greatly to the development and establishment of a wide range of translational approaches aiming to regenerate the bone tissue. In this regard, the calvarial defect model has found great application in basic and applied research, nonetheless the controversial rationalization for the use of critical size defects – defects that are unable to report spontaneous healing – or sub-critical size defects in the proposed applications. Accordingly, this work aims to review the advantages and limitations of the use of rodent models in biomedical bone-related research, emphasizing the problematic issues of the use of calvarial critical and sub-critical size defects. Additionally, surgical protocols for the establishment of both defects in rat calvarial bone, as well as the description and exemplification of the most frequently used techniques to access the bone tissue repair, are portrayed.

The bone tissue is characterized by an adequate capacity to regenerate itself following the establishment of a lesion or a defect, when the physiological stimuli converge to establish a proper response. Nevertheless, determined conditions associated with an unfavorable micro-environment, sub-optimal surgical techniques or biomechanical instability can lead to a poor prognosis on bone tissue regeneration [1]. Furthermore, large orthopaedic defects, in which the physiological regenerative capabilities are exceeded, rely on the application of mechanically- and biologically-suited biomaterials, including ceramics, metals, polymers and composites, for adequate tissue reconstruction [2]. The reported situations are established major clinical and socio-economic burdens with serious implications in patients life-style and life quality [3]. Furthermore, several systemic conditions are known to affect bone physiological equilibrium and may contribute to the impairment of an adequate healing process [4-6].

Regenerative medicine and tissue engineering approaches to the bone tissue enclose a wide range of applications that aim to repair, augment, substitute and regenerate lost tissues [2]. De novo bone formation relies on the recruitment, transplantation, homing or modulation of progenitor or differentiated cells. These cells require the availability of an adequate substrate to play their biological function by adhering, proliferating and differentiating in a controlled way, giving rise to a mature tissue with adequate biomechanical properties [2, 3].

The design of experimental models to evaluate the efficacy and biosafety of these regenerative strategies – that encompass cells, materials and modulators – requires both methodical control and modulation of specific variables – situations that cannot be met on a single model. According to Muschler et al, in order to aim the clinical translation of bone tissue engineering strategies, used models should meet several criteria: mimic the clinical and biological environment in which the experimental methodology will be assessed; allow quantifiable parameters to access the success, in a quantitative and qualitative way, and functional performance of the regenerated tissue; and identify and foresee relevant differences in the biological performance between assayed methods [7].

In vitro assays give great contribution to the comprehension of fundamental biological mechanisms (i.e., transcription, translation, intra-cellular signaling events, regulation of the cell cycle, ligand-receptor interactions, etc.), screening of the biological activity, toxicity and immunogenicity of specific compounds, and evaluation of the direct or indirect cell response to a seeded material [8, 9]. Additionally, in vitro models of higher complexity have been developed, enclosing the use of bioreactors to access the biological response of 3D constructs and co-culture models with different

cell populations, to further recreate the complexity of multiple cell interactions [10, 11]. Even so, in vitro assays reveal significant limitations in the capacity to recreate the intricacies of the in vivo milieu and though, are incapable of predicting clinical output and performance.

In vivo research with animal models has been a preferred experimental system since, by approximation, provides relevant data regarding physiological and pathological conditions that could be of use to establish more effective clinical interventions. *In vivo* research establishes a link between in vitro studies and clinical trials. Experimental animal models are essential to provide an adequate approximation to the real settings. Accordingly, the selection of the appropriate design and model relies, in the very end, in the therapeutic modality that is being tested [7]. In this context, and in which relies to the bone tissue, one may consider five domains of biological activity: 1) Osteogenesis – associated with the cellular function – i.e, the biological process by which committed cells at different stages of differentiation are recruited, activated, proliferate and differentiate in order to produce de novo bone tissue; 2) Osteoconduction – associated with the support function – i.e., the process by which a specific volume of tissue is preserved from the infringement of neighboring tissues and allows osteogenic cells to play their biological role; 3) Osteoinduction – associated with the modulators function – i.e., the process by which soluble or matrix-associated molecules influence the biological fate of osteoblastic cells; 4) Mass transfer and 5) Biophysical effects – processes which are mainly associated with biochemical and biomechanical events that contribute to the establishment of an adequate tissue healing [12].

Animal models, and more specifically rodent models, have been extensively used and have contributed greatly to the development and establishment of a wide range of approaches to regenerate the bone tissue. For instance, and focusing on osteogenesis, rodent models have provided great amount of data regarding the cellular behavior of multiple populations relevant to bone regeneration [13-15]. Moreover, and in which regards to osteoconduction, rat and mouse models have also proven to be of great importance regarding the assessment of the biocompatibility of granular, scaffolds or bulk materials, in the evaluation of the surface osteoconduction and specific toxicity, and degradation rate of synthetic materials aiming bone repair [7, 15, 16]. These models have been also used for the evaluation of the biosafety profile of the osteoinduction process, following the administration of biomodulators [15, 17, 18].

Among the available orthotopic models to evaluate the bone function, calvarial bone defects have gained a widespread reputation and use in the published literature, reporting valuable data from basic and applied research. Nonetheless, a major point of

debate relies on the selection of either critical size defects – the ones that do not report spontaneous healing during the lifetime of the animal – or sub-critical size defects – defects in which complete bone regeneration is expected, without the contribution of induced-recruited or added factors.

In this way, we aim to review the advantages and limitations of the use of rodent models in biomedical bone-related research, in particular the calvarial bone model, emphasizing the problematic issues of the use of critical size and sub-critical size bone defects. Additionally, surgical protocols for the establishment of both defects in rat calvarial bone, as well as the description and exemplification of the most frequently used techniques to access the bone tissue repair, are portrayed.

Selection of animal species – the relevance of rodents

A large variety of mammalian species have been used in bone-related research. O'Loughlin reviewed the use of animal models in fracture repair studies published for the past 10 years in 6 orthopaedic journals and realized the following relative order of frequency: rat 38%, rabbit 19%, mouse 13%, sheep 11%, dog 9%, goat 4% and other 4% [19]. This report clearly states the relevance of rodents in orthopaedic research. Fundamental research, feasibility and bioactivity testing greatly rely on the use of mice and rats due to the high definition of the models in a biological, genetic and immunological point of view, which allows the attainment of a high level of experimental reproducibility.

In fundamental research, the availability of biological tools (e.g., primers for PCR testing, microarrays, probes, antibodies, etc.), the fast turnover of individuals and the rapid occurrence of biological processes are of the utmost importance, allowing for a facilitated observation of the processes under study. In an additional way, the sequencing of mouse [20] and rat [21] genome smoothed the progress of transgenic and knockout models which contributed to the knowledge of the function and modulation of specific genes [22, 23].

Going one step further fundamental research, feasibility and bioactive testing directs the research process along the translational application pathway. Specific evaluation broadly includes the efficacy of materials' or agents' delivery, cytotoxicity and biocompatibility testing and screening for adverse or unwanted reactions. The same models used in feasibility studies, with relevance for both mice and rat, are also utilized for the quality control screening and bioactivity of products or implants. In addition, route of administration and assessment of the target tissues may be evaluated in compliance with the proposed clinical setting.

The assessment of clinical modeling and efficacy, also referred as preclinical testing, is broadly performed in large skeletally mature animals including dogs, goats, sheep and pigs, reporting phylogenetical resemblance. Structure and composition of these animals' bone tissue has been found to be highly similar to those of humans [24]. Point variations are generally associated with modest differences in cancellous and cortical density, response to uferectomy and diet restriction, extent of sexual dismorphism, age of peak bone mass, and rate and extension of harversian remodeling [7, 24, 25]. Nevertheless the stated variations, there is no substantiation that one model proves to be a better match than other to address clinical translation of assayed therapeutic approaches. As a result, individual selection should rely on economic issues, local access, housing requirements and availability, staff expertise, and considerations of the experimental protocol. Nonhuman primates (NHPs) have also been used in the study of bone repair, nevertheless the established increase in the research cost and the raise of cultural and ethical questions. Arguments substantiated by the evolutionary proximity and anatomic and physiological resemblance converge to indicate NHPs as first choice models in bone-related research. Nevertheless, the diversity and variability attained in effector responses limit the efficacy of clinical translation – response variations between primate species has been shown to be greater than in quadrupeds and even humans [26, 27]. In addition, biomechanical differences have been largely stated and reports concerning differential biological responses – e.g., baboons seem to be hypersensitive to the administration of bone morphogenic proteins [28] – contribute to the fact that NHPs do not attain a valid consensus as providing a first choice model, comparing to other large animals [7].

As stated, a wide range of animal models is available not only for fundamental, feasibility and bioactivity bone-related biomedical research, but also for pre-clinical testing. Individual choice should be made according to the knowledge of established biological differences, advantages and inconveniences, but also taking into account methodological and operational features of each model. Comparing the characteristics of the bone tissue between the described animals, several differences can be outputted. For instance, rodents continue to model their skeleton throughout their life cycle - regarding grow and reshape - and growth plates remain open throughout adulthood. Mice and rats also report limited trabecular bone content and haversain remodeling - by tunneling osteoclasts - does not occur, although cancellous remodeling is established [29, 30]. Furthermore, rodent models are not suited to the establishment of long-term studies, in which multiple biopsies or large blood samples are required, due to biological constrains. On the other hand, and comparing to large animal models, rodents are inexpensive, easy to house and manipulate, and report minimal social

concern. Furthermore, if trustworthy and validatable data can be acquired, animals placed at the lower end of the phylogenetic scale should be preferably used – in the case, rodents are a first choice option over large mammals. Due to their widespread utilization, much is known regarding the biological processes associated with bone turnover, diet modifications and drug administration. Furthermore, the reduced lifespan of these animals allows for the study of the influence of aging in the bone metabolism and regeneration processes.

Over viewing the stated arguments, rodent models prove to be quite useful in bone-related research, being among first choice models for in vivo testing of regenerative and/or therapeutic approaches to the bone tissue.

In vivo models of bone regeneration – the calvarial defect model

Currently, several in vivo models are used to evaluate the bone regeneration process, the bone-biomaterial interaction and the physiological or pathological evidence of the modulation of the ossification pathway. Experimental models can be classified as heterotopic or orthotopic, based on the vicinity to the autologous bone tissue. The characterization of materials aiming bone regeneration is generally assayed, on a first approach, in a heterotopic model, i.e. subcutaneous, intramuscular, intraperitoneal or mesentery location, which are generally used prior to the assessment of the materials' behavior in direct contact with the bone tissue. Moreover, if the material reveals a paste-like consistency, it can be easily injected into the targeted site.

The surgical implantation of granular, scaffolds or bulk materials has been widely conducted in rodents. Accordingly, the rat heterotopic model has been used successfully to show the sequence of events involved in the ossification process [31]. Most common implantation sites include the subcutaneous tissue on the back or upper abdominal area [32]. Although the use of heterotopic bioassays in rodent models prevails in the biocompatibility assessment of materials, there is a scarcity of data regarding translational and clinical applications, no matter how quantitative the data from the heterotopic bioassay may be [33].

In order to solve inherited limitations from heterotopic applications, intraosseous defects have been used to test for the capacity of materials and constructs to promote the repair of discontinuous and weight-bearing lesions. The selection of orthotopic models in bone research relies broadly in one of the following options: calvarial, long bone or mandible segmental, partial cortical and cancellous bone defects [34]. The calvarial model outreaches as an adequate model to evaluate complex materials and tissue engineering constructs aiming bone regeneration, especially in which refers to the regeneration of craniofacial defects. This model has been established in a wide

range of animal species including, mice, rats, rabbits, dogs, sheeps, goats, pigs and non-humane primates, although rats and rabbits are the most commonly used animals.

The calvarial model is very adequate and popular among researchers, mainly due to the following reasons: the calvarial bone structure allows the establishment of a uniform, reproducible and standardized defect that is easily evaluated by radiographic and histological analysis; the anatomic location reflects an adequate size for surgical access and intra-operative handling; the dura and the overlaying skin set up an adequate support for implanted materials, without the need of internal or external fixation; and the model has been widely used and studied, allowing a precise comparison of grafted substances [32]. Nonetheless, it does not allow the assessment of the biological response of the implanted material to a physiological biomechanical loading which may be a limitation in some applications. In this case, alternative anatomical load bearing locations, like the mandible, the femur or tibia, should be preferably selected.

Calvarial critical size and subcritical size defect models

The use of the calvarial model implies the selection of the defect size, particularly the knowledge of the critical size of the defect, which varies according to the animal species, strain, gender, age, anatomic site, shape, size and micro-mechanical environment [35-37]. According to Schmitz et al, the CSD can be described as the smallest wound established intraosseously in a particular bone, which does not report spontaneous healing during the lifetime of the animal [35, 36]. Accordingly, the CSD can be considered the prototype of discontinuity defects, as a specific condition of failed osteogenesis for overcoming the threshold of the physiological process of tissue repair/regeneration.

Nevertheless the stated knowledge, the processes associated with the cease of bone healing during the repair of CSD have not been fully understood. Honma et al compared the regeneration process in sub-critical (3.8 mm in diameter) and critical (8.8 mm in diameter) size defects established in Wistar rats' calvaria [38]. New bone formation was observed in both defect sizes, with small defects being almost completely filled by 24 weeks, while large defects remained unrepaired, becoming non-unions with fibrous connective tissue in the areas in which the bone formation was absent. Radiographic analysis reported that the bone formed per week was maximal at week 4, for both defect sizes, data supported by a high expression of collagen type I and osteocalcin, by osteoblasts and osteocytes, as assessed by in situ hybridization. Moreover, collagen and osteocalcin production was very low at week 24 – for both defect sizes – suggesting that bone cells may greatly reduce bone formation and the

differentiation process of new osteoblasts may be severally impaired at this time point. In this way, the authors suggested that the bone formation process ceases within 24 weeks, regardless the dimension of the defect size and completation of defect repair [38]. The influence of the post-surgical inflammatory response on the osteogenic activity may be important to substantiate the attained data, and has been reported in several in vitro and in vivo models [39-42].

All the same, the evaluation of the CSD relies not only on the assessment of the repair of the wound size but, above all, on the quality of the regenerated tissue. This evaluation should be based on the relativity of the model, i.e. according to the specificities of the experimental protocol and time points, since the best tissue quality ought to be achieved in the shortest lapse of time. Regarding tissue quality on bone regeneration, it is wide established that fibrous connective tissue regenerates faster than bone, relying on the faster migration of fibroblasts to the wound site, comparing to osteoblasts [43-46]. Early works, in the 1970's, by Najjar et al showed that the first healing of bone wounds in animal models was set on fibrovascular connective tissue, followed by immature bone replacement , which in turn remodeled into mature bone [47]. Accordingly, one ought to attain a fast osseous healing which can prevent the establishment of undesirable results such as fibrous non-union or fibrous encapsulation of implanted materials [48, 49].

Furthermore, apart from the size of the defect, other factors determine the quantity and quality of the new bone tissue formed. For instance, the anatomical site and its stability are relevant since the load stress and the degree of mobility can have a profound effect on the final outcome [50, 51]. Other factors, proven to be relevant, include the intrinsic structure of the bone tissue, adequacy of vascular supply, involvement of the cortical bone, and presence or absence of periosteum [35, 36, 46, 52]. Animals' age is also an important point to consider in experimental planning since juvenile animals have been shown to report an increased healing capacity of calvarial defects, which may be related to differential transcriptional gene expression profiles [53-56]. Wu et al, in order to determine the CSD in neonatal mice, established circular defects of 0.8, 1.0, and 1.5 mm in diameter, in the parietal bone. Healing assessment reported statistically significant differences in bone filling percentages: 1.5 mm defects (4.49%), 1.0 mm defects (47.65%), and 0.8-mm defects (73.45%) [57]. These result output the 0.8 and 1.0mm defects as sub-critical size defects and the 1.5 mm as a CSD. In another experimental setting, Aalami et al aimed to compare the bone regeneration process in juvenile and adult mice. Non-suture associated cranial defects, with 3mm, 4mm and 5mm in diameter, established in the calvarial bone of juvenile (6-day old) and adult (60-day old) mice, were evaluated. Following 8 weeks of

healing, histological and radiographic evaluation allowed to conclude that all three defect sizes were found to be critical in the adult, whereas significant healing (59, 65 and 44%, respectively, of the total defect area) was seen in juvenile mice [53].

In rats, controversial data regarding the dimensions of CSD have been reported. Turnbull et al. described the surgical establishment of a 2mm in diameter defect, in Wistar rats' calvaria, and their incapacity to heal up to 3 months, as assessed by radiographic and histological techniques [58]. Following, Mulliken et al. reported a 4 mm CSD in Charles River rats [59]. Takagi et al. characterized the CSD as 8 mm in diameter, in 6 months Sprague Dawley rats [60] as it has been reported earlier by Ray et al for Long Evans rats [61]. Later on, Hollinger et al substantiated the 8 mm defect as the CSD for Long Evans and Walter Reed rats, reporting the inability of the defect to heal spontaneously, following 13 months, and a maximum of 10% of de novo bone formation [35, 36].

Other bibliographic reports have acknowledged the 5mm defect as a CSD for adult rats. Bosh et al reported that a 5 mm defect, apart from minor bone formation on the defects' margins, was unable to heal spontaneously up to 12 months after the surgery [62]. The stated advantages of the use of 5mm CSD include the possibility to establish 2 defects per animal, and the avoidance of the inclusion of the sagittal suture in the defect, minimizing the risk of midsagittal sinus lesion [62]. On the other hand, laterally performed craniotomies – opposing those which include the sagittal suture, like in the 8mm defect – may allow substance diffusion and impair local repair/regeneration, due to the close vicinity of adjacent defects, which may blight the relevance of the model [63]. Accordingly, the 8mm defect continues to be used in many reports aiming to assess different bone therapeutic strategies. This is established not only for the described limitations of the 5mm CSD design, but also due to the increased challenge associated with the higher diameter of the defect.

Apart from the need to establish a CSD, with an increased challenge for the regenerative process, sub-critical size calvarial defects allow to evaluate the impact that a wide range of conditions, biological processes or added substances have on the physiological equilibrium of the bone tissue regeneration, through an intramembranous ossification process. Specifically, sub-critical size calvarial defects have been generally used to evaluate the biological response of the bone regeneration process following the establishment of pathological conditions [64, 65], within the evaluation of therapeutic options to enhance bone regeneration [66, 67] and optimization of hard tissues-related surgical techniques [68, 69]. In mice, 1 mm diameter defects have been routinely used as sub-critical size defects due to the fast healing – normally complete around 14 days – allowing the determination of stimulatory or inhibitory effects of locally or systemically

applied substances. In rats, defects created with 3 mm trephines, or less, have found generalized application as standardized sub-critical size defects.

These surgical procedures, due to the technique-dependent and sensitive applied protocol, as well as the significance of the anatomical neighboring structures, should be conducted by clinical professionals with surgical expertise, following an adequate training period. Additionally, due to the expected amount of pain induced by the orthopedic procedure, a local anesthetic should be used in conjunction with a general anesthetic, as well as an appropriate regimen of post-operative analgesia.

Following we describe a refined surgical protocol for the establishment of CSD and sub-critical size defects in Wistar rats' calvarial bone, for the evaluation of the biocompatibility of a ceramic granular material.

Establishment of calvarial critical size and subcritical size defects on rodents

The animals – male Wistar rats with 3 months, weighing between 260-280g – were purchased from Charles River Laboratories. National regulations for the care and use of laboratory animals were observed at all times. All experiments were approved by the local IACUC. Animals were housed in plastic cages in a monitored environment (21°C; 12h light/dark cycle).

Anaesthesia and pain control followed recommended routines for the species. Prior to the surgical intervention, the animals were anesthetized using sevoflurane inhalation anesthesia (4% to 5% induction; 2% to 3% maintenance). Following, the skin that covered the skull, around the incision area, was shaved and disinfected with iodopovidone solution. An intraperitoneal injection of tramadol (10 mg/kg) for post-operative analgesia was given, and the animals were then transferred onto a heating pad, maintained at 37 °C, in the operating field. A subcutaneous injection of 0.3-0.4 mL of 1% lidocaine, used as a local anesthetic, was administered along the sagittal midline of the skull. Following, a surgical blade was used to perform a midline incision, from the nasofrontal area to an anterior location of the external occipital protuberance (Figure 1A). The skin was then reflected bilaterally and a new midline incision, of around 3 cm, allowed the division of the subcutaneous fascia and the bilateral reflection of the periosteal flaps following blunt dissection, to expose the calvarial bone surface (Figure 1B-D). Careful drilling with an 8 mm diameter trephine bur, mounted on a low-speed dental handpiece, was done around the sagittal suture, and a standardized, round, segmental defect was made. During drilling, the area was continuously irrigated with sterile saline solution and extreme care was taken not to damage the dura mater or the underlying blood vessels and sinus (Figure 1E-F). The obtained calvarial disk was carefully removed to avoid tearing of the subjacent cranial structures (Figure 1G). After

thoroughly rinsing of the defect with physiological saline, to wash out any bone fragments, the material in the granular form – a modified hydroxyapatite – was implanted within the defect (Figure 1H-I). The periosteum and scalp were closed over in layers with interrupted 4-0 Vicryl resorbable sutures (Figure 1J-K). Following surgical intervention, the animals were given a subcutaneous injection of sterile saline (10 mL/kg/hr of surgery). The rats were placed into soft-bedded plastic cages and housed individually after the procedure. Each animal received a subcutaneous injection of tramadol (10 mg/kg) at 12, 24, and 36 hours after surgery for continued post-operative analgesia. Animals were given free access to food and water and were monitored daily, in the post-operative period until euthanasia, for any complications or abnormal behavior.

Alternatively, the establishment of sub-critical calvarial defects, in rats, can be carried out with the use of 3 mm trephines or less in diameter, allowing the establishment of multiple defects in the calvarial bone (Figure 1L).
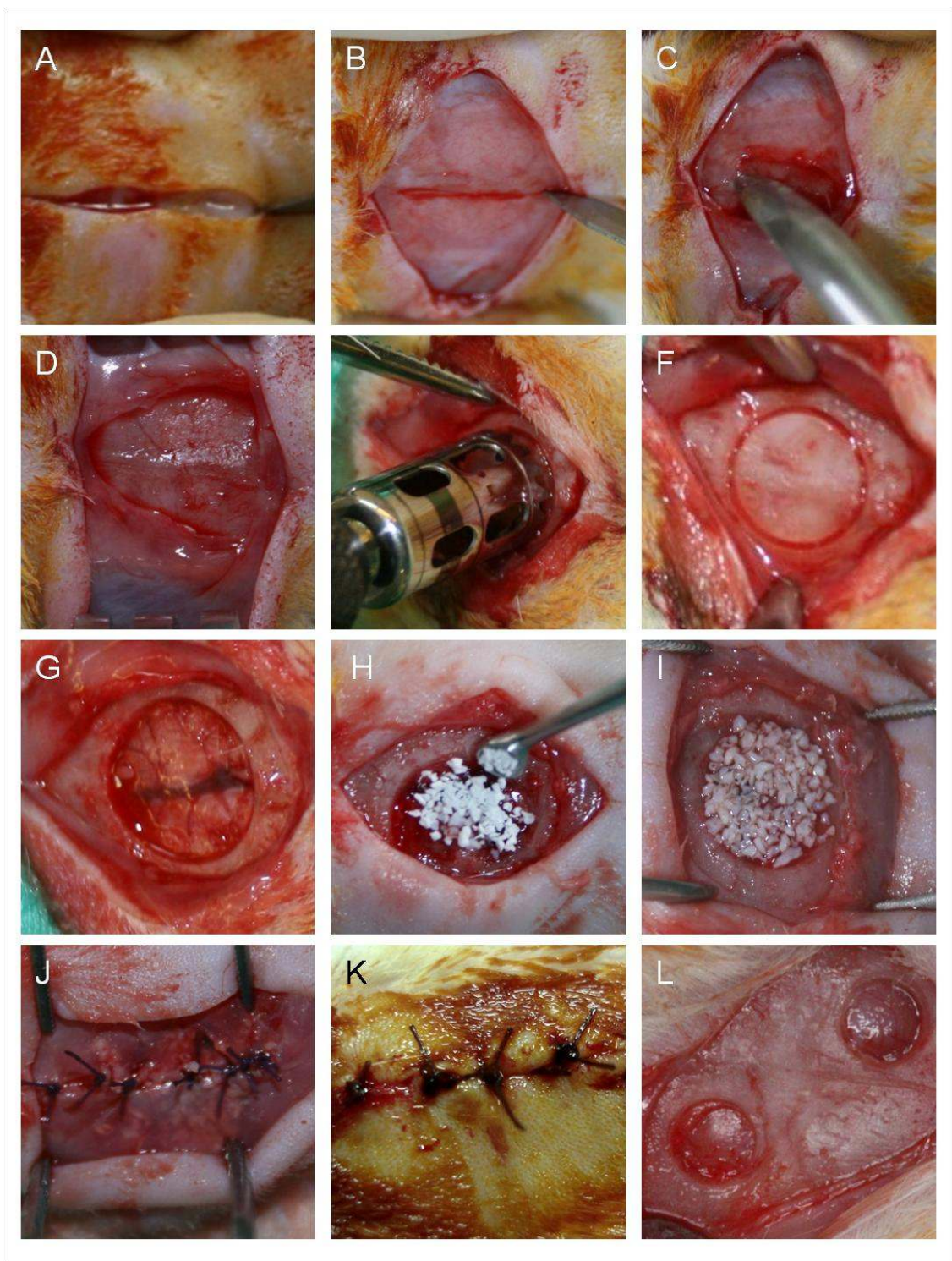
Figure 1 – Surgical protocol for the establishment of critical size defects (A-K) and subcritical size defects (L), on rat calvarial bone.

Evaluation methodologies of the bone regeneration process

The assessment of the bone regeneration process can be carried out by reaching hand of multiple and complementary methodologies. Histological analysis, electron microscopy and radiological techniques are among the most commonly used. As follows, the authors described the most relevant techniques used with given examples from their personal experience.

Histological evaluation

Characterization of the regenerated bone tissue is commonly performed by histological evaluation with light microscopy, following standard dying of the sample. Descriptive histology and histomorphometry are the two major classes of histological evaluation. Descriptive histology is used to provide a general assessment of the tissue of interest, giving data regarding cell morphology, structure and arrangement within the interface with the extracellular matrix or with an implanted material. Semi-quantitative analysis could be performed using a score system, in which the data can be evaluated using nonparametric analysis of variance. Histomorphometry allows quantitative analysis of histological data, namely regarding length and distance, area and number of the components of interest [29, 70]. These are the basic parameters which can be assessed in two-dimensional histomorphometric analysis. Three-dimensional evaluation can be conducted from two-dimensional sampled images following specific considered assumptions. Due to the use of multiple designations and misinterpretations in histomorphometric analysis, a consensus report aimed to establish a system for standardization of nomenclature, symbols, and units, and has generally been adopted [71]. Despite the aim to perform a reproducible analysis in the evaluation of the attained results, histological observation is lined by significant inter-method and inter-observer variability, especially in which regards histomorphometric analysis [72].

Bone tissue can also be labeled in vivo with intravital markers, in order to assess the quantitative evaluation of bone formation and remodeling events [73]. Used fluorochromes are irreversibly deposited and rely on their calcium-binding properties to be embedded into the mineralization fronts of the remodeling bone [73]. Prepared samples can be visualized under fluorescent light. Specific binding to newly mineralizing surfaces of mineralized tissues may be due to the smaller size of the apatite crystals formed during the early stages of the mineralization process, compared with older mineralizing sites [74, 75]. The most commonly used fluorochromes are tetracycline, calcein dyes, alizarins and xylenol [76].

Immunohistochemistry (IHC), by a direct or indirect technique, could also be used to identify and specifically localize peptides or proteins of interest in bone tissue section, based on the principle of the specific interaction between antibodies and antigens [77]. In order to improve reproducibility and standardization of the data attained with IHC, quantitative methodologies have been developed, relying upon pixel-counting and cumulative signal strength algorithms [78, 79].

As an example, on Figure 2, representative images of some of the depicted techniques are shown.
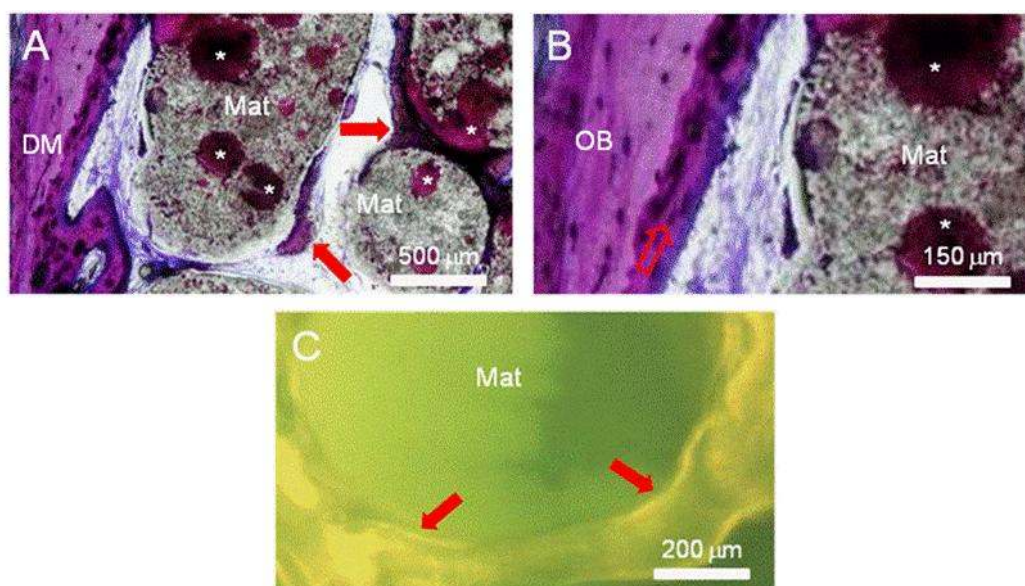

Figure 2 –Images of non-decalcified resin-embedded calvarial samples, following the surgical establishment of an 8 mm CSD on rat calvarial bone and the implantation of a ceramic material. Figure 2A and 2B are stained with toluidine blue, 15 days following implantation. Figure 2C shows a tetracycline-stained sample, 3 months following material implantation. Mat – pellets of the implanted material; DM – defect margin; Arrows – areas of new bone formation; OB – old bone; * - areas of primary ossification.

Electron microscopy

Scanning electron microscopy (SEM) is also an important tool used on the evaluation of the structure and morphology of the bone tissue. In biomedical bone-related research, it has been used to characterize trabecular and cortical bone surfaces, implant surfaces, wear debris, implant beds and implant-tissue interfaces [80-82]. With the use of corrosion-cast tissues, SEM has been able to assess the vascular structure in the evaluated tissues – which is of the utmost importance for the development and maintenance of an adequate bone tissue quality [83, 84]. Major

limitations associated with SEM application are related to the relative small size of the evaluated samples and the need for drying the specimen for observation, which has been shown to induce modifications in morphology and spatial structure of the tissues [85]. New technologies have allowed the development of low-temperature or cryo-SEM, and environmental SEM systems, which aim to solve the dehydration-related problems [80].

As an example, on Figure 3, images of rat calvaria specimens assessed by environmental SEM are portrayed.
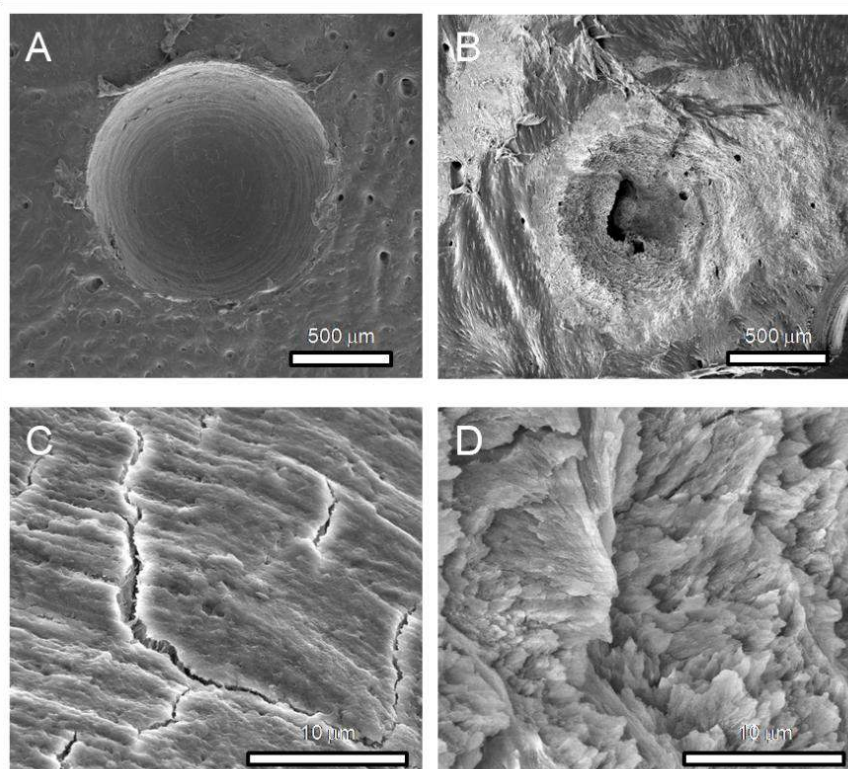

Figure 3 – Micrographs of rat calvaria assessed by environmental SEM, 3 days following the establishment of sub-critical monocortical defects, are presented. The defects were established with a 1mm diameter burr (A and C) and with a high-intensity Erb:YAG laser (B and D). Figures 3C and 3D are detailed high magnification images of Figures 3A and 3B, respectively.

Electron microscopy techniques also make use of transmission methodologies – TEM, transmission electron microscopy – in which a beam of electrons is transmitted through an ultra thin specimen, interacting with the specimen as it passes through. This is a very powerful methodology to evaluate the ultrastructure and morphology of subcellular components, cells and tissue-biomaterial interaction [86-88]. Nevertheless the very high resolution, samples require extensive sample preparation and the field of view is relatively small, raising the possibility that the analyzed region may not be

characteristic of the whole sample. Additionally, samples may suffer modifications from the preparation process or directly damaged by the electron beam [87, 88].

Illustrating this application, two images of ceramic-based materials' debris interacting with rat calvarial osteoblastic cells, are shown on Figure 4.
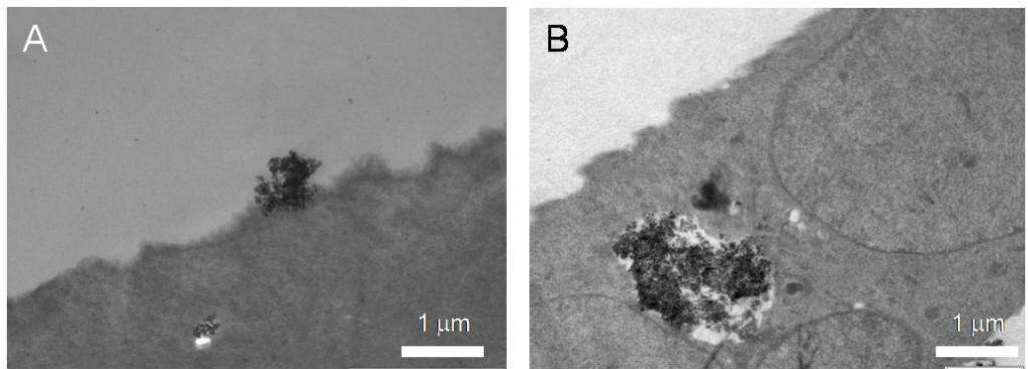

Figure 4 –Transmission electron micrographs of ceramic-derived material debris interacting with osteoblastic cells from rat calvarial bone.

Radiological techniques

Radiologic techniques have also been employed with success in the evaluation of the bone repair and regeneration processes. Radiography is the basic method for the evaluation of fracture healing and bone-defect repair. In clinical or experimental settings, pre-surgical evaluation allows the assessment of the specific anatomy and bone dimensions, facilitating the selection of fixation devices and implants. Post-operative evaluation also benefits from the radiographic assessment allowing the determination of the fracture placement or the quality of the defect fill. Periodic evaluation permits the monitoring of the repair process. High-resolution radiography and microradiography are complementary techniques that allow the evaluation of the detailed structure of the bone tissue. Quantification of bone aposition and densitometric analysis can be conducted, even in the neighboring of an implant [89].

Sample radiographic images of the rat calvarial bone, with or without a grafted material, are shown on Figure 5.
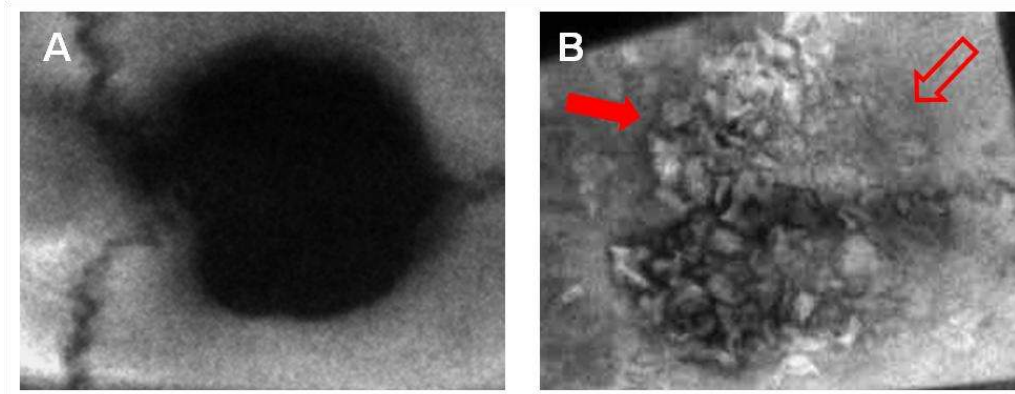
Figure 5 – Radiographic images of the rat calvarial bone, without (Fig. 5A) or with (Fig. 5B) a grafted ceramic material, 6 months following the surgical establishment of an 8 mm CSD. Areas of newly formed bone following material resorption (open arrow) can be identified, simultaneously with areas of implanted biomaterial content, interspersed with the newly formed bone tissue (full arrow).

X-ray computed microtomography (µCT) is a miniaturized form of conventional computerized axial tomography (CAT) that has been found to be a valuable application in bone-related research. This technology enables 3D reconstruction of the internal structure of small X-ray opaque objects in a noninvasive and non destructive way. µCT allows to qualitatively and quantitatively assess the spatial and temporal mineralization of bone formation. The availability of 3D analysis techniques, coupled to specific image processing methods opens up new possibilities for the analysis of bone structures [90, 91]. Recent reports outline the use of µCT for the monitorization of the in vivo bone remodeling process [92].

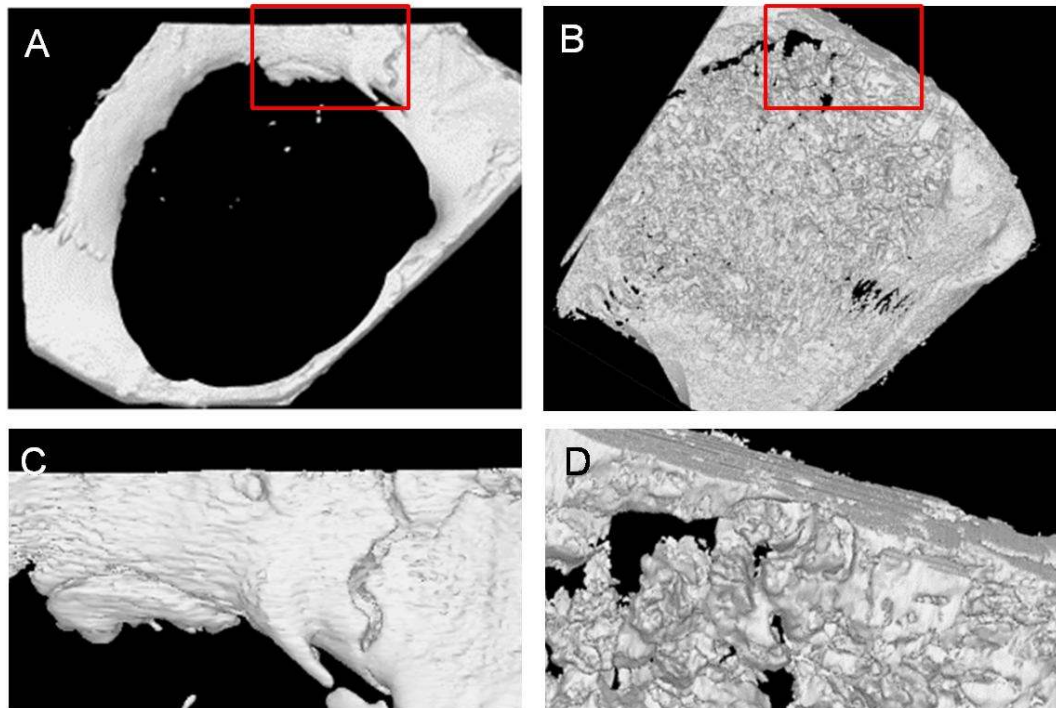On Figure 6, µCT-reconstructed 3D images of rat calvarial bone are shown.

Figure 6 – µCT-reconstructed 3D images of rat calvarial bone, 3 months following the establishment of a 8 mm CSD, without (Fig. 6A and 6C) and with the implantation of a ceramic material (Fig. 6B and 6D). Figures 6C and 6D are detailed high magnification images of Figures 6A and 6B, respectively.

Conclusion

Animal models play an important role in bone tissue-related research by providing methodological approaches to study detailed events and regenerative advances, which aim to establish adequate translational applications with clinical relevance. While no species fulfils the requirements of an ideal animal model, rodents reach out as easily available, easy to house and handle, and account for a high amount of background data due to the widespread use in the reported literature. Furthermore, the described models established on rodents calvarial bone allow the establishment of a standardized, reproducible orthotopic defect which permits not only the evaluation of the biocompatibility of implanted biomaterials or tissue engineering constructs, but also the assessment of the intramembranous ossification process in physiological and pathological conditions. Multiple methodologies, including histological analysis, electron microscopy and radiological techniques have reported relevant and complementary data, with proven adequacy, in the assessment of bone repair/regeneration process.

References

1. Perry C. Bone repair techniques, bone graft, and bone graft substitutes. Clin Orthop Res 1999;360:71-86.

2. Burg K, Porter S, Kellam J. Biomaterial developments for bone tissue engineering. Biomaterials 2000;21:2347-2359.

3. Giannoudis P, Pountos I. Tissue regeneration. The past, the present and the future. Injury 2005;36 (Suppl. 4):S2-S5.

4. Raisz L. Physiology and pathophysiology of bone remodeling. Clin Chem 1999;45:1353-1358.

5. Lu H, Kraut D, Gerstenfeld L, Graves D. Diabetes interferes with the bone formation by affecting the expression of transcription factors that regulate osteoblast differentiation. Endocrinology 2003;144:346-352.

6. Quarto R, Thomas D, Liang C. Bone progenitor cell deficits and the age-associated decline in bone repair capacity. Calcif Tissue Int 1995;56:123-129.

7. Muschler G, Raut V, Patterson T, Wenke J, Hollinger J. The design and use of animal models for translational research in bone tissue engineering and regenerative medicine. Tissue Eng Part B 2010;16:123-145.

8. Kirkpatrick C, Bittinger F, Wagner M, Köhler H, van Kooten T, Klein C, et al. Current trends in biocompatibility testing. Proc Inst Mech Eng H 1998;212:75-84.

9. Schoonen W, Westerink W, Horbach G. High-throughput screening for analysis of in vitro toxicity. EXC 2009;99:401-452.

10. Kirkpatrick J, Fuchs S, Hermanns I, Peters K, Unger R. Cell culture models of higher complexity in tissue engineering and regenerative medicine. Biomaterials 2007;28:5193-5198.

11. Yu X, Botchwey E, Levine E, Pollack S, Laurencin C. Bioreactor-based bone tissue engineering: the influence of dynamic flow on osteoblast phenotypic expression and matrix mineralization. Proc Natl Acad Sci U S A 2004;101:11203-11208.

12. Muschler G, Nakamoto C, Griffith L. Engineering principles of clinical cell-based tissue engineering. J Bone Joint Surg Am 2004;86-A:1541-1558.

13. Bruder S, Fox B. Tissue engineering of bone. Cell based strategies. Clin Orthop Relat Res 1999;367 Suppl:S68-83.

14. Cancedda R, Dozin B, Giannoni P, Quarto R. Tissue engineering and cell therapy of cartilage and bone. Matrix Biol 2003;22:81-91.

15. Reddi A. Morphogenesis and tissue engineering of bone and cartilage: inductive signals, stem cells, and biomimetic biomaterials. Tissue Eng 2000;6:351-359.

16. Hutmacher D. Scaffolds in tissue engineering bone and cartilage. Biomaterials 2000;21:2529-2543.

17. Boden S. Bioactive factors for bone tissue engineering. Clin Orthop Relat Res 1999;367 Suppl:S84-94.

18. Canalis E, McCarthy T, Centrella M. Growth factors and the regulation of bone remodeling. J Clin Invest 1988;81:277-281.

19. O'Loughlin P, Morr S, Bogunovic L, Kim A, Park B, Lane J. Selection and development of preclinical models in fracture-healing research. J Bone Joint Surg Am 2008;90 Suppl 1:79-94.

20. Waterston R, Lindblad-Toh K, Birney E, Rogers J, Abril J, Agarwal P, et al. Initial sequencing and comparative analysis of the mouse genome. Nature 2002;420:520-562.

21. Gibbs R, Weinstock G, Metzker M, Muzny D, Sodergren E, Scherer S, et al. Genome sequence of the Brown Norway rat yields insights into mammalian evolution. Nature 2004;428:493-521.

22. Bockamp E, Maringer M, Spangenberg C, Fees S, Fraser S, Eshkind L, et al. Of mice and models: improved animal models for biomedical research. Physiol Genomics 2002;11:115-132.

23. Filipiak W, Saunders T. Advances in transgenic rat production. Transgenic Res 2006;15:673-686.

24. Pearce A, Richards R, Milz S, Schneider E, Pearce S. Animal models for implant biomaterial research in bone: a review. Eur Cell Mater 2007;13:1-10.

25. Reinwald S, Burr D. Review of nonprimate, large animal models for osteoporosis research. J Bone Miner Res 2008;23:1353–1368.

26. Aspenberg P, Wang E, Thorngren K. Bone morphogenetic protein induces bone in the squirrel monkey, but bone matrix does not. Acta Orthop Scand 1992;63:619-622.

27. Giannobile W, Finkelman R, Lynch S. Comparison of canine and non-human primate animal models for periodontal regenerative therapy: results following a single administration of PDGF/IGF-I. J Periodontol 1994;65:1158-1168.

28. Barnes B, Boden S, Louis-Ugbo J, Tomak P, Park J, Park M, et al. Lower dose of rhBMP-2 achieves spine fusion when combined with an osteoconductive bulking agent in non-human primates. Spine 2005;15:1127-1133.

29. Vignery A, Baron R. Dynamic histomorphometry of alveolar bone remodeling in the adult rat. Anat Rec 1980;196:191-200.

30. Erben R. Trabecular and endocortical bone surfaces in the rat: modeling or remodeling? Anat Rec 1996;246:39-46.

31. Edwards J, Diegmann M, Scarborough N. Osteoinduction of human demineralized bone: characterization in a rat model. Clin Orthop Relat Res 1998;357:219-228.

32. An Y, Friedman R. Animal Models of Bone Defect Repair. In: An Y, Friedman R, editors. Animal Models in Orthopaedic Research. Boca Raton: CRC Press, Inc, 1999. p. 241-260.

33. Glowacki J. A review of osteoinductive testing methods and sterilization processes for demineralized bone. Cell Tissue Bank 2005;6:3-12.

34. Salgado A, Coutinho O, Reis R. Bone tissue engineering: state of the art and future trends. Macromol Biosci 2004;4:743-765.

35. Schmitz J, Hollinger J. The critical size defect as an experimental model for craniomandibulofacial nonunions. Clin Orthop Relat Res 1986;205:299-308.

36. Hollinger J, Kleinschmidt J. The critical size defect as an experimental model to test bone repair materials. J Craniofacial Surg 1990;1:60-68.

37. Liebschner M. Biomechanical considerations of animal models used in tissue engineering of bone. Biomaterials 2004;25:1697-1714.

38. Honma T, Itagaki T, Nakamura M, Kamakura S, Takahashi I, Echigo S, et al. Bone formation in rat calvaria ceases within a limited period regardless of completion of defect repair. Oral Diseases 2008;14:457-464.

39. Rifas L, Arackal S, Weitzmann M. Inflammatory T cells rapidly induce differentiation of human bone marrow stromal cells into mature osteoblasts. J Cell Biochem 2003;88:650-659.

40. Shen F, Ruddy M, Plamondon P, Gaffen S. Cytokines link osteoblasts and inflammation: microarray analysis of interleukin-17- and TNF-alpha-induced genes in bone cells. J Leukoc Biol 2005;77:388-399.

41. Aikawa E, Nahrendorf, Figueiredo J, Swirski F, Shtatland T, Kohler H, et al. Osteogenesis associates with inflammation in early-stage atherosclerosis evaluated by molecular imaging in vivo. Circulation 2007;116:2841-2850.

42. Harder A, An Y. The mechanisms of the inhibitory effects of nonsteroidal anti-inflammatory drugs on bone healing: a concise review. J Clin Pharmacol 2003;43:807-815.

43. Mundell R, Mooney M, Siegel M, Losken A. Osseous guided tissue regeneration using a collagen barrier membrane. J Oral Maxillofac Surg 1993;51:1004-1012.

44. Stetzer K, Cooper G, Gassner R, Kapucu R, Mundell R, Mooney M. Effects of fixation type and guided tissue regeneration on maxillary osteotomy healing in rabbits. J Oral Maxillofac Surg 2002;60:436-437.

45. Dahlin C, Linde A, Gottlow J, Nyman S. Healing of bone defects by guided tissue regeneration. Plast Reconstr Surg 1988;81:672-676.

46. Aaboe M, Pinholt E, Hjørting-Hansen E. Healing of experimentally created defects: a review. Br J Oral Maxillofac Surg 1995;33:312-318.

47. Najjar T, Kahn D. Comparative study of healing and remodeling in various bones. J Oral Surg 1977;35:375-379.

48. Dahlin C, Sandberg E, Alberius P, Linde A. Restoration of mandibular nonunion bone defects. An experimental study in rats using an osteopromotive membrane method. Int J Oral Maxillofac Surg 1994;23:237-242.

49. Heiple K, Chase S, Heendon C. A comparative study of the healing process following different types of bone transplantation J Bone Joint Surg Am 1963;45:1593-1616.

50. Friedenberg Z, Lawrence R. The regeneration of bone in defects of varying size. Surg Gynecol Obstet 1962;113:721-726.

51. Carter D, Beaupré G, Giori N, Helms J. Mechanobiology of skeletal regeneration. Clin Orthop Relat Res 1998;355 Suppl:S41-55.

52. Frame J. A convenient animal model for testing bone substitute materials. J Oral Surg 1980;38:176-180.

53. Aalami OO, Nacamuli RP, Lenton KA, Cowan CM, Fang TD, Fong KD, et al. Applications of a Mouse Model of Calvarial Healing: Differences in Regenerative Abilities of Juveniles and Adults. Plastic and Reconstructive Surgery 2004;114:713-720.

54. Aalami O, Nacamuli R, Salim A, Fong K, Lenton K, Song H, et al. Differential transcriptional expression profiles of juvenile and adult calvarial bone. Plast Reconstr Surg 2005;115:1986-1994.

55. Wan D, Kwan M, Gupta D, Wang Z, Slater B, Panetta N, et al. Global age-dependent differences in gene expression in response to calvarial injury. J Craniofac Surg 2008;19:1292-1301.

56. Meyer Jr R, Tsahakis P, Martin D, Banks D, Harrow M, Kiebzak G. Age and ovariectomy impair both the normalization of mechanical properties and the accretion of mineral by the fracture callus in rats. J Orthop Res 2001;19:428-435.

57. Wu X, Downes S, Watts D. Evaluation of critical size defects of mouse calvarial bone: An organ culture study. Microsc Res Tech 2010;73:540-547.

58. Turnbull R, Freeman E. Use of wounds in the parietal bone of rat for evaluating bone marrow for grafting into periodontal defects. J Periodont Res 1974;9:39.

59. Mulliken J, Glowacki J. Induced osteogenesis for repair and construction in the craniofacial region. Plast Reconstr Surg 1980;65:553-560.

60. Takagi K, Urist M. The reaction of the dura to bone morphogenetic protein (BMP) in repair of skull defects. Ann Surg 1982;196:100–109.

61. Ray R, Holloway J. Bone Implants: Preliminary Report of an Experimental Study. J Bone Joint Surg Am 1957;39:1119-1128.

62. Bosch C, Melsen B, Vargervik K. Importance of the critical-size bone defect in testing bone-regenerating materials. J Craniofac Surg 1998;9:310-6.

63. Viateau V, Logeart- Avramoglou D, Guillemin G, Petite H. Animal Models for Bone Tissue Engineering Purposes. In: Conn P, editor. Sourcebook of Models for Biomedical Research: Humana Press, 2008.

64. Santana R, L X, Chase H, Amar S, Graves D, Trackman P. A Role for Advanced Glycation End Products in Diminished Bone Healing in Type 1 Diabetes Diabetes 2003;52:1502-1510.

65. Shyng Y, Devlin H, Sloan P. The effect of streptozotocin-induced experimental diabetes mellitus on calvarial defect healing and bone turnover in the rat Int J Oral Maxillofac Surg 2002;30:70-74.

66. Khadra M, Kasem N, Haanaes H, Ellingsen J, Lyngstadaas S. Enhancement of bone formation in rat calvarial bone defects using low-level laser therapy. Oral Surg Oral Med Oral Pathol Oral Radiol Endod 2004;97:693-700.

67. Aghaloo T, Cowan C, Chou Y-F, Zhang X, Lee H, Miao S, et al. Nell-1-Induced Bone Regeneration in Calvarial Defects. Am J Pathol 2006;169:903–915.

68. Pourzarandian A, Watanabe H, Aoki A, Ichinose S, Sasaki K, Nitta H, et al. Histological and TEM examination of early stages of bone healing after Er:YAG laser irradiation. Photomed Laser Surg 2004;22:342-350.

69. Yoshino T, Aoki A, Oda S, Takasaki A, Mizutani K, Sasaki K, et al. Long-term histologic analysis of bone tissue alteration and healing following Er:YAG laser irradiation compared to electrosurgery. J Periontol 2009;80:82-92.

70. Parfitt A, Drezner M, Glorieux F, Kanis J, Malluche H, Meunier P, et al. Bone histomorphometry: standardization of nomenclature, symbols and units. Report of the ASBMR Histomorphometry Nomenclature Committee. J Bone Miner Res 1987;2:595-610.

71. Parfitt A. Bone histomorphometry: proposed system for standardization of nomenclature, symbols, and units. Calcif Tissue Int 1988;42:284-286.

72. Wright C, Vedi S, Garrahan N, Stanton M, Duffy S, Compston J. Combined inter-observer and inter-method variation in bone histomorphometry. Bone 1992;13:205-208.

73. Aaron J, Makins N, Francis R, Peacock M. Staining of the calcification front in human bone using contrasting fluorochromes in vitro. J Histochem Cytochem 1984;32:1251-1261.

74. Frost H. Tetracycline-based histological analysis of bone remodeling. Calcif Tissue Int 1969;3:211-237.

75. Tam C, Anderson W. Tetracycline labeling of bone in vivo. Calcif Tissue Int 1980;30:121-125.

76. Sun T, Mori S, Roper J, Brown C, Hooser T, Burr D. Do different fluorochrome labels give equivalent histomorphometric information? Bone 1992;13:443-446.

77. Yang R, Davies C, Archer C, Richards R. Immunohistochemistry of matrix markers in Technovit 9100 New®-embedded undecalcified bone sections Eur Cell Mater 2003;6:57-71.

78. Cregger M, Berger A, Rimm D. Immunohistochemistry and quantitative analysis of protein expression. Arch Pathol Lab Med 2006;130:1026-1030.

79. Rojo M, Bueno G, Slodkowska J. Review of imaging solutions for integrated quantitative immunohistochemistry in the Pathology daily practice. Folia Histochem Cytobiol 2009;47:349-354.

80. Boyde A, Jones S. Scanning electron microscopy of bone: instrument, specimen, and issues. Microsc Res Tech 1996;33:92-120.

81. Tracy B, Doremus R. Direct electron microscopy studies of the bone - hydroxylapatite interface. J Biomed Mater Res 1984;18:719-726.

82. Neo M, Kotani S, Fujita Y, Nakamura T, Yamamuro T, Bando Y, et al. Differences in ceramic-bone interface between surface-active ceramics and resorbable ceramics: a study by scanning and transmission electron microscopy. J Biomed Mater Res 1992;26:255-267.

83. McDonald D, Choyke P. Imaging of angiogenesis: from microscope to clinic. Nat Med 2003;9:713-725.

84. Kanczler J, Oreffo R. Osteogenesis and angiogenesis: the potential for engineering bone. Eur Cell Mater 2008;15:100-114.

85. Tran Van P, Vignery A, Baron R. An electron-microscopic study of the bone-remodeling sequence in the rat. Cell Tissue Res 1982;225:283-292.

86. Rubin M, Jasiuk I, Taylor J, Rubin J, Ganey T, Apkarian R. TEM analysis of the nanostructure of normal and osteoporotic human trabecular bone. Bone 2003;33:270-282.

87. Bakker D, van Blitterswijk C, Hesseling S, Daems W, Grote J. Tissue/biomaterial interface characteristics of four elastomers. A transmission electron microscopical study. J Biomed Mater Res 1990;24:277-293.

88. Daculsi G, LeGeros R, Deudon C. Scanning and transmission electron microscopy, and electron probe analysis of the interface between implants and host bone. Osseo-coalescence versus osseo-integration. Scanning Microsc 1990;4:309-314.

89. Schortinghuis J, Ruben J, Meijer H, AL B, Raghoebar G, Stegenga B. Microradiography to evaluate bone growth into a rat mandibular defect. Arch Oral Biol 2003;48:155-160.

90. Rüegsegger P, Koller B, Müller R. A microtomographic system for the nondestructive evaluation of bone architecture. Calcif Tissue Int 1996;58:24-29.

91. Stock S, Ignatiev K, Foster S, Forman L, Stern P. MicroCT quantification of in vitro bone resorption of neonatal murine calvaria exposed to IL-1 or PTH. J Struct Biol 2004;147:185-199.

92. Waarsing J, Day J, van der Linden J, Ederveen A, Spanjers C, De Clerck N, et al. Detecting and tracking local changes in the tibiae of individual rats: a novel method to analyse longitudinal in vivo micro-CT data. Bone 2004;34:163-169.

Chapter 11

Concluding remarks

The adequacy and success of any material in the biological milieu is defined by its reaction to and from the surrounding environment. In this framework, apart from wide accepted generalizations, there is no specific universal consensus regarding the definition of biomaterial, or even strict directives for its biocompatibility assessment. Nonetheless, biocompatibility remains the central theme concerning the clinical application of biomaterials, and it is generally accepted that this term reflects not only the mere absence of cytotoxic effects, but also embraces a positive action in the sense of biofunctionality, i.e. the promotion of biological processes which further extend the intended aim of the application of a biomaterial.

The national and international standards for testing regimes represent a lowest common denominator for such applications and do not necessarily ensure that optimal function is expected to be achieved. The most popular and accepted series of standards in this area are depicted in ISO 10993: Biological evaluation of medical devices, and address the issue of biocompatibility by categorizing the materials based on the nature and estimate duration of contact with the organism. Local and systemic reactions, acute or chronic effects during contact with tissues or blood, delayed sensitization reactions, potential of the material to elicit chromosomal aberrations, carcinogenic potential, etc. are of particular interest while designing and conducting qualification studies. Both *in vitro* and *in vivo* testing is addressed in ISO 10993, in order to evaluate local and systemic reactions. Hence, no individual test can be used for ascertaining the biocompatibility of a material and a material cannot be categorically stated as broadly biocompatible; on the other hand, it can be inferred, through a series of properly selected qualification studies, that a material is suitable for use in a specific application.

An obvious first step approach regarding *in vitro* biomaterial biological testing embraces the *general cytocompatibility* evaluation and usually involves the use of various cell lines which can be easily cultivated and passaged in the laboratory for long periods. Within the scope of this thesis, reported examples are shown in chapters 2 to 5, based on the use of human fibroblastic or osteoblastic-like cell lines with a wide variety of candidate materials, including ceramics, composites and surface-modified materials. A generic approach to the biological behaviour of candidate materials is possible and allows the detection of cytotoxic and/or mutagenic compounds in direct or indirect culture systems. As portrayed, used cultures allow for the assessment of cell adhesion, cell morphology, cell viability/proliferation, as well as the expression of generic cellular markers, parameters that can all be compared to the ones verified on cultures grown in standard control conditions, usually on the surface of the culture plate. This characterization methodology seems to be convenient and highly sensitive

for recognizing and exclude broadly cytotoxic materials at an early stage in the testing process. Nonetheless, these methods cannot be regarded as exhaustive and definitive regarding the *in vitro* cytocompatibility evaluation and it is proposed that such screening methodologies be followed by a second *in vitro* phase, in which the *specific cytocompatibility* assessment is conducted. In this stage, the material response to primary or early passaged cells of a type relevant to the proposed application of the medical device is thoroughly characterized. Accordingly, in chapters 4 to 9, this evaluation phase is exemplified within a wide range of materials. In the illustrated examples, human fibroblastic, osteoblastic and endothelial cells were cultured in direct contact with the testing materials and evaluated regarding broadly cell functions e.g., cell adhesion, viability and proliferation, and most of all, markers of functionality and expression of the specific phenotype. The later included the evaluation of, for osteoblasts, the expression of alkaline phosphatase, the gene/protein expression associated with the osteogenic commitment, and the formation of a mineralized extracellular matrix; and for endothelial cells, the formation of multicellular cord-like structures in pro-angiogenic conditions, and the expression of genes or proteins associated with the specific phenotype. The *in vitro* cytocompatibility evaluation is an attempt to simulate the *in vivo* situation as closely as possible, by selecting cell populations most likely to modulate the behaviour of implanted materials. In the case of materials aiming to perform in close contact with the bone tissue, osteoblasts and endothelial cells are of the upmost relevance within the bone regeneration, since they contribute directly and indirectly to the osteogenic and angiogenic processes.

In the described biological systems it is thus possible to assemble a spectrum of *in vitro* changes, ranging from inhibition of growth with truthful cell death or inadequate expression of cell markers (cytotoxic materials), to stimulation of cell proliferation and/or other cell biological parameters (cytocompatible materials with eventual bioactivity). An expansion of *in vitro* testing methods can offer a methodology to tailor biomaterials, but does not eliminate the need to address the candidate biomaterial/tissue engineering construct in an *in vivo* biological system.

Animal models are essential for evaluating biocompatibility, tissue response and mechanical function of candidate materials, prior to clinical use in human trials. Animal models allow the evaluation of materials in loaded or unloaded situations, over a wide range of time frames, ages, and in different biological constrains (e.g. healthy/physiological tissues or within pathological conditions). Moreover, not only tissues in the immediate vicinity of the implant can be assessed, but also tissues in remote locations, which is of particular relevance within the study of wear particle debris or degradable implants.

While animal models may closely represent the mechanical and physiological conditions of the clinical situation, it must be remembered that it is only an estimated approximation, with each model having unique advantages and disadvantages. Currently there are numerous models for testing implant materials *in vivo*, ranging in purpose from the assessment of orthotopic cellular behaviour and soft tissue adherence, to the osseointegration process and the dissemination of implant wear particles. A wide range of animal species and specific orthotopic models have been developed but currently, rodents reach out as easily available, easy to house and handle, and account for a high amount of background data due to the extensive use in the reported literature. These conditions broadly facilitate the widespread selection of these animals for bone related basic and translational research. In chapter 10, the rodents' calvarial defect model is discussed regarding the evaluation of the biocompatibility of implanted biomaterials or tissue engineering constructs, and also regarding the assessment of the intramembranous ossification process in physiological and pathological conditions. Critical appraisal is given to the choice of critical size *vs* non-critical size defects, and several methodologies to address the bone regeneration process are discussed.

Overall, researchers working in bone tissue regeneration field are faced with highly complex biological systems that output a large amount of extremely intricate and multidisciplinary data that need adequate processing in order to output reliable and valuable information. From the biological point of view, recent advances have contributed to shed a new light into the development of investigative research tools, and in the understanding of the mechanisms involved in cell and tissue cross-talk with biomaterials, during bone regeneration. At the same time, material development (in regards to design and fabrication methodologies) have become increasingly sophisticated. The greatest challenge that has emerged as the result of the synergic multidisciplinary approach is the exponential increase of possibilities that have to be tested and validated. Trustworthy and effective paths have to be carefully considered in order to evaluate the increasing number of potential materials aiming human contact. High-throughput screening technologies can be combined with biological systems for rapid evaluation of cellular effects caused by the underlying substrates. With the technological advances, new tools will enable the rapid assessment of the interaction between cells and biomaterials, at the cellular, molecular and gene levels, offering a window of opportunity to comprehend the regulatory signals that rule the cell/biomaterial interaction. *In vivo*, screening models and biomarkers have been developed to more efficiently select the biomaterials from the great plethora of available options. Additionally, increased knowledge of laboratory animal

experimentation and the establishment of representative models of the human settings, in physiological and pathological conditions, have considerably increased the throughput of valuable data for subsequent stages of biocompatibility evaluation.

Closer to mimicking the complexity of biological tissues, biomimetic approaches to regenerate damaged tissues will continue to emerge and further evolve due to the continued convergence of multiple fields of research. *In vitro* and *in vivo* biocompatibility testing will continue to set the ground base from which candidate materials aiming clinical application stand for, prior to the use in clinical settings.